CHEMICAL AND PHYSICAL ASPECTS OF WEAR PROCESSES IN POLYMERS.

by M.O.W. Richardson, B.Tech.(Hons), A.R.I.C., A.P.I.

A thesis submitted for the degree of DOCTOR OF PHILOSOPHY from the Department of Polymer Science and Technology,

Brunel University, Uxbridge, Middlesex. September, 1972.

ABSTRACT

A series of homogeneous halogen containing polymers have been studied whilst sliding against mild steel and oxides present on mild steel. The degradation characteristics of P.V.C. and Cl^{d}P.V.C. have been correlated in terms of current mechano-chemical comminution theory and the process causing the wear of P.V.C., Cl^{d}P.V.C., P.T.F.E. and P.C.T.F.E. described in relation to the chemical and physical conditions at the sliding interface. In addition the potential importance of the chemical role of oxide free iron surfaces in wear processes has been demonstrated by interacting an analogue compound of P.T.F.E. ($n\text{-}C_5F_{12}$) with clean iron under ultra high vacuum conditions. The resulting fragmentation of the perfluorinated compound is discussed and a simplified degradation mechanism suggested.

INDEX

SECTION TWO

1. GENERAL LITERATURE SURVEY

1.1 Introduction

It is widely accepted that the study of wear processes in polymeric materials, both in composite and homogeneous form, is in many areas in its infancy. Although polymers such as nylon filled with molybdenum disulphide, PTFE filled with bronze and lead, and polyesters filled with glass-fibre are used in commercial 'wearing' applications, little is really understood of their intrinsic chemical and physical wear mechanisms. It is intended to outline a few of the topics of interest in this area and to present a survey of the findings of present workers. The first four sections, dealing with transfer films, melting effects, topography and surface layers, obviously fall in the closely related fields of surface physics and physical chemistry, and it was felt that a brief survey of their significance was necessary before attempting to review the seemingly more obvious chemical aspects of polymer wear processes. The topics of surface treatment, degradation, polymerisation and cross-linking cover this latter area and reveal some interesting possibilities for research and development work in the field of 'tailor-made' composites.

1.2 Film Transfer

When organic polymers are involved in bearing applications the phenomenon of material transfer to or from the shaft is of major importance[1-9]. An understanding of the mechanism of wear must take into account the laying down and subsequent removal of any transferred films[8]. Thus in the case of PTFE bearings and a steel shaft, after a period of time, the situation can change from one of PTFE rubbing on

steel to one of PTFE rubbing on PTFE, with a subsequent reduction in friction. Under exceptional circumstances metals can, however, transfer preferentially to the polymer, e.g. PTFE rubbing on silver[6], but this phenomenon is unusual and certainly not likely to be encountered with common engineering materials.

For PTFE rubbing on glass the character of the film is said to be related to speed and environmental temperature[2,10]. Broadly speaking either high speeds and/or low temperatures tend to cause a fairly massive movement of polymer, and the film, although averaging 0.1 μm thick, includes lumps and small particles. Low speeds and moderate temperatures, however, produce a continuous thin film 10-40 nm thick, which reduces the coefficient of friction from 0.3 to 0.07. The explanation given[2] is one of shearing between crystalline regions in the PTFE which are said to be separated by amorphous regions that are subject to time-dependent flow effects. Current workers[10] in this field, however, are tending to discount this hypothesis and can see no apparent connection between the bulk properties of the polymer and the nature of the film produced.

PRATT[11], quoting HANFORD AND JOYCE[119], has shown that if in the ideal case a highly orientated mono-molecular layer of PTFE bonded to a metal surface rubs on a perfectly smooth PTFE substrate, then one contributing factor to adhesive wear would be reduced because of the lack of van der Waals' forces between molecules. This is attributed to fluorine atoms screening the carbon backbone chain. Orientation effects are also discussed elsewhere[66].

MAKINSON AND TABOR[2], however, while drawing attention to the low surface energy of PTFE compared with analogous hydrocarbons, conclude that the difference is not large enough to discount all bonding of the van der Waals' type. Attention is drawn to the

importance of adhesion by electrostatic attraction caused by charge separation, and it is pointed out that some workers (e.g. DERYAGIN[12]) have attributed the whole of the adhesion of polymers to these effects, while others (e.g. SKINNER et al.[13]) consider them to play only a minor role.

The maintenance and generation of the beneficial transfer film has been a subject of considerable speculation, especially as certain fillers are thought to enhance its adherence[7]. The use of lead, either in the form of metal or oxide, is an interesting case in point even though Russian work[57] is contradictory. HARGREAVES AND TANTAM[4] suggest that the lead oxide acts as a chemical polishing agent by transferring oxygen to the rough parts of the mating surface. The basic assumption here, of course, is that the degree of roughness determines the extent of adherence of film. A later paper by PRATT[7] discounts this hypothesis for PTFE bearing materials by virtue of the fact that one cannot successfully interchange bronze/lead/PTFE composites with say copper/lead/PTFE or iron/lead/PTFE versions, the point being that although both copper and iron are capable of producing the local hot spots for the proposed lead oxide and shaft reactions, great reductions in wear are not achieved. He believes, however, in the importance of interfacial chemical effects and cites the example of an ill-defined green compound produced by rubbing the surface of a bronze/PTFE composite. The function of copper oxide, phosphates, lead and lead oxide in these bearing materials is thought to be one of increasing bond strength between shaft and film by an unknown mechanism. The exothermic reaction that takes place between lead oxide and PTFE at 300-360 °C may be of significance in this matter. Polyethylene [7] compositions sliding against water cooled silver steel shafts are said to exhibit similar wear properties to P.T.F.E. compositions but the improvement induced in other polymers by the bronze + lead types of addition decreases as the molecular structure of the polymer deviates from the simple CF_2 or CH_2 repeat unit. The reason for this is not offered.

The exact role of oxygen or metal oxides in this field is thus open to further study, but it is worth noting that in the powder coating and sintering industry good adhesion of polyethylene to steel is obtained by first oxidising the polymer surface[14]. (N.B. as distinct from metal.)

PACKHAM[14] has also pointed out the importance of mechanical keying by the polymer to porous surfaces such as metal oxides. VINOGRADOV[9] reports that the presence of oxidised polypropylene on the surface of steel enhances its anti-wear properties in experiments concerned with polymer and steel friction couples.

The study of PTFE filled with partially graphitic carbon fibres, lead or copper composites has drawn LANCASTER AND GILTROW[5] to an alternative explanation of the action of metal fillers in increasing film transfer. They claim that copper or lead counterfaces against steel induce low wear and hence it is possible that preferential transfer of these metals to the steel shaft may provide a soft surface in which debris can be embedded. Their work also shows that there is a critical value of stress at the interface below which a film can be transferred readily.

The presence of degradation products from local hot spots on polymer bearing surfaces may also be significant in the chemistry of film forming[6]. Under high vacuum conditions with loads of the order of 10.0 N and speeds between 1.95 and 4.91 m s^{-1}, fluoride fragments are said to be produced when rubbing P.T.F.E. on stainless steel.[6] Other workers[15] report that rare earth fluorides are good film formers on certain metals, and it would be interesting to establish whether metal halides are formed when halogen-containing thermoplastics are used as bearing materials.

In metal/metal systems even a 0.1% O_2 content in an argon atmosphere can be shown to affect the silver to steel transfer,[120,16] and in leaded brasses the wear has been shown to be affected by the chemical composition of the oxide layers which form during rubbing. Obviously the effect of the environment must also be taken into account when extending the study to polymeric systems, especially in respect of external humidity and oxygen entrapped in the fabrication itself.

The geometry of the sliding system and its relation to the direction of material transfer has been mentioned or discussed by several authors[16,40,124] quoting examples of work that used both similar[125, 126] and dissimilar[17,18,19] metal couples. ANTLER[124] states that even in the unambiguous case where riders and rings are of the same material (e.g. copper) unsymmetrical transfer often occurs when mating surfaces are not geometrically identical, with metal tending to be displaced from the larger to the smaller surface.

In the field of solid lubricant films such as graphite, mica and lead di-iodide etc., which are all lamellar solids, LANCASTER[20] has demonstrated the importance of substrate hardness in film build-up. He suggests that the endurance of the coating is inversely proportional to the hardness, i.e. soft substrates encourage the film build-up. The mechanism is said to be one of embedding suitably orientated crystallites of the lamellar solid into metal surfaces such as copper.

In view of the potentially beneficial effects of transferred films, it may be possible to tailor-make bearing materials that will form semi-permanent transfer films by chemical bonding. For example, an uncured epoxy resin could be cross-linked with phthalocyanine derivatives, which are known to produce thermosets with relatively good

high-temperature properties[21]. When allowed to wear against a steel shaft, a strongly adhering transfer film may form by virtue of chemical complexing between nitrogen in the phthalocyanine component and the metal surface. Thus one could effectively anchor epoxide layers to the surface. Adherence of straight metal-free phthalocyanine lubricants to metal surfaces is already well established[22], but it must be noted that metal complexes of the same compounds (pigments) are vastly inferior as far as wear properties are concerned[23].

In the field of plastic coatings advances have already been made[58] in producing films of fluorocarbons 13-50μm thick by sintering on to metal. Similarly in situ transfer coating has been investigated by constructing roller bearing cages of PTFE[59]. R.F. sputtering of PTFE on to metal and glass surfaces has also been described[80].

1.3 The Influence of Surface and Environmental Temperatures on Wear

The energy dissipated at rubbing surfaces nearly always appears in the form of heat and is produced by friction. In most sliding situations contact is made at isolated junctions and not over the whole apparent area of contact, giving rise to local hot spots. The area being of the order of an asperity junction[25] (P.36,49,50) whose diameters vary greatly but are estimated to be in the region of 1.0μm. Their temperatures generally agree to within 30% of those theoretically calculated. A number of workers[24,25,61] have produced or quoted theoretical formulae in this field, but there are a number of major drawbacks in applying them reliably. For example, the use of most of the equations involves measuring such parameters as the coefficient of friction and the diameter of the contact junction, and assumes that the heat generated at individual junctions does not interact.

More recently, however, RABINOWICZ[25] has quoted an expression which incorporates surface energy data, and apart from the sliding velocity it contains no parameter that is not a constant for the material or a conversion factor:

$$\theta_m = \frac{9400 f \gamma V}{J(K_1+K_2)}$$

where J = mechanical equivalent of heat, θ_m = rise in temperature, f = coefficient of friction, γ = surface energy (softer material), V = velocity, and K_1 = thermal conductivity of sliding surface, K_2 = thermal conductivity of countersurface.

Typical values of θ_m that are obtained are 0.75 (°C/cm/sec) for steel/steel, 2.2 for bakelite/bakelite, and 0.07 for steel/nylon. Using expressions quoted by ARCHARD[24] it should also be possible to estimate in advance combinations of load and speed that will induce wear breakdown in polymer/steel systems because these parameters are involved in his alternative equations.

It is generally accepted by most workers that for wear in polymers (especially PTFE), increasing wear occurs with increasing interface temperature[26, 27]. Indeed, it is well known that when the surface temperature approaches the melting point of the polymer, breakdown occurs[24, 28, 29], and usually the flash temperatures obtained in general practice closely approach the melting temperature of the lower melting of the two sliding materials[25]: BEZBAROD'KO has demonstrated that with GRP's involving phenol-formaldehyde, polyamide, or epoxy systems, both the coefficient of friction and hardness decrease with time. Surface temperatures were estimated by reference to colour changes in the plastic and were found to be 50–60°C higher than the thermocouples indicated. When the systems were lubricated with glycerine the cooling effect was an important means of increasing wear resistance. Chemical changes at the interface were claimed to occur above a certain loading, and eventually the

coefficient of friction was independent of load and temperature of the test-piece was constant. It is claimed[29] that with polymers such as polymethyl methacrylate and ebonite at high loads, again the coefficient of friction decreases due to the melting phenomenon. It was concluded, however, that where glycerine was used as a lubricant, heating of the surface layers was not the sole cause of reduction of coefficient of friction, and modification of the steel surface was important, i.e. formation of glycerates. eg 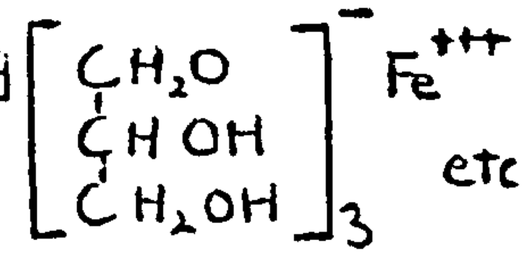 etc

AWATANI et al.[28] have deduced an expression to relate the usable limit of plastic materials to load and velocity. This was produced as a result of their study of nylon 6 and polyethylene rubbing on steel.

$$T_o + K\mu PV = T_s$$

where T_o = temperature of surface, K = a constant related to experimental conditions, μ = coefficient of friction, P = load, V = velocity, and T_s = characteristic temperature of polymer. For example, T_s = 120°C for high-density polyethylene and 190 °C for nylon 6.

The increase in frictional coefficient early on in their tests and then the decrease to a final constant was explained from adhesion theory taking into account the temperature dependence of yield pressure and shear strength.

LANCASTER[3] has shown that in the case of abrasive wear of a number of polymers, where no transfer is taking place, there is a minimum value of wear rate at a characteristic temperature for each sample although the ratio of plastic deformation to elastic deformation, as characterised by ratio of hardness to elastic modulus, is independent of temperature. He establishes, however, that the product of the elongation to break and the breaking strength is an important

parameter in the abrasive wear of polymers, and shows that $1/s\varepsilon$ varies with temperature in the same way that wear rate does.

1.4 Surface Topography

When polymeric materials rubbing on metal surfaces are considered, the concepts of surface roughness and surface profile have particular significance. This is due to the potentially beneficial or harmful influences of transfer films that are liable to form on the metal counterface, because the rate of formation in many cases is influenced by the degree of roughness[3, 5]. It is claimed that relatively ductile polymers such as polyethylene, polypropylene and polytetrafluoroethylene form transfer films which effectively smooth out the counterface and reduce wear rate. On the other hand polymers possessing relatively small elongation such as polystyrene, poly-acrylonitrile-butadiene-styrene etc. do not easily form beneficial transfer films and hence the degree of counterface roughness is only effective in increasing the wear rate. Other workers[10] claim that materials such as low-density polyethylene do not form continuous thin transfer films under any of their experimental conditions, although transferred lumps are in evidence.

As previously stated in the case of abrasive wear conditions, LANCASTER has shown that for certain polymers such as polyacetal, polypropylene and polymethyl methacrylate, there is a characteristic temperature at which wear is at a minimum. The individual values for this temperature are increased by increasing the counterface roughness.

In the particular case of filled PTFE rubbing on steel there are said to be critical values for the counterface roughness beyond which wear increases rapidly[30]. The upper limit is approximately 0.8 μm c.l.a.

but the value for the lower limit is still in dispute. However, 0.2-0.4μm is quoted to be the 'safe' range for good wear resistance. In addition, STEIJN[31] has reported that even for a change of surface finish on the steel component of 0.025-0.09μm (r.m.s.), there is a microscopically observable change in the degree of smoothing of the PTFE surface during the course of a wear experiment. Other workers record measurable changes in friction with changes in surface finish of the steel component but these do not necessarily correlate with wear rates[62].

As any wear experiment progresses, of course, the nature of the rubbing interfaces must change accordingly until some form of equilibrium situation is established. For wear studies on metals, ARCHARD AND HIRST[32] state that for all types of wear mechanism, once equilibrium surface conditions are produced the wear rate becomes independent of the apparent area of contact. A further point of interest is that some workers claim[33] that the equilibrium surface finish attained by a friction pair (of an unspecified sintered anti-friction material) is independent of the initial surface roughness. A minimum value for wear rate is said to be associated with the approach of this equilibrium surface condition.

In the field of 'wear' theory, considerations of surface finish also tend to play an important role. BAYER[8], for example, includes this parameter in his 'wear' equations. Roughness also must be taken into account when considering friction theory, and as RABINOWICZ[25] points out, the friction force is only independent of this parameter over a given range of surface finish (approximately 0.4-1.25μm).

Another aspect of this particular topic is the means of producing the finish. There are reports[30] that polymers exhibit better wear resistance against ground metal surfaces than turned ones. An explanation for this phenomenon is not, however, offered.

There are a number of general reviews in the literature dealing with methods of determining surface roughness and the relationships between wear rate and surface topography[63-65].

1.5 Surface Layers

Surface films such as oxides, soft metals, and molybdenum disulphide in a resin binder, etc., have been shown to possess low wear characteristics when the film thickness lies between 10^{-8} and 10^{-5}m (10-10,000 nm)[34]. At the upper (10^{-5}m) limit a rise in friction occurs because the load is then carried by the film rather than by the substrate, and a corresponding increase in wear develops due to the formation of large wear particles. The experimental data appear to agree reasonably well with theoretical predictions based on concepts of characteristic junction size and wear particle size as proffered by RABINOWICZ.

DE GEE[35] has pointed out that in the case of steel/steel systems, thick oxide films generally inhibit the formation of adhesive joints and thus reduce friction and wear. For thin oxide films, however, adhesion between sliding surfaces may well increase due to the formation of monomolecular layers which can locally 'glue' (as he puts it) the surface together.

In air at room temperature clean mild steel oxidises predominantly to ferrosoferric oxide[36,67] (Fe_3O_4) 2-10 nm thick. By heating in a vacuum furnace in a restricted oxygen supply (1.0-10.0 N m^{-2} at 500-750K) 100nm thick films can be produced[68] and their surface lubrication properties compared with oxides of the Fe_2O_3 type. In the case of steel/steel sytems, only Fe_3O_4 imparted good lubrication properties to the surface said to be due to localised stresses shattering the oxide into lamellar plate-like pieces from cleavage parallel to the octahedral faces of the crystal[36,121]. More recent work[69] has drawn attention to the greater number of 'easily sheared' planes in the cubic crystalline structure of Fe_3O_4 compared with the hexagonal close packed $\propto Fe_2O_3$ system (where the indexing is based on a hexagonal cell derived from the obverse rhombohedron[70]). Thus Fe_3O_4 is said to have a low wear structure. Presumably this is intended to imply that low wear is induced in the countersurface as a consequence of sacrificial oxide break-up (lubrication) across the interface. If this is not the case then paradoxically the argument for a greater number of slip planes and systems is used by other workers[71;72,73] to explain why close hexagonally packed metals such as zinc or titanium have greater wear resistance than cubic metals such as iron or copper. In these cases it is suggested that multiple slip planes in cubic systems will intersect each other so that shearing produces heavy wear. For hexagonal metals dislocation movement in one plane only leads to uninterupted glide, thus dissipating the shearing forces without heavy wear.

Care must be taken, of course, when comparing oxide and metal crystalline materials because of the differences in the

structure and bonding (i.e. quite apart from the 'close packing of spheres' concept) e.g. iron oxides are held together by electrostatic (ionic) bonding between Fe^{++}, Fe^{+++} and O^{--} ions arranged in close proximity in fixed orderly arrays throughout the crystal lattice. The crystalline metallic state, however, is often described as consisting of positive metal ions embedded in a cloud of electrons[130 (P.975) 131 (P.675)]. The significant difference being that the electrons (here considered as partially analagous to negative ions) are not associated with particular atoms and are labile even at absolute zero temeperatures. One point, however, on which there is substantial agreement is that for an oxide to act as a lubricant the hardness must not exceed 1 - 2 x that of the substrate and the thickness must fall within critical limits[74 - 79] (see earlier).

DRAIGOR et al.[37] have reported a novel method of measuring oxide film thickness using an electron emission intensity counter for which is claimed the specific advantage of being contact free and requiring only 10 - 15 seconds for a reading. ROWE et al.[38] have used the X-ray microanalysis technique for studying metal oxide surfaces, which gives not only an indication of thickness but also the change of metal to oxygen atomic proportions with different depths of probe. A simple assessment of chemical structure on the surface, however, can easily be obtained by examining electron diffraction patterns.

This particular technique and some other modern physical methods of analysis have recently been reviewed by QUINN[71] with special emphasis on tribological applications.

1.6 Surface Treatment for Polymers and The Surface Chemistry of Polymer Wear.

REIHSMANN[39] has successfully produced low-friction surfaces on elastomers such as neoprene, butyl rubber and Buna N rubber by one of two basic processes. The first involves one-step graft fluorination carried out in an autoclave containing sulphur tetrafluoroethylene and acrylic acid plus the rubber. The resulting materials had coefficients of friction of 0.40-0.60 at low speeds (30.4-61.0 mm s^{-1}) and 0.15-0.25 at high speeds (3040 mm s^{-1}). The second process grafts partially fluorinated oligomers of ethylacrylate and acrylic acid onto the surface after first swelling the rubber with a suitable solvent and then irradiating with ultraviolet light. HORAN reports similar work[81].

The grafting of PTFE and PVC onto other polymers by electron irradiation is also possible[82].

Russian authors[29] claim that when glass-reinforced polymers such as phenolformaldehyde, epoxides etc. are used as friction couples in conjunction with steel and using glycerine lubrication, boundary layers are formed on the plastic surfaces. This is in addition to glycerates formed on the metal surface. Frictional heat is also cited as causing chemical modification to the polymer surface and, of course, under extreme conditions the polymer melts.

It must be noted that the concept of anchoring suitable boundary layers on a plastic is further complicated by more general difficulties of defining the thickness and nature of the film required[127].

The wear resistance of metal surfaces is often markedly improved by diffusion hardening treatments, the most widely adopted[40(P.8) 41] being carbonising, nitriding, and sulphiding. Perhaps a similar line of treatment might be derived for polymers using other materials and techniques.

Recent developments in electron beam curing of polymers[42] make it possible to locally harden surfaces by another method. For example, polyethylene could be cross-linked in the upper few microns of surface for sliding applications. Japanese authors[28] have tried irradiating polyethylene with gamma rays from a cobalt 60 source with beneficial results with doses above 10^8 roentgens.* Nylon, however, does not improve after receiving similar treatment. Polymer surfaces can also be cross-linked by plasma techniques[83] (ionised low pressure gases).

1.7 The Degradation of Polymers Under Wearing Conditions

Local areas of hot material are formed when polymers slide on metals under dry conditions. BUCKLEY AND JOHNSON[6] claim that decomposition mechanisms for polymer compositions depend on the mode of heat dissipation from the sliding interface, though aspects of this are later challenged by other workers[43]. PTFE was studied at 1.33×10^{-7} N m^{-2} pressure and with various fillers and metal couples. With unfilled PTFE the principal degradation products were CF^+ and CF_2^+ ions (in the spectrometer). With glass filled polymer, however, the principal product was F^+ ion, indicating a C-F bond cleavage at the interface.

* R.S. 776 (1970)

This was attributed to the greater mechanical strength imparted by the filler reducing the amount of local heat being carried away by wear particles. The decomposition products detectable when copper metal fillers were used in PTFE were very small due to the dissipation of heat. Very low concentrations of F^+ and CF^+ ions were observed. Silver was anomalous in so far as, although its thermal conductivity is greater than copper, large quantities of decomposition products were produced. This was stated to be due to silver transference to the PTFE, giving effectively silver rubbing on silver (the reaction of disc surfaces with hydrogen sulphide produced a continuous layer of silver sulphide). In the case of coke flour and graphite fillers it was found that the coke flour gave more favourable heat dissipation, due to orientation effects in fabrication which resulted in better wear characteristics. Work currently being carried out at Brunel University[44] into the effects of orientating fillers in thermoplastics may confirm a connection with good wear properties. There are reports[66] that the molecular weight of PTFE at the wearing surface decreases and it is well known of course that even polymers in solution will degrade under shear[84].

Russian authors[45,46] claim that high molecular weight polymers at the moment of mechanically induced degradation are capable of activating the deformation and fracture of metals. This may explain why excessive wear is sometimes encountered in metal parts when operating in contact with polymeric materials. The technique used in this study was ball milling of polyethylene, PTFE, polystyrene, polymethyl methacrylate and polyphenol-formaldehyde emulsions with iron powder followed by particle size analysis of the ground material. Conversely, recent work by MORECROFT[85] has demonstrated the capacity of oxide free iron to promote degradation of organic molecules and the conclusions might logically extend to include polymers in specific

'wearing' circumstances e.g. in the presence of iron fatigue cracks at U.H.V.

Other work has shown how under extreme conditions of wear[29] both CRP's containing polyphenol formaldehyde, polyamide and glass fibre and thermoplastics such as polymethyl methacrylate first soften and melt at the rubbing interfaces and then degrade. Techniques have been developed[47] which allow the experimenter to follow the decomposition of a monolayer of surface using mass ion spectrometry and electron microscopy, but as yet these methods have not been applied to tribological problems.

In the field of liquid lubrication of steel/steel surfaces considerable work has been done on additive degradation[48], but it will not be discussed here. In view of the considerable volume of work carried out on the beneficial action of solid lubricants producing low interfacial shear strength and easily sliding surfaces, however, it may be relevant to speculate at this point on whether use could be made of surface polymer degradation to the same advantage.

1.8 Polymerisation and Cross-Linking Effects on Rubbing Interfaces

In 1962 CAMPBELL AND LEE[49] did an exploratory study of frictional polymers formed as a consequence of mechanical activation during the sliding of various metals in organic vapours. The resin produced when palladium was rubbed by itself in limonene vapour and disobutylene vapour did not, however, reduce wear. In the presence of a monolayer of stearic acid copious polymer was produced from the organic vapour which reduced both wear and friction. o-Chlorobenzotrifluoride vapour induced wear reduction in all three metal couples i.e. steel/steel, palladium/palladium and chromium/chromium, but polymeric material was not observable. It was concluded that the nature of the film which preceded the polymer formation was the determining factor in wear and friction reduction.

The results were explained by assuming that free radicals, produced by shearing the adsorbed stearic acid film in the presence of a catalyst, initiated polymerisation of the organic gases.

Similar conclusions about mechanism were cited by CHAIKIN[50] when he detected minute amounts of a complex, cross-linked, amorphous, oxygen-containing material on the surfaces of rubbing platinum, palladium, ruthenium, and rhodium in environments of over 60 simple saturated and unsaturated organic compounds such as alcohols and hydrocarbons, etc. On work with oils ROUNDS[86] has commented on the roll of additives and the environment on friction polymer formation.

Current work at Cambridge[51,52] has added to this the feasability of using these films produced in situ as boundary lubricants. TABOR AND WILLIS have used low molecular weight dimethyl-silicone fluids, which when used alone are poor lubricants for steel, to produce polysiloxane films. These films are mechanically unstable, but while they are present, definitely reduce wear. Further work has revealed that inclusion of a small quantity of a fatty acid surfactant in the silicone fluid, such as stearic acid, produces a film with superior lubricating properties. In this case the polysiloxane acts as an anchor for the stearic acid which is chemically attached to the metal surface. It is claimed that metal oxides act as a catalyst.

JEMMETT[53] has shown how the relative thickness of bonded polysiloxane films can be estimated using attenuated total reflectance infra-red spectrophotometry techniques (silicon-mthyl peak at 7.9μm). The ease of formation of the film is shown to be related to the ease of oxidation of the metal itself, and the thickness of the film is shown to be proportional to the mean molecular diameter of the linear polysiloxane involved. It is claimed that one could

theoretically produce coatings of required thickness and exercise control of their adhesion to the metal surface by changes in the chemical structure of the siloxane skeleton.

A recent paper by KOUTKOV AND TABOR[54], in which nylon 6:6 was slid against steel in the presence of siloxane fluids, has introduced the idea of interaction between the methyl groups on the polysiloxane film produced and amide radicals on the substrate. It is also suggested that the newly formed polymer may plasticise the surface of the nylon and so produce a low friction surface. It is added, however, that further study is needed to establish with greater certainty the detailed mode of action of the silicone.

In the light of this present work a number of interesting technological possibilities could be emerging. Is it feasible, for instance, to produce a composite plastic bearing with a built-in potential for producing its own wear-resistant surface friction polymer, e.g. using a polymer containing a potentially cross-linkable plasticiser. On the other hand perhaps a suitable cross-linkable additive could be incorporated in the lubrication system of a polymer/steel bearing couple. With unplasticised PVC it should be noted that excess HCl (from the degradation process), metal chlorides or organo tin stabilisers can actually promote cross-linking while surrounding areas are degrading[87].

1.9 Conclusions

Although a very great amount of money has been spent on lubrication technology and materials development[55,56] there is a surprising lack of knowledge concerning the basic chemical and physical phenomena which occur when surfaces interact in relative motion. While interesting and lucrative advances have been made, for instance in the

use of plastics in bearing applications, the fundamental reasons and explanations of the chemical and physical mechanisms involved still require further study. It is hoped, therefore, that this thesis will be a useful contribution in the right direction.

2. AIMS OF THE PRESENT WORK

The primary objective was to take a series of homogeneous halogen containing polymers (namely P.V.C., $Cl^dP.V.C.$, P.T.F.E. and P.C.T.F.E.) and study their mode of wearing or interaction when slid or contacted with a variety of conditioned mild steel surfaces. Three types of countersurface were chosen for study.

(i) mild steel with associated 100nm thick oxides

(ii) mild steel with the nominal 2-14nm thick oxide.

(iii) mild steel without oxide.

The experiments concerned with countersurfaces (i) and (ii) are presented in SECTION ONE & involve a detailed assessment of the degradation characteristics of P.V.C. (and to a lesser extent $Cl^dP.V.C.$) under a variety of loadings, sliding speeds, temperatures and surface conditions. More general studies of wear rates and film transfer phenomena have been attempted for P.T.F.E. and P.C.T.F.E. as well as P.V.C. and $Cl^dP.V.C.$

For countersurface conditions (iii) experimental data and discussion is presented separately in SECTION TWO For experimental reasons this necessarily involved introducing an analogue compound of P.T.F.E. (namely nC_5F_{12}) under ultra high vacuum (U.H.V.) conditions onto the surface of simulated oxide free mild steel (namely clean iron) and studying reaction products.

The philosophy behind the adoption of particular lines of study, materials and techniques etc., is discussed and developed further in the individual introductions to the sections that follow.

SECTION ONE

3. A STUDY OF THE WEAR PROPERTIES OF P.V.C., Cl^dP.V.C., P.T.F.E., AND P.C.T.F.E. UNDER VARIOUS CONDITIONS OF SLIDING SPEED, LOADING, TEMPERATURE AND IRON OXIDE COUNTERSURFACE WITH PARTICULAR REFERENCE TO MECHANO-CHEMICAL EFFECTS AND THE DEGRADATION MECHANISM OF P.V.C.

3.1 Introduction and General Philosophy

Much of the published work dealing with wear processes in polymers has concentrated on searching for relationships between steady state wear rate, the bulk properties of the materials and certain experimental parameters such as sliding velocity, load etc. As the literature survey has revealed although this is both useful and necessary work benefits would also accrue from complimentary studies aimed at looking at the process from a tribochemical point of view. It is generally accepted that potentially high stresses can be developed between sliding surfaces even with seemingly light loads due to the fact that the real area of contact is invariably, and sometimes considerably, lower than the apparent area of contact. This can cause significant local elastic and plastic deformation of the interface that in turn can lead to an increase in temperature, molecular rupture and exposure of new (potentially catalytic) surfaces under conditions of high pressure. Thus chemical changes at the sliding surface would seem, intuitively, inevitable. This SECTION ONE therefore, is an attempt to set up a series of dry wear situations (involving several different polymers sliding on a variety of types and thicknesses of oxide associated with mild steel) with a view to answering two basic questions.

(1) How are certain of the polymers chemically and physically degrading in relation to the changing sliding conditions?

(2) How do the polymer wear rates correlate to the changing sliding conditions?

A series of homogenous halogen containing polymers were chosen for the study representing both substantially amorphous materials (P.V.C. and Cl^{d}P.V.C.) and crystalline materials (P.T.F.E. and P.C.T.F.E.) respectively. By choosing homogenous thermoplastic polymers it was intended to eliminate complicating factors due to fillers etc. and difficulties in fabricating them into simple flat specimens. None of the samples required final machining thus minimising degradation effects on the surface due to cutting and frictional heat that would have been developed during the finishing process.

P.V.C. was singled out for an 'in depth' study of degradation characteristics for a number of important practical reasons. Firstly it is readily soluble in certain common solvents, such as tetrahydrofuran and hence more amenable to molecular weight analysis techniques such as gel permeation chromatography (cf. P.T.F.E. which has a very low solubility in all common solvents at room temperature). Secondly its mode of thermal degradation is such that very sensitive colour changes herald the onset of such heat induced processes and can beused as an indicator of areas suitable for further investigation. This would normally take the form of infra-red and ultra-violet absorption spectrophotometry the latter technique also being particularly sensitive to certain degradative effects e.g. induced hyperconjugated main chain unsaturation (SEE RESULTS/DISCUSSION). In addition any evolution of HCl from the polymer molecule (a distinct possibility with P.V.C.) could lead to readily detectable changes on the iron oxide

surfaces e.g. ferric chloride formation.

For many practical applications where polymers are expected to fulfil a sliding role (e.g. plastic bearings) the mating surface involved is mild steel. With this in mind it was decided in the present experiments to produce oxide countersurfaces representative of those found on mild steel. Although in this case there are several varieties of iron oxide possible, Fe_3O_4 and Fe_2O_3 were selected as being the most common. These were grown in varying proportions on the steel surface by heating in controlled environmental conditions so that up to 100nm thick films were produced. Control experiments with only the nominal 2-14nm Fe_3O_4 oxide associated with freshly polished mild steel were also carried out. In order to complete the picture of the potential chemical activity at tribochemical surfaces more specialised experiments involving oxide free iron have been attempted and described in SECTION TWO. Full details of all the materials used and how they were produced etc. is presented in later sections dealing with sample preparation etc.

A survey of the experimental methods used for the study of unlubricated wear and friction processes in both plastics and metals (the results of which have been discussed in the literature survey) revealed a potentially wide choice of approach[123,25].

Firstly the geometry of sliding systems can vary between pin on disc, pin on ring, pin on drum, pin on flat, crossed cylinders, flat on cylinder, ring on ring, etc., etc. Each system presents its own individual advantages and disadvantages according to whether one is interested in repetitive or non-repetitive wear, or setting out to accentuate a particular mode of wear (e.g. adhesive, abrasive, corrosive or surface fatigue[25] wear etc.). For example the pin on disc arrangement can be useful for measuring non-repetitive abrasive wear of

the pin. This is achieved by designing the pin to traverse the surface of an abrasive disc in a decreasing spiral (much like a needle in the grooves of a gramaphone disc). In most of these methods the area of contact has been localised so that sliding takes place over a narrow track. In fact in some cases the track is narrowed further by tapering or rounding off the end on the pin so that initially the apparent and real areas of contact are very nearly equal[25(P.105)] at the interface when sliding commences. This makes it easy to locate areas on the surface for microscopic examination and theoretically one should be able to extrapolate[25(P.105)] the wear and friction results to cover similar systems where the load is dissipated over a large apparent area (providing of course the wear and friction forces are still related to real area of contact and, more particularly in the case of polymers, the melting, viscous flow and transfer effects at the surface are still operating in the same way).

The second major consideration in choosing a wear test method is the manner in which the actual wear rate is to be monitored. Usually one of four generally accepted techniques[25(P.119)] are employed namely, weighing,mechanical gauging, optical guaging or radiotracer analysis. For weighing the limit of resolution is restricted by such factors as the ability to adequately remove loose debris from the specimen prior to weighing and the accuracy and sensitivity of the chemical balance used. Generally speaking the limit is said to be about 10^{-4}g[25(P.120)]. Mechanical gauging is restricted to a similar resolution of about 10^{-4}g calculated on the assumption that the micrometer has its own resolution of approximately 10^{-2}mm and the rider sliding face has a surface area of 1.0mm^2. Typical of optical methods is the microscopic measurement of wear scars produced from interacting crossed cylinders where the wear scar diameter is related to the volume of material

removed. In this case the limits of resolution are set by the accuracy of the travelling microscope and, more poignantly in the case of thermoplastics, the degree to which the wear scar edge definition and geometry is distorted by heating, visco-elastic and stress relaxation effects. Actual resolution limits thus depend on the system and could typically vary between 10^{-3} - 10^{-5}g. Use of radiotracers to measure wear is usually confined to certain metal/metal sliding systems and is potentially the most accurate method of all providing measurements down to 10^{-9} - 10^{-12}g.

For the present experiments where it was intended to examine the thermal and mechano-chemical degradation of polymers in addition to their wear performance against oxides present on mild steel the following requirements influenced the final choice of apparatus geometry and method of wear measurement.

(1) Easy access to polymer wear scar for chemical and optical examination of wear debris.

(2) Easy removal of polymer specimens and mild steel countersurfaces (in the latter case for heat treatment in air or vacuum furnace).

(3) Polymer specimen must be in a readily mouldable form not requiring final surface machining (which could cause local thermal or mechano-chemical damage).

(4) System of wear measurement must be suitable for amorphous polymers heated to or beyond their glass transition temperatures (Tg).

To fulfil these conditions a polymer flat on revolving mild steel cylinder arrangement was chosen as illustrated in FIGS. 1, 2 and 4. Apart from satisfying the accessibility and removal requirements of the first and second conditions it also allowed the polymer specimens to be in the form of cut down compression moulded sheet (not needing surface machining) thus meeting condition three. The direct weighing method was used to record wear rate as this alleviated the possibility (however remote) of wear scar distortion due to heating effects implied in requirement four.

Some of the analysis techniques adopted to study the degradation effects at the sliding interface have already been mentioned and the principles involved will be discussed more fully in the APPENDIX.

Sub-sections entitled APPARATUS, SAMPLE PREPARATION AND ANALYSIS and EXPERIMENTAL PROCEDURE etc., now follow describing the actual experimental equipment, materials and test methods in greater detail.

3.2 Apparatus

3.2.1 Wear Rig

This consisted essentially of horizontally rotating 5cm. mild steel drums on which stationary flat microscope slide size plastic specimens were allowed to slide under applied loads. (See Fig.1.).

A series of drums along the same drive shaft was powered by an electric motor linked to the system by a pulley belt. At either end of the belt were variable diameter pulleys allowing the speed of sliding to be varied from 1.44 ms^{-1} - 5.33 ms^{-1} in three stages. A carefully designed drive assembly (see fig. 2.) allowed the drums to be interchanged or easily removed for examination without disturbing the shaft alignment. This alignment was critical in avoiding excessive vibration at high speed; also requiring meticulously accurate shaft trueness and the use of double bearings between each wear head station. The plastic specimens were clamped in specimen arms and held in a permanent horizontal plane against the appropriate drums by action of the pivot and arm steady that restricted horizontal vibrations by a tongue and slot arrangement illustrated in fig. 1. The load was provided by weights hung at the end of the arm and the actual applied load at the sliding interface measured by a spring balance connected to the hook positioned centrally above the specimen. The whole assembly, drums shafts and arms were maintained in rigid tubular framework designed for easy access (see fig.3). Additional strengthening bars were attached at various angles to rigidify the structure and hence reduce vibration.

For some experiments an electric heater was positioned a few centimetres below the rotating drums to allow the steel surfaces to

THE WEAR RIG HEAD ARRANGEMENT.

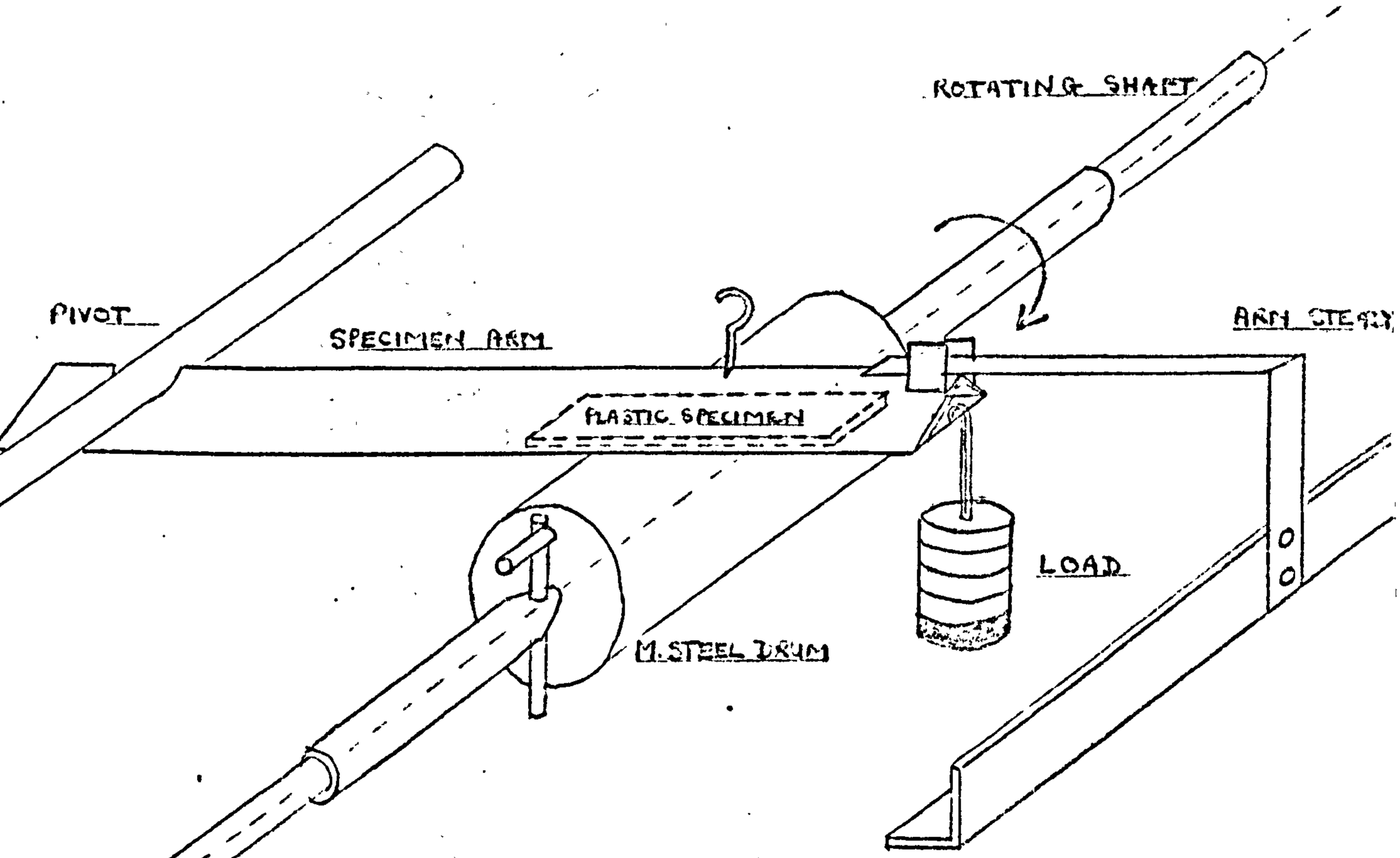

FIG. 1.

THE WEAR RIG DRIVE ASSEMBLY.

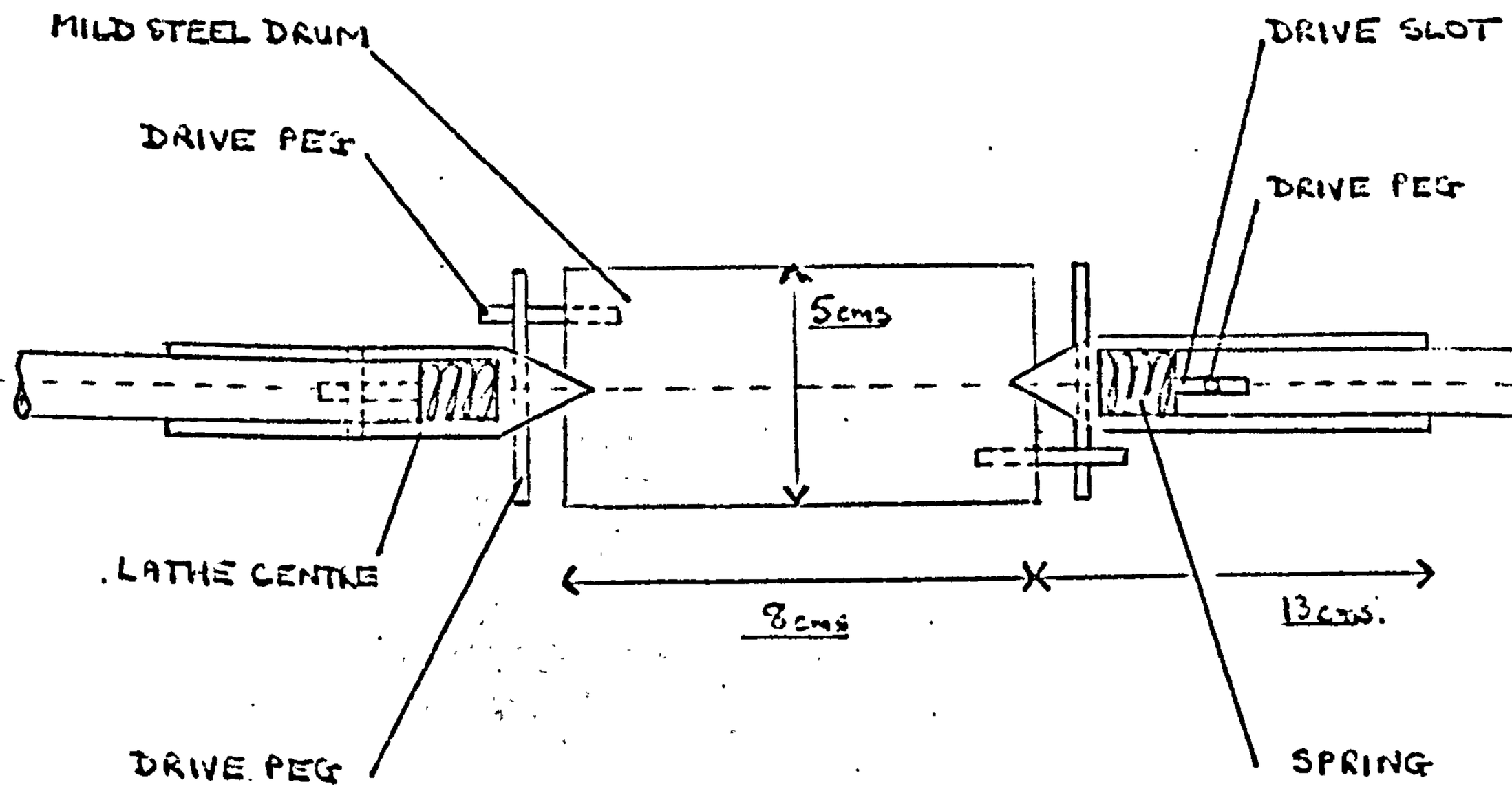

FIG. 2.

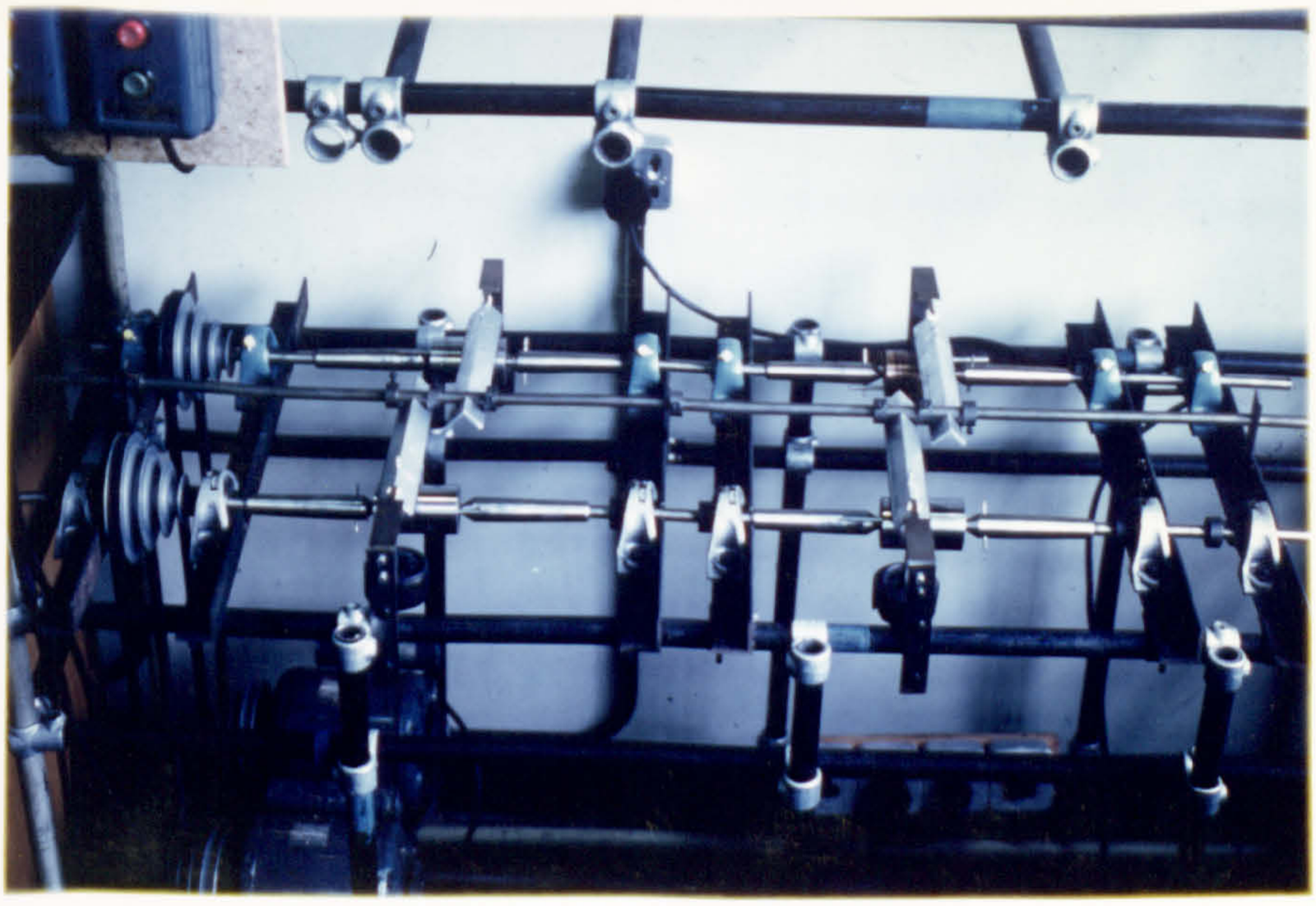

FIG.3 . The wear rig apparatus.

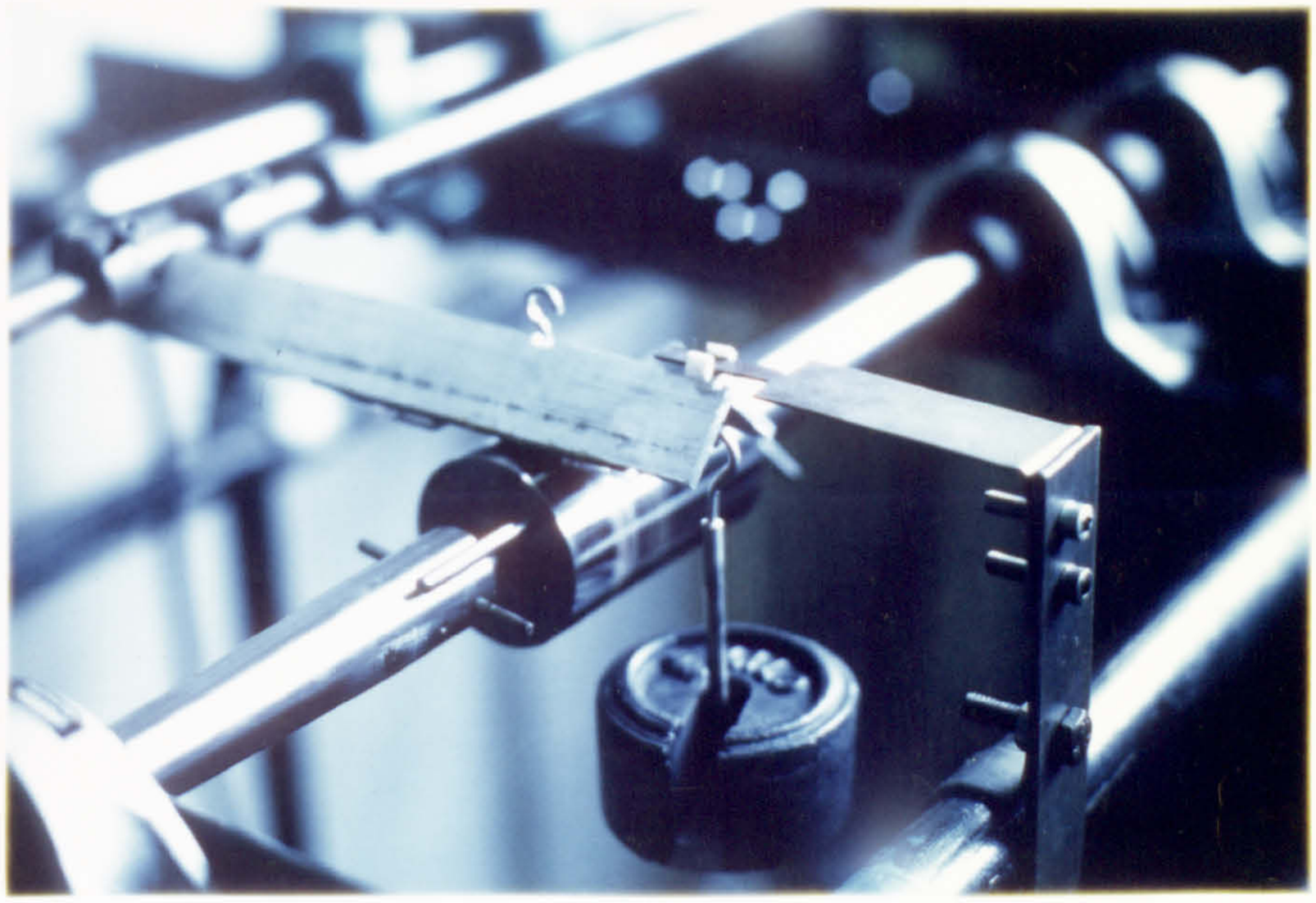

FIG.4 . The wear rig apparatus - showing drum and specimen arm.

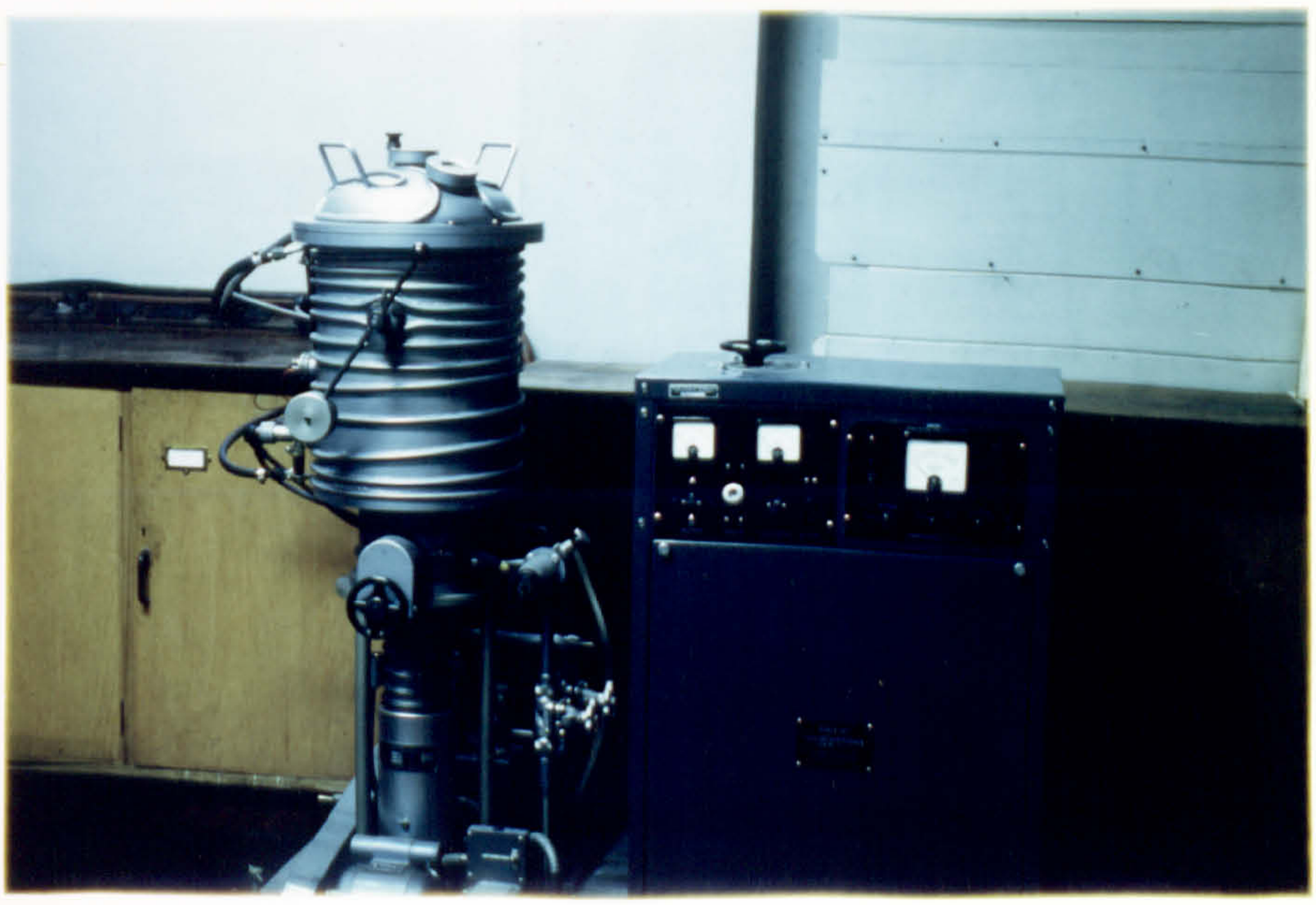

FIG.5 . The 'Speedivac' vacuum furnace.

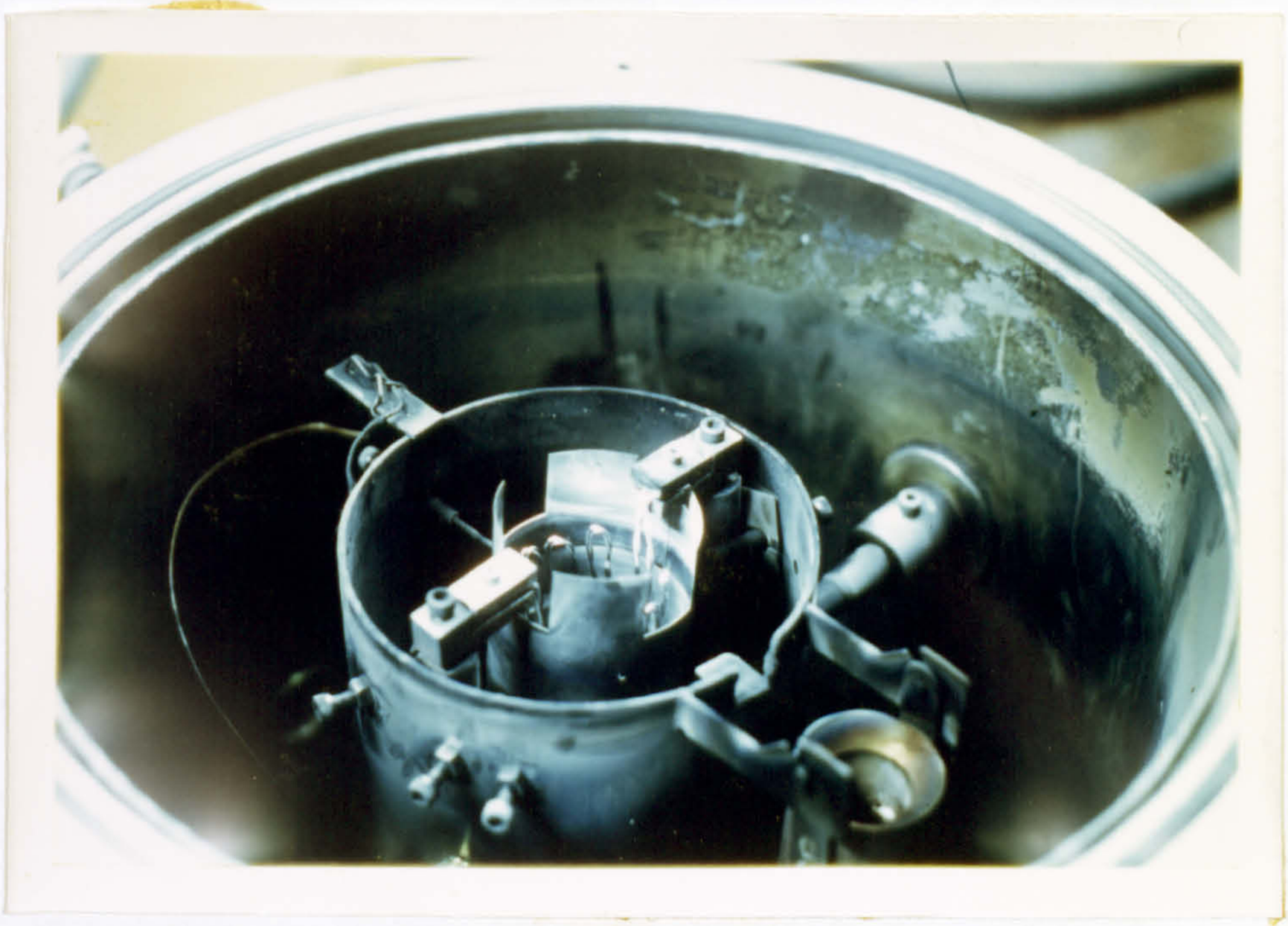

FIG. 6 The 'Speedivac' vacuum furnace - showing modified element.

be heated between (20-90°C) 293-363K . Temperatures were measured by a sliding platinum band thermocouple held momentarily to the drum surface.

In the course of a typical experiment the plastic specimens were removed at 600 s intervals from their arms and weighed on a Stanton five decimal place metric balance. Loose debris was removed in each instance by clean tissues.

3.2.2 Ancillary Equipment

In order to produce the suitable 100nm thick Fe_3O_4 oxides on the surface of the mild steel countersurfaces a modified vacuum furnace was built. It consisted basically of a 50cm long and 33cm diameter evacuated chamber heated internally by a 300-400 watt radiant electric heater and cooled externally by a water jacket. Certain aspects of the design and operation were critical in achieving the required result. Firstly, nickel/chromium heating elements were required to eliminate the possibility of coating the specimen with oxide contamination from the heater itself. Secondly, even though the pressure required was only $\simeq 1.0\ N\ m^{-2}$ an oil diffusion pump was incorporated into the system with an appropriate leak valve. This arrangement avoided the back diffusion of contaminating oil. (Further details and diagrams are presented in the APPENDIX 1).

3.3 Sample Preparation and Analysis

3.3.1 Metal Drums

3.3.1.1 Polished Steel Surface Production

Mild steel drums of approximately 5 cm. diameter and 8 cm. length were turned on a lathe and then ground and polished to a surface finish of 0.075 - 0.1μm (3 - 4μin) c.l.a. as measured on a Rank Taylor Hobson Talysurf surface finish apparatus. For consistency, the drums were surfaced with fresh 600 grade silicon carbide paper before each experiment, cleaned and degreased with 'analar' acetone and trichloroethylene and then carefully dried with microscope tissues. This procedure was found to give a surface finish of(3.0μin $\pm$ 1.0) 0.075μm $\pm$ 0.025 c.l.a. Under these conditions it was reasonable to assume that a 2 - 1/4 nm thick Fe_3O_4 oxide surface had been formed. [67]

Mild steel specifications :- EN 35

Tensile strength 494 M Nm^{-2} (71680 p.s.i.)

C	0.2% w/w
Si	0.15% w/w
Mn	0.06% w/w
S	0.04% w/w
P	0.035%w/w

5.3.1.2 100nm Fe_3O_4 Surface Oxide Formation

Taking drums treated as in (3.3.1.1) they were heated in a vacuum furnace for a total average time of (1 hr. 15 mins.) 4.5 ks . The first 15 mins. involved a steady build up of temperature to (500 °C) 873 K with the pressure maintained between (0.035 - 0.1 torr) 4.5 - 13 Nm^{-2}. Heating was continued for a further hour and then the whole system allowed to cool under vacuum. This procedure produced an approximately 100 nm. thick

oxide film [36] exhibiting the characteristic blue interference colours. [130 (P.20)] Experience showed that both time of heating, temperature and pressure were critical in producing the required oxide thickness. Intermediate stages of light straw, yellow brown, purple, violet were observed similar to those described by Osborne [88] as the transparent layer built up. With the temperature maintained at (500°C) 873K, and a vacuum of (3.5×10^{-2} torr) $\leq 1.0\ Nm^{-2}$ once the light straw colour had formed then the other colours appeared at intervals of approximately 5 minutes. The conditions were so chosen to promote formation of Fe_3O_4 as the major oxide following the work of Boggs [68] et al and Johnson [36] et al.

The former demonstrates an inverse relationship between the likelihood of Fe_3O_4 as the major oxide and temperature and pressure. Hence a degree of compromise was required in being able to produce the required result. For analytical purposes some oxide was stripped from the drums [89] using Booker's technique. This involved coating with a thin layer of formvar and then with collodion. When dry the double film was removed along with the adhering oxide. The collodion was dissolved away using amyl acetate and the remaining oxide/formvar rubbed into small rolls and inserted in a standard X-ray powder diffraction camera. Only Fe_3O_4 oxide was found (See Results). Similarly electron diffraction patterns on an identically prepared mild steel surface (removed by the standard extraction replica technique) confirmed the presence of Fe_3O_4.

3.3.1.3 $\alpha Fe_2O_3/Fe_3O_4$ Surface Oxide Formation

This was produced by heating the polished mild steel drums in an electrically heated air furnace for 45-60 minutes at (500°C) 873K. The blue interference colours were again indicative of the required oxide

thickness and X-ray and electron diffraction pattern analysis indicative of the expected $\alpha Fe_2C_3/Fe_3O_4$ oxide. (See Results).

3.3.2 Plastic Specimens

Samples of flat pressed P.V.C., chlorinated P.V.C., P.T.F.E., and P.C.T.F.E., were cut down from sheet, trimmed and prepared into microscope slide size (2.5 x 6.0 x 0.3 cm.) specimens ready for clamping in the wear-rig arm. Specific details for each sample were as follows:-

P.V.C.

Source: R.A.P.R.A. (P.S.C.C.) P.V.C.2.

Additives: 2% lead stearate stabiliser/lubricant* (dibasic)

Fabrication: Dry blended then hot pressed.

Formula:

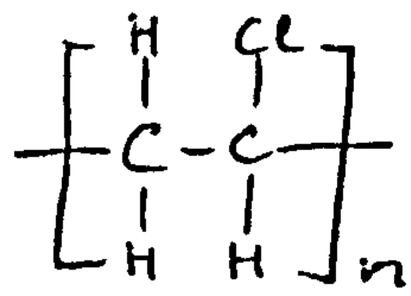

Cl^{d}P.V.C.

Source: British Traders and Shippers Ltd., Kanevinyl M.608.

Additives: 2% lead stearate stabiliser/lubricant* (dibasic)

Fabrication: Dry blended, roll mill 463K for 120s press 468K for 600s.

Formula:

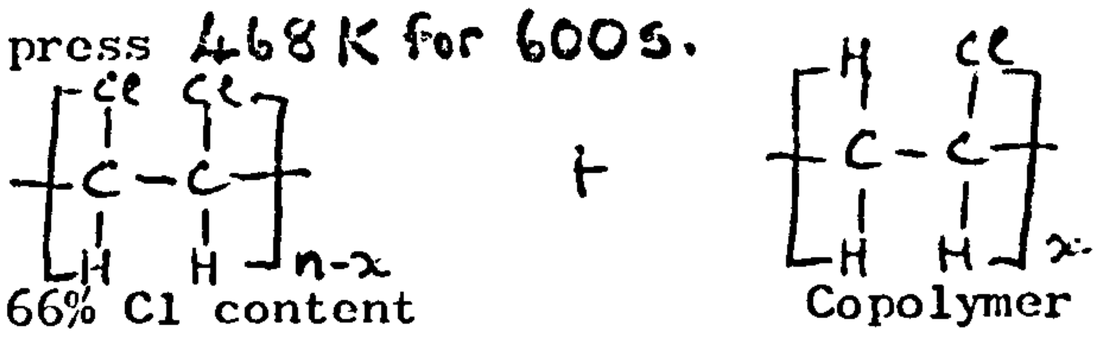

66% Cl content — Copolymer

P.T.F.E.

Source: G.H.Bloore/J. Klinger Co. Ltd., Permaflon DuPont Teflon.

Fabrication: Preformed in a press at 293°K then 2-3 hrs. in sintering oven at (360-390°C) 633-663K.

Formula:

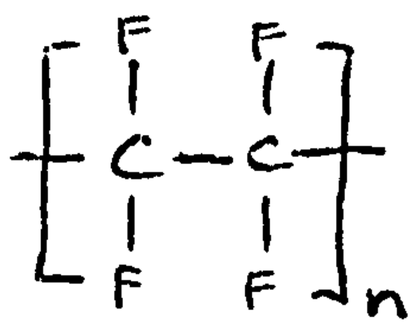

P.C.T.F.E.

Source: Fluorocarbons Co. Ltd., Voltalef 302 (Eugene Kuhlmann, France).

Fabrication: Heated press(274°C) 548K then quenched in cold water to increase amorphous content.

Formula:

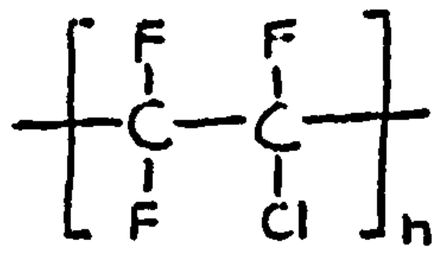

* Stabiliser must be added to these particular polymers[107] to reduce thermal degradation and inadequate flow effects during compression moulding. In these instances the minimum percentage of dibasic lead stearate was added (2%) to ensure a satisfactory moulding. Before each experiment the surfaces of the plastics were carefully cleaned with organic solvents such as 'analar' trichloroethylene to remove any traces of stabiliser that may have migrated to the surface. Although it would be practically impossible to remove every trace of contamination nevertheless I.R. absorption spectra of an unworn control sample of P.V.C. (APPENDIX 3) did not reveal any unexpected peaks that could be associated with significant amounts of stabiliser e.g. Control I.R. absorption analysis indicated that one might expect a small peak at $1510cm^{-1}$ when traces of dibasic lead stearate were present in P.V.C. (APPENDIX 3).

Dibasic lead stearate was chosen as the stabiliser in preference to lead stearate because in quantities $<3\%$ it does not generate stearic acid in the course of its stabilising action[107 (P.109)].

3.4 Experimental Procedure

3.4.1 Measurement of Polymer Wear Rate

The particular polymer samples were weighed on a five decimal place balance, clamped into a wear-rig arm and fitted in place above a suitably prepared mild steel drum. The required sliding velocity was selected by adjusting the motor pullies and checked with a revolution counter in contact with the drum surface. The correct static loading was applied by weights hung in the holder and checked by a spring balance connected momentarily to the centrally placed hook above the specimen. If required, the electric heater below the appropriate drums was switched on to heat the mild steel surface to the temperature required and checked with a thermocouple. Finally the drums were set in motion for ten minute intervals with weight measurements of the plastics taken each time. Any loose debris on plastic or metal was carefully removed with tweezers and stored in a specimen tube for gel permeation chromatography (G.P.C.) analysis, infra-red A.T.R. analysis or U.V. spectrometry analysis. Before each weighing the polymer surface was thoroughly cleaned with a dry tissue as experience showed that unless this was done trailing edge debris (no longer in the wear track) tended to promote erroneous results.

A series of 6 - 8 weight loss measurements were made for each polymer in each wearing situation over a period of 60 - 80 minutes. The experiment was repeated several times on different stations and different samples of the same specimen. Reproducibility of results was checked by a computer analysis (see results) and, if satisfactory, an average value of the wear rate, obtained in terms of weight loss in 10^{-3} kg per unit time of sliding in seconds. These values could easily be converted into alternative expressions of wear rate e.g. cm^3/cm by simple conversion factors involving specific gravities.

3.4.2 Analytical Techniques

A variety of analytical techniques were adopted both for the initial characterisation of materials and for the estimation of chemical and physical changes after being worn. Much of the procedure adopted was typical standard practice and so only unusual aspects will be elaborated at this point. (Full details may be found in the APPENDIX).

Analysis of the oxides on the mild steel countersurfaces were carried out by powder camera X-ray diffraction techniques with confirmation by electron diffraction. In the former case the oxides were removed by means of a plastic backing strip, (SEE SAMPLE PREPARATION AND ANALYSIS), rolled into thin rods and mounted directly into the apparatus. The intensity and spacing of the 'd' lines produced on the exposed photographic film were accurately determined using a Joyce microdensitometer and the data translated into qualitative and quantitative information about the oxide by reference to A.S.T.M. powder diffraction files. Confirmation of these results were achieved by taking electron diffraction photographs of the same oxides this time removed using carbon extraction replicas. Once again use of the microdensitometer and A.S.T.M. powder files led to positive identification of the oxides involved.

Estimates of the relative oxide hardnesses were made using a standard Vickers Micro-Hardness Indenter in conjunction with an M55 microscope. Flat specimens of the same mild steel material as the drums were used and subjected to the same heat treatment. As is discussed elsewhere (see APPENDIX 8)caution was exercised in the interpretation of results because of thinness of the oxide layer in comparison with the depth of penetration.

As the P.V.C. experiments proceded some of the loose wear debris pushed out of the wear track was examined by infra-red attenuated total reflectance spectrophotometry. The samples were mounted on adhesive backed tape with the side that had slid against the mild steel 'sandwiched' against the prism. Further details such as infra-red incidence angles, energies and estimated depths of penetration etc., etc., are found in APPENDIX 3 along with the spectra obtained.

Other pieces of P.V.C. wear debris were collected and 1.0% tetrahydrofuran solutions made up ready for ultraviolet spectrophotometry. Once again simple absorption spectra were obtained and compared to control samples.

Wear debris from both the P.V.C. and Cl^{d}P.V.C. samples were also subjected to gel permeation chromatography. This involved the preparation of 0.2% tetrahydrofuran solutions and passing them through a column containing calibrated polystyrene gel. (It is important to note that in the present work both the P.V.C. and the Cl^{d}P.V.C. samples were totally soluble in the T.H.F. indicating that little or no cross-linking had occurred at the polymer sliding interface). The rate of passage through the columns was dependent on the particular molecular weight of individual molecules. Thus the apparatus automatically plots concentration versus elution volume graphs and estimates of the molecular weight distribution and the various average molecular weights can be calculated using the appropriate mathematical conversion factors (see RESULTS/DISCUSSION and APPENDIX 2).

3.5 Results/Discussion

3.5.1 Introduction and Presentation of Experimental Data

The presentation of results has been so arranged as to allow easy cross reference with the corresponding interpretation developed in the discussion. It must be borne in mind that whilst performing the central basic experiments of sliding certain flat pieces of polymer against various revolving mild steel cylinders, two basic questions have been posed.

(1) How are the polymers physically and chemically degrading in relation to the changing sliding conditions?

(2) How do the polymer wear rates correlate to the changing sliding conditions?

The results therefore reflect this basic philosophy and fall into three groupings. The first two involve data from experiments directly concerned with answering questions (1) and (2) and the third a glossary of more general, ancillary information. The presentation may be categorised as follows:-

1. Analyses Connected With the Polymer Degradation Process During Sliding.

   1.1 Gel permeation chromatography

   1.2 Infra-red attenuated total reflectance absorption spectrophotometry

   1.3 Ultra-violet absorption spectrophotometry

   1.4 Macro and micro optical examination of surfaces.

2. Measurements of polymer wear rate during sliding on mild steel and oxide countersurfaces.

3. Ancillary analyses of materials

3.1 X-ray and electron diffraction

3.2 Vickers Micro-Hardness Testing

3.3 Differential scanning calorimetry

3.5.1.1 Analyses Connected With The Polymer Degradation Process During Sliding.

3.5.1.1.1 Gel Permeation Chromatography.

Only molecular weight analyses of P.V.C. and Cl^{d}P.V.C. were carried out due to the practical problems that would have been associated with finding suitable solvents for P.T.F.E. and P.C.T.F.E. Thus the gel permeation chromatography analyses of debris emanating from the wear scars of P.V.C. and Cl^{d}P.V.C. sliding on mild steel cylinders are presented in TABLE 1. The numbers in the first column identify the particular experiment followed by a brief description of the wearing system involved. Unless otherwise stated the polymer flats were sliding at $1.44 ms^{-1}$ on mild steel cylinders polished to 0.076μm (c.l.a.) surface finish, carrying a nominal 2-14 nm Fe_3O_4 oxide, and with a normal loading of 8.83 N e.g. experiment 10 involved P.V.C. sliding under the conditions just mentioned except that the mild steel cylinder had been heat treated in a vacuum furnace producing an approximately 100nm thick Fe_3O_4 countersurface (see sample preparation section). The next two major columns tabulate the number average molecular weights (definitions given in the discussion) of the polymers before $[(\bar{M}n)_v]$ and after $[(\bar{M}n)]$ the sliding experiments. The further sub division into parts A and B refer to the particular G.P.C. column the results were obtained from(details of the difference between the two are outlined in APPENDIX 2.)

It is sufficient to mention that only measurements from the same

G.P.C. column should be used for individual comparisons. Next are listed the $\left[\frac{(M\bar{n})}{(M\bar{n})_v}\right]$ ratios which give an indication of the fraction of the original number average molecular weights the polymer had been reduced to after each experiment. Finally the ratio between the various individual number average ($M\bar{n}$), weight average ($M\bar{w}$) and 'Z' average ($M\bar{z}$) molecular weights are presented in the last four sections thus allowing an estimate to be made of the degree of molecular weight spread (polydispersion) of the individual molecules contributing to the 'averaged' molecular weights (see DISCUSSION). For simplification, some of the information presented in TABLE 1. has been drawn in histogram form in FIG. 7. allowing an immediate appreciation of the relation between certain experimental parameters and the change in the average polymer molecular weight of the wear debris. The polymer type is indicated below each block of rectangles with the parameters being changed listed immediately above. Unless otherwise stated all other experimental conditions were as described for TABLE 1.

TABLE 1

A SYNOPSIS OF THE G.P.C. M.WT. ANALYSES OF POLYMERS AFTER SLIDING ON TREATED MILD STEEL.

EXPT. NOS	WEARING SYSTEM	ORIGINAL M.WT. (POLYMER) $\bar{M}_n$ G.P.C. COLUMN A	ORIGINAL M.WT. (POLYMER) $\bar{M}_n$ G.P.C. COLUMN B	DEBRIS M.WT. (POLYMER) $\bar{M}_n$ G.P.C. COLUMN A	DEBRIS M.WT. (POLYMER) $\bar{M}_n$ G.P.C. COLUMN B	$\bar{M}_n$ [A] ($\bar{M}_n$)	$\bar{M}_n$ [B] ($\bar{M}_n$)	ORIGINAL (A) N:W:Z	ORIGINAL (B) N:W:Z	DEBRIS (A) N:W:Z	DEBRIS (B) N:W:Z
5.	P.V.C. | M.S.	31200	37000	17450	18700	0·56	0·51	1:30:23·5	1:291:7·86	1:214:4·30	1:2·21:4·63
6	P.V.C. | M.S.	31200	37000	17450	18700	0·56	0·51	1:30:23·5	1:291:7·86	1:214:4·30	1:2·21:4·63
7.	P.V.C. | M.S. (Air furnace)	31200	37000	14150	15400	0·45	0·42	1:30:23·5	1:291:7·86	1:192:3·85	1:2·1:4·28
8.	P.V.C | M.S (Air furnace)	31200	37000	14150	15400	0·45	0·42	1:30:23·5	1:291:7·86	1:192:3·86	1:2·1:4·28
9.	P.V.C. | M.S. (Vacuum Furnace)		38100		15700		0·41		1:30:8·5		1:2·5:5·35
10.	P.V.C. | M.S. (Vacuum Furnace)		38100		15700		0·41		1:30:8·5		1:2·5:5·35
25	P.V.C. | M.S ($2·88\ ms^{-1}$)		33500		22000		0·66		1:30:7·1		1:2·2:4·2
26.	P.V.C | M.S. ($2·88\ ms^{-1}$)		33500		22000		0·66		1:30:7·1		1:2·2:4·2
27.	P.V.C. | M.S. ($5·33\ ms^{-1}$)		33500		24500		0·73		1:30:7·1		1:2·5:5·1
28.	P.V.C. | M.S ($5·33\ ms^{-1}$)		33500		24500		0·73		1:30:7·1		1:2·5:5·1
29.	P.V.C | M.S. ($\overset{3·93N}{400g}$)	35600		18300		0·51		1:2·8:140		1:1·9:3·4	
30	P.V.C. | M.S ($\overset{3·93N}{400g}$)	35600		18300		0·51		1:2·8:140		1:1·9:3·4	
31.	P.V.C. | M.S ($\overset{3·93N}{400g}$)	35600		18300		0·51		1:2·8:140		1:1·9:3·4	
32.	P.V.C | M.S ($\overset{3·93N}{400g}$)	35600		18300		0·51		1:2·8:140		1:1·9:3·4	
33	Cl^{d} P.V.C | M.S (Vac furnace)	34500		11200		0·33		1:2·2:4·7		1:1·7:3·1	

TABLE 1 (Contd.)

EXPT. NOS	WEARING SYSTEM	ORIGINAL MWT. (POLYMER) $\bar{M}_v$ G.P.C. COLUMN A	ORIGINAL MWT. (POLYMER) $\bar{M}_v$ G.P.C. COLUMN B	DEBRIS MWT. (POLYMER) $\bar{M}$ G.P.C. COLUMN A	DEBRIS MWT. (POLYMER) $\bar{M}$ G.P.C. COLUMN B	$\bar{M}$ [A] $(\bar{M}\bar{a})_v$	$\bar{M}$ [B] $(\bar{M}\bar{a})_v$	ORIGINAL [A] n:W:Z	ORIGINAL [B] n:W:Z	DEBRIS [A] n:W:Z	DEBRIS [B] n:W:Z
34.	Cl^d P.V.C. / M.S. (Vac. furnace)	34500		11200		0·33		1:2·2:4·7		1:1·7:3·1	
35.	Cl^d P.V.C. / M.S. (Air furnace)	34500		12800		0·37		1:2·2:4·7		1:1·9:8·2	
36.	Cl^d P.V.C. / M.S (Air furnace)	34500		12800		0·37		1:2·2:4·7		1:1·9:8·2	
43.	P.V.C. / MS ($1600_{9}^{15·7\,N}$)	35600		18100		0·50		1:2·8:140		1:2·2:39	
44.	P.V.C / MS ($1600_{9}^{15·7\,N}$)	35600		18100		0·50		1:2·8:140		1:2·2:39	
45.	Cl^d P.V.C. / M.S.	34500		18900		0·55		1:2·2:4·7		1:1·5:2·4	
46.	Cl^d P.V.C. / MS.	34500		18900		0·55		1:2·2:4·7		1:1·5·2·4	
47.	P.V.C / M.S. (346–363K)	29 593		24458		0·83		1:2·7:6·7		1:2·0:3·9	
48.	P.V.C / MS (308–323K)	29 593		18045		0·61		1:2·7:6·7		1:2·0:3·7	

FIG 7.

MOLECULAR WEIGHT (M_n) STUDIES OF POLYMER WEAR DEBRIS AFTER SLIDING ON MILD STEEL.

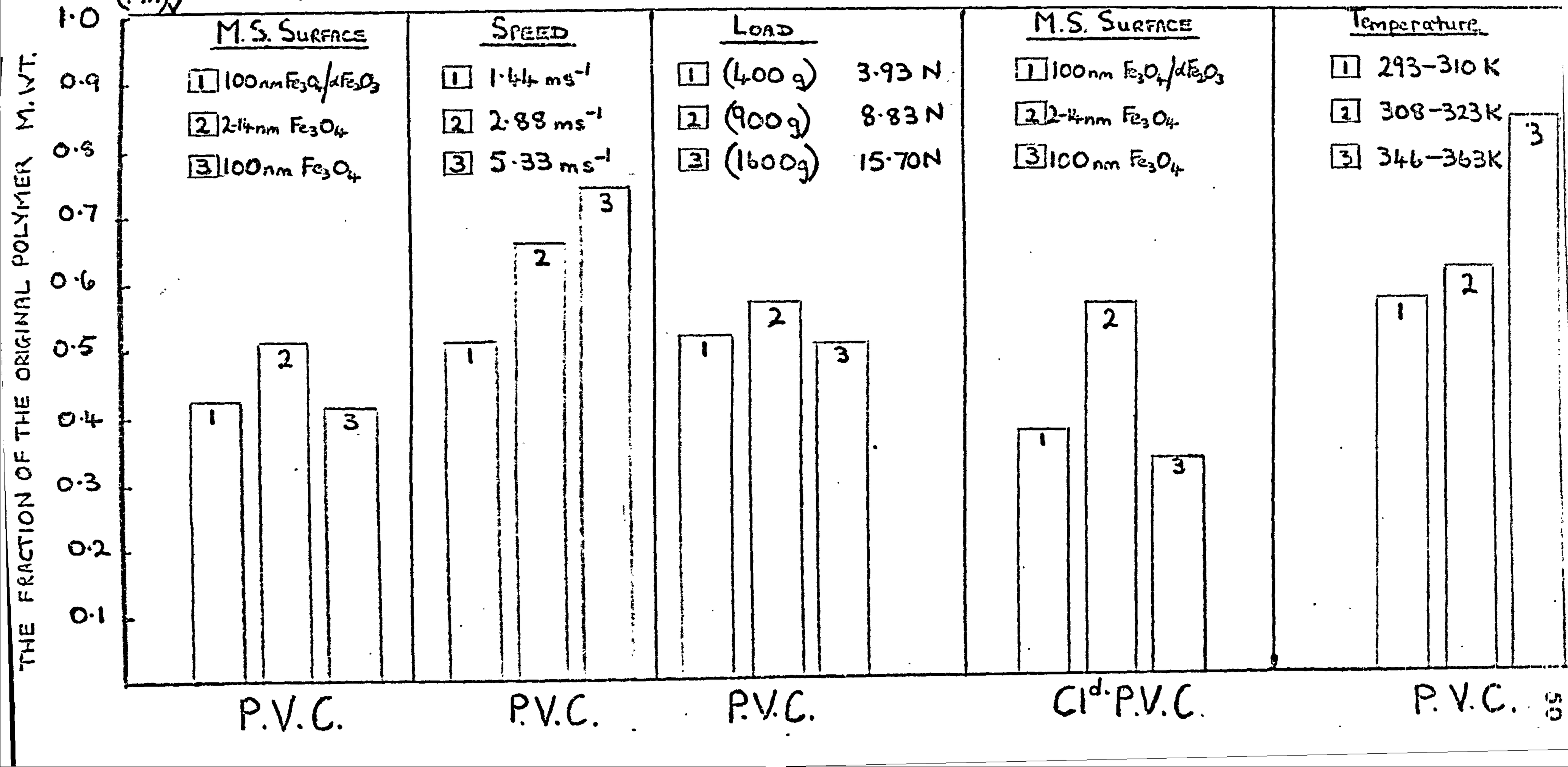

3.5.1.1.2 Infra-red attenuated total reflectance absorption spectrophotometry.

Individual A.T.R. graphs of the surface of P.V.C. before and after being worn are collated in the appendix. The most salient features of the absorption spectra are presented in TABLE 2. After quoting the debris code number (allowing comparison with graphs in APPENDIX 3.) a brief description of each system is given. Once again unless otherwise stated the experimental conditions were as quoted earlier in TABLE 1. The next three columns detail the wavenumbers where significant changes have occurred in the individual absorption spectra. An example is the occurrence of a new 1380 cm^{-1} peak with almost all the worn P.V.C. samples. This is illustrated further in FIG.8.

TABLE 2.

A synopsis of the significant features of the infra-red (A.T.R.) analysis of polymeric debris after P.V.C. had slid on conditioned mild steel.

DEBRIS CODE	WEARING SYSTEM	ABSORPTION CHARACTERISTICS		
		NEW PEAKS	INCREASED PEAKS	DECREASED PEAKS
D_1	P.V.C./MILD STEEL	1380 cm^{-1}	2950 cm^{-1}	—
D_2	P.V.C./VACUUM FURNACE OXIDE	1380 cm^{-1}	—	—
D_3	P.V.C./AIR FURNACE OXIDE	1380 cm^{-1}	2950 cm^{-1}	1339 cm^{-1}
D_{13}	P.V.C./M.S. (15.7N (1600g))	1380 cm^{-1}	2950 cm^{-1}	—
D_{14}	P.V.C./M.S (3.93N (400g))	1380 cm^{-1}	2950 cm^{-1}	1255 cm^{-1}
D_{15}	P.V.C./M.S. (2.88 ms^{-1})	1380 cm^{-1}	2950 cm^{-1}	1255 cm^{-1}
D_{16}	P.V.C/MS (5.33 ms^{-1})	1380 cm^{-1}	2950 cm^{-1}	—

FIG.8.
An example of the change in infra-red absorption characteristics of the surfaces and debris on P.V.C. after sliding on mild steel.(See also APPENDIX 3)

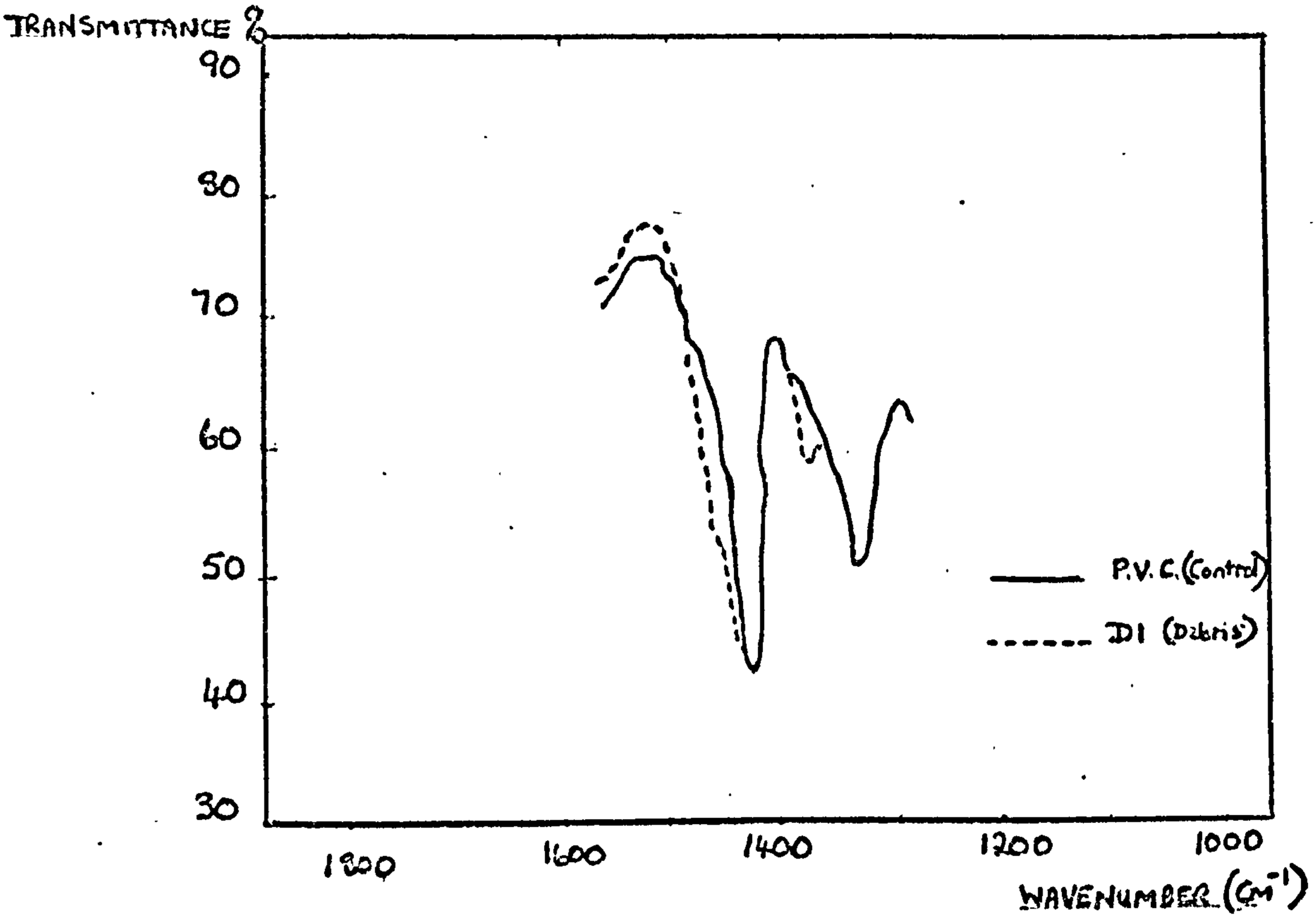

3.5.1.1.3 Ultra-violet absorption spectrophotometry

The original U.V. spectrophotometry absorbance spectra of P.V.C. samples before and after being worn are collated in the appendix. A summary of the most important features are listed in TABLE 3. After defining the conditions of measurement e.g. initial concentration of P.V.C. in solvent etc., the relative % absorbance values at wavelengths 254nm and 293nm are compared and general remarks recorded in the final column.

TABLE 3.

A synopsis of the ultra violet absorption characteristics of polymeric (PVC) debris after sliding on mild steel.
(See also APPENDIX 4).

SAMPLE	INITIAL CONCN.	SOLVENT	PATH LENGTH	ABSORBANCE		RATIO $\frac{A_{293}}{A_{254}}$	REMARKS.
				(λ) 254nm	(λ) 293 nm		
1. P.V.C. CONTROL	1·0%	T.H.F.	1cm	0·66	0·43	0·65	
2. THERMALLY DEGRADED P.V.C. (HEATED TO 500K OVER 2HRS. THEN COOLED OVER 2HRS)	1·0%	T.H.F.	1cm	0·78	0·87	1·11	THE PEAK INTENSITY AT 293 nm HAS CONSIDERABLY INCREASED RELATIVE TO THE 254nm PEAK.
3. P.V.C. WEAR DEBRIS (P.V.C./M.S. 30' (900g) 8·83N 1·44 ms^{-1})	1·0%	THF.	1cm	0·41	0·36	0·88	THE PEAK INTENSITY AT 293nm HAS CONSIDERABLY INCREASED RELATIVE TO THE 254nm PEAK BUT NOT TO THE SAME EXTENT AS SAMPLE 2.
4. SOLVENT (TETRAHYDROFURAN)	—	—	1cm	—	—	—	NO OBSERVABLE ABSORBANCE PEAKS 200–400 nm

3.5.1.1.4 Macro and Micro optical examination of worn surfaces.

As each wear experiment was performed a record was kept of all the visible changes occurring at interface. Where necessary optical microscopy was used to examine the process more carefully. A summary of this record is presented in TABLE 4. and includes a final column of photographic figure numbers for cross-reference. The process of identification of thin polymer transfer films that sometimes formed on the mild steel countersurfaces was amplified by a new 'interference colour' technique described later in APPENDIX 5. and exemplified in FIGS. 37, 44.

A summary of the macro and micro optical examination of worn surfaces.

TABLE 4.

EXPT. CODE NOS.	WEARING SYSTEM	CHANGES AT THE PLASTIC/METAL INTERFACE	FIG. NOS.
1,2,5,6,11, 12	PVC/MS	Initially loose brown flakes of polymer debris speckled with areas of black appeared, progressing finally (1 hour) to strips of transferred material 4.0 cms x 2.0 m.m x 5.0 μm.	APPENDIX 5
9,10	PVC/MS (VAC.FURNACE)	Surrounding metal areas visibly polished after only 10m sliding. Larger amounts of transferred polymer appeared on the drums than for other P.V.C/MS sliding combinations and each strip reached a maximum dimensions of 3.5 cms x 3.0 mm x 5.0 μm. Where the drum oxide was broken (in 3 mm strips) reciprocal blackening of the P.V.C. was observed due to abraded and embedded oxide.	11-13 28-30 34
3,4,7,8	PVC/MS (AIR FURNACE)	The oxide surface stayed mainly unmarked apart from a small brown band of 3 mm wide transferred polymer film that could be dissolved away with T.H.F. solvent. The reciprocal polymer surface contained shiny smooth bands in the direction of sliding suggesting localised melting. In the relatively rare occurrence of the oxide fracturing a brown strip was promoted on the mating plastic area. Polymer debris collected on the edge of the metal wear, scar and in some cases contained a red coloration.	14-16 31-33 35 36

TABLE 4 (Contd.)

EXPT. CODE NOS.	WEARING SYSTEM	CHANGES AT THE PLASTIC/METAL INTERFACE	FIG. NOS.
25, 26	P.V.C/MS (2.88 ms^{-1})	Long transferred streaks of polymer appeared on the metal drum after 30 min. These were typically shaped like 2.0 cms x 2 mm equilateral triangles with the apex leaving the interface site last. There was also some evidence of minute specks of transferred metal in the polymer during the first few minutes of sliding.	
27, 28	P.V.C/MS (5.33 ms^{-1})	Ditto	
29-32	P.V.C/MS (400 g)	Small strips of adhering debris began to appear on the metal drums after 100 min.	
43, 44	P.V.C/MS (1600 g)	Small strips of adhering debris began to appear on the metal drums after 30 min.	
45, 46	Cl^{d}P.V.C./MS	After 10 -20 min sliding fine specks of transferred polymer appeared on the drums, leading to extensive square flaky deposits after 20 -30 min. Longer, streaky transferred fragments were generated after 30 -70 min. When the transferred material was removed the light brown tinge remaining on the metal was tested with potassium ferri and ferro cyanide for traces of any iron salts generated, but none were found.	
33, 34, 37-40	Cl^{d}P.V.C/M.S (Vacuum Furnace)	Two types of transfer phenomena were observed correlatable to either high or low wear rates. Low transfer was associated with low wear rate and extensive patchy transfer with a higher wear rate. In the latter case a brown line first developed on the steel progressing to transferred polymer patches 1.0 x 0.3 cms. in dimension.	

TABLE 4 (Contd.)

EXPT. CODE NOS.	WEARING SYSTEM	CHANGES AT THE PLASTIC/METAL INTERFACE	FIG. NOS.
35, 36	Cl^{d} P.V.C/M.S (Air Furnace)	Very little transfer of the polymer occurred or rupture of the oxide surface.	
11, 12	P.T.F.E/M.S.	After 10min sliding powdery flakes of P.T.F.E. 3 mm square were transferred to the steel drum. As the experiment progressed the polymer became increasingly polished and eventually developed eight grooves approximately 0.5 mm diameter, and 0.1 mm deep in the direction of sliding. There was some evidence that at the end of the run a very fine smeared film of polymer had appeared on the drum but this did not occur on every occasion.	37
15, 16	P.T.F.E./M.S (Vacuum Furnace)	After 10-45min sliding the oxide began to rupture and lumpy smeared deposits of P.T.F.E. were observable on both the intact and removed areas of drum surface. Oxide fragments were found embedded in the P.T.F.E., surface at the end of the experiment.	38-40
13, 14	P.T.F.E./M.S (Air Furnace)	Much less polymer transfer occurred than on the vacuum furnace oxide surface. That which did appear was preceded by flaky deposits developing later into thin smeared ribbons. The P.T.F.E. became polished during the experiment and only slightly grooved in three or four places. Very little oxide was observably embedded in the P.T.F.E. at the conclusion of the run.	41
17-20	P.C.T.F.E./M.S.	After 10min polymer debris was adhering to the steel drum in short semi-continuous smeared ribbons.	42-44

TABLE 4 (Contd.)

EXPT. CODE NOS.	WEARING SYSTEM	CHANGES AT THE PLASTIC/METAL INTERFACE	FIG. NOS.
21, 22	P.C.T.F.E./M.S. (Vacuum Furnace)	Little observable polymer transfer to drum.	
23, 24	P.C.T.F.E./M.S. (Air Furnace)	Polymer transfer to drum almost entirely inhibited.	

3.5.1.2 Measurements of Polymer Wear Rate During Sliding on Mild Steel and Oxide Countersurfaces.

TABLE 5. lists the measured wear rate values for different types of polymer flat in loaded sliding interaction with various types of rotating mild steel cylinder. Experimental code numbers are presented in the first column followed by the wear station identification letter i.e. A, B, C or D, (further details are given in Apparatus and Experimental Procedure Sections). Reading horizontally, information is presented about both the type and nature of the polymer flats and the metal countersurfaces used in the experiments followed in the next two columns by the applied relative sliding speeds and loadings. Next the average wear rates are recorded for individual experiments and finally the appropriate overall mean values for where the same experiment had been performed at different wear stations e.g. the average wear rate for P.C.T.F.E. on 2-14nm Fe_3O_4 oxide, under the conditions described in experiments 17-20 where the measurements were carried out twice on each of two different stations (C and D), was $2.07 \times 10^{-9} cm^3/cm$.

It must be noted that the wear rateslisted correspond to the computer averaged values of the slopes of the polymer wear curves(See APPENDIX 6) 'appropriately converted from gs^{-1} to cm^3/cm . The correlation coefficients for each set of results from individual wear experiments (APPENDIX 6) are expressed in TABLE 6 along with the calculated standard t-test significance values for comparisons of similar experiments performed at different wear stations.

For simplicity the most salient features of TABLE 5 have been further presented in histogram form in FIG. 9. thus allowing

easier comparisons of wear rate. Beneath each block of rectangles A-F is indicated the polymer type and above each block the pertinent metal oxide countersurface or wearing conditions that were being varied and examined for their effect on polymer wear rate. Unless otherwise stated the experiments may be regarded as having been carried out on mild steel cylinders under the same experimental conditions as described for TABLF 1. e.g. block B in FIG. 9. gives a graphical comparison of wear rates of P.V.C. sliding on mild steel cylinders under the conditions just implied except that the load was varied between 3.93 - 8.83 - 15.70 N (400 - 900 - 1600g).

A tabulation of the materials and conditions adopted for the wear experiments and the subsequent wear rates recorded. The mild steel countersurface may be considered as having an initial surface finish of 0.076μm and an initial surface temperature of 293 K.

TABLE 5.

EXPERIMENT CODE NOS	WEAR STATION	POLYMER FLAT			MILD STEEL COUNTERSURFACE	SPEED (ms^{-1})	LOAD (N)	WEAR RATE ($cm^3\,cm^{-1}$)	AVERAGE ($cm^3\,cm^{-1}$)
		TYPE	T_g (K)	T_m (K)					
1	A	P.V.C	356		2-14nm Fe_3O_4	1·44	8·83	59×10^{-9}	7.26×10^{-9}
2	B	P.V.C.	356		2-14nm Fe_3O_4	1·44	8·83	8.62×10^{-9}	
3	A	P.V.C.	356		100nm $Fe_3O_4/\alpha Fe_2O_3$	1·44	8·83	1.12×10^{-8}	9.21×10^{-9}
4	B	P.V.C.	356		100nm $Fe_3O_4/\alpha Fe_2O_3$	1·44	8·83	7.23×10^{-9}	
5	C	P.V.C.	356		2-14nm Fe_3O_4	1·44	8·83	6.50×10^{-9}	6.62×10^{-8}
6	D	P.V.C.	356		2-14nm Fe_3O_4	1·44	8·83	6.75×10^{-9}	
7	C	P.V.C.	356		100nm $Fe_3O_4/\alpha Fe_2O_3$	1·44	8·83	1.25×10^{-8}	1.10×10^{-8}
8	D	P.V.C.	356		100nm $Fe_3O_4/\alpha Fe_2O_3$	1·44	8·83	9.45×10^{-9}	
9	C	P.V.C.	356		100nm Fe_3O_4	1·44	8·83	6.90×10^{-9}	6.77×10^{-9}
10	D	P.V.C.	356		100nm Fe_3O_4	1·44	8·83	6.65×10^{-9}	
11	C	P.T.F.E.		603	2-14nm Fe_3O_4	1·44	8·83	4.88×10^{-8}	4.90×10^{-8}
12	D	P.T.F.E.		603	2-14nm Fe_3O_4	1·44	8·83	4.92×10^{-8}	
13	C	P.T.F.E.		603	100nm $Fe_3O_4/\alpha Fe_2O_3$	1·44	8·83	4.22×10^{-8}	4.03×10^{-8}
14	D	P.T.F.E.		603	100nm $Fe_3O_4/\alpha Fe_2O_3$	1·44	8·83	3.83×10^{-8}	
15	C	P.T.F.E		603	100nm Fe_3O_4	1·44	8·83	4.29×10^{-8}	$3.9\% \times 10^{-8}$

TABLE 5. (Contd.)

EXPERIMENT CODE NOS	WEAR STATION	POLYMER FLAT			MILD STEEL COUNTERSURFACE	SPEED (ms^{-1})	LOAD (N)	WEAR RATE ($cm^3\,cm^{-1}$)	AVERAGE ($cm^3\,cm^{-1}$)
		TYPE	T_g (K)	T_m (K)					
16	D	P.T.F.E.		603	100nm Fe_3O_4	1·44	8·83	3.63×10^{-5}	3.96×10^{-5}
17	C	P.C.T.F.E.		484	2-14nm Fe_3O_4	1·44	8·83	2.15×10^{-9}	2.07×10^{-9}
18	D	P.C.T.F.E.		484	2-14nm Fe_3O_4	1·44	8·83	2.00×10^{-9}	
19	C	P.C.T.F.E		484	2-14nm Fe_3O_4	1·44	8·83	2.13×10^{-9}	
20	D	P.C.T.F.E.		484	2-14nm Fe_3O_4	1·44	8·83	2.00×10^{-9}	
21	C	P.C.T.F.E.		484	100nm Fe_3O_4	1·44	8·83	7.63×10^{-10}	5.70×10^{-10}
22	D	P.C.T.F.E.		484	100nm Fe_3O_4	1·44	8·83	9.77×10^{-10}	
23	C	P.C.T.F.E.		484	100nm Fe_3O_4 / αFe_2O_3	1·44	8·83	8.00×10^{-10}	7.96×10^{-10}
24	D	P.C.T.F.E.		484	100nm Fe_3O_4 / αFe_2O_3	1·44	8·83	7.92×10^{-10}	
25	C	P.V.C.	356		2-14nm Fe_3O_4	2·88	8·83	1.07×10^{-5}	1.07×10^{-5}
26	D	P.V.C.	356		2-14nm Fe_3O_4	2·88	8·83	1.07×10^{-8}	
27	C	P.V.C.	356		2-14nm Fe_3O_4	5·33	8·83	1.26×10^{-8}	8.94×10^{-9}
28	D	P.V.C.	356		2-14nm Fe_3O_4	5·33	8·83	7.62×10^{-9}	
29	C	P.V.C.	356		2-14nm Fe_3O_4	1·44	3·93	3.51×10^{-9}	2.51×10^{-9}
30	D	P.V.C.	356		2-14nm Fe_3O_4	1·44	3·93	1.51×10^{-9}	

TABLE 5. (Cont^{d}).

EXPERIMENT CODE NOS	WEAR STATION	POLYMER FLAT			MILD STEEL COUNTERSURFACE	SPEED (ms^{-1})	LOAD (N)	WEAR RATE ($cm^3\,cm^{-1}$)	AVERAGE ($cm^3\,cm^{-1}$)
		TYPE	T_g (K)	T_m (K)					
31	C	P.V.C.	356		2-14 nm Fe_3O_4	1·44	3·93	2.05×10^{-9}	2.51×10^{-9}
32	D	P.V.C.	382		2-14 nm Fe_3O_4	1·44	3·93	1.59×10^{-9}	
33	C	Cl^{d} P.V.C.	382		100nm Fe_3O_4	1·44	8·83	4.41×10^{-9}	5.16×10^{-9}
34	D	Cl^{d} P.V.C.	382		100nm Fe_3O_4	1·44	8·83	5.90×10^{-9}	
35	C	Cl^{d} P.V.C	382		100nm Fe_3O_4 / αFe_2O_3	1·44	8·83	2.12×10^{-9}	2.10×10^{-9}
36	D	Cl^{d} P.V.C.	382		100nm Fe_3O_4 / αFe_2O_3	1·44	8·83	2.08×10^{-9}	
37	C	Cl^{d} P.V.C	382		100nm Fe_3O_4	1·44	8·83	(TRANSFER) 5.76×10^{-9}	7.49×10^{-9}
38	C	Cl^{d} P.V.C.	382		100nm Fe_3O_4	1·44	8·83	(NO TRANSFER) 3.05×10^{-9}	2.81×10^{-9}
39	D	Cl^{d} P.V.C.	382		100nm Fe_3O_4	1·44	8·83	(NO TRANSFER) 2.56×10^{-9}	
40	D	Cl^{d} P.V.C.	382		100nm Fe_3O_4	1·44	8·83	(TRANSFER) 9.22×10^{-9}	7.49×10^{-9}
43	C	P.V.C.	356		2-14nm Fe_3O_4	1·44	15·70	9.9×10^{-9}	9.21×10^{-9}
44	D	P.V.C.	356		2-14nm Fe_3O_4	1·44	15·70	8.51×10^{-9}	
45	C	Cl^{d} P.V.C.	382		2-14nm Fe_3O_4	1·44	8·83	2.19×10^{-8}	2.25×10^{-8}
46	D	Cl^{d} P.V.C.	382		2-14nm Fe_3O_4	1·44	8·83	2.31×10^{-8}	

A summary of the statistical analysis and significance of the wear rates of polymer flats sliding against conditioned mild steel cylinders.

TABLE 6 (See also TABLE 5 and APPENDIX 6)

EXPT. CODE NOS	WEARING SYSTEM		CORRELATION COEFFICIENT	DEGREES OF FREEDOM	T	T-TEST SIGNIFICANCE	REMARKS
1	P.V.C./M.S.	A*	0·835	36	2·32	2-5%	SIGNIFICANT
2	P.V.C./M.S.	B	0·937				
3	P.V.C./M.S. (A.F.O.)*	A	0·981	34	3·00	0·2-1·0%	HIGHLY SIGNIFICANT
4	P.V.C./M.S. (AFO.)	B	0·829				
5	P.V.C./M.S.	C	0·992	20	0·36	72.5%	NO SIGNIFICANCE
6	P.V.C/M.S.	D	0·971				
7	P.V.C./M.S. (A.F.O.)	C	0·978	22	3·11	0·2-1·0%	HIGHLY SIGNIFICANT
8	P.V.C./M.S. (AFO.)	D	0·978				
9	P.V.C./M.S. (V.F.C.)	C	0·969	44	0·35	>25%	NO SIGNIFICANCE
10	P.V.C./M.S. (V.F.C.)	D	0·951				
11	PTFE/M.S.	C	0·991	32	0·21	72.5%	NO SIGNIFICANCE
12	PTFE/MS.	D	0·999				
13	PTFE/M.S. (A.F.O.)	C	0·994	32	1·30	10-25%	SLIGHT SIGNIFICANCE
14	PTFE./M.S. (AFO)	D	0·961				
15	PTFE./M.S. (V.F.O.)	C	0·998	20	6·05	0·1%	V. HIGHLY SIGNIFICANT
16	PTFE/M.S. (V.F.O)	D	0·998				
17	PCTFE/M.S.	C	0·728	20	0·17	>25%	NO SIGNIFICANCE
18	PCTFE/M.S.	D	0·722				
19	PCTFE./MS	C	0·982	20	0·52	>25%	NO SIGNIFICANCE
20	PCTFE/MS.	D	0·958				
21	PCTFE/M.S. (V.F.O.)	C	0·964	20	1·87	5-10%	SLIGHT SIGNIFICANCE
22	PCTFE/MS (V.F.O)	D	0·956				
23	PCTFE./M.S. (A.F.O.)	C	0·765	20	0·03	>25%	NO SIGNIFICANCE
24	PCTFE/MS (AFO)	D	0·945				
1	P.V.C./M.S.	A	0·835	35	4·85	<0·1%	V. HIGHLY SIGNIFICANT
3	P.V.C./M.S. (AFO.)	A	0·981				

TABIE 6 (Contd.)

EXPT CODENCS	WEARING SYSTEM	CORRELATION COEFFICIENT	DEGREES OF FREEDOM	T	T-TEST SIGNIFICANCE	REMARKS
25	P.V.C. | M S ($0.95 ms^{-1}$) C	0·995	20	0·09	> 25%	NO SIGNIFICANCE
26	P.V.C. | M S ($2·88 ms^{-1}$) D	0·996				
27	P.V.C. | M S ($5·33 ms^{-1}$) C	0·979	19	2·67	1·0–2·0%	SIGNIFICANT
28	P.V.C | M S ($5·33 ms^{-1}$) D	0·830				
25	P.V.C. | M·S ($2·88 ms^{-1}$) C	0·995	19	8·45	< 0·1%	V. HIGHLY SIGNIFICANT
27	P.V.C. | M.S ($5·33 ms^{-1}$) C	0·979				
26	P.V.C | M S ($2·88 ms^{-1}$) D	0·996	20	1·36	10–25%	SLIGHT SIGNIFICANCE
28	P.V.C. | M S ($5·33 ms^{-1}$) D	0·830				
29	P.V.C. | M S. (3·93N) C	0·958	28	5·73	< 0·1%	V. HIGHLY SIGNIFICANT
30	P.V.C. | M S. (3·93N) D	0·880				
31	P.V.C. | M.S. (3·93N) C	0·956	16	1·56	10–25%	SLIGHT SIGNIFICANCE
32	P.V.C. | M S (3·93N) D	0·941				
33	Cl^{d} P.V.C. | M S. (V.F.O.) C	0·896	20	0·82	> 25%	NO SIGNIFICANCE
34	Cl^{d} P.V.C | M S (V F O) D	0·740				
35	Cl^{d} P.V.C. | M.S (A.F.O.) C	0·792	20	0·05	> 25%	NO SIGNIFICANCE
36	Cl^{d} P.V.C. | M.S (A F O) D	0·853				
29	P.V C. | M.S. (3·93N) C	0·958	22	3·73	0·1–0·2%	HIGHLY SIGNIFICANT
31	P.V.C. | M.S (3·93N) C	0·956				
30	P.V.C. | M.S. (3·93N) D	0·880	22	0·32	0·2–0·1%	HIGHLY SIGNIFICANT
32	P.V.C. | M S (3·93N) D	0·941				
33	Cl^{d} P.V.C. | M S (V F O) C	0·896	20	2·67	1·0–2·0%	SIGNIFICANT
35	Cl^{d} P.V.C. | M.S (A F O) C	0·792				
34	Cl^{d} P.V.C. | M.S (V F O) D	0·740	20	2·22	2·0–5·0%	SIGNIFICANT
36	Cl^{d} P.V.C | M.S (A F O) D	0·853				
37	Cl^{d} P.V.C. | M.S (V.F.O.) C	0·990	8	3·89	1·0–2·0%	SIGNIFICANT
40	Cl^{d} P.V.C. | M S (V F O) D	0·995				

TABLE 6 (Contd.)

EXPT. CODE NOS	WEARING SYSTEM	CORRELATION COEFFICIENT	DEGREES OF FREEDOM	T	T-TEST SIGNIFICANCE	REMARKS
39	Cl^{d} P.V.C. | M.S. (VFO.) D	0·996	8	2·16	5·0-10·0%	SLIGHT SIGNIFICANCE
38	Cl^{d} P.V.C. | M.S. (V.FO) C	0·992				
37	Cl^{d} P.V.C. | MS (VFO.) C	0·990	8	6·02	<0·1%	V. HIGHLY SIGNIFICANT
38	Cl^{d} P.V.C. | MS (VFO) C	0·992				
39	Cl^{d} P.V.C. | M.S (VFO) D	0·996	8	8·31	<0·1%	V. HIGHLY SIGNIFICANT
40	Cl^{d} P.V.C. | MS (VFO) D	0·985				
43	P.V.C. | MS (15·70N) C	0·985	20	1·20	>25%	NO SIGNIFICANCE
44	P.V.C. | M.S. (15·70N) D	0·935				
45	Cl^{d} P.V.C | MS. C	0·946	20	0·44	>25%	NO SIGNIFICANCE
46	Cl^{d} P.V.C. | M.S. D	0·976				

* N.B.

V.F.O. = Vacuum furnace oxide on mild steel (Fe_3O_4)

A.F.O. = Air furnace oxide on mild steel ($\alpha Fe_2O_3 / Fe_3O_4$)

A = Wear station 'A'

B = Wear station 'B' etc etc

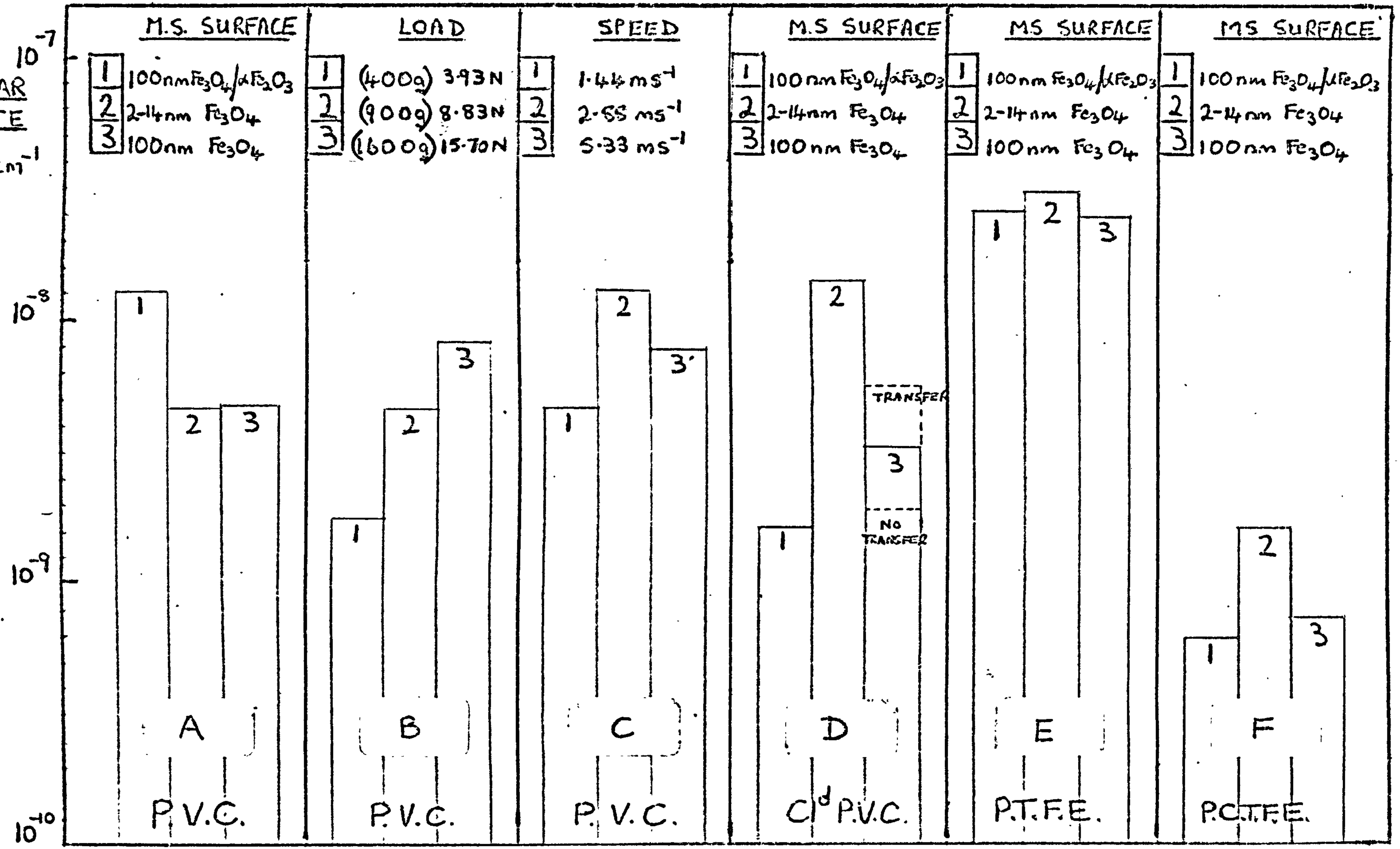

FIG 9. A histogram summary of the wear rates of various polymer flats sliding against several different conditioned mild steel surfaces under a variety of experimental conditions. (See also TABLE 5).

3.5.1.3 Ancillary Analyses of Materials.

3.5.1.3.1 X-ray and Electron Diffraction.

Both the x-ray and electron diffraction information and the corresponding microdensitometer details of the oxides present on the surface of mild steel cylinders are collated in the appendix. A summary of the results of these analyses however are tabulated in TABLE 7. The original experimental code numbers are listed alongside a description of the sample allowing easy comparison with the more detailed information in the appendix. Taking X7, for example, the table shows that this was a sample of the oxide present on the mild steel surface after 3½ hours heating at 773K in a vacuum furnace at 4.7-10 N m^{-2} pressure. The oxide had been removed using the Booker, Norbury and Sutton (B.N.S.) technique described in the sample preparation section and mounted in a standard X-ray powder diffraction camera. The X-ray diffraction pattern obtained indicated that the specimen was substantially Fe_3O_4 with a trace of αFe_2O_3.

X-RAY AND ELECTRON DIFFRACTION ANALYSIS RESULTS.

TABLE 7.

CODE NO.	SAMPLE	PREPARATION	RESULT
X7	OXIDE ON MILD STEEL	B.N.S. TECHNIQUE	Fe_3O_4
	AFTER 3½ HRS. 773K	THEN ROLLED INTO	+ trace αFe_2O_3
	$10-4{\cdot}7\ N_m^{-2}$	POWDER CAMERA	
		CAPILLARY.	
X10	OXIDE ON MILD STEEL	B.N.S. TECHNIQUE	$Fe_3O_4/\alpha Fe_2O_3$
	AFTER 2 HRS. 773 K	THEN ROLLED INTO	
	IN AIR	POWDER CAMERA	
		CAPILLARY	
X13	MAGNETITE	POWDER SHAKEN	Fe_3O_4
	(STANDARD)	INTO CAPILLARY.	
X14	HAEMATITE	POWDER SHAKEN	αFe_2O_3
	(STANDARD)	INTO CAPILLARY	
X15	MAGNETITE/HAEMATITE	PHYSICALLY MIXED	$Fe_3O_4/\alpha Fe_2O_3$
	(1:1 STANDARD)	POWDERS SHAKEN	
		INTO CAPILLARY	
X17	VACUUM FURNACE	ROLLED AND	Fe_3O_4
	OXIDE EMBEDDED IN	MOUNTED IN	+ trace αFe
	P.V.C. AFTER WEAR EXPT.	POWDER CAMERA	

ELECTRON CODE NO.	SAMPLE	PREPARATION	RESULT
E14	M.S. VACUUM FURNACE OXIDE	STANDARD CARBON	Fe_3O_4
	(1HR 773K $10-4{\cdot}7N_m^{-2}$)	REPLICA TECHNIQUE	
E16	AIR FURNACE OXIDE	STANDARD CARBON	$Fe_3O_4/\alpha Fe_2O_3$
	(1HR 773K.)	REPLICA TECHNIQUE	+ trace FeO

3.5.1.3.2 Vickers Micro-Hardness Testing.

TABLE 8. is a largely self-explanatory summary of Vickers hardness measurements made on the various types of oxide present on the mild steel countersurfaces. After a brief description of the oxide in question the next four columns list the loading on the indenter and aspects of the resulting indentation geometry. The final column gives the appropriate mean Vickers hardness number associated with the measured indentation diameter. For reasons already discussed under 'experimental procedure' these values are only very approximate and strictly relative.

3.5.1.3.3 Differential Scanning Calorimetry

The D.S.C. measurements on the samples (carried out and supplied by R.A.P.R.A.) of glass transition point (Tg) and melting point (Tm) for substantially amorphous and crystalline polymers respectively are conveniently recorded in TABLE 5.

Vickers micro-hardness number (V.H.N.) measurements made on mild steel/iron oxide countersurfaces.

TABLE 8

SAMPLE SURFACE	(g) LOAD	DIAGONAL LENGTH (μm)	DEPTH OF PENETRATION (μm)	V.H.N.	MEAN V.H.N.
2-14 nm Fe_3O_4 on	10	66		239	
mild steel.	10	71		207	
	10	73	10·1	196	210
	10	72		201	
	10	69		219	
	10	72		201	
100 nm Fe_3O_4/x Fe_2O_3 on	10	60		290	
mild steel.	10	59	8·7	300	282
	10	63		263	
	10	62		271	
100 nm Fe_3O_4 on	10	65		247	
mild steel.	10	67		232	
	10	65	9·6	247	235
	10	65		247	
	10	69		219	
	10	69		219	

3.5.2 The Degradation Mechanism of P.V.C. as it Slides on Mild Steel and Oxides Present on Mild Steel.

3.5.2.1 Introduction.

Many reviews of P.V.C. degradation have appeared in the last few years[98, 106, 107, 108] and they all codify four main types of chain modification process.

(i) Mechano-chemical degradation

(ii) Thermal dehydrochlorination degradation

(iii) Photodegradation

(iv) Irradiation degradation.

Since photodegradation processes require prolonged exposure to sunlight (especially λ 270 - 310nm) over many days to produce observable changes in mechanical properties[98] and degradation by high energy radiation such as electron beams or X-rays obviously requires the specific environment to be artificially manufactured, only (i) and (ii) are considered in this discussion. This is not to assume that other types of interaction or chemical action cannot occur on metal or metal oxide surfaces and conceivably affect polymer degradation. For example the action of ultra violet and visible light or even physical polishing of an oxide surface has been shown by KRAMER[109,37] et al to excite electron emission. Similarly H_2O_2 has been shown to have been produced on fresh metal surfaces by a process of radical ion formation following electron excitation. Thus, although the whole concept of interface changes during sliding must necessarily be considered complex the predominant features of such processes should be readily observable allowing simplified interpretations.

The relative importance of mechano-chemical breakdown and/or thermal degradation can be deduced from interpretation of the results of the infra red A.T.R. spectrophotometry, gel permeation chromatography (G.P.C.), ultra violet spectrophotometry and general macro and microscopic examination of surfaces. These will be considered individually.

3.5.2.2 Infra-Red Attenuated Total Reflectance (A.T.R.) Studies.

The most salient feature of the spectra of the worn P.V.C. debris samples (APPENDIX 3) occurs at wave number 1380cm^{-1} (SEE TABLE 2). Here a new peak is consistently appearing (when compared to the unworn P.V.C. control sample) and appears to be accompanied by a general broadening of the $-CH_2-$ in plane deformation absorption peak at 1439cm^{-1} (SEE FIG. 8). These are characteristics of the I.R. absorption pa ttern that might be expected when $-\overset{|}{\underset{|}{C}}-CH_3$ groups are present in t he polymer molecule. Indeed it has been established[96] that any such new end-groups may be expected to differ from the structure of the terminal groups which are characteristic of the given polymer before degradation. For P.V.C. these original groups would probably have been unsaturated[97]. Thus terminal methyl groups are consistent with a strong peak between 1385-1370cm^{-1} due to a symmetrical deformation mode and a medium intensity peak between 1470-1435cm^{-1} due to assymmetrical deformation[92, 95]. The latter absorption in this case is obviously being partially masked by the stronger 1439cm^{-1} peak. A possible mechanism for the production of these entities can be cited in terms of a *disproportionation[93] or chain transfer reaction following mechano-chemical shearing. (See also G.P.C. analysis & FIG. 10)

*This is the term applied to one of the processes whereby two adjacent free radicals can mutually destroy each other by electron spin pairing. The most common example is where a hydrogen atom from one of the radicals is transferred to the other giving two new molecules, one saturated and the other possessing an olefinic double bond at one end [122].

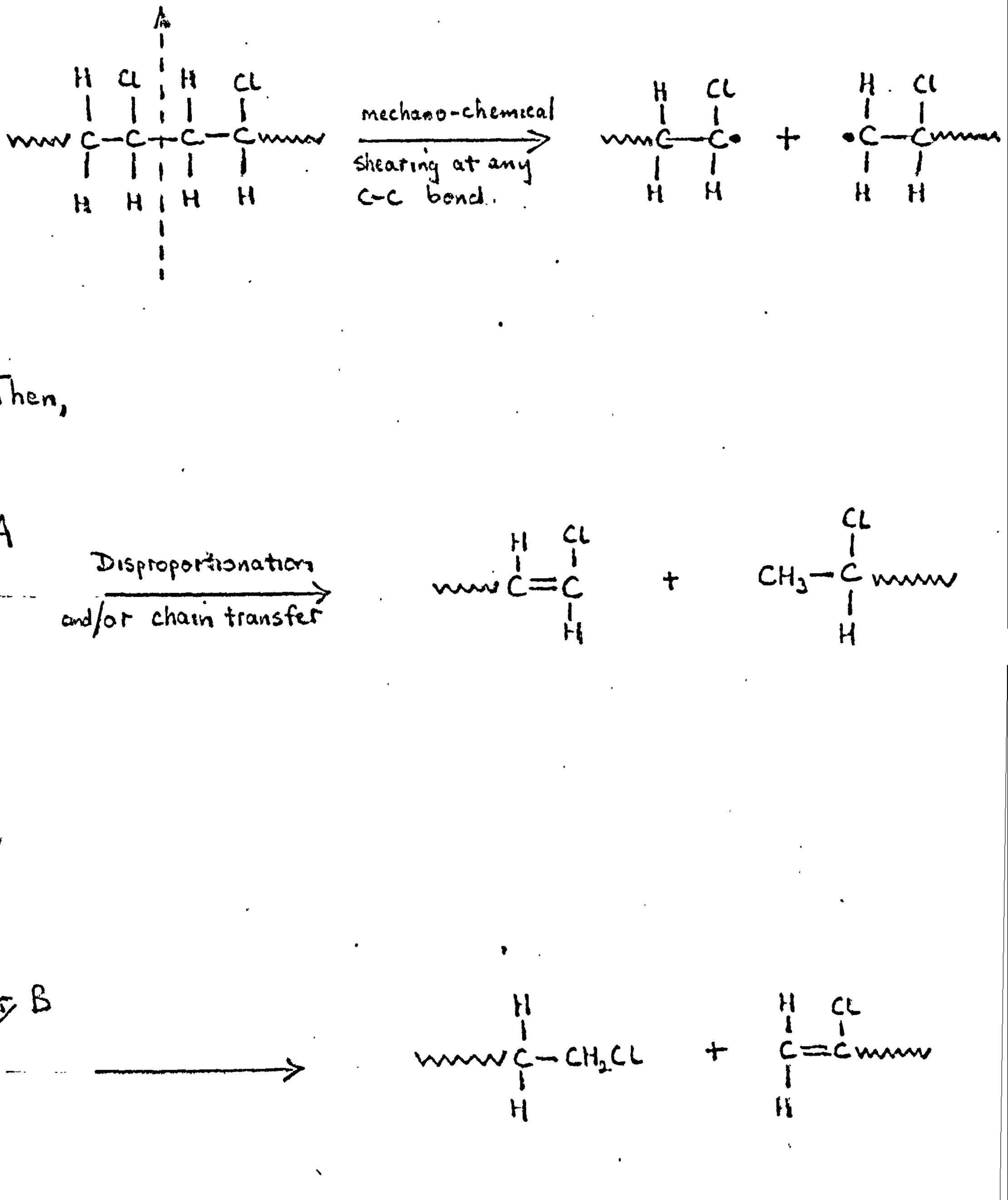

FIG 10.

A proposed mechanism for the mechano-chemical breakdown of P.V.C. when slid against mild steel or iron oxides.

The fact that some form of increased C = C stretching vibration peak does not also occur between 1680-1580cm^{-1} in the spectra may be explained in terms of the low or variable intensities of absorption associated with such entities. It is interesting to note however that in nearly all cases increased absorption occurs in the 3000-2950cm^{-1} region which would be consistent with C-H stretching and deformation vibrations for groups attached to double bonds. A further mitigating factor is that metal halides such as $FeCl_3$ have been shown to promote crosslinking of the P.V.C. chains by interaction of -C-Cl and -C=C chain ends[87] thus reducing the degree of unsaturation. In the present work it is reasonable to assume the presence of some $FeCl_3$ due to the reaction between the mild steel surface and dehydrochlorinating (thermally degrading) P.V.C. Extensive removal of -C=C end-groups from worn P.V.C, cannot be explained by this mechanism however as significant amounts of cross-linked material would have impaired the solubility of wear debris in T.H.F. (See G.P.C. analysis in EXPERIMENTAL PROCEDURE section).

It should be mentioned at this point that changes in polymer end-groups are not always easily detectable by I.R. analysis. This is particularly true of high molecular weight molecules due to the relatively small number of end-groups compared to say $-CH_2-$ groups which occur repeatedly all along the P.V.C. chain. This reservation can be off-set slightly by the fact that a number of examples can be quoted from the literature[94] where polymer end groups analysis has been used to determine molecular weights up to $\bar{M}n$ 100,000. Indeed some authors claim by implication[95] that in the polyethylene (Marlex) case methyl group concentration is quantitively measurable down to 0.5 theoretical Me groups per 1,000 carbon atoms. In the present case the average molecular weight of the sheared P.V.C. is $\bar{M}n$ 15,000 which corresponds to an average chain length of approximately 475 carbon atoms. Assuming that only between one in two and one in four of the polymer chains possess a terminal methyl group

(by virtue of disproportionation) then the methyl group concentration is equivalent to 0.5 - 1.0 Me per 1,000 carbon atoms. Hence these should be readily observable.

Obviously the reaction cited can only be a tentative proposal and requires considerable further work for confirmation. Typically this would involve electron spin resonance studies (E.S.R.) at low temperatures thus characterising radicals by their spectra and furnishing evidence of their concentration.

3.5.2.3 Gel Permeation Chromatography (G.P.C.) Analysis.

It is well established that most synthetic polymers are polydisperse and the distribution of the molecular weights in any given sample can be represented by a weight fraction versus molecular weight graph.

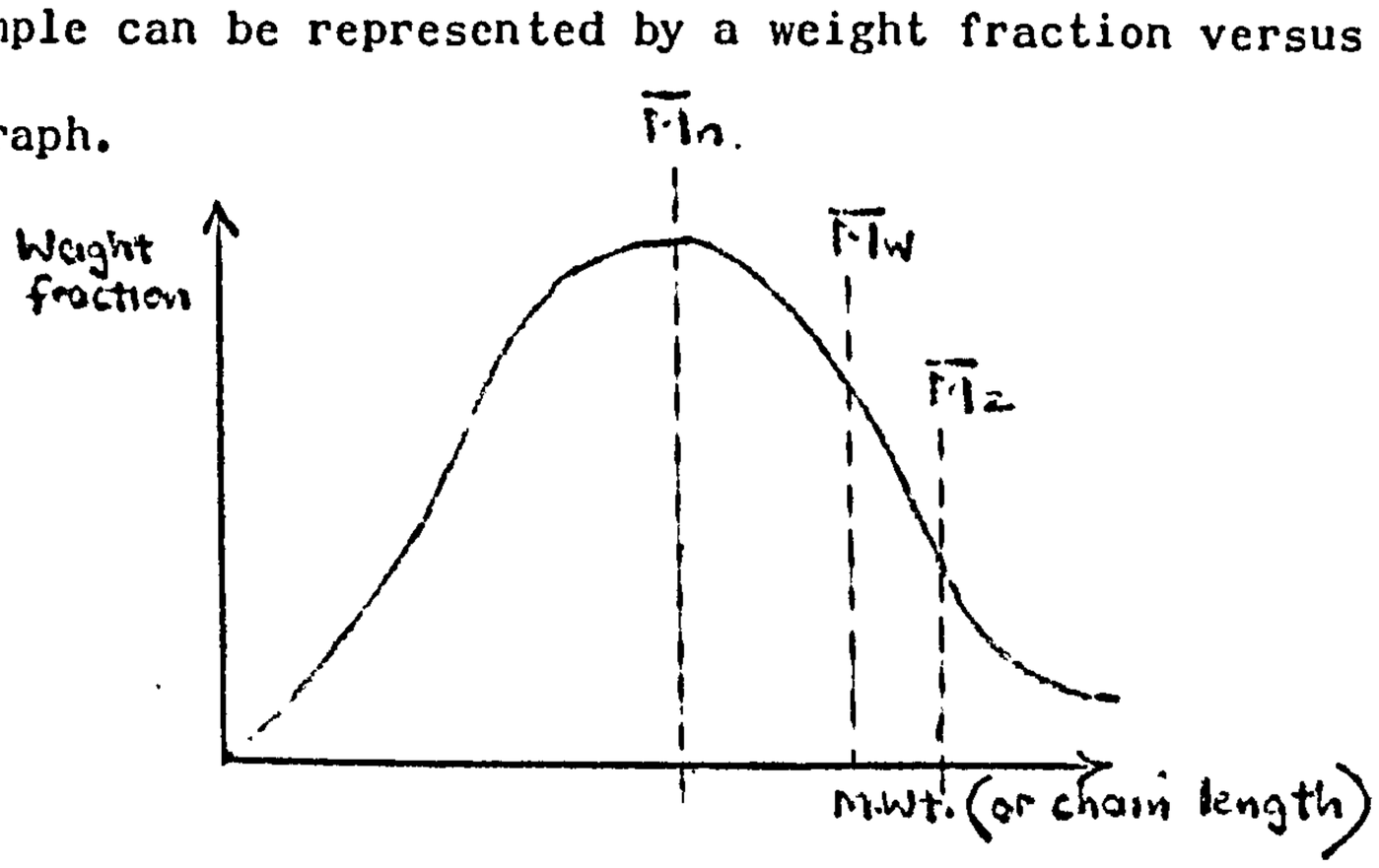

Average molecular weights can be defined mathematically by a number of different methods, the most common being number average ($\overline{M}n$), weight average ($\overline{M}w$) and the 'Z' average ($\overline{M}z$). The general formula used may be stated as -

$$\overline{M} = \frac{\sum_{i=1}^{\infty} N_i M_i^a}{\sum_{i=1}^{\infty} N_i M_i^{a-1}}$$

where N_i is the number of molecules of m.wt. M_i and a =1 for ($\overline{M}n$),

a = 2 for ($\overline{M}w$), and a = 3 for ($\overline{M}z$)

Different formulae are used according to whether the contribution of large molecules is to be stressed to allow for differences in shape and configuration[94(P.171)]. Consequently each type of average molecular weight effectively corresponds to a different point (see above) on the mass fraction (or concentration) versus molecular chain length (or elution volume) curves as obtained by G.P.C. analysis. The definition of 'number' average molecular weight ($M\bar{n}$) is derived from the normal counting process whereby the mass of the sample is divided by the number of molecules it contains. This numerically includes every molecule equally irrespective of its particular mass. Simple analogies for the 'weight' average molecular weight ($M\bar{w}$) and the 'Z' average molecular weight ($M\bar{z}$) etc., do not exist[94 (P.171)] but it is sufficient to say that, mathematically, in these cases increased emphasis is given to individual molecules with high molecular weights such that $Mn < Mw < Mz$. These higher types of average are particularly significant when used to compare polymers in which molecular size, shape, and orientation have an important effect on physical properties e.g. viscosity. Alternatively $M\bar{z}$ and $M\bar{w}$ can be computed (in addition to $M\bar{n}$) to get an indication of the range of molecular weights present in a polymer sample.

It can be seen that $M\bar{n} < M\bar{w} < M\bar{z}$ for polydisperse systems and $M\bar{n} = M\bar{w} = M\bar{z}$ for theoretically monodosperse systems. Thus the ratio of $M\bar{n} : M\bar{w} : M\bar{z}$ gives some indication of the breadth of the molecular weight distribution curve[94].

In the present work with P.V.C. wear debris (TABLE 1) a sharpening of the distribution has noticeably occurred in every case (except experiments 35 and 36) and is indicative of a predominantly mechano-chemical degradation process[96 (P.54)]. Thermal and chemical degradationare more commonly associated with polymer fragments of both high and low molecular weight [96 (P.128)]* although in the present P.V.C. case the thermally promoted dehydrochlorination reaction does not necessarily include main chain scission[98] but merely HCl removed from the sides of the main chain.

All of the P.V.C. samples have had their $\bar{M}n$: $\bar{M}w$ ratios reduced from approximately 3.0 to approximately 2.0 which is supplementary evidence to the tentative A.T.R. conclusions that disproportionation reactions may be taking place during mechano-chemical shearing. This is derived from BILLMEYER'S statement[94 (P.163)] that polymers terminated by disproportionation give rise to $\bar{M}n$: $\bar{M}w$ values of 2.0 whereas normal high conversion vinyl polymers have ratios between 2.0 - 5.0.

3.5.2.4 Macro-and Microscopic Examination of Worn P.V.C. for Thermal Degradation.

A careful macro and microscopic examination of worn polymer surfaces was made before, during and after sliding on mild steel and mild steel oxides. Particular attention was payed to P.V.C. and Cl^{d} P.V.C. and an attempt made to assess the degree of

* Although initially the middle of the polymer main chain may be ruptured by chemical or thermal energy influences, thereafter a depolymerisation or decomposition reaction could be propogated. For example, in the case of a depolymerisation reaction, monomer units could be progressively removed from the molecule. Thus over a period of time only short chain monomer units or undegraded high polymer molecules would be left.

dehydrochlorination by reference to colour changes. It is well established that during degradation HCl is progressively removed from the sides of the carbon chain resulting in an increasingly conjugated polyene structure. This promotes discolouration of the plastic in the form of a pink-red-brown-black development in an inert atmosphere probably due to the intensity of one species[98]. In other atmospheres and with certain additives a yellow-orange-brown-black sequence is obtained. Absolute measurement of colour is difficult although some workers[111] have used the Munsell Colour Method which quantifies it in terms of comparative values of 'lightness' and 'hue'. Others have tried standard iodine titrations[112], ultra-violet/visible spectrometry[113] or even the reflectance of degraded polymer powder[114]. In the present work observation of any colour development in the polymer surface was used as a qualitative qualification of evidence furnished by U.V. Spectrophotometry. Indeed it can be shown that in inert atmospheres even a 0.1% loss of HCl is detectable by visual examination[111] and corresponds to a conjugated polyene structure of at least 7 double bonds[115].

TABLE 4 only reveals evidence of colour development in the case of P.V.C. sliding on the 100nm air furnace oxide ($Fe_3O_4/\alpha Fe_2O_3$) surface. The colour red suggests that the degradation process had not developed to any great extent and indeed even this discolouration did not occur in debris from every sliding experiment. The darkening of polymer surface in the initial stages of the P.V.C./Fe_3O_4, P.V.C./mild steel sliding combinations was judged, after microscopic examination, to be very fine areas of removed oxide embedded in the surface. This occurred to a much greater extent in the P.V.C./100nmFe_3O_4 case. Overall, this absence of coloration (in conjunction with the evidence furnished by chemical tests and both I.R. and U.V. spectrophotometry discussed on pages 72 - 82 would tend to suggest that in the particular context of the

present work thermal dehydrochlorination plays a relatively minor role in the general degradation of P.V.C. when sliding at $1.44ms^{-1}$ on oxides with a load of(900g) 8.83 N for periods between 10 and 70 minutes. As a corollary bulk surface temperatures can be generally assumed to be below the 423K region which is the usual temperature at which discolouration first appears in inert atmospheres[98 (P.2)]. Smoothness of the polymer surface in the case of P.V.C./Fe_3O_4/αFe_2O_3 experiments however indicate that surface temperatures had at least reached the T_g (356K) level and presumably would facilitate any mechano-chemical processes taking place.

After each wear experiment the surface of the mild steel drums were analysed for traces of ferrous or ferric chloride salts as might be expected if dehydrochlorinating P.V.C. had reacted with the countersurface. Treatment of the wear scar with solutions of potassium ferri or ferro cyanide (taking care to remove any transfer films so that the contacting drop spread out on an apparently hydrophilic surface[25 (P.72)]) failed to produce the characteristic Prussian blue precipitate associated with quantities of iron chloride. This added further weight to the conclusions that little of the P.V.C. surface was thermally degrading.

3.5.2.5 Ultra-Violet (U.V.) Spectrophotometry Studies.

As is discussed elsewhere, if thermal degradation of P.V.C. had recurred it would have been initially associated with the development of a conjugated polyene structure as dehydrochlorination took place. Changes of this character are readily detected by U.V. absorption techniques which generate spectra characterised by increased absorption peak intensity, wave shifts or peaks at an increased number of wave lengths.
Unfortunately in order to properly analyse the complex absorption spectra

of degraded P.V.C. it is desirable to have spectral details of all the individual polyenes concerned (in terms of wavelength and extinction coefficients of absorption maxima). However, in spite of the great volume of work published in this area[98, 115, etc.] this vital information is still unresearched. GEDDES[98 (P.45)] claims that there is a general tendency to assume that each individual adsorption maxima in the degraded P.V.C. spectra corresponds to the longest wavelength peak of an individual polyene but points out that fortuitous overlap of several minor peaks may in fact produce spurious peaks in the composite spectrum. Experimental evidence for this hypothesis is not quoted, however.

In the present work no attempt was made (or intended) to draw detailed qualitative or quantitative conclusions for the reasons outlined above. All that was required was a simple assessment of whether extensive dehydrochlorination had taken place in P.V.C. sliding on mild steel at $1.44 ms^{-1}$ and (900g) 8.83 N load. As TABLE 3. (and the spectrometer traces in APPENDIX 4) show, only slight thermal degradation has taken place in the bulk of the debris sample. This can be deduced from the relative heights of the λ maxima at 293 and 254. For the unworn P.V.C. specimen (sample 1) the ratio is 0.65 and it changes to 1.11 for a heavily degraded brown-black specimen (sample 2) which presumably may be assumed to possess polyenes with up to 25 double bonds in the main chain[116]. The wear debris sample however only has a ratio of 0.88 thus indicating either a few selected areas of high degradation (with the associated absorption maxima weakened by unaffected polymer in solution) or a generally low level of thermal degradation throughout the specimen. In view of the 'flash temperature'* concept (discussed in the literature survey) and evidence proffered by visual examination (discussed elsewhere) the former is the more likely.

*This involves the idea of small hot spots of frictional heat developing across a wearing surface[25(P.86)] rather than a general, even, temperature rise..

3.5.2.6 Summary.

Generally speaking when P.V.C. is worn on mild steel and mild steel oxides at a speed of $1.44ms^{-1}$ and (900g) 8.83 N load the main degradative action is in the form of mechano-chemical comminution with some thermal degradation in localised areas.

3.5.3 Mechano-Chemistry and its relation to the wear of P.V.C., Cl^dP.V.C., P.T.F.E., P.C.T.F.E.

3.5.3.1 General Principles.

The interpretation of the molecular weight analyses for P.V.C. and Cl^dP.V.C. require discussion and review of the mechano-chemical principles which are separately or collectively contributing to the polymer chain length modifications occuring during wear.

The rupture of molecular chains can take place when there arises at some point in the molecule a localised stress exceeding the critical value for the chemical covalent strength between atoms at that site. In the present case that is likely to be 4.0 - 6.0 n N per bond[96 (P.13)]. An important factor affecting this is the way in which the applied energy from the shearing forces dissipates itself between the principle valency bonds and inter and intra molecular interactions. This in turn is dependent on the physical nature of the polymer and, for linear amorphous plastics, whether they are in the glassy, high elastic, or viscous state. Transitions between these states occur at different temperatures for different polymers according to their chemical nature, molecular weight and rate of deformation etc.

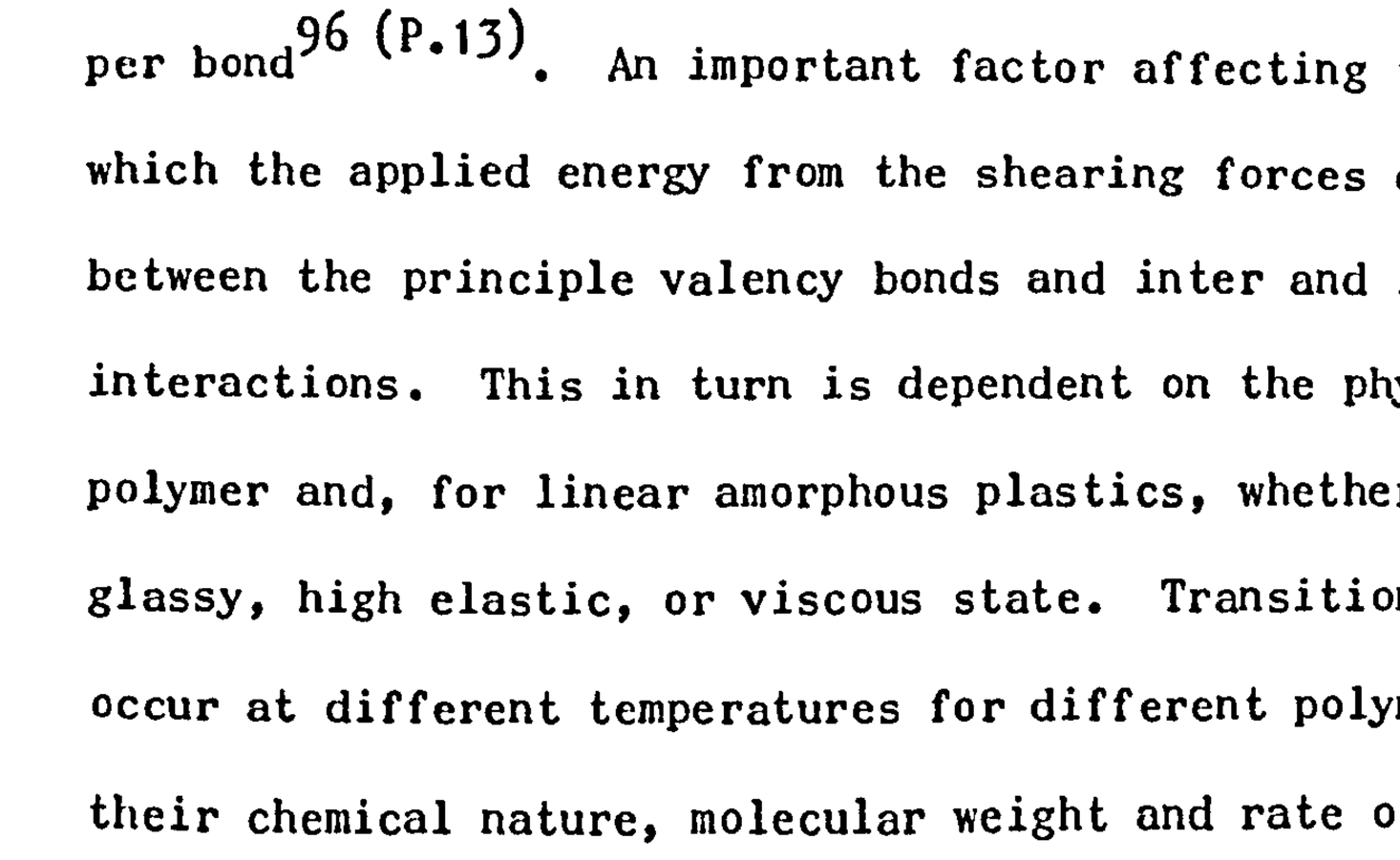

A summary of some of the literature with respect to types of mechano-chemical degradation may be presented in tabular form as follows:-

STATE	PRINCIPAL CHARACTERISTICS OF DEFORMATION	MECHANO-CHEMICAL DEGRADATION
Glassy	Reversible, time and temperature independent changes in valency angles, interatomic and intermolecular distances. $\sigma = E_1 S$	* $\frac{ds}{dt} < \frac{\sigma}{3}$ redistribution of molecules without scission. $\frac{ds}{dt} > \frac{\sigma}{3}$ stress increases until mechano-chemical degradation or brittle failure. Tg increases with rate of deformation. Tg little dependent on mwt. Scission always associated with comminution. Degradation mainly occurs on polymer

* NB Maxwell's equation is $\frac{ds}{dt} = \frac{\sigma}{3} + \frac{1}{E}\frac{d\sigma}{dt}$ which rearranged becomes

$\frac{d\sigma}{dt} = E\left(\frac{ds}{dt} - \frac{\sigma}{3}\right)$ Thus the overall sign of the term in brackets determines the slope (if negative then the stress is 'relaxing' if positive the stress is 'building up').

STATE	PRINCIPAL CHARACTERISTICS OF DEFORMATION	MECHANO-CHEMICAL DEGRADATION
Glassy cont....		96(P.18,188,208) surfaces and planes of cleavage.* Degradation is independent of temperature up to Tg.
Forced - Elastic (transition)	As above but contains additional irreversible changes in chain configuration. Orientation of chains occur and anisotropic mechanical properties.	As above but scission also possible in the bulk of the polymer.
High - Elastic (Visco-elastic)	Complex combination of time dependent/independent effects. But deformation may be considered as mainly time dependent reversible changes in chain configuration. The deformation that can be effected is several orders higher than in the forced-	Degradation by even small deformations continues until the mwt low enough to effectively lower T_v. Increased rate of deformation increases

* When the polymer is well below its glass transition temperature, the energy, from mechanical working tends to dissipate itself mainly by simple material splitting. Consequently mechano-chemical degradation and hence free macro radicals are said to form (in the course of the process) only on the newly cleaved surfaces and not in the polymer bulk 96 (P.18).

STATE	PRINCIPAL CHARACTERISTICS OF DEFORMATION	MECHANO-CHEMICAL DEGRADATION
High - Elastic cont....	elastic state. $\sigma = E_2 S + \eta_2 \frac{dS}{dt}$	the probability of degradation. Scission without final comminution is possible.
Forced - Plastic (transition)	Similar to high elastic state with superimposed non-reversible chain slip (flow).	As T_v approached then the likelihood of chain scission decreases.
Viscous Flow	Complex state but may be ccnsidered as a mainly time dependent, mwt dependent irreversible flow of material (chain slip). $\sigma = \eta_3 \frac{dS}{dt}$ $\ln \eta_3 = A + \sqrt{m}$	In the ideal case chain scission cannot take place.

N.B. Although the stress/strain relationships quoted above are mainly applicable to individual states, in practice they are all (to varying degrees) simultaneously applicable. For example, the equation containing the viscosity coefficient could equally apply (but to a markedly smaller degree) to the other states In such cases:-

η_1 = viscosity coefficient for the glassy state
η_2 = " " " " high elastic (visco-elastic)state
η_3 = " " " " viscous state

Symbols

σ = stress

S = strain

t = time

η = coefficient of viscosity

E = Young's modulus

A = constant

$\bar{M}$ = average molecular weight

T_b = forced elastic transition temperature

T_g = glass transition temperature

T_{pl} = forced elastic transition temperature

T_v = flow transition temperature

For predominantly crystalline polymers the rigid crystallites direct the mechano-chemical shearing forces to the amorphous areas which separate them. After a period of time the crystalline areas themselves are destroyed (cold melting) and from that moment the same mechano-chemical principles may be employed as above.

In the present context P.V.C. may be regarded as a highly amorphous material with mainly atactic polymer chains interspersed with occasional regions of syndiotactic molecular arrangement[105(P163) 99(P92)]. The glass transition temperature (T_g) was measured by differential scanning calorimetery (D.S.C.) to be approximately 357K and so with the exception of experiment 48 the mechano-chemical process may be regarded as starting in the glassy state. Similar arguments apply to the CL^dP.V.C. with a measured T_g of approximately 382K.

3.5.3.2 The Limiting Molecular Weight M_∞

There is a theoretically and empirically limiting value to the average molecular weight of a polymer after mechano-chemical action[96(P.40)] and this may be expressed in two different mathematical forms.

$$M_\infty = \frac{E_v m S_2}{q S_1} \qquad \text{(1)}$$

$$M = ae^{-kt} + M_\infty \qquad \text{(2)}$$

Where,

M_∞ = limiting value to the molecular weight
E_v = energy associated with principal valency bonds
m = molecular weight of monomer
q = energy of intermolecular attraction
S_1 = limiting interatomic distance (at rupture)
S_2 = limiting inter molecular distance (at rupture)
M_t = number average molecular weight at time t
M_o = initial molecular weight
a = $M_o - M_\infty$
k = rate constant (dependent on chemical nature of polymer especially the packing density)
t = time

The polymer cannot be fragmented by mechano-chemical forces beyond M_∞ because at this point the cumulative effect of intermolecular attraction and the physical entanglement of chains etc. have reached a critically low value by virtue of their shorter length. Thus mechanically induced internal stresses that formally could have been relaxed by the breaking of covalent bonds are preferentially re-distributed by the displacement of the smaller, more mobile, molecules themselves.

Examination of TABLE 1. and FIG. 7. reveals that the molecular weight of the P.V.C. debris (after 10 minutes sliding is dependent on

the prevalent sliding conditions e.g. chemical surface of the mild steel drum, loading, sliding velocity and surface temperature. But if equation (1) is assumed substantially correct then the experimental parameters just stated are altering the rate of mechano-chemical scission but not the ultimate M_∞ value. This follows from the fact that the same type of P.V.C. was used in all the experimentswith only a slight individual variance in the average molecular weight. Thus all the potential variables in (1) (apart from a component of k) are effectively constant including t which in this case was (10 minutes) 600s . Hence the varying values of $\bar{M}n$ recorded for the different experiments must all be tending at different rates to the same M_∞ value.

3.5.3.3 The Effect of Speed and Temperature on the Rate of Mechano-Chemical Degradation of P.V.C. Sliding on Mild Steel.

The effect of sliding speed on the molecular weight of the Polymer debris produced can be seen in FIG. 7 here as the speed was increased by factors of approximately 1:2:4 ((keeping the load (900gf) 8.83 N and initial surface finish (0.076μm) of the mild steel constant)) then the ratio of initial mwt $(\bar{M}n)_v$ to final molecular weight $(\bar{M}n)$ increased steadily between 0.51 and 0.73. An increase in the bulk temperature of the drums was observed to accompany these changes reaching approximately 310, 320 and 350K respectively as the speed was increased through 1.44, 2.88 and 5.33 ms^{-1}. The temperature build up is partially the result of the mechanical deformation process causing molecules in the polymer bulk to be forced past one another producing internal frictional heat. For example, when successive stretching occurs (in an elongation process) through a narrow 'flow zone' then the localised temperature build up has been estimated at 55 deg. K[102]. Also, of course, it must be noted that

Under 'wearing' conditions and following the RABINOWICZ[25] (P.89) formula quoted in the LITERATURE SURVEY, P.12, θm, the mean 'flash temperature' rise above the temperature of the surrounding material is directly proportional to the sliding velocity (providing other factors, such as coefficient of friction, stay constant). Assuming values of 0.4 for the coefficient of friction of P.V.C. on mild steel, 39.0 mN m^{-1} for the surface energy (same units as surface tension) of P.V.C., 1.44 ms^{-1} for the relative sliding velocity, 62.8 W m^{-1} K^{-1} and 0.146 W m^{-1} K^{-1} for the thermal conductivities of mild steel and P.V.C. respectively then the calculated 'flash temperature' is 2.4 deg. K above the ambient material temperature for every ms^{-1} increase in sliding velocity. Thus hot spots that developed within the P.V.C./mild steel interface.are theoretically likely to have reached approximately 313, 327 and 362 K respectively as the speed varied between 1.44, 2.88 and 5.33 ms^{-1}.

If the same formula is used for Fe_3O_4/P.V.C. and $\alpha Fe_2O_3/Fe_3O_4$ sliding couples then the calculated flash temperature rises(above the ambient material temperatures) become approximately 27.0 deg. K and 18.3 deg. K respectively for every ms^{-1} incremental increase in sliding velocity.This assumes thermal conductivities[136] of 4.18 $Wm^{-1}K^{-1}$ for Fe_3O_4, 8.37 Wm^{-1} K^{-1} for αFe_2O_3, 6.27 Wm^{-1} K^{-1} for 1:1 $Fe_3O_4/\alpha Fe_2O_3$ and 0.4 for the coefficient of friction.

Thus, the P.V.C. at the sliding interface may be regarded as being in the forced elastic or high elastic physical state described earlier corresponding to temperatures immediately below the glass transition temperature (T_g) of 356 K and immediately above. Consequently, according to mechano-chemical theory this should lead to increased dissipation of the applied stresses by facilitated chain movement, in turn leading to less chain scission and a larger $\frac{\overline{Mn}}{(\overline{Mn})_v}^*$ value. This was born out in practice as the results show and was confirmed by an additional experiment (FIG.7) where the initial surface temperatures of the mild steel drums were maintained between 293-310K, 308-323K and 346-363K respectively keeping all other factors constant i.e. speed ($1.44ms^{-1}$), load (8.83N), initial surface finish of drum ($0.076\mu m$). Here a similar trend in the m.wt analysis of the resulting wear debris was observed with the increased temperature again instrumental in reducing chain rupture.

Complimentary to this 'increased surface flow' hypothesis is the fact that transferred polymer developed more quickly on the surface of the drums as speed and temperature increased (TABLE 4). N.B. Throughout the the experiments a specially developed 'interference film' technique was found useful in establishing the existence of transfer films (see APPENDIX 5)

A comparison of the changing wear rates (FIG. 9) and the changing m.wt. of debris with increased speed (FIG. 7) indicates that the improved surface flow (as opposed to bulk flow) of polymeric material suggested earlier can also lead to improved wear properties (within strictly specific circumstances). On this basis the drop in wear rate in the $5.33ms^{-1}$ region could be associated with the characteristic wear rate minima reported as occuring with many thermoplastics.

* This ratio signifies the fraction of the original molecular weight any particular sample has been reduced to and has no other theoretical significance

at critical temperatures[3,129 (P.7)] e.g. P.M.M.A. 388K (Vicat softening point 378K), P.P. 351K (Vicat softening point 423K), polyacetal 383K (Vicat softening point 438K). This wear rate minima is said to be closely followed by a deterioration of wear properties as the bulk softening point is approached or surpassed[3,24,28,29,129 (P.7)]. Direct correlations are difficult here, however, because the present experiments were of a repetitive nature that encouraged transfer films whereas the latter work was strictly non-repetitive abrasive wear avoiding transfer. Nevertheless in the present case the temperature build up through the forced elastic regime and towards T_g could be contributing to the facilitated transfer of material to the drum.

3.5.3.4 The Effect of Load on the Rate of Mechano-Chemical Degradation of P.V.C. Sliding on Mild Steel.

The effect of loads between (400 - 1600g) 3.93 - 15.7N on the m.wt. of debris produced by P.V.C. sliding at $1.44ms^{-1}$ on a polished ($0.076\mu m$ c.l.a.) steel drum was surprisingly constant* (FIG. 7 and TABLE 1). With slight variations the initial molecular weight of the P.V.C. at the sliding interface was roughly halved. One explanation for this can be found by correlating these measurements with the fact that wear rate, however, was measured to increase with load in agreement with some published reviews of wear rate theory[71 (P.4), 25, 16]. If wear is increasing then removal of material from the interface must be increasing taking with it some of the heat energy developed by frictional and mechanical shearing forces. Thus the temperature build up at the interface would be periodically interupted or reduced and only allowed to rise again while that fragment of the interface was

* It is interesting to note that according to RABINOWICZ[25 (P.89)] the flash temperature build-up is also independent of load though of course this conflicts with older equations 25 (P.88) for calculating hot spot temperatures.

intact. Apart from individual flash temperature spots the bulk temperature of the polymer surface is probably such that it remains in the glassy or forced elastic state described earlier. These conditions would favour the fairly extensive rupture of polymer chains (irrespective of load) that was reflected in the G.P.C. analysis. Also favoured would be the smaller bands of debris recorded in TABLE 4 when compared with the longer bands associated with increased speed (and/or temperature). These ideas are complimentary to the increased sliding speed conclusions where the softening of the polymer reaches the point where mechano-chemical energy can be readily dissipated by chain mobility (and/or flow) thus reducing the extent of chain scission.

3.5.3.5 The Effect of Surface Oxide Conditions on the Mechano-Chemical Degradation of P.V.C. and Cl^{d}P.V.C. Sliding on Mild Steel.

The polymeric wear debris from P.V.C. and Cl^{d}P.V.C. (FIG. 7 and TABLE 1) when worn against various types and thicknesses of oxides present on steel show some interesting similarities with respect to molecular weight analysis. The presence of either a mixed 100nm iron oxide ($Fe_3O_4/\alpha Fe_2O_3$) or a single 100nm iron oxide (Fe_3O_4) on the steel drums appears to induce increased rate of chain scission in both polymers. Both oxides possess higher Vickers hardness numerals (V.H.N. TABLE 8.) than the mild steel substrate although the figures quoted can only be regarded as relative and in no sense accurate absolute values (see EXPERIMENTAL PROCEDURE AND APPENDIX 8). Thus it is reasonable to assume that mechano-chemical energy is more readily transferred to the polymer interface by the rigid oxides than the more ductile mild steel substrate. Equation (2) reveals that the

mechano-chemically induced path from the initial polymer molecular weight M_o to the limiting molecular weight M_∞ is mathematically exponential. Therefore the differences in the apparent rates of degradation between the two different oxide systems are likely to be considerably masked as M_∞ is approached.

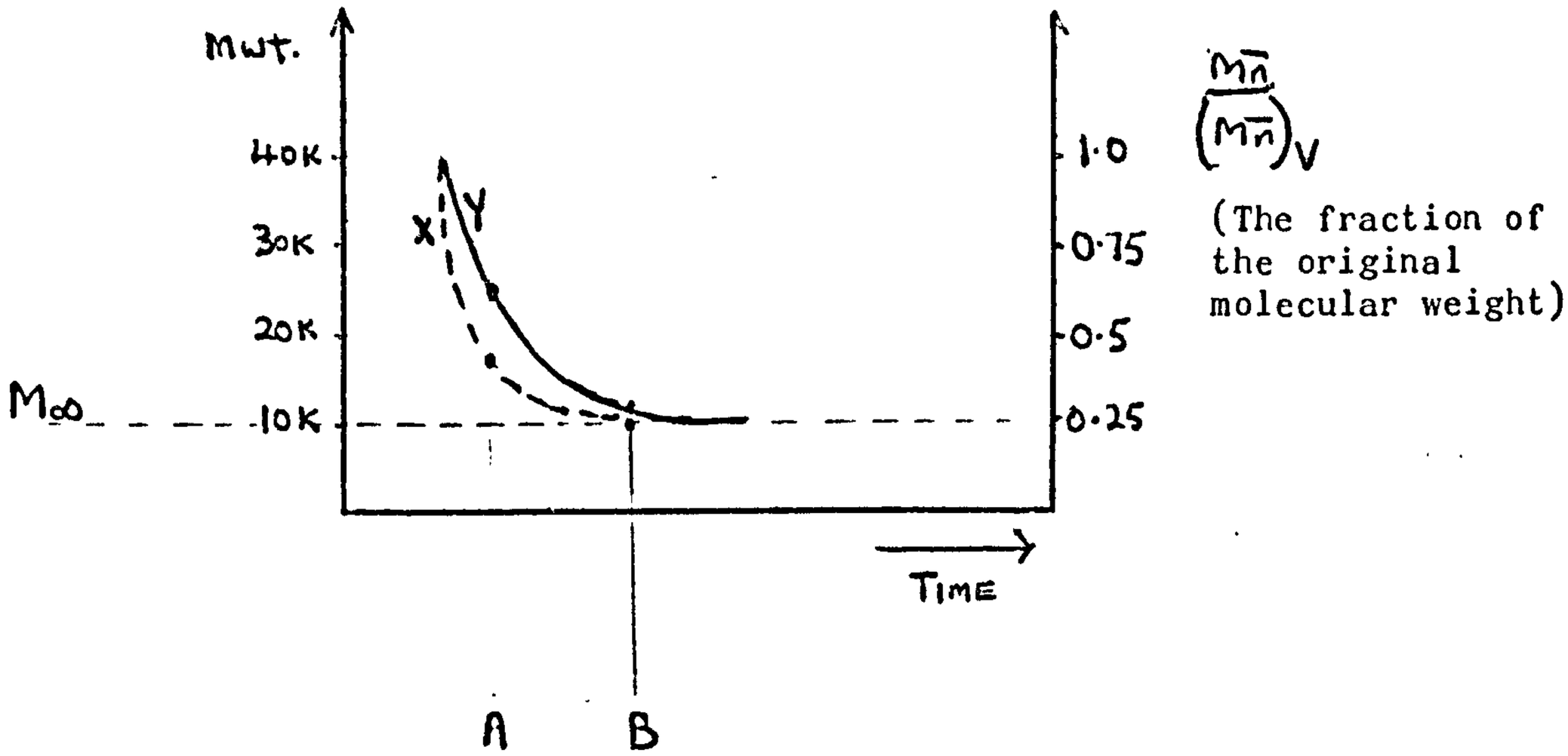

E.g. Assume the hypothetical case of a polymer of M_o = 40,000 and M_∞ = 10,000 and allow it to degrade by two exponential paths X and Y according to the surface conditions. Thus at time A the molecular weight and $\frac{\overline{Mn}}{(\overline{Mn})_V}$ differences between the two curves at that point is far greater than at time B as M_∞ is approached.

Thus the possibility of differing wear rates induced by the differences in hardness between the two oxides themselves would not be evident because it is possible (but not proved) that degradation had progressed in both cases to the point where the exponential curves were tailing off[96(P.40)].

Although there are similarities in the mechano-chemical degradation of P.V.C. and Cl^{d}P.V.C. when slid on different oxides the actual effect on the wear rate introduces some further important factors. These include polymer film transfer to the drum and the mechanical properties of the oxides and polymers themselves. All these topics have been discussed in the literature survey (1) and so only empirical observations need be added here.

Firstly the massive lumpy transfer described in TABLE 4 appeared, in the Cl^{d}P.V.C. case, to increase wear rate, Since both P.V.C. and Cl^{d}P.V.C. may be regarded as relatively non-ductile glassy polymers at room temperature (P.V.C. 40% elongation to break; Cl^{d}P.V.C. 21.5% elongation to break) then this result is not unexpected[3, 104(P.6)]. Reference to APPENDIX 6 (33,34) and FIG. 9 shows this more clearly. When the Cl^{d}P.V.C. was worn against 100nm Fe_3O_4 two different wear rates were recorded according to whether the transfer film developed or not (TABLE 4). The influence of temperature in stabilising the transfer process was born out by pre-heating the drums to approximately 310K and repeating the experiment whereupon debris readily developed on the surface. Presumably the enhanced cold flow of the polymer is critical as the T_g temperature is approached and the T_g of 382K for Cl^{d}P.V.C. must be noted in this case to be 25 deg.K higher than that for P.V.C. Thus following this hypothesis the surface softening temperature for P.V.C. is reached in the experiments and transfer films form easily. This is not so for Cl^{d}P.V.C. and experimental fluctuations in temperature (above and below its T_g) cause uncertainty in the establishment of a transfer film process.

Secondly in the P.V.C. case there is evidence of both Fe_3O_4 and $Fe_3O_4/\alpha Fe_2O_3$ oxide breaking-up during the course of the experiments the rupture being much more extensive on Fe_3O_4 than $Fe_3O_4/\alpha Fe_2O_3$. This process was examined in more detail by scratching the surface of the unworn oxide surfaces with a steel scalpel and examining the result under a stereoscan microscope (FIGS.11-27) The flaky platelike break-up of the Fe_3O_4 surface contrasting with the less broken granular $Fe_3O_4/\alpha Fe_2O_3$ comparison. Embedded oxide fragments of similar platelike appearance are clearly discernable in the surface of the P.V.C. after sliding on Fe_3O_4 (FIGS. 28-33). X-ray analysis of these fragments at the end of a wear experiment (X17 TABLE 7) shows that the chemical composition of the oxide has not changed substantially during the embedding process. Thus it can be argued that although both oxides are to some degree breaking-up, the Fe_3O_4 alone substantially embeds into the P.V.C. surface and effectively offsets any coarse abrasive action by virtue of its low shear strength, mode of lamellar rupture and lower relative hardness (SEE LITERATURE SURVEY). Indeed a beneficial polishing action could be occuring similar to that reported by LANCASTER[104] (P.8) with certain types of filler. Polishing[25] (P.184) is defined as a special form of abrasive wear promoted by very small grains (of the order of magnitude 5μm diameter or less) on an elastic backing. Reference to FIG. 30 confirms that in the present context the plate like Fe_3O_4 fragments embedded in P.V.C. during the wear process fulfils these conditions. It is of interest to note at this point that metal bearings are sometimes deliberately designed with one relatively soft surface so that any potentially abrasive particles entering the sytem may get conveniently buried.

In the examples discussed earlier the observed transfer of both lumps and thin films of polymeric material and harder oxide fragments across

the sliding interface suggests that a complicated combination[129] of adhesive, abrasive and fatigue wear processes[25] are occurring. Even when the oxide does not break-up abrasive processes cannot necessarily be ruled out.

Using BURWELL'S[128] classifications there are two main types of abrasive wear, one involving a hard, rough surface at the interface and the other hard abrasive grains. These are referred to as two-body and three-body wear processes respectively. According to RABINOWICZ[25] (P.167) abrasive wear of the two-body kind is greatly reduced when the sliding surface is smooth and hard. Similarly three-body abrasive wear is greatly reduced when the particles in the system are small, or when they are softer than the sliding materials. Thus the three-body concept aptly describes the earlier P.V.C. example where the oxide countersurface was breaking up. In the Cl^{d}P.V.C. case, however, shattering and removal of the countersurface oxides was not recorded to any extent during the wear experiments and this fact seems to be reflected in the substantially improved polymer wear rates. It is reasonable to conclude therefore that in this two-body process, providing the oxides remain intact, their smooth surface topography (i.e. relative to the mild steel substrate and revealed in the scanning electron microscope pictures FIGS. 11, 14, 17) coupled with their greater hardness (see results) is beneficial to the wear of Cl^{d}P.V.C.

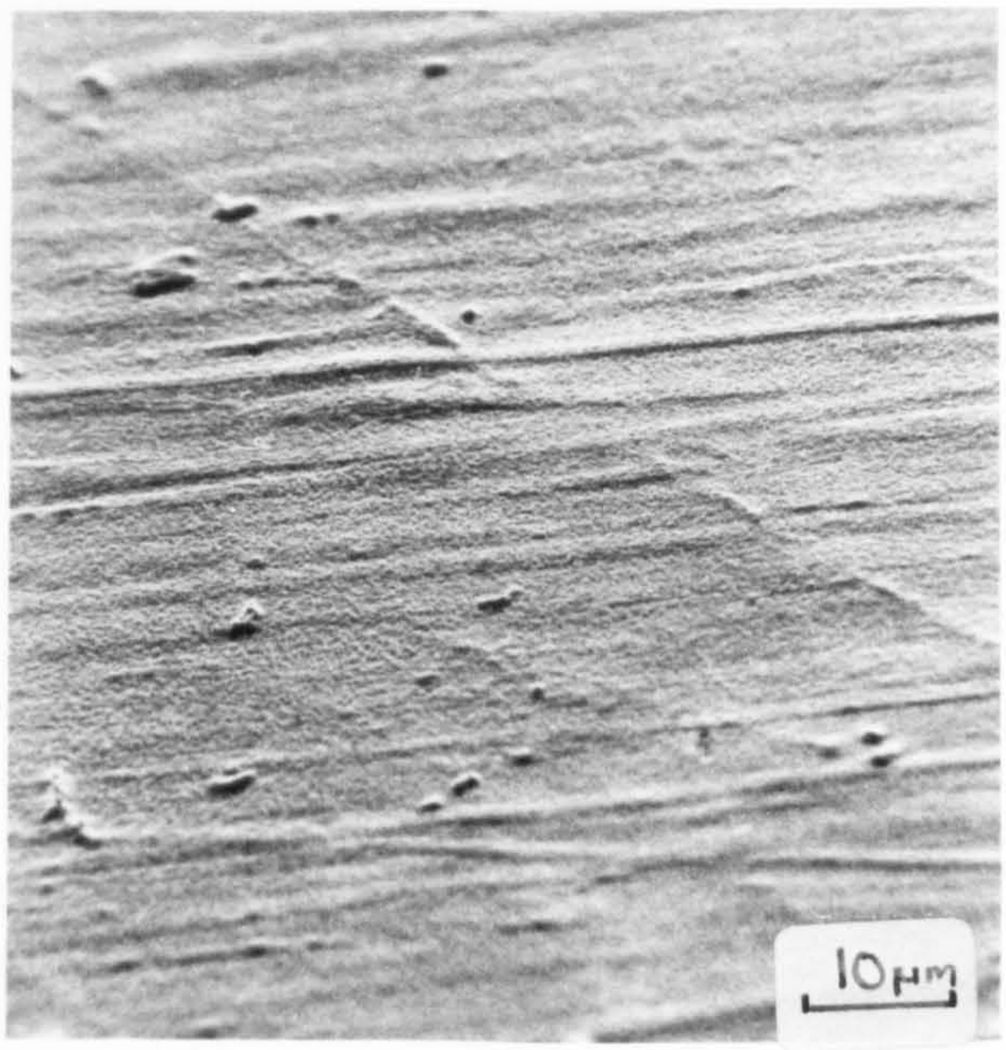

FIG. II

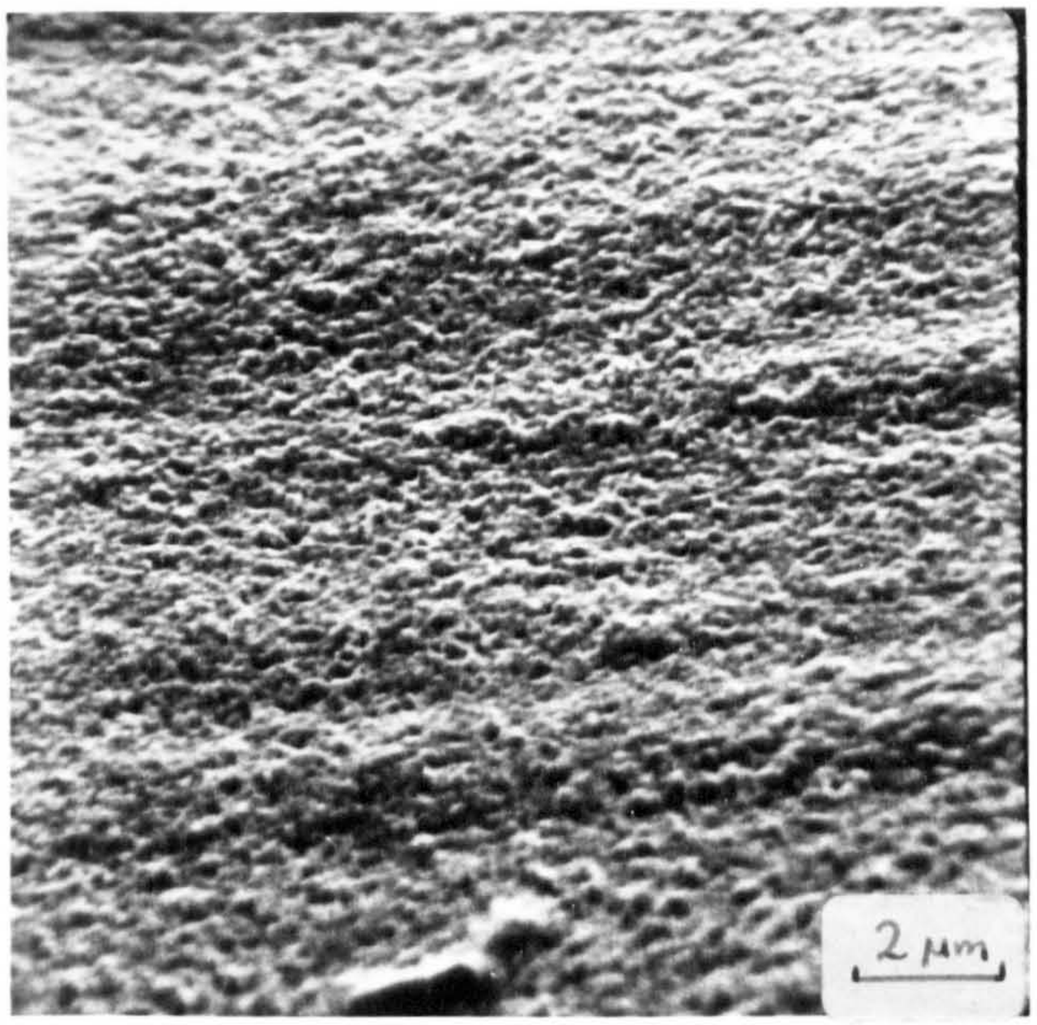

FIG. 12

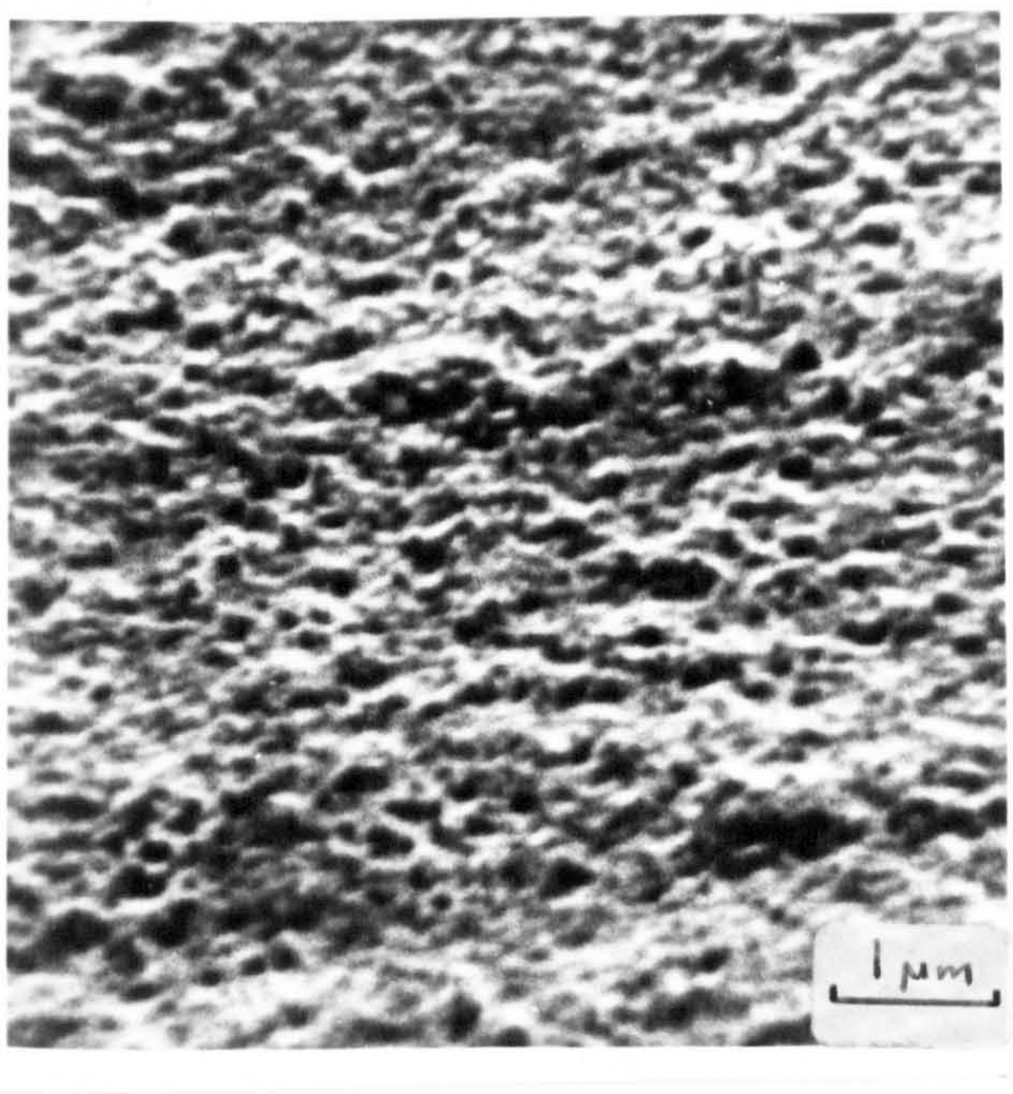

FIG. 13

Stereoscan photographs of the surface of 100nm thick Fe_3O_4 oxide (i.e. mild steel heated in a vacuum furnace) to illustrate the relatively smooth profile compared to the mild steel substrate. (cf. Figs. 17, 18, 19.)

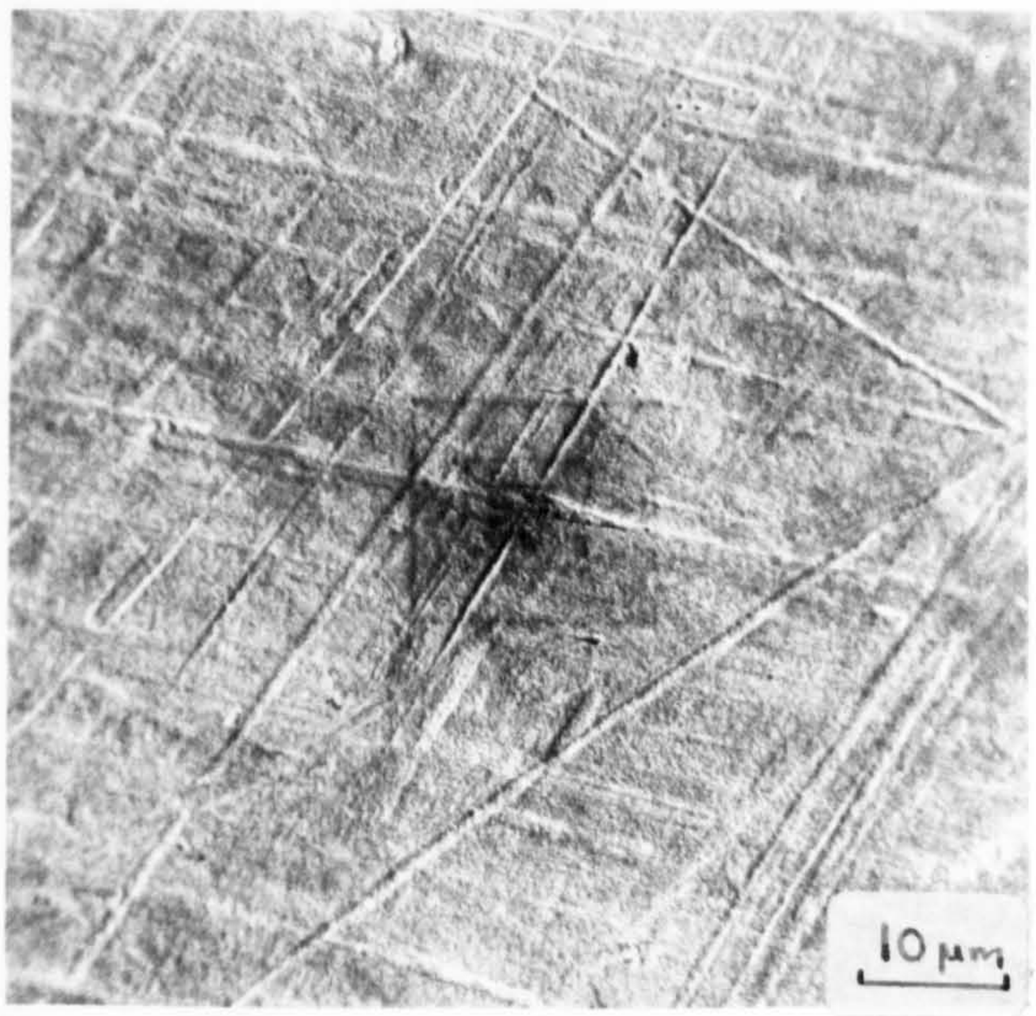

FIG. 14

FIG. 15

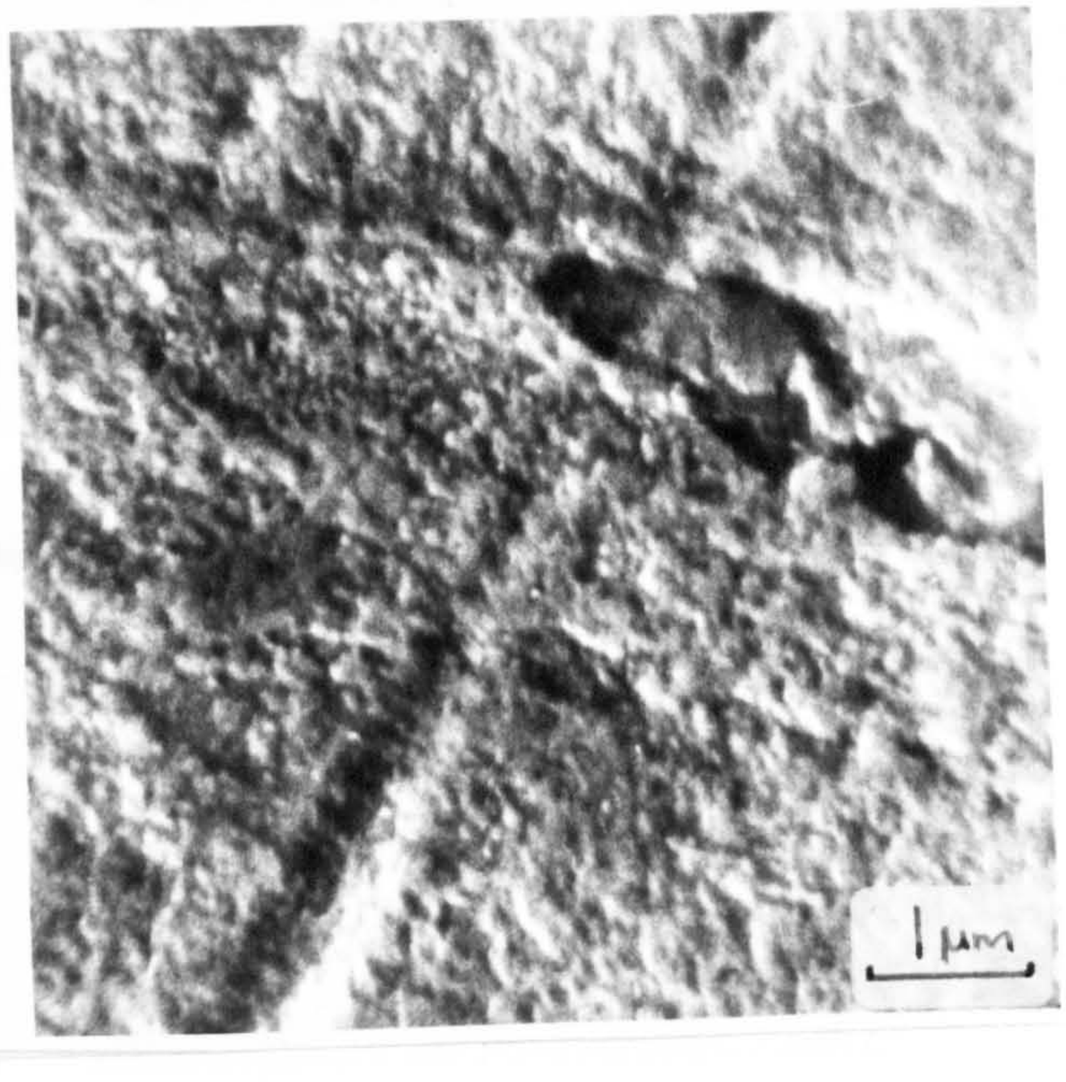

FIG. 16

Stereoscan photographs of the surface of 100nm thick $Fe_3O_4/\alpha Fe_2O_3$ oxide (i.e. mild steel heated in an air furnace) to illustrate the relatively smooth profile compared to the mild steel substrate (cf. Figs. 17, 18, 19.)

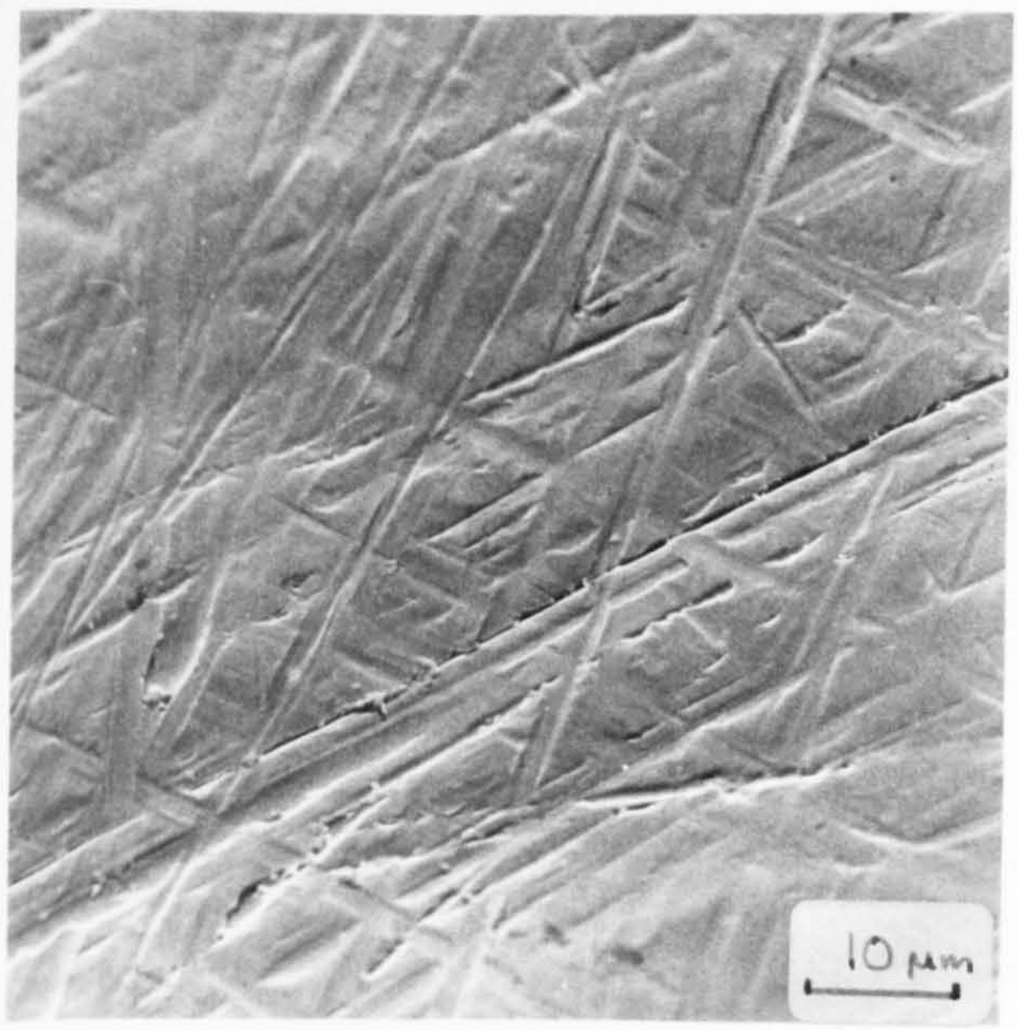

FIG. 17

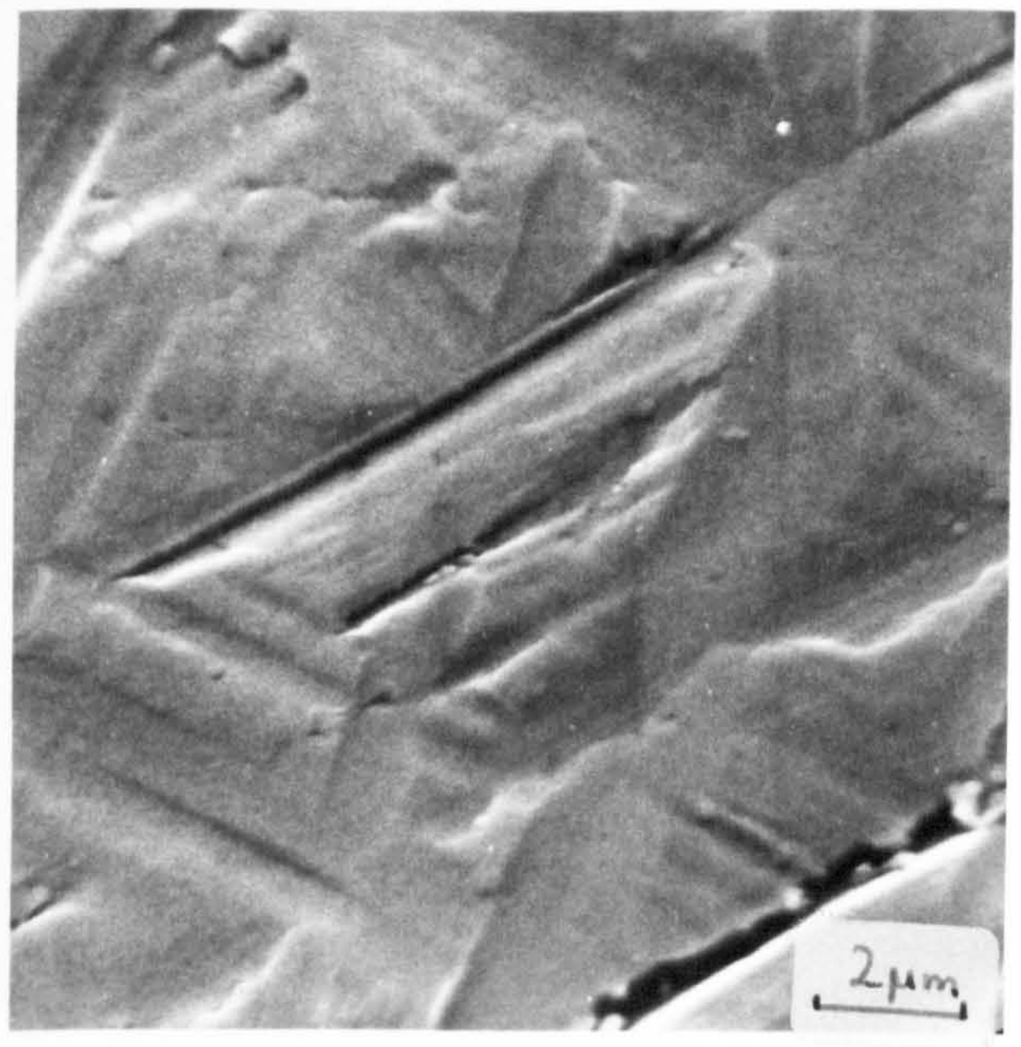

FIG. 18

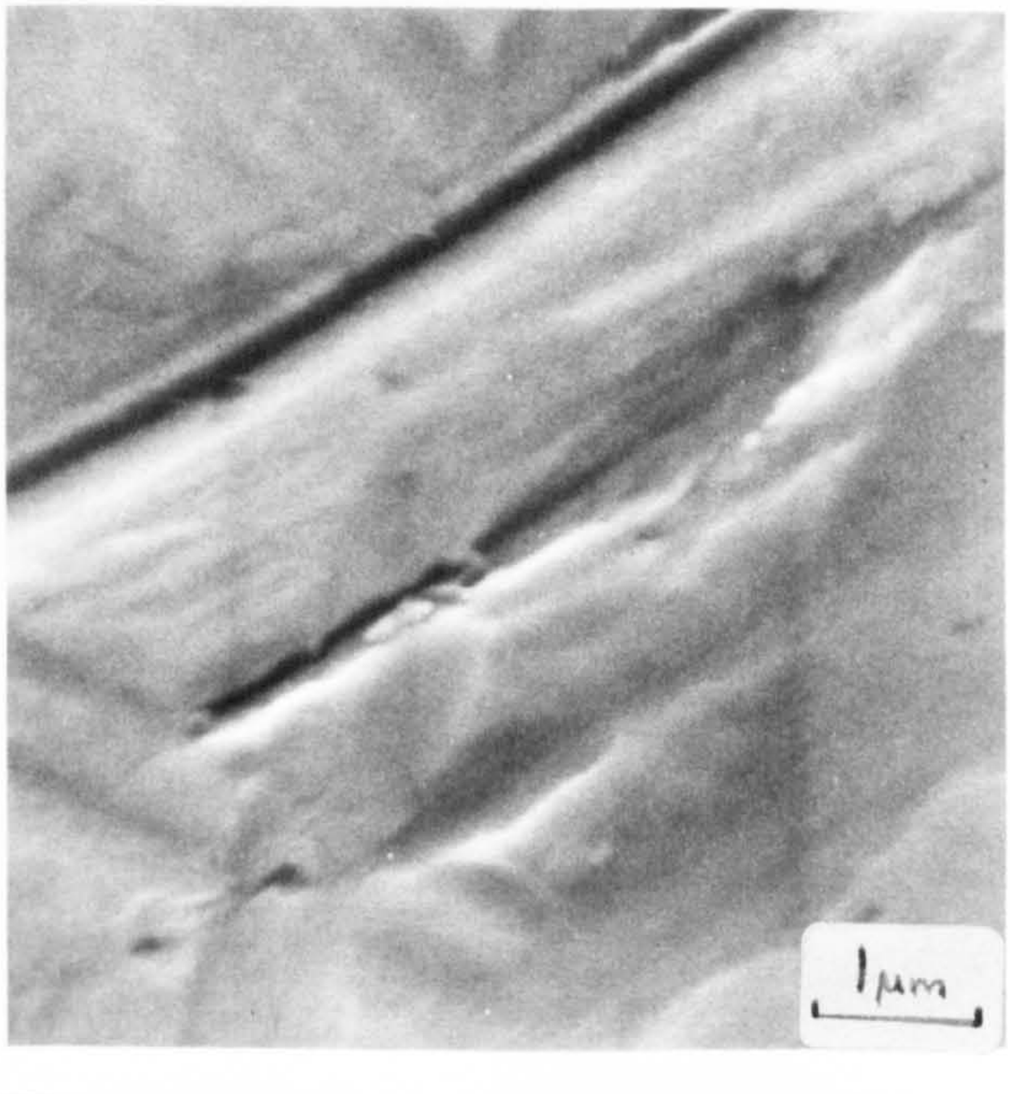

FIG. 19

Stereoscan photographs of the surface of mild steel (polished with 600 grade silicon carbide paper to a finish of 0.075 - o.1µm c.l.a.) to illustrate the relatively sharply grooved profile compared to Fe_3O_4 or Fe_3O_4 & Fe_2O_3 oxide surfaces (cf. Figs. 11 -13 or 14 - 16.)

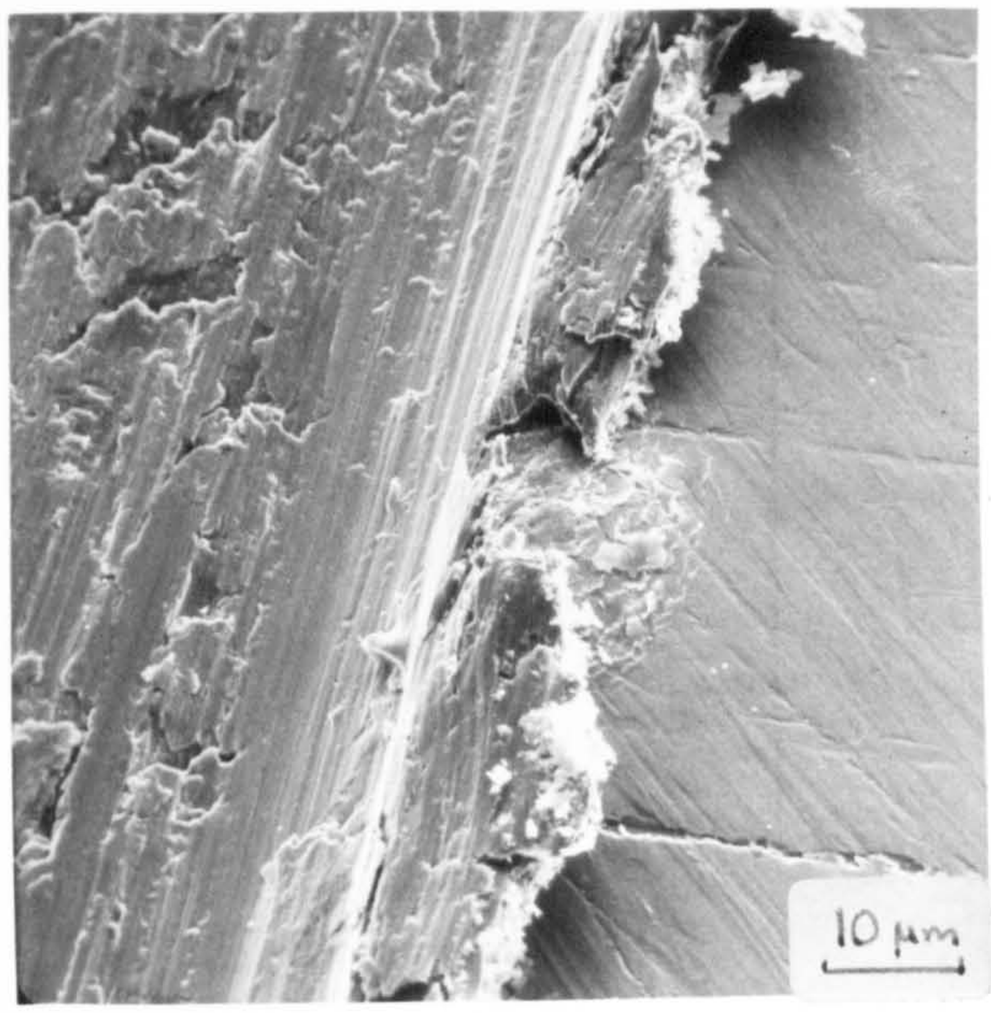

FIG. 20

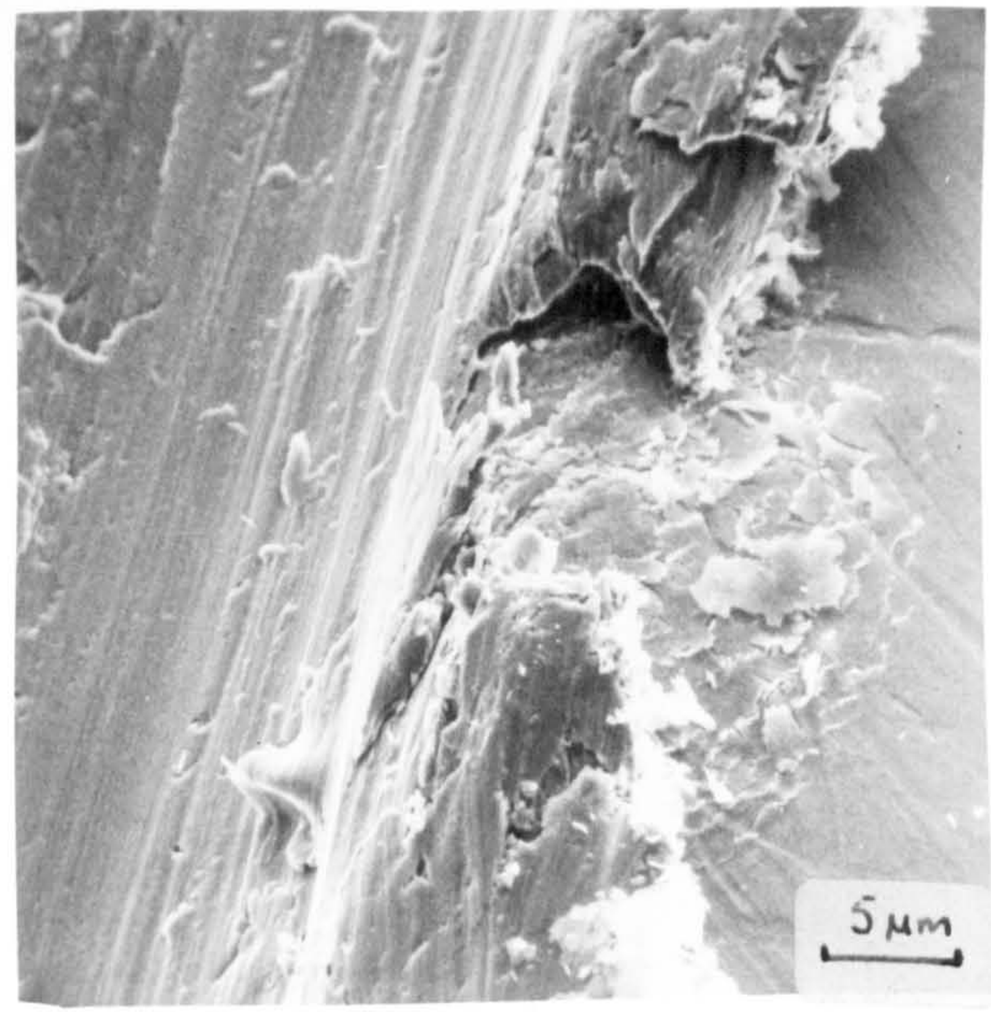

FIG. 21

FIG. 22

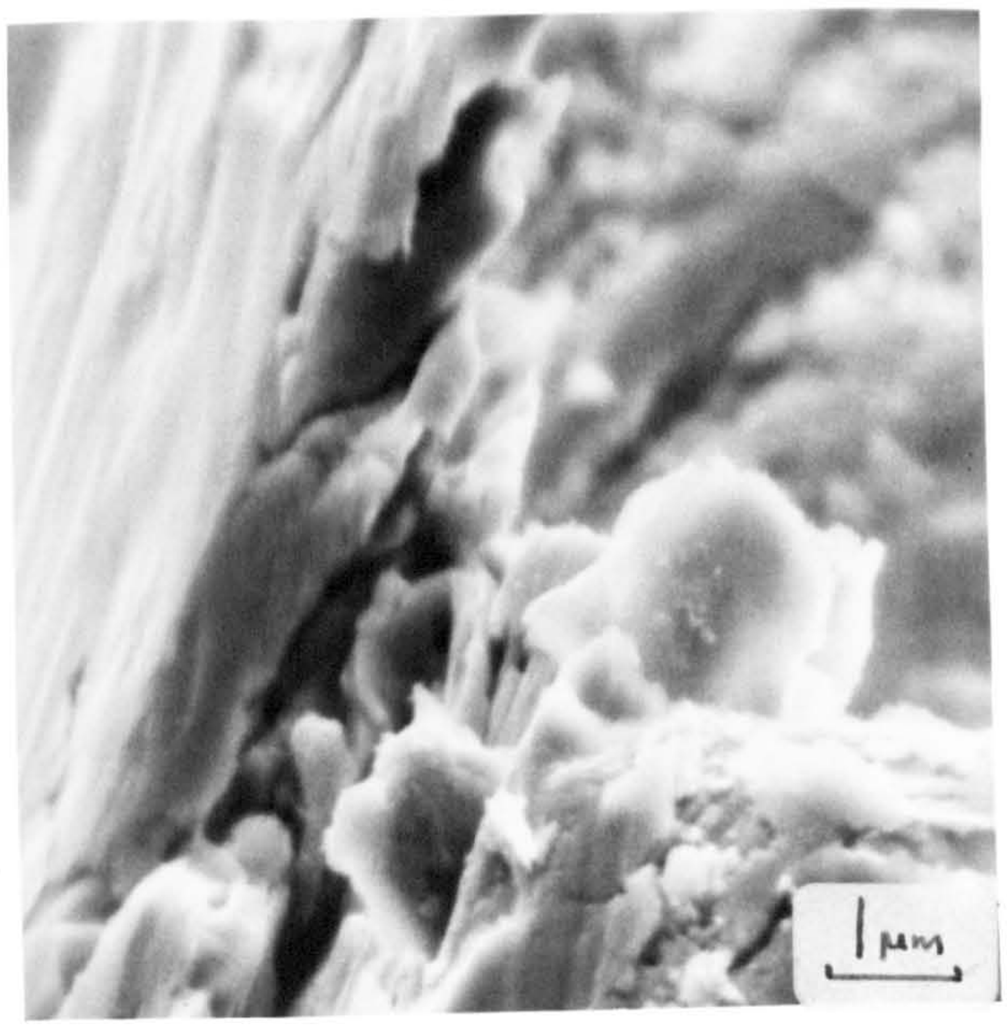

Fig. 23

Stereoscan photographs of a stressed (scratched) surface of 100 nm thick $Fe_3O_4/\alpha Fe_2O_3$ oxide (mild steel heated in an air furnace) showing the mode of rupture. The friable, but less extensive oxide fragmentation contrasts markedly with the larger plate-like oxide fragmentation (and observable over a wider area) obtained by stressing a 100nm thick Fe_3O_4 oxide surface illustrated in Figs. 24 - 27.

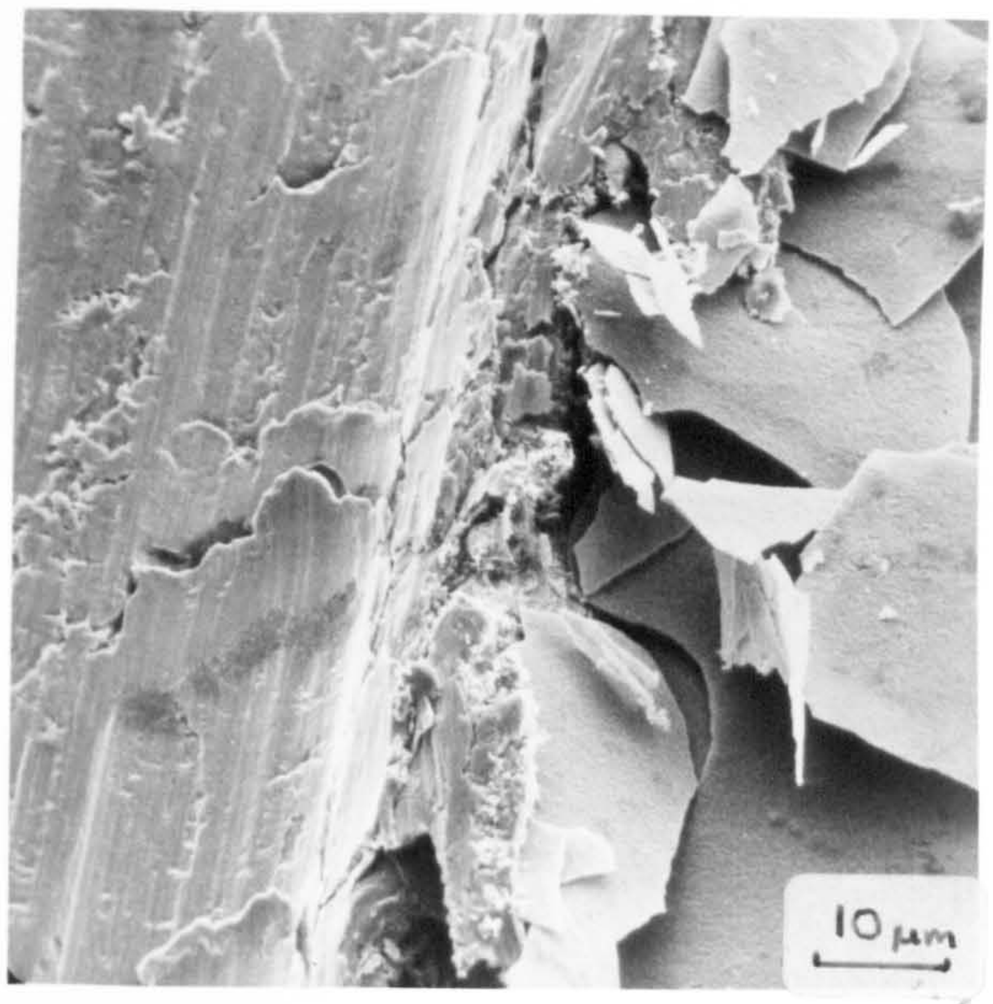

FIG. 24

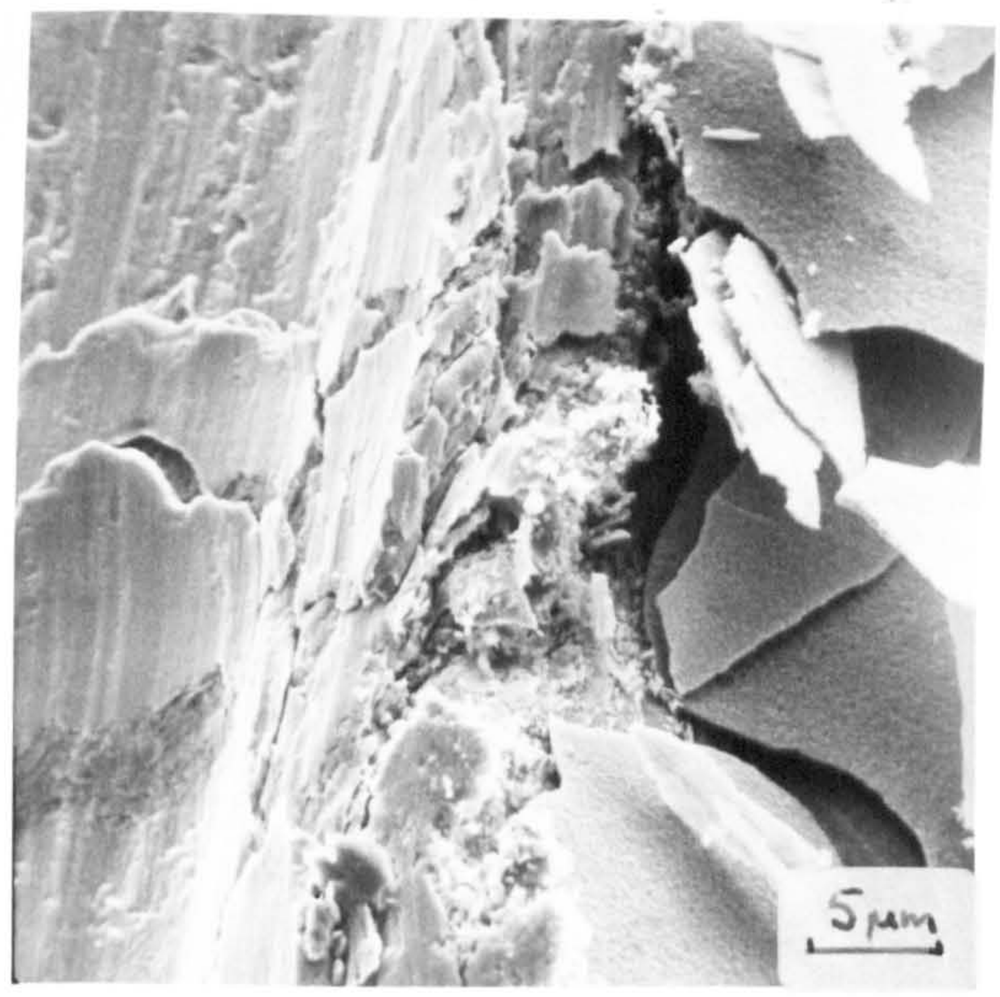

FIG. 25

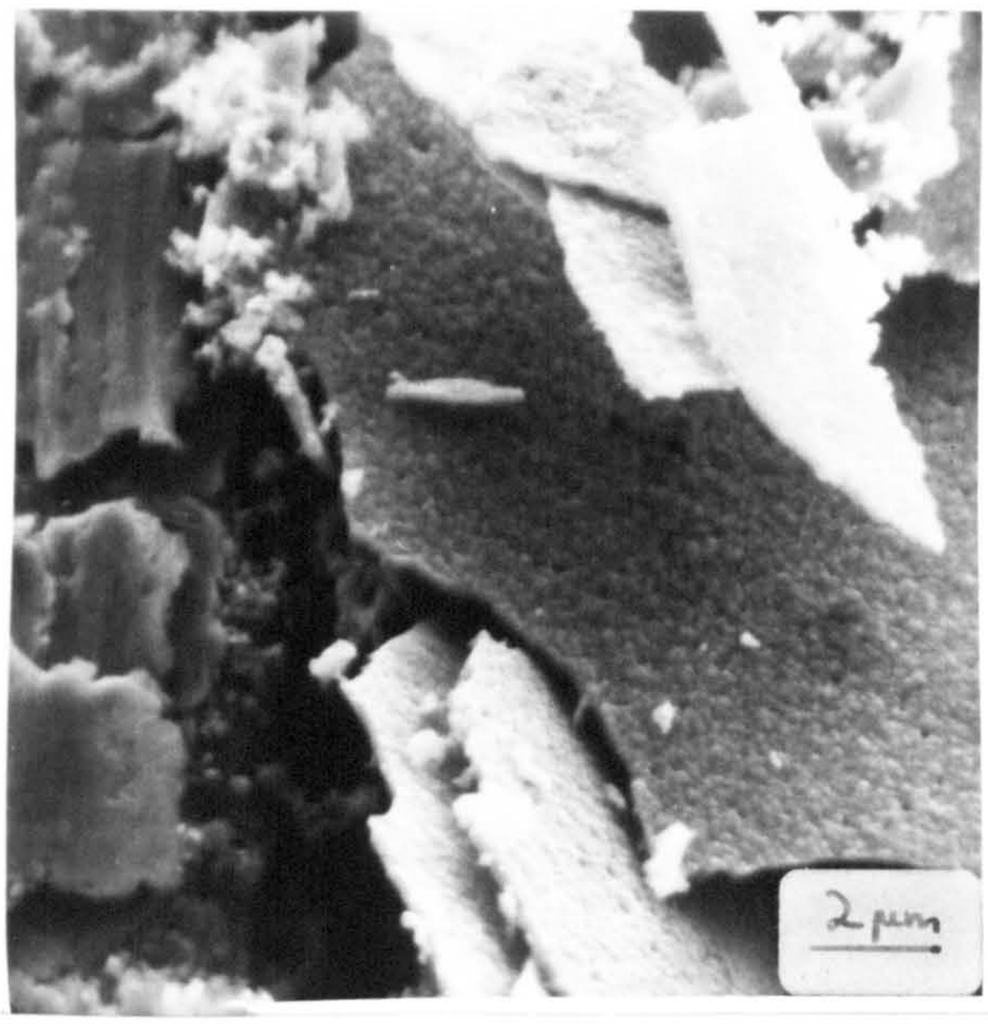

FIG. 26

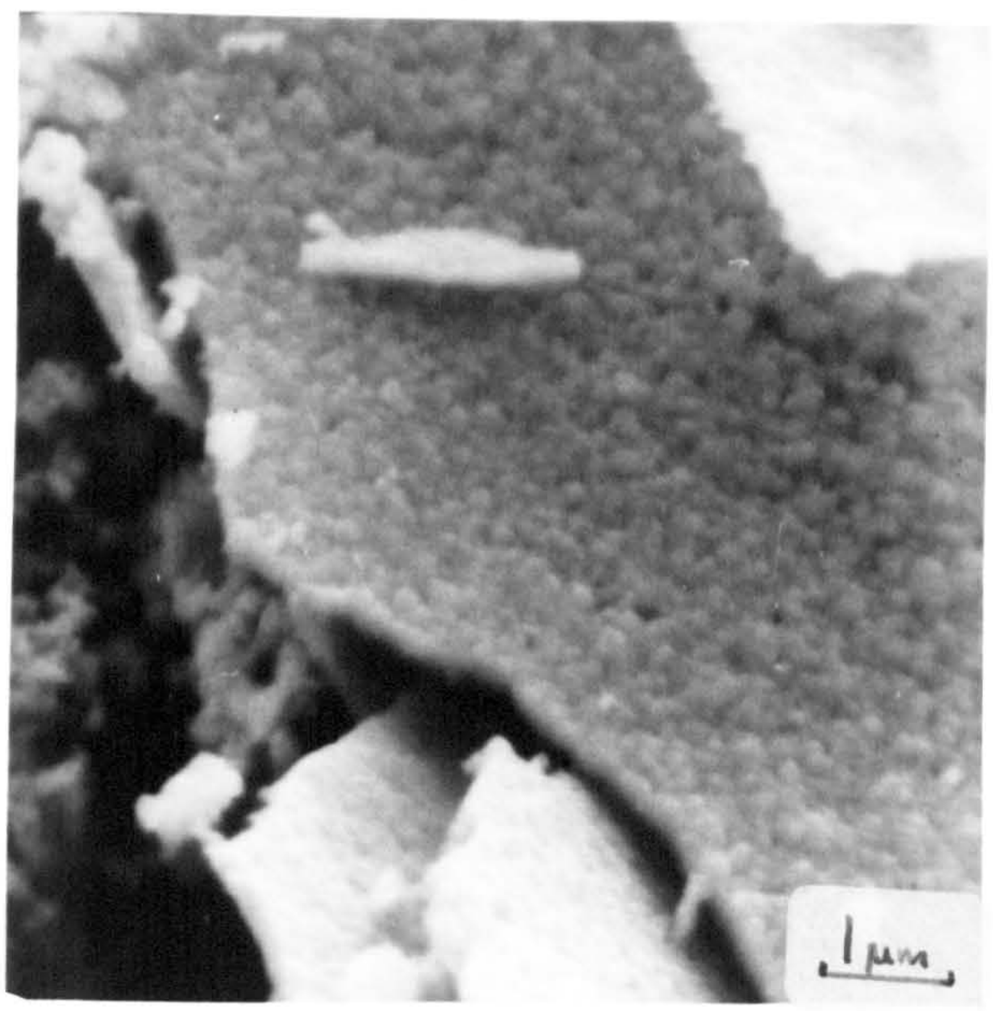

FIG. 27

Stereoscan photographs of a stressed (scratched) surface of 100nm thick Fe_3O_4 oxide (mild steel heated in a vacuum furnace) showing the mode of rupture. The extensive laminar plate-like oxide fragmentation contrasts markedly with the much less extensive smaller friable oxide fragmentation obtained by stressing a 100nm thick $Fe_3O_4/\alpha Fe_2O_3$ oxide surface illustrated in Figs. 20 - 23.

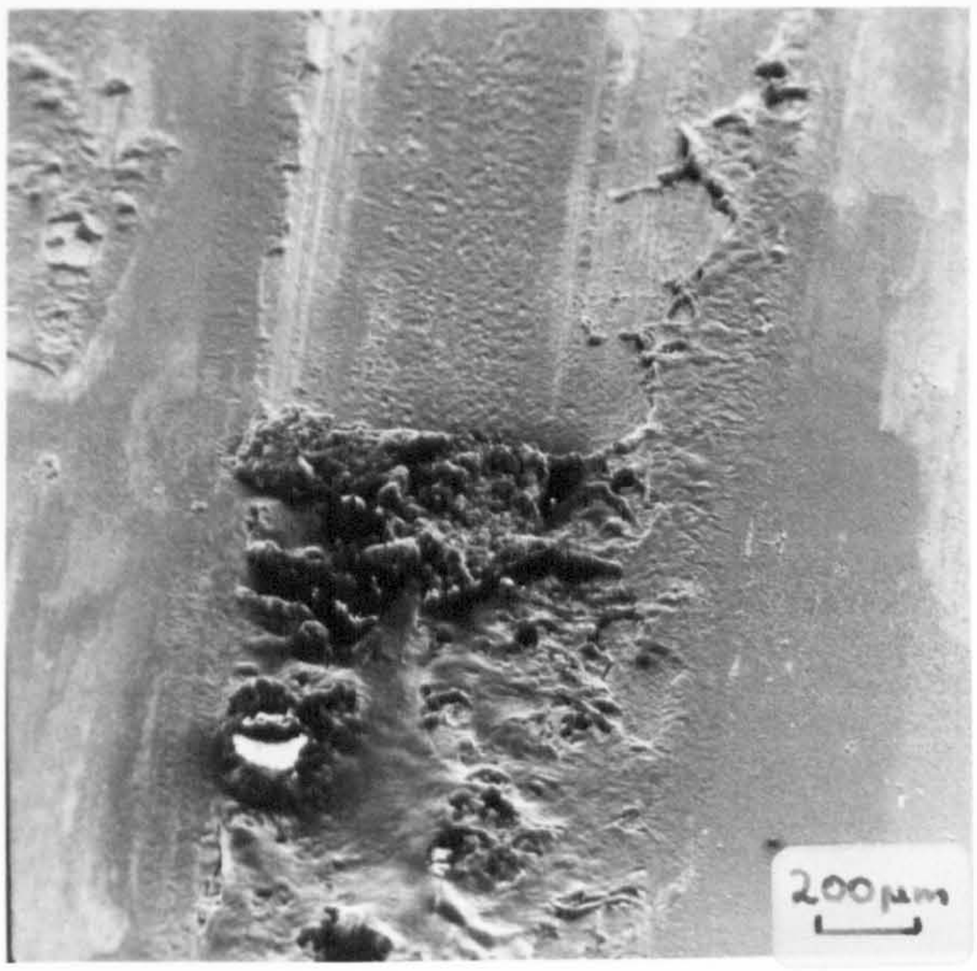

FIG. 28

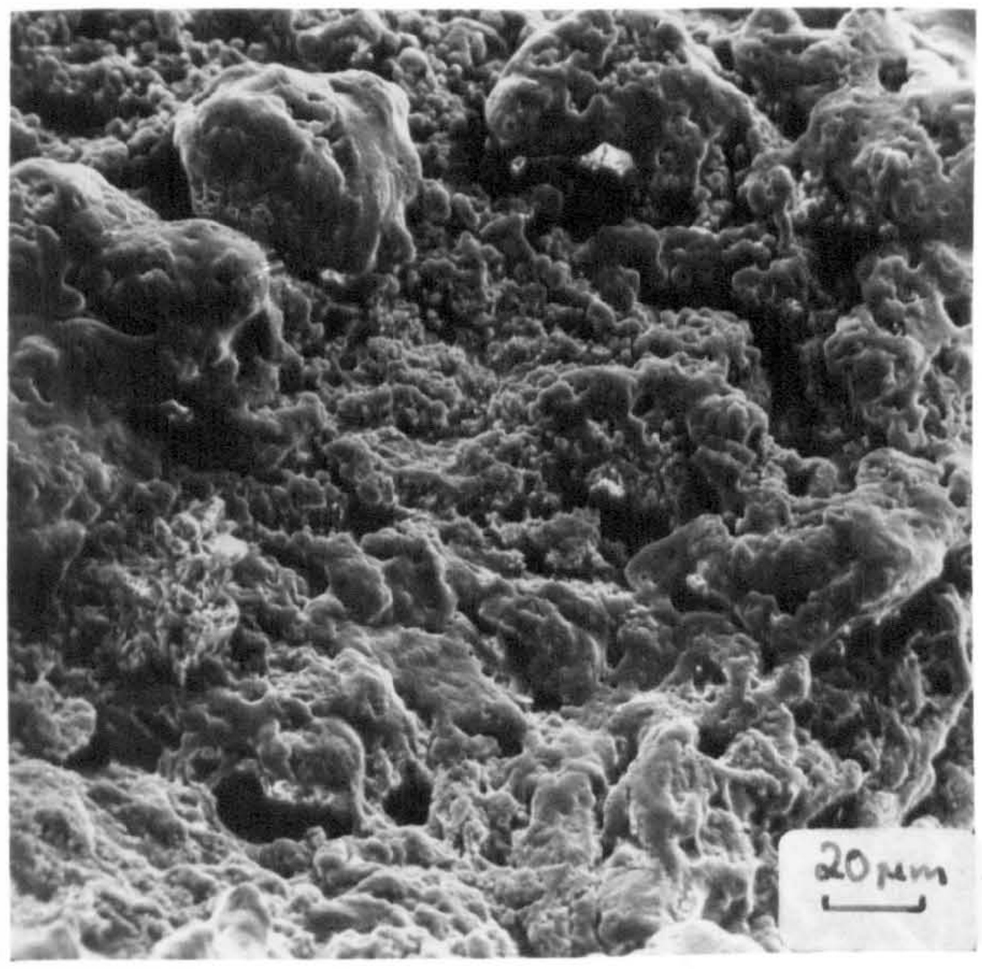

FIG. 29

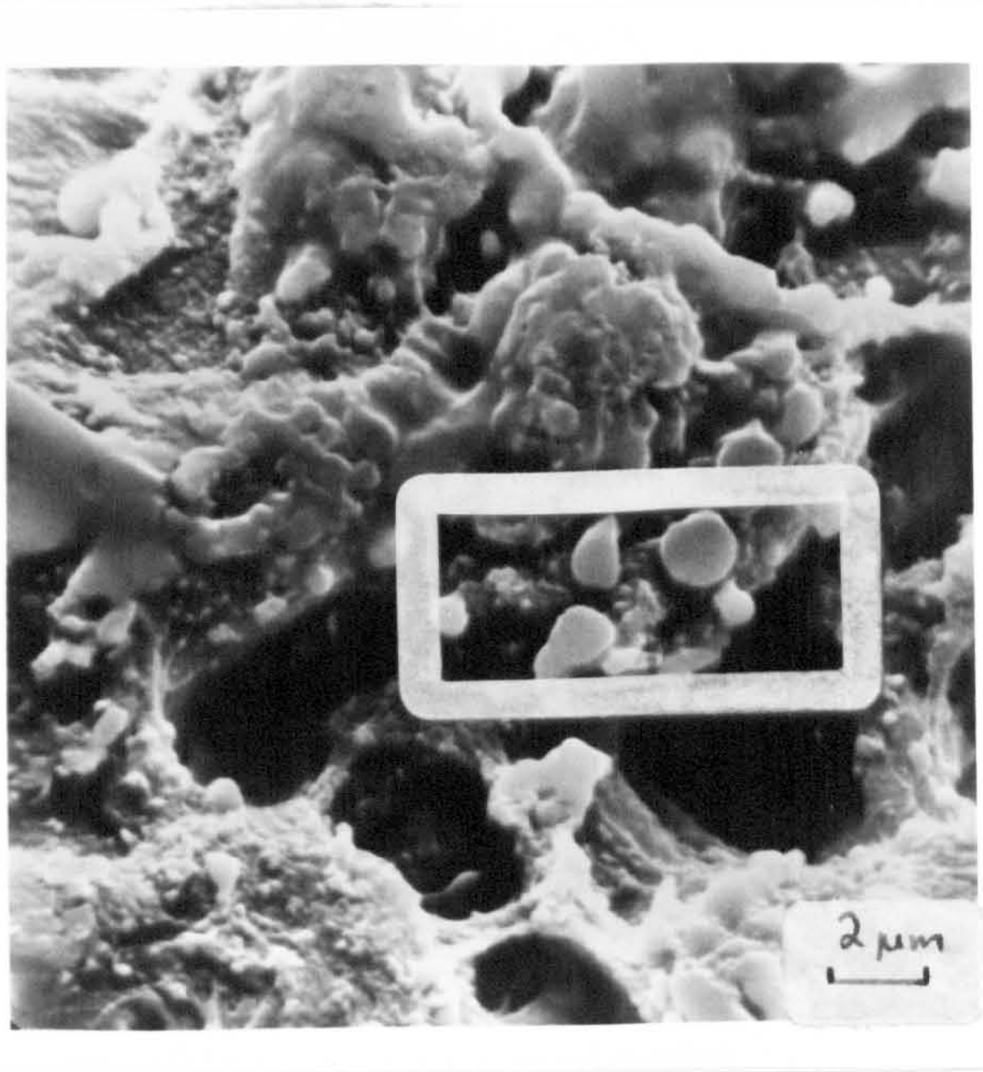

FIG. 30

Approximately 2.0µm diameter plate-like fragments embedded in P.V.C. after this polymer had been slid on a 100nm thick Fe_3O_4 surface.

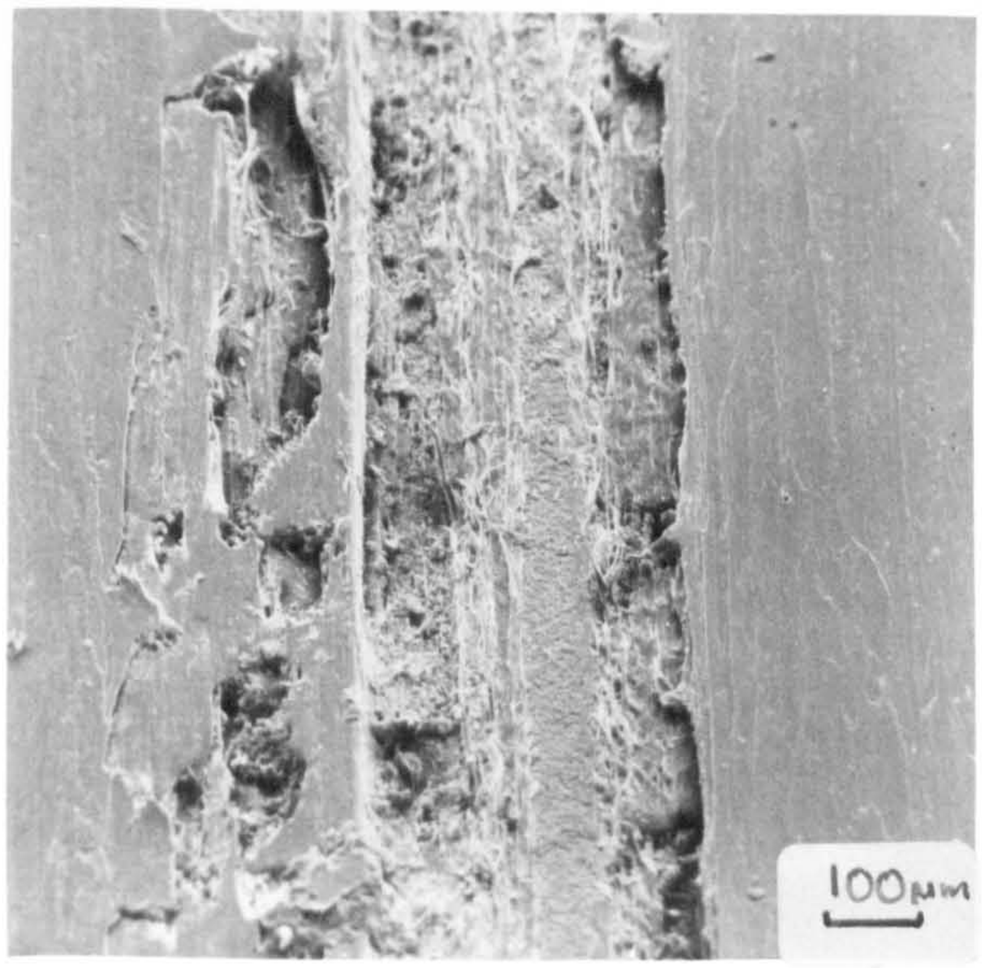

FIG. 31

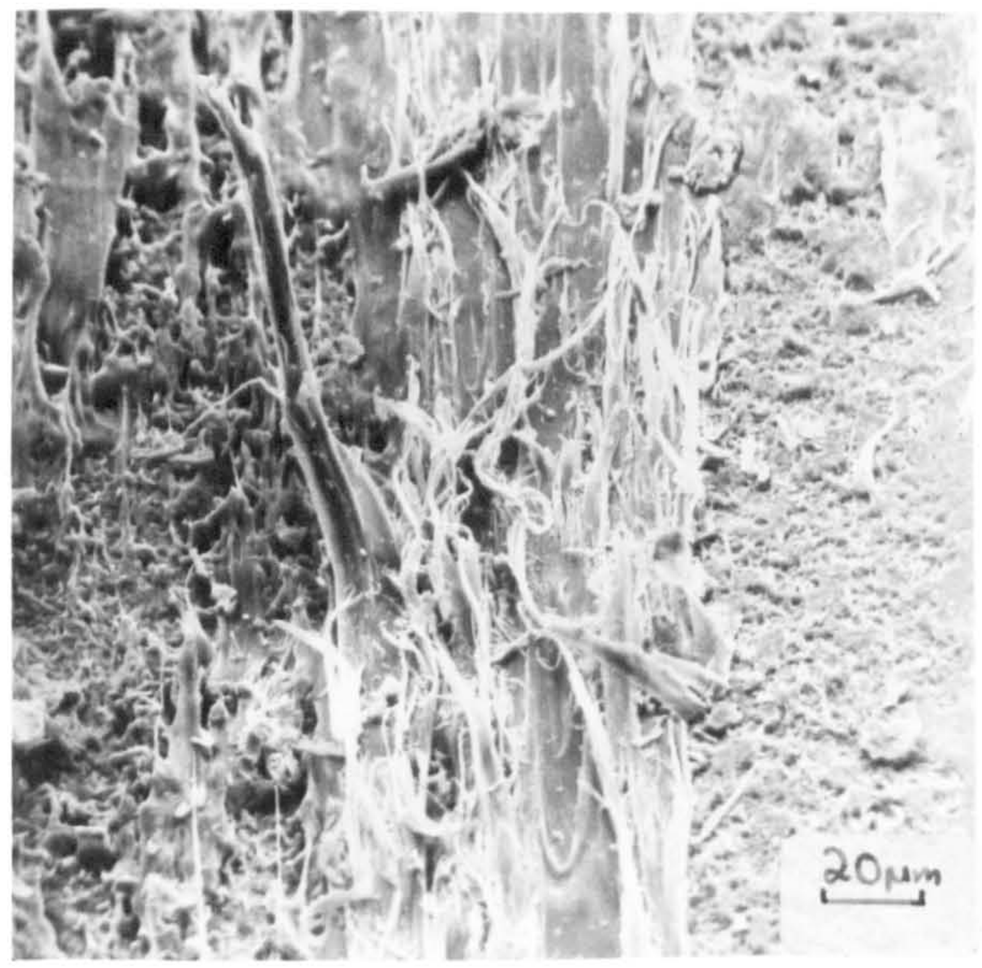

FIG. 32

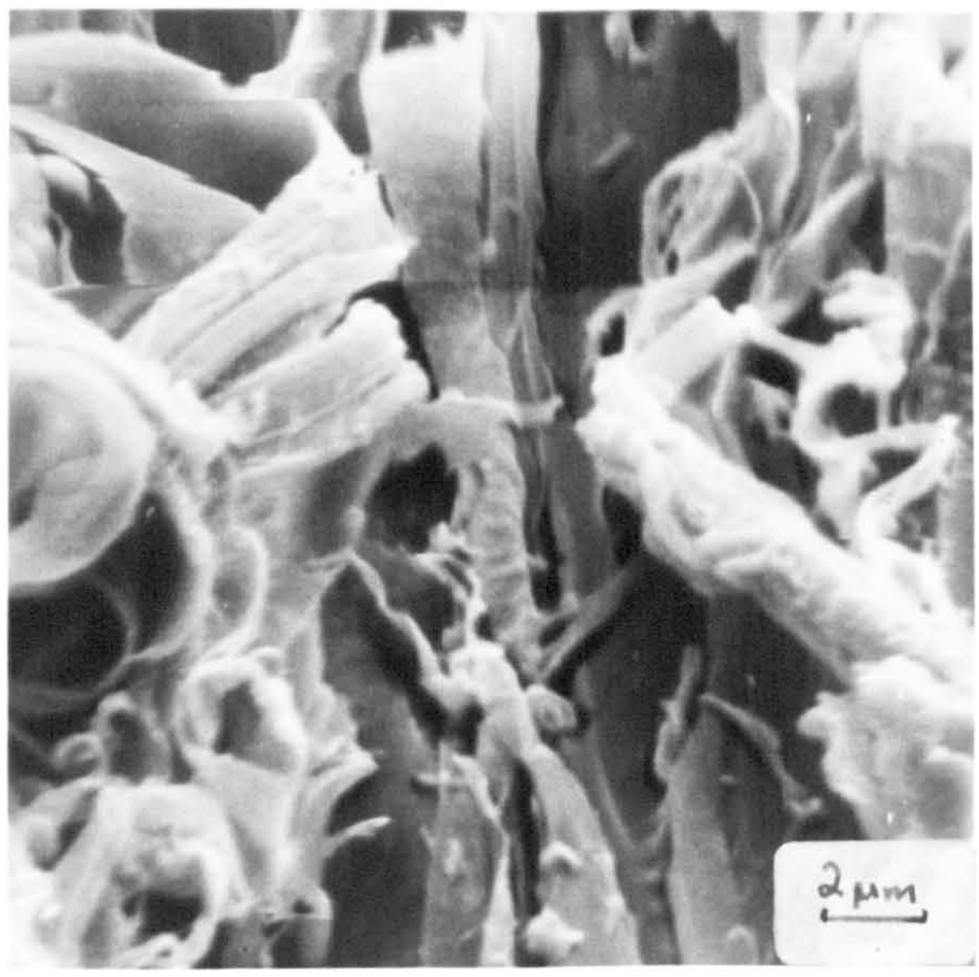

FIG. 33

The worn, but almost oxide free, surface of P.V.C. after it had been slid on a 100nm thick $Fe_3O_4/\alpha Fe_2O_3$ oxide surface.

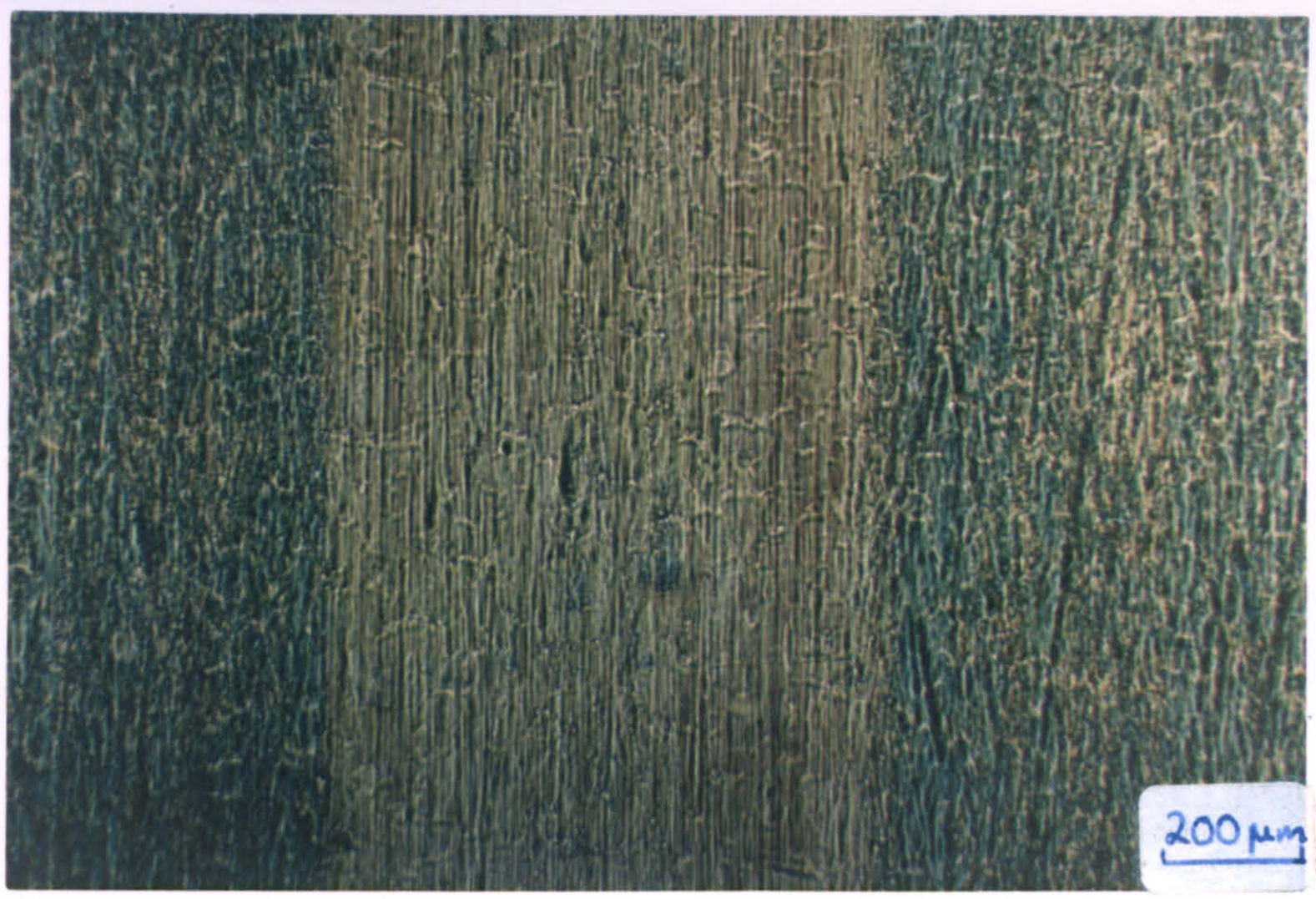

FIG. 34 Band of partially removed oxide on surface of 100nm Fe_3O_4 after P.V.C. had been sliding for 10 minutes.

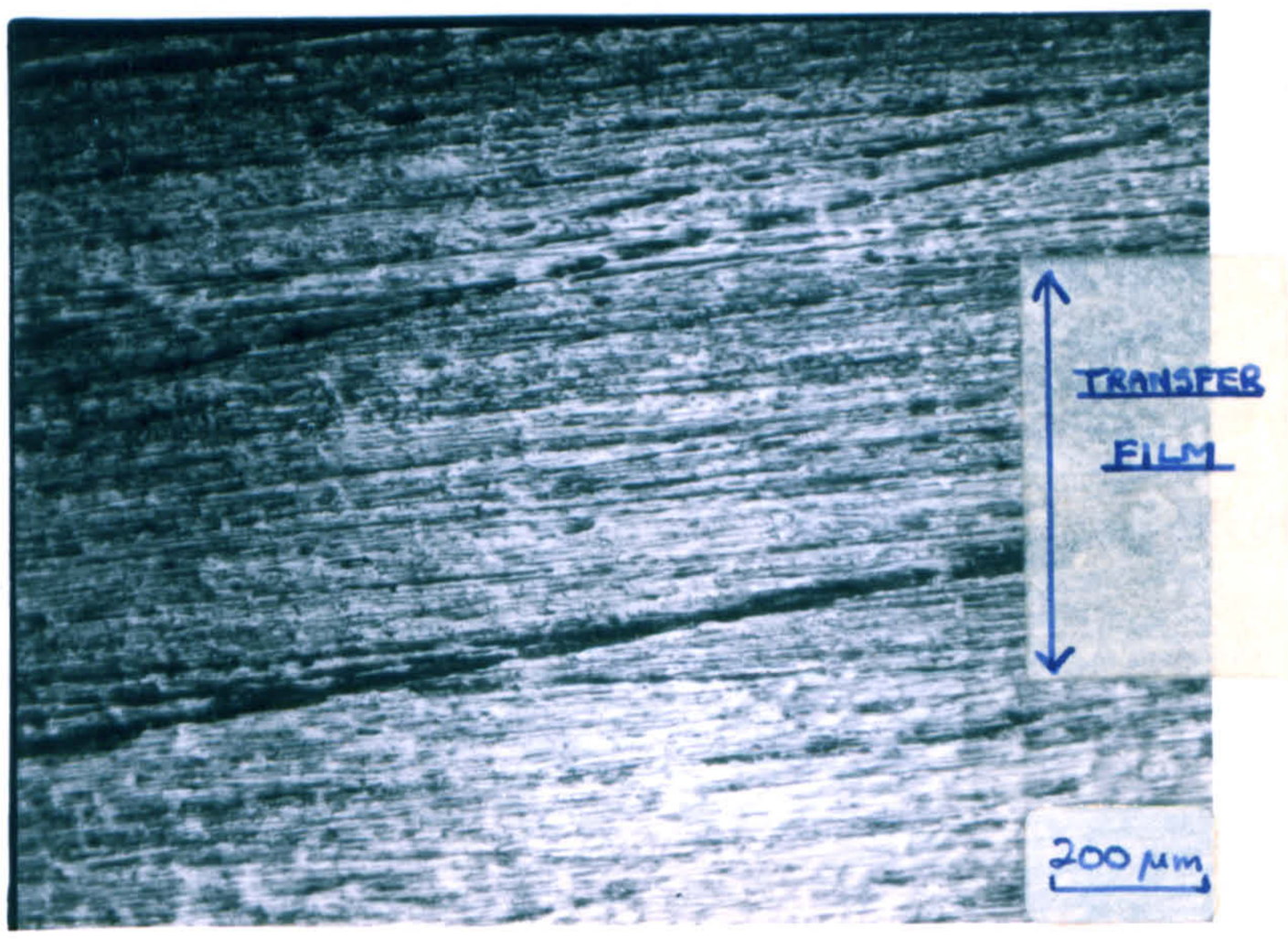

FIG. 35 Band of transferred polymer on surface of 100nm $Fe_3O_4/\alpha Fe_2O_3$ after P.V.C. had slid for 30 minutes.

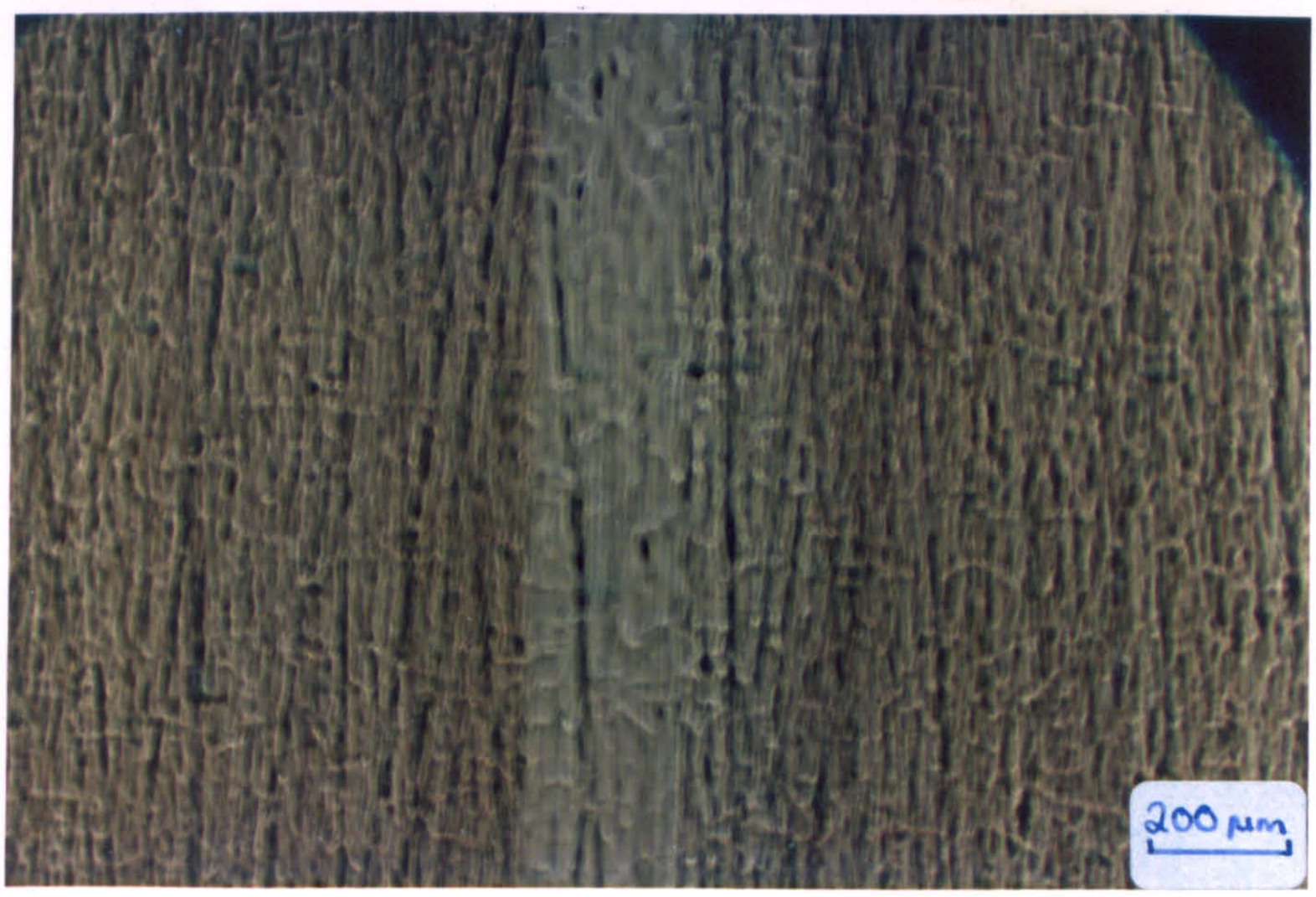

FIG. 36 Band of transferred polymer on surface of intact 100nm $Fe_3O_4/\alpha Fe_2O_3$ oxide after P.V.C. had been sliding for 40 minutes.

3.5.3.6 The Effect of Surface Oxide Conditions on the Wear Rate of P.T.F.E. and P.C.T.F.E. Sliding on Mild Steel.

P.T.F.E. and P.C.T.F.E. may be conveniently considered together here due to their predominantly crystalline characteristics (P.T.F.E.>P.C.T.F.E.) when compared to substantially amorphous polymers such as P.V.C. and Cl^{d}P.V.C. Both the P.T.F.E. and P.C.T.F.E. samples may be regarded as being highly crystalline. e.g. P.T.F.E. ≙ 90% * and P.C.T.F.E. ≙ 60% * and possessing melting points (Tm) of 603K and 484K respectively. P.T.F.E. is generally regarded as a unique polymer with respect to its low frictional properties. These are currently attributed to its smooth molecular profile and orientation and transfer during sliding[100]. No correlation between the coefficient of friction and wear properties, however, is generally regarded to exist and so additional factors must be included in the present discussion.

The generally high wear rate of P.T.F.E. on all types of surface examined may be partially ascribed to its inherently poor mechanical (tensile, compressive, shear) strength. For instance, the tensile strength of the P.T.F.E.used was measured as 16.9 MN m^{-2} (Standard ASTMmethod) which is very low compared with 33.0 MN m^{-2} (P.C.T.F.E.) 50.0 MN m^{-2} (P.V.C.) and 62.5 MN m^{-2} (Cl^{d}P.V.C.). It must be noted of course that in common with other plastics the mechanical properties in general change dramatically with temperature and strain rate etc. (as might be expected in 'wearing' situations).
When heated above its melting point P.T.F.E. becomes a transparent gel that is mechanically weak and will not flow without fracture. The zig-zag carbon chain of P.T.F.E. is twisted into a helical configuration to relieve repulsions between fluorine atoms on alternate carbon atoms[101]. Thus the tight sheath of fluorine atoms effectively reduce interchain forces to a minimum and help keep the chains extended, both factors contributing to high thermal stability at the cost of mechanical strength. The existence of fine transfer films on all the surfaces examined, however, seems to have had quite a considerable and significant

* The Manufacturer's figure.

levelling effect on the magnitude of wear rate (FIG. 9). Thus although in other polymer systems the wear rate had either been raised or lowered (by for instance a 100 nm Fe_3O_4 / $\propto Fe_2O_3$ counter surface on the mild steel drums) in this case the rate stayed relatively stable in the region of 4×10^{-8} cm^3/cm. This is in spite of the fact that Fe_3O_4 oxide fragments were observed on the surface of the P.T.F.E. specimens at the end of the experiment suggesting some small degree of break up. In common with the P.V.C. and Cl^dP.V.C. results the air furnace oxide (100 nm Fe_3O_4 / $\propto Fe_2O_3$) remained much more intact throughout the sliding.

In the P.C.T.F.E. experiments the presence of both systems of thick oxide seem to have had a markedly beneficial effect on the wear rate in similar fashion to Cl^dP.V.C. Clearly the absence of thick transfer films in both cases seem to be the rate controlling parameters. This coupled with the fact that both oxides remained intact throughout the experiment would seem to suggest that their smoothness and greater hardness, rather than any low shear properties, were important in promoting good wear properties in this instance. It must be noted here too that P.C.T.F.E. was distinctly less ductile than P.T.F.E. at room temperature. cf. P.C.T.F.E. 22% elongation to break; P.T.F.E. 175% elongation to break. Hence, very thin, continuous, beneficial transfer films were not likely to occur. Indeed if transfer had occurred this undoubtedly would have had a deleterious effect on wear rate in common with other polymers of low ductility[3,104 (P.6)]. In the current situation for P.C.T.F.E. the full effect of low wear rate associated with sliding on intact hard surfaces (oxides) was able to manifest itself without the complication of the transfer film levelling effect previously described for P.T.F.E.

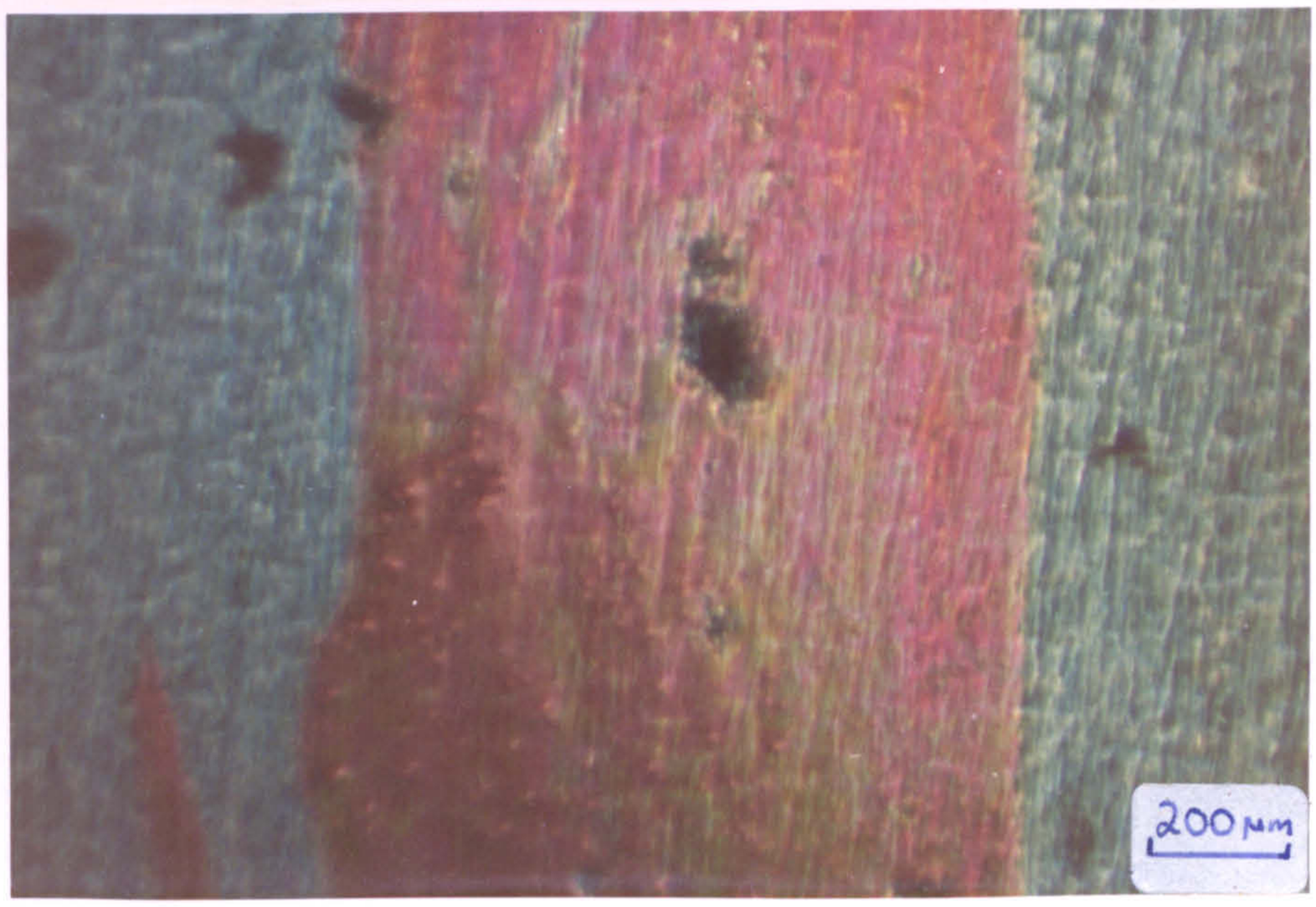

FIG. 37 Band of transferred polymer on surface of mild steel after P.T.F.E. had slid for 45 minutes. (The sample was heat treated in an air furnace for 15' at 750K to promote interference colour contrast.)

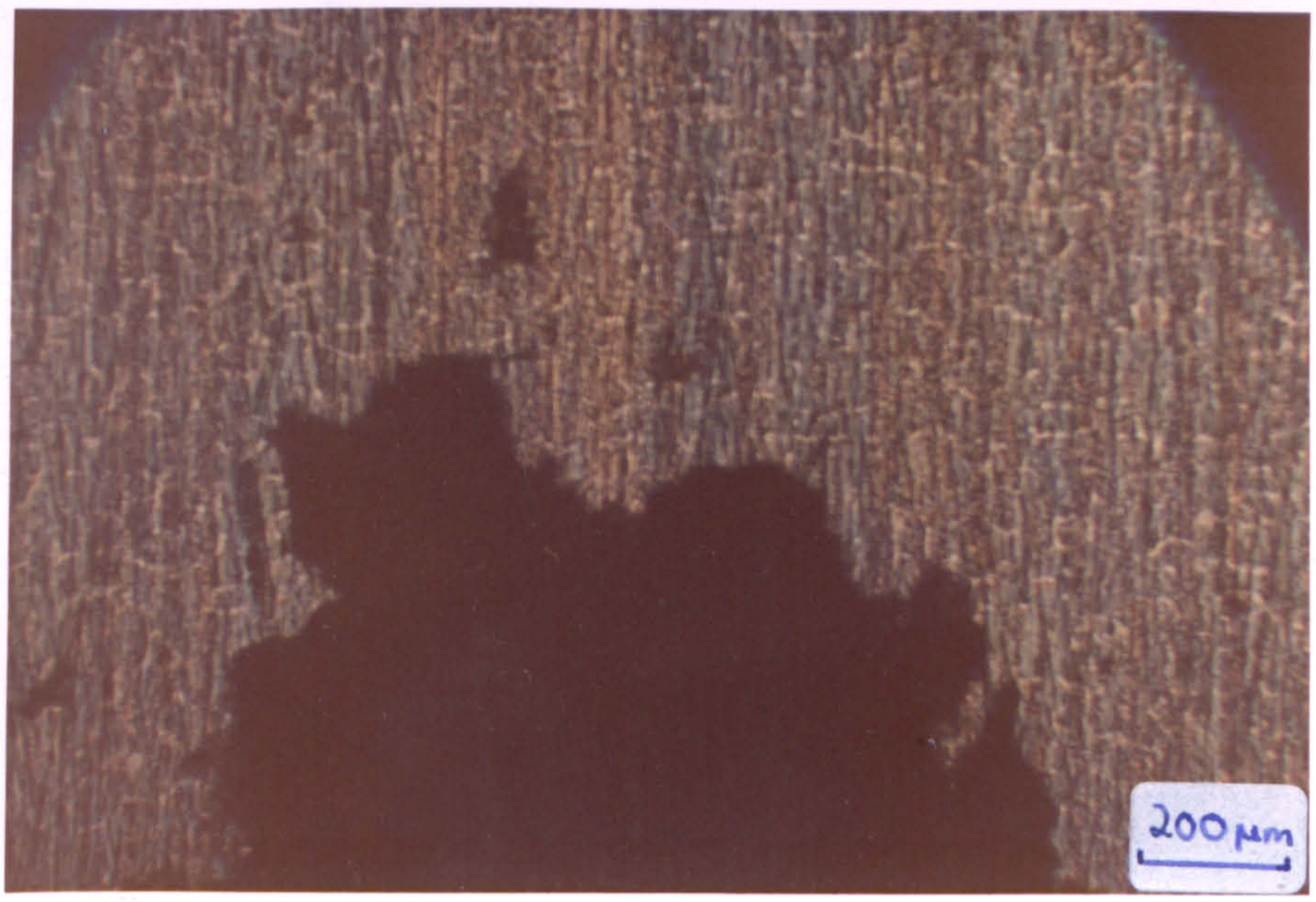

FIG. 38 Transferred lump of polymer on oxide surface after P.T.F.E. had slid on 100nm Fe_3O_4 for 45 minutes - note areas of removed oxide.

FIG. 39 Ditto- showing P.T.F.E. smeared on both ruptured and intact oxide.

FIG. 40 Ditto - showing embedded oxide fragments in P.T.F.E. sample surface.

FIG. 41 Polished oxide surface after P.T.F.E. had slid on 100nm Fe_3O_4/αFe_2O_3 for 45 minutes - only small evidence of oxide rupture and polymer transfer.

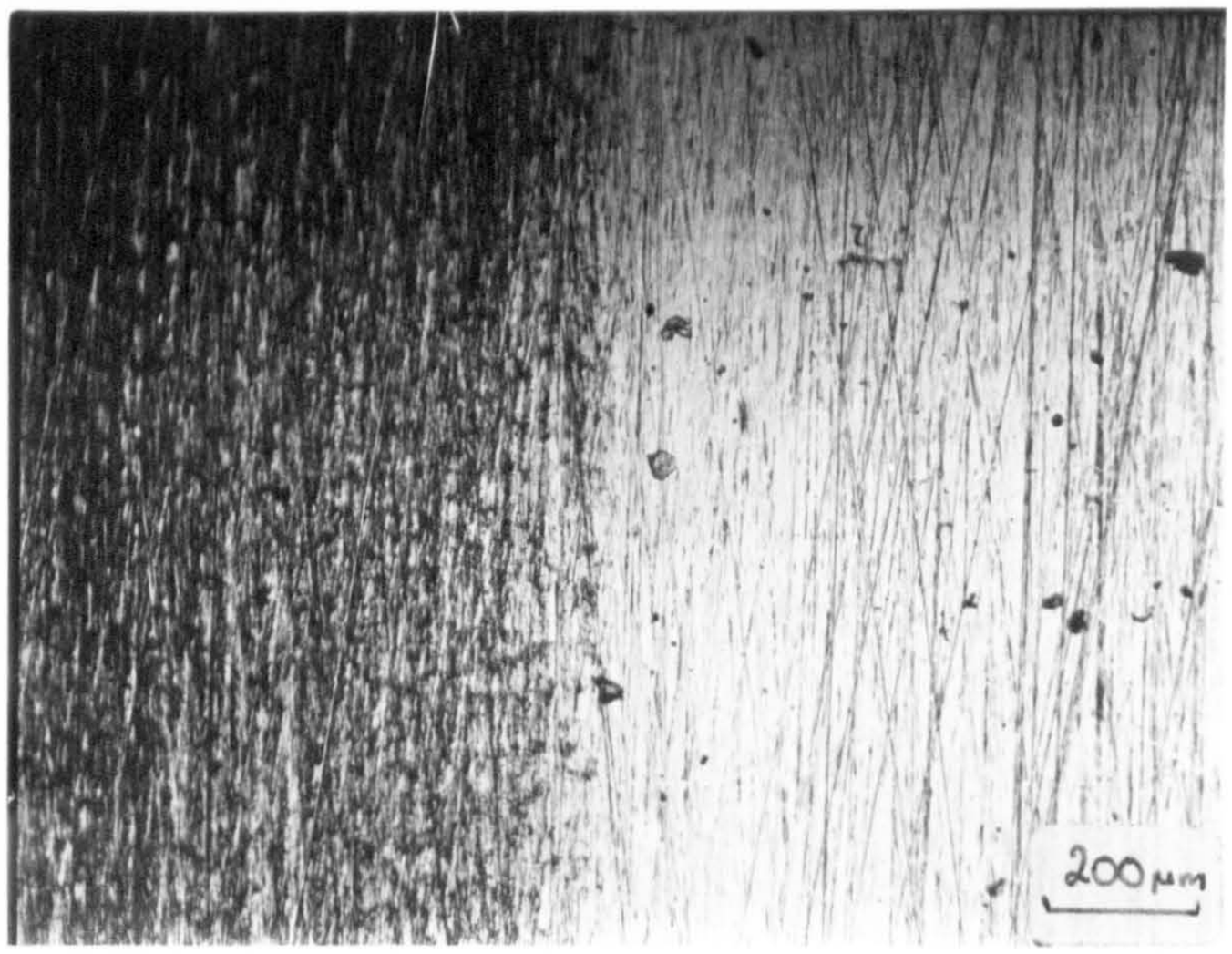

FIG. 42 Left. Smeared polymer on mild steel surface after P.C.T.F.E. had slid for 30 minutes.

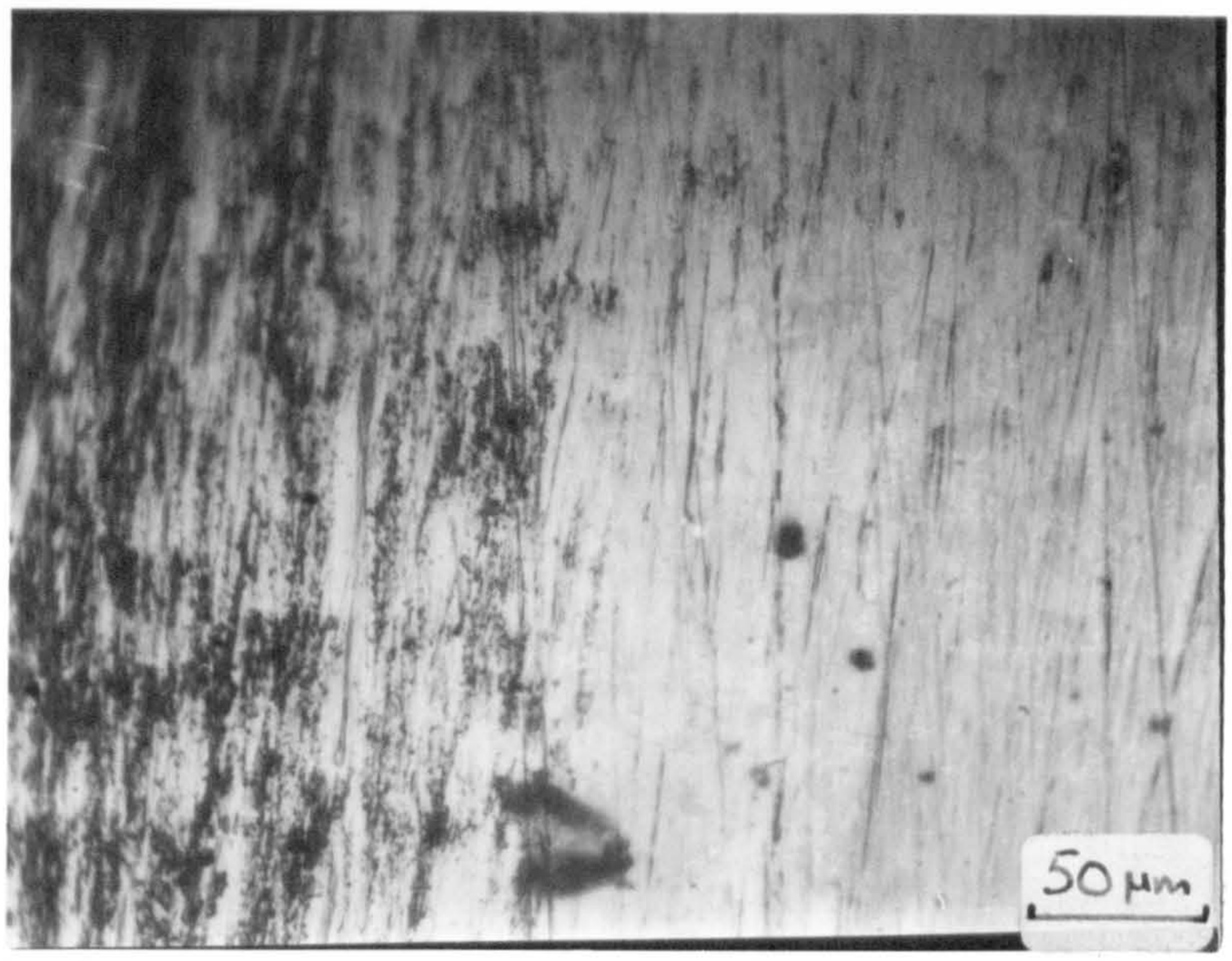

FIG. 43 Ditto - showing discontinuous nature of the smearing.

FIG. 44 Ditto - heat treated.

3.6 Specific Conclusions (SECTION ONE)

Within the experimental constraints of the current investigations the following conclusions are proposed:-

3.6.1 The Degradation Characteristics of P.V.C. and Cl^{d}P.V.C. During Sliding.

(1) The main degradation process associated with the wear and sliding of P.V.C. on mild steel is fundamentally mechano-chemical with only small localised areas being thermally degraded. (Cl^{d}P.V.C. may behave similarly but was not specifically studied in this respect).

(2) It is most likely that the P.V.C. mechano-chemical degradation process proceeds via random polymer chain rupture and subsequent disproportionation reaction mechanisms.

(3) The degree of polymer degradation when P.V.C. and Cl^{d}P.V.C. are slid on mild steel or mild steel oxides is fundamentally linked to the physical state and flow characteristics of the polymers before and during the wearing process.

(4) The temperature build up at a polymer/mild steel interface can change the flow characteristics of the plastic which in turn can alter the mode of dissipation of the mechano-chemical forces. The result is that any wearing process that increases surface temperatures can

potentially decrease the degree of polymer chain scission.

(5) If there are thick (100nm) oxides present on a mild steel surface and they are harder and more rigid than their substrate then greater mechano-chemical degradation takes place in the associated 'wearing' polymer countersurface. This is a result of the facilitated transfer of mechano-chemical energy to the sliding interface.

3.6.2 Wear Rate Characteristics of P.V.C., Cl^dP.V.C., P.T.F.E., and P.C.T.F.E. During Sliding.

(6) When undamaged 100nm thick Fe_3O_4 and $Fe_3O_4/\alpha Fe_2O_3$ oxides are present on the surface of a mild steel countersurface on which the polymers are worn then improved wear rates are obtained due to the smoother surface topography and the greater hardness of the oxides relative to their substrate.

(7) The wear rate of P.V.C. on mild steel increases approximately linearly with increasing load. (As predicted, within certain limits, by simplified abrasive and adhesive wear theories).

(8) The wear rate of P.V.C. on mild steel varies non-linearly with increasing speed in such a way as to suggest the approach of a wear minima apparently due to a critical surface temperature region.

(9) Macro transfer films appear to be delcterious to wear rate and their appearance controlled by the temperature rises at the interface and the ductility, tensile strength and flow characteristics of individual polymers.

(10) Micro transfer films (as produced by P.T.F.E.) promote a 'levelling' effect on the wear rates when polymers are slid on mild steel and mild steel oxide countersurfaces.

(11) Polymers with high values of ductility (% elongation to break) appear to be associated with the rupture of thick (100nm) oxides on mild steel surfaces.

(12) 100nm Fe_3O_4 layers on mild steel tend to break up more easily into lamellar fragments than equivalent surfaces of 100nm thick $Fe_3O_4/\alpha Fe_2O_3$. When embedded in a polymer however, and in the absence of micro-transfer films, Fe_3O_4 acts as a polishing agent in contrast to the coarser abrasive action of $Fe_3O_4/\alpha Fe_2O_3$.

SECTION TWO

4. A STUDY OF THE POTENTIAL REACTIVITY OF OXIDE FREE IRON SURFACES IN THE PRESENCE OF AN ANALOGUE COMPOUND OF P.T.F.E. ($n\text{-}C_5F_{12}$)

4.1 Introduction and General Philosophy

The wear process of various polymers such as P.V.C., P.T.F.E., etc. have been studied and described in SECTION ONE. The experiments involved mild steel countersurfaces possessing varying thicknesses of oxide layers (i.e. 2-100nm). In order to compliment this work it was thought desirable to examine the possibility of interactions between one of these polymers and a mild steel countersurface completely free of any interfacial oxide. The following SECTION TWO is a description of experiments designed to meet this objective.

The use of specialised ultra high vacuum apparatus was essential and in view of the experimental complexity the work had to be confined to a few, carefully chosen, investigations. Furthermore as it is difficult to produce and maintain an exact representation of an oxide free mild steel surface with all the usual trace elements (such as carbon, silicon, sulphur, etc., etc.) in a free or chemically combined state, pure iron was selected instead. Mild steel consists of approximately 99.6% w/w pure iron and so this was not an unreasonable substitution.

It has been reported by MORECROFT [138-140] and others that, under conditions of ultra high vacuum, oxide free iron will promote the breakdown of long chain alkanes and aliphatic carboxylic acids into smaller molecules. More recently a comprehensive survey of this type of reaction has appeared[141] (Vol. 2 P.66) in tabular review form. As freshly exposed metal surfaces are continually being generated by processes such as wear and metal fatigue, it is reasonable to suppose that interface sites are therefore potentially very reactive for at least a few

nanoseconds before the usual oxides form. It was decided, therefore, to establish whether a material such as P.T.F.E. (used in bearing manufacture) might reasonably be expected to degrade under such conditions. Dodecafluoro-n-pentane n C_5F_{12} was chosen to simulate part of the P.T.F.E. chain allowed to come in contact at 10^{-7} N m^{-2} and ambient temperature with a freshly prepared clean iron film on borosilicate glass (Pyrex) produced by an evaporation process in situ from an iron wire wrapped round a tungsten filament. Other techniques could have been used for film formation[142] such as ion bombardment but in this particular case evaporation followed by condensation was the most readily available. My calculations showed that by conductiong the experiment at U.H.V. (i.e.$<10^{-7}$ N m^{-2} pressure) there were not sufficient molecules of of oxygen present in the reaction chamber to form even one monolayer of oxide on the iron surface*. Hence the term 'clean iron' is essentially one of indirect implication by virtue of the conditions chosen but does not necessarily preclude impurities other than oxygen.

The events inside the reaction chamber were followed with an M.S.10 mass spectrometer and ε modified Pirani gauge. As the results subsequently endorsed, the high volatility of the fragments produced ruled out analysis by an alternative technique such as gas/liquid chromatography which would have given lower resolution in this case. This is quite apart from the experimental difficulties of sweeping the low quantities of reaction species into the column with argon gas.

More specific details of technique, apparatus design and sample preparation etc., etc., appear in sections immediately following this introduction.

* See 'calculations' in APPENDIX 9

4.2 Description of Apparatus

(1) Reaction Vessel.

(2) Vacuum System.

(3) Mass Spectrometer.

4.2.1 Reaction Vessel. (FIGS. 45 - 49)

This consisted of a(500ml) $5 \times 10^{-4} m^3$ Pyrex glass flask inside which were positioned a pair of stainless steel electrodes culminating in an(0.011") 280μm tungsten wire filament wrapped with fine iron wire. Experiment showed that the tungsten wire had to be the correct thickness to promote vapourisation of the iron without alloying when the current was applied. The current required for this was approximately 8-9 amperes at 12 volts.

Connected to the chamber was a modified Pirani gauge for monitoring pressure changes in the region$(10^{-1}\text{-}10^{-5}$ torr$)$ $10\text{-}10^{-3}$ N m^{-2} and a cold trap for removing condensible vapours when necessary.

Sample vapour introduction to the reaction chamber was restricted initially by a glass break-seal and later in time, after this seal had been broken, controlled by a high vacuum leak valve.

FIG. 45 — "CLEAN" IRON REACTION VESSEL

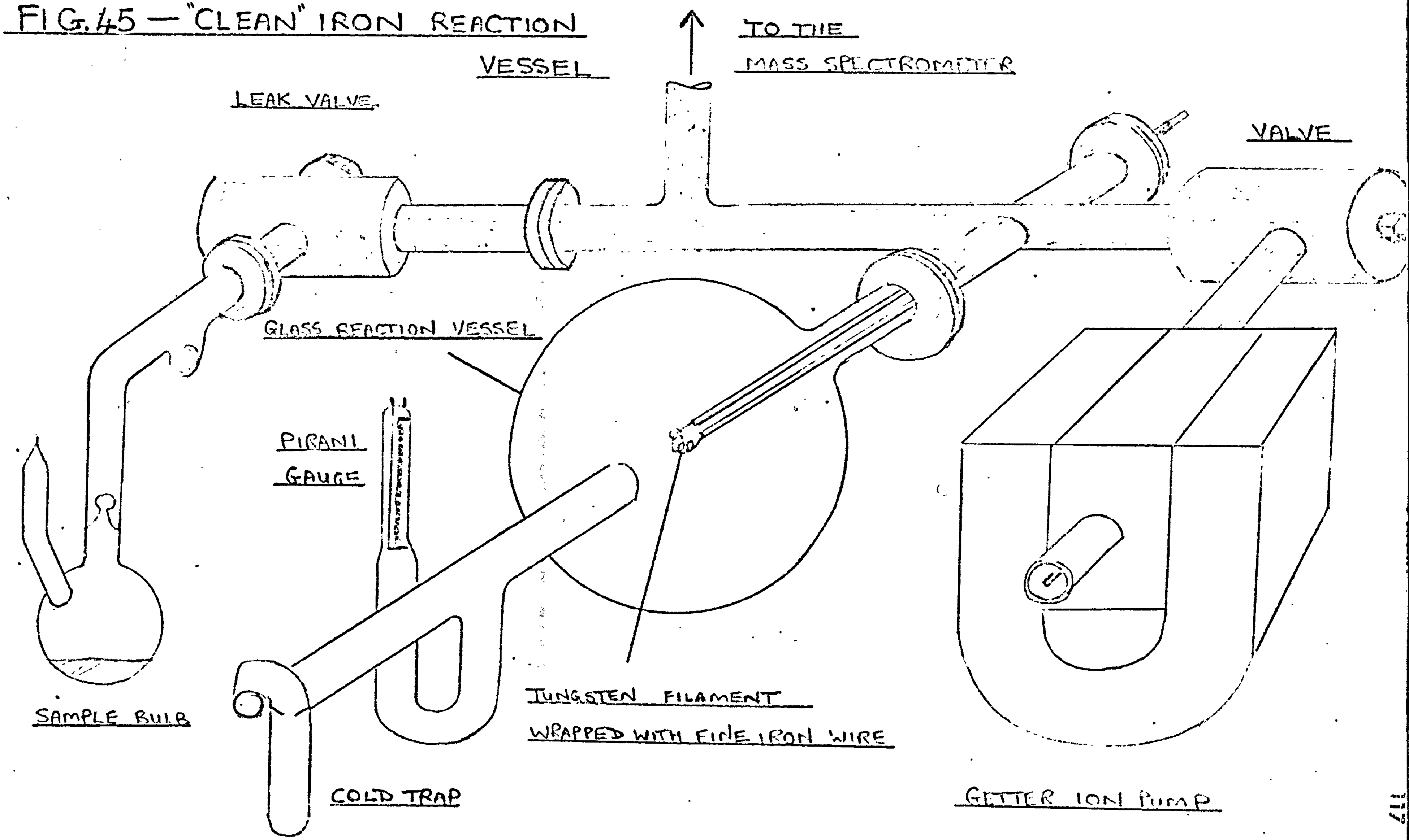

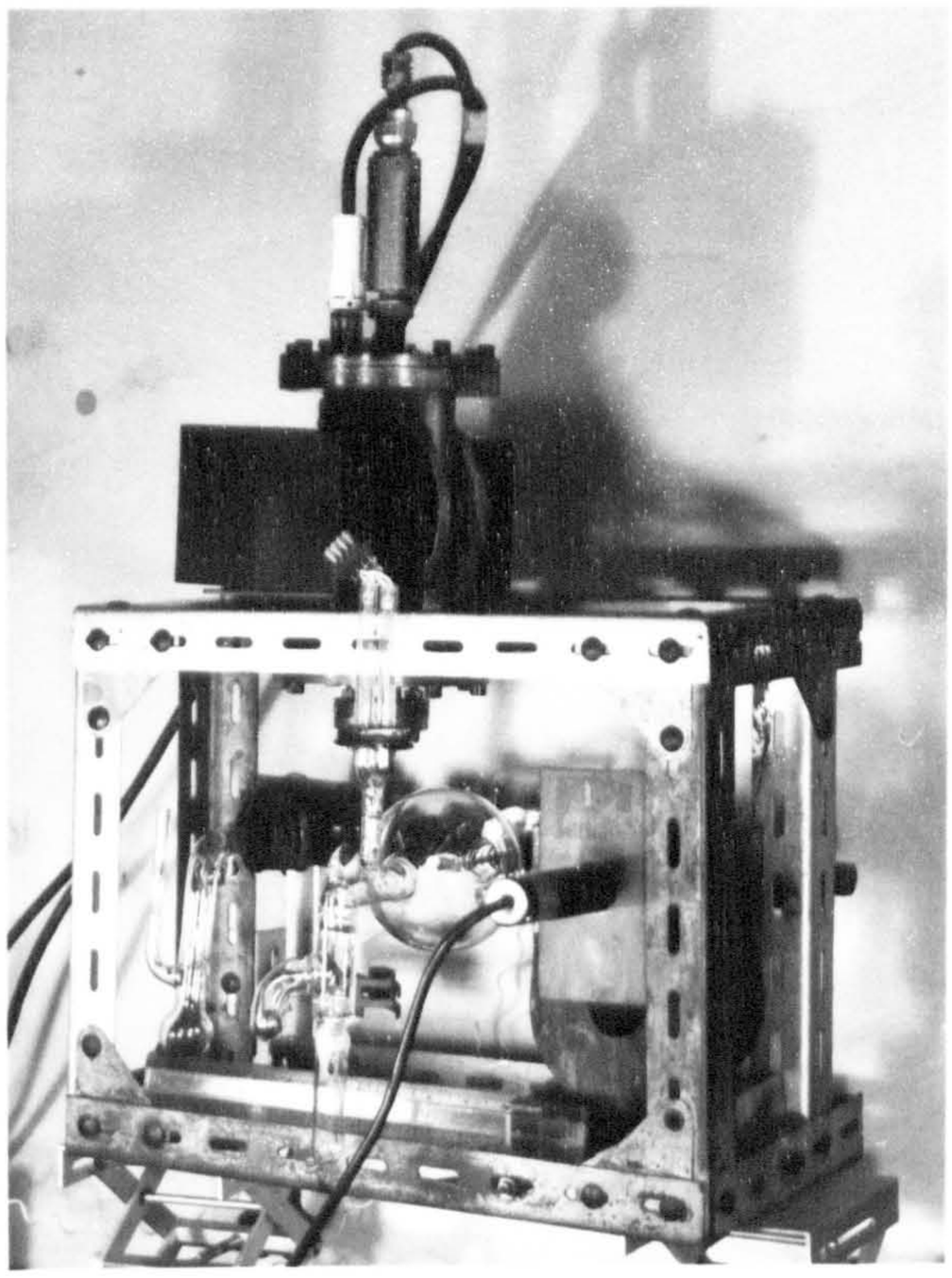

FIG. 46 The clean iron apparatus and mass spectrometer.

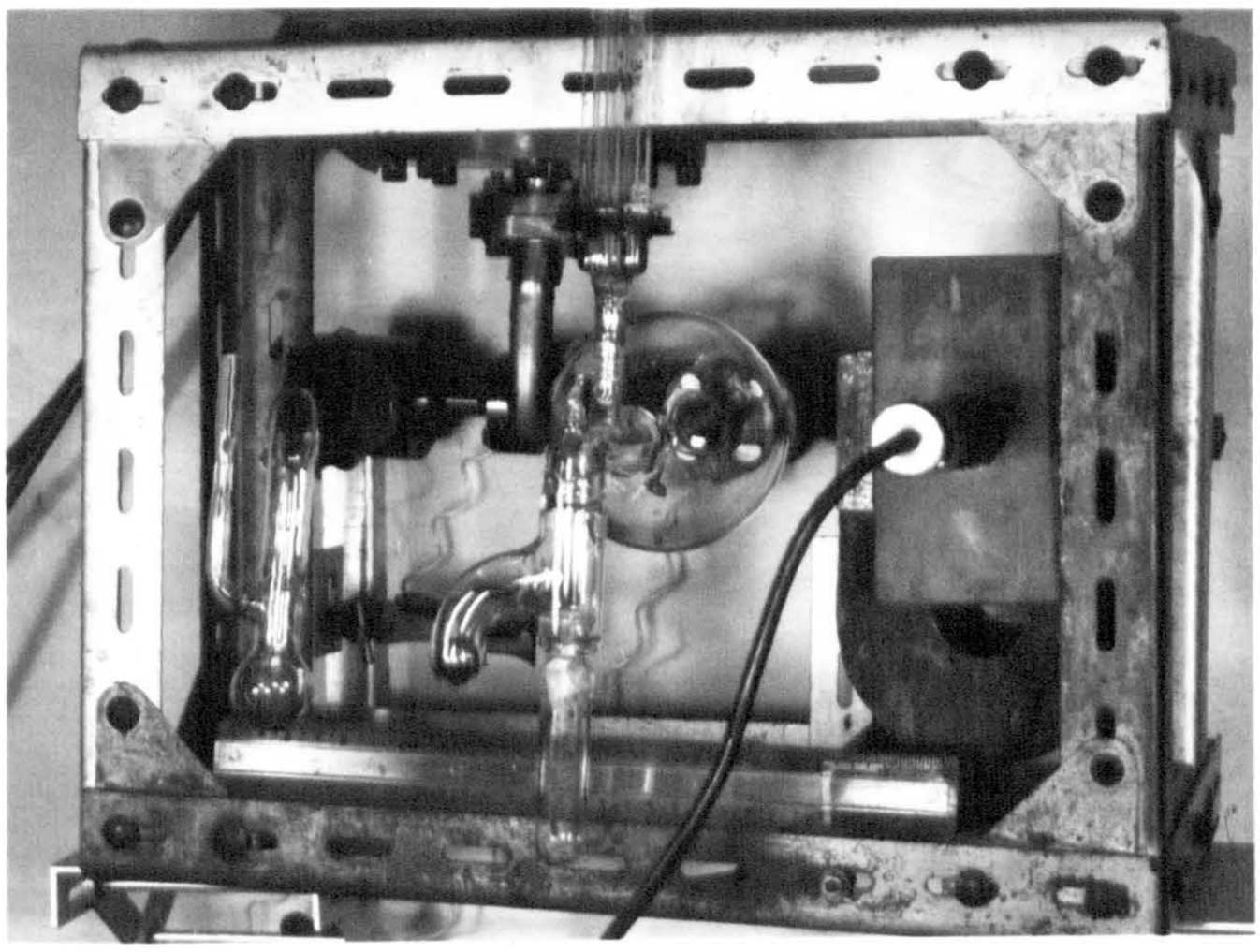

FIG. 47 The clean iron apparatus showing sample bulb reaction chamber and getter ion pump.

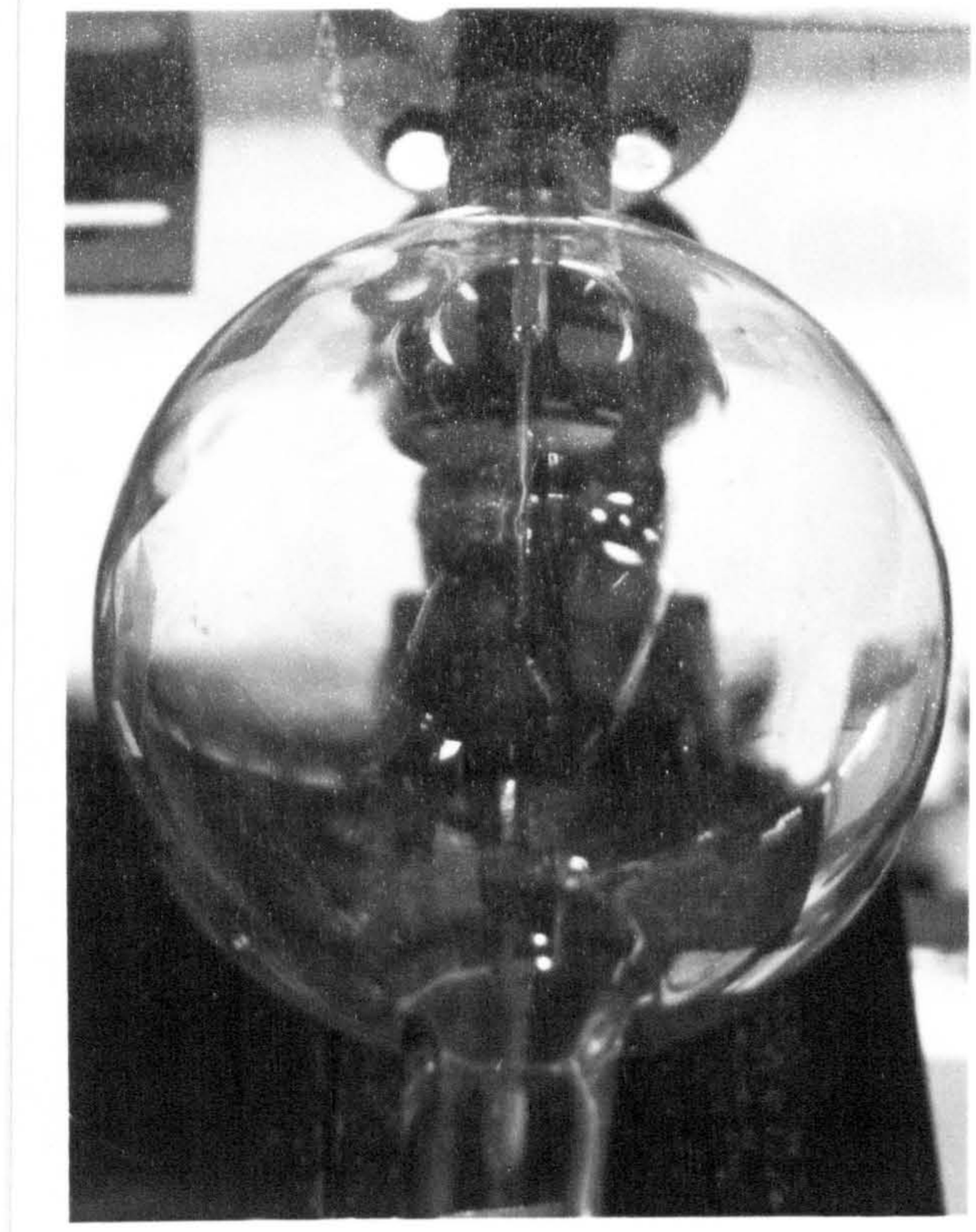

FIG. 48 The clean iron apparatus showing close-up of reaction chamber.

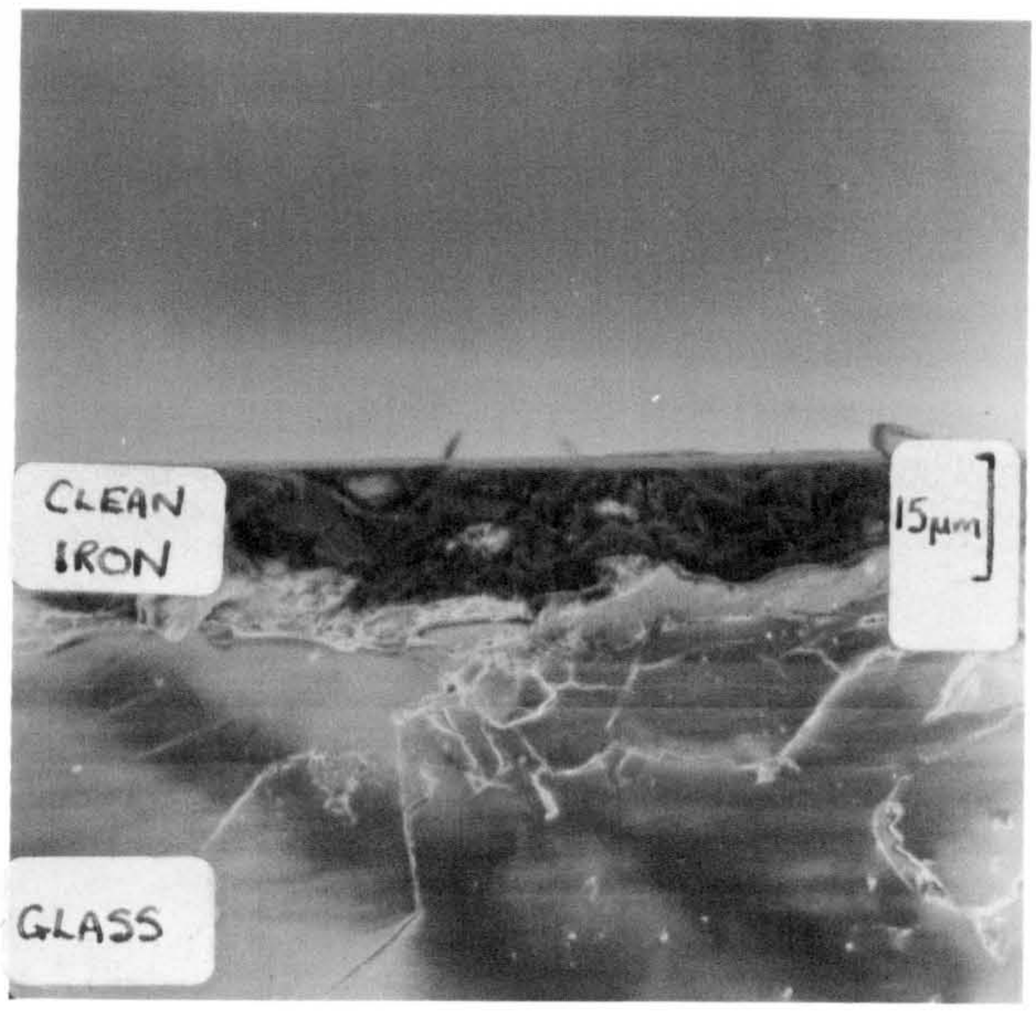

FIG. 49 A side view of an evaporated iron film on the surface of a microscope slide.

4.2.2 Vacuum System

In order to produce the ultra high vacuum (U.H.V.) required in the reaction chamber a three stage pumping arrangement was required.

(i) Rotary backing pump to produce

$(10^{-2}$ torr$)$ 1.0 N m^{-2}

(ii) Oil diffusion pump to produce

$(10^{-2}$-10^{-6} torr$)$ 10^{-2}-10^{-4} N m^{-2}

(iii) Getter ion pump to produce

$(10^{-4}$-10^{-10} torr$)$ 10^{-2}-10^{-8} N m^{-2}

In addition special metal tubes and flanges were employed requiring gold seals and considerable care and cleanliness in assembly and operation. In practice the rotary and diffusion pumps pumped the apparatus via an inlet above the cold trap until, by flaming exposed glass areas to remove adsorbed (and to some extent chemisorbed) water, the pressure fell to $\simeq$ $(10^{-5}$ torr$)$ 10^{-3} N m^{-2} . At this point the Ferranti FJD/FPD - 15 getter ion pump was cut in until vacuum of $(10^{-6}$ torr$)$ 10^{-4} N m^{-2} reached whereupon the connection to the diffusion pump was sealed off and pumping continued by the getter ion pump alone.

Contamination and arcing inside the getter ion pump tended to cause initial short circuiting problems that were overcome by improvising a programmed heat treatment. This consisted of raising the temperature of the pump by wrapping in heating tapes and supplying an activating current with the 'cut-out' circuit by-passed. At the same time the apparatus was outgassed by pumping on diffusion and rotary pumps for several hours. After allowing the system to cool down again the 'gettering' action was found to operate smoothly and efficiently and to cut in at the correct pressure.

4.2.3 Mass Spectrometer

This was essentially an A.E.I. Ltd. M.S.10 modified to cover the mass range (m/e) 12-200.

A stream of electrons from filament to trap ionises the sample gas inside the cage and these ions are repelled to the outside by the ion repeller. The particles then describe a circular path due to the combined effect of the accelerating potential supplied by the cage and an externally applied magnetic field. The geometric and electronic arrangement is such that different ions arrive to give a signal on the ion collector according to the accelerating voltage applied. Hence the ion current gives a measure of the various quantities of molecular species present.

Avoiding unnecessary detail the basic specifications are as follows:-

(i) Tube Specifications.

Ionising current filament/trap	(10-50 μA. (76 V
Filament heater	(3.4 A (1.7Va.c.
Ion repeller potential	-5 to +10 V (normally +1 V w.r.t. cage)
Cage potential	40-2000 V d.c. w.r.t. earth.

(ii) General Performance.

Working pressure $(10^{-4}-10^{-10}$ torr) $10^{-2}-10^{-8}$ N m^{-2}

Mass range (modified) m/e 2, 3, 4.

m/e 12-45.

m/e 36-200.

Resolving power Unit mass separation m/e 170

Useful Spectra m/e 200

Valley overlap at m/e 40 is 2%.

N.B. A control analysis of n-C_5F_{12} was also carried out for confirmation purposes on a standard A.E.I. Ltd. M.S.9 mass spectrometer (belonging to Shell Research Ltd.)that had a much greater resolution than the M.S.10 (see SAMPLE PREPARATION AND PURITY). For the main experimental work, however, only the M.S.10 could be conveniently used due to the problems involved in 'baking-out' the apparatus.

4.3 Sample Preparation and Purity

The mass spectrum of the n-C_5F_{12} (perfluoro-n-pentane) sample from Fluoro-Chem Ltd. was obtained using an A.E.I. M.S.9. high resolution mass spectrometer. The sample was introduced via the hot box inlet system at a temperature of $\simeq$ 550K.

The cracking pattern obtained contained additional peaks not due to n-C_5F_{12} and occurring in many instances fourteen mass numbers higher than the expected carbon/fluorine peaks. In view of the usual preparation technique[143] for this material (i.e. electrochemical fluorination of pyridine) the major impurity was most likely to be undecafluoropiperidine giving rise to carbon/fluorine/carbon containing peaks.

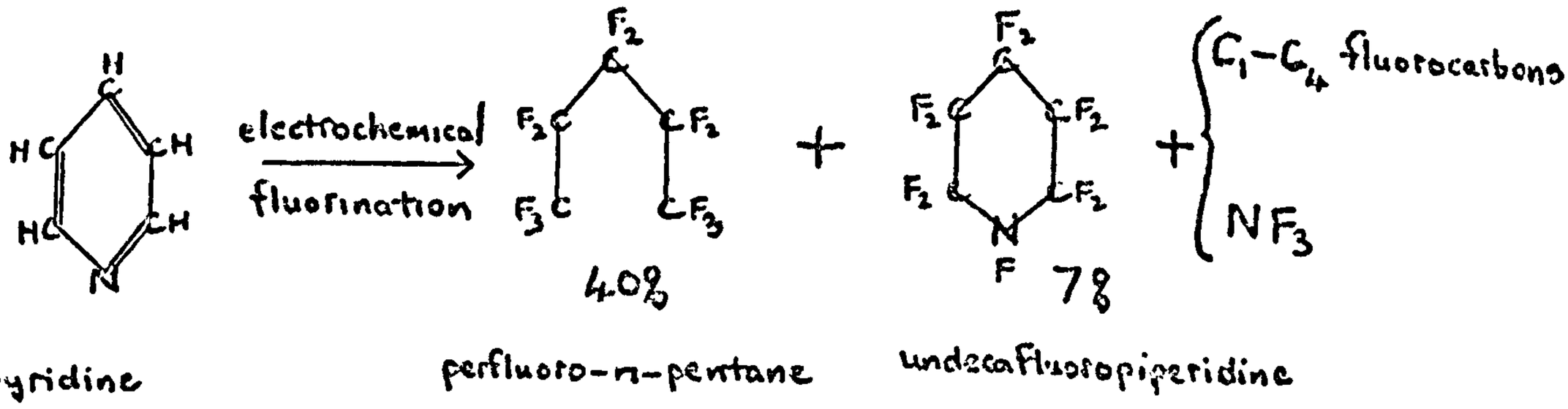

The parent ion for this impurity appeared at m/e 283 and for the sample at m/e 288.

Combined mass spectrometry and gas/liquid chromatography revealed an impurity level of $\simeq$ 5% probably due to the undecafluoropiperidine and C_5F_{12} isomers. As the specialised long column chromatography equipment for further purification was not readily available in allotted time the sample was used as characterised.

Compound	B.P.
n-C_5F_{12}	(29.3 °C) 302.45 K
iso-C_5F_{12}	(30.1 °C) 303.25 K
C_4F_{10}	(-1.0 °C) 272.15 K
$C_5F_{11}N$	(49.5 °C) 322.65 K

4.4 Experimental Procedure

The reaction vessel was evacuated to about $(10^{-6}$ torr$)$ 10^{-4} N m^{-2} using the three stage pumping system described earlier. The whole apparatus was then placed in a specially built electric oven to bake out over a period of two days at temperatures up to 700K to remove gases and moisture from the walls. Similarly the Pirani gauge mass spectrometer and tungsten filaments were outgassed by passing a current through them over a period of several days with care taken not to overheat the latter and vapourise the iron wire. By this technique the getter ion pump brought the system down to a vacuum of better than $(10^{-8}$ torr$)$ 10^{-6} N m^{-2} and ultimately to the region of $(10^{-10}$ torr$)$ 10^{-8} N m^{-2}.

At this stage $\simeq(3$cc$)$ 3×10^{-6} m^3 of n-C_5F_{12} were introduced into the sample bulb and frozen with liquid nitrogen. An auxiliary high vacuum system was used to remove remaining volatiles and then, isolating the pumps, the sample was allowed to melt and gently boil. By repeating this 'freeze drying' technique several times any air, moisture or volatile impurities were removed and then the sample sealed in and isolated in the usual way.

Next the clean iron film was formed by applying 8-9A at 12V across the tungsten filament which was sufficient to vapourise the fine iron wire which in turn condensed on the inside of the glass reaction vessel leaving a 'mirror'. With liquid nitrogen around the cold trap the break-seal between the sample and clean iron chamber was broken and a controlled amount of n-C_5F_{12} vapour allowed to enter until the Pirani gauge recorded about $(10^{-4}$ torr$)$ 10^{-2} N m^{-2}.

At this point mass spectrometer scans were started to analyse any non-condensible vapours produced. After a period of (30 - 45 minutes) 1.8 - 2.7 Ks the cold trap was removed and the pressure increased to $\simeq$ (10^{-1} torr) 10 N m^{-2} . The cold trap was reapplied and a record kept of any changes in Pirani readings due to production of non-condensible gases in the interim period. Further mass spectrometer analyses were carried out and then the pressure change experiment repeated.

At a later date the complete experiment was repeated several times on these occasions allowing the sample vapour into the reaction chamber before forming the iron film. Mass spectrometer analyses were made before and after production of the film and the results compared with the earlier experiments.

4.5 Results/Discussion

4.5.1. Presentation of Results

As has already been outlined in the introduction the object of the experiments presented in this SECTION TWO was to observe and record the breakdown of n-C_5F_{12} as it came in contact with a 'clean' iron film free of the usual surface oxides. Thus the tables of results and appropriate histograms deal mainly with mass spectrometry analyses conducted at appropriate intervals during the interactions. The results refer in general to three main experimental runs during which fresh 'clean' iron films were produced and new samples of n-C_5F_{12} introduced in each case. TABLE 9 is a brief record of the sequence of operations involved in the experiments with corresponding comments on the resulting mass spectrometer analyses. The experimental analysis code numbers 1-7, 8-9, and 10-14 in the left hand column refer to the first, second and third complete experimental runs respectively. Double horizontal lines have been drawn in the table to indicate where these discontinuities due to different experiments occur. In the case of the first group of analyses (1-7) these refer to changes occuring in the reaction chamber when the n-C_5F_{12} vapour was introduced onto previously formed 'clean' iron film. In the latter two groups of analyses (8-9 and 10-14) the 'clean' iron film was formed after initially allowing n-C_5F_{12} vapour into the system and then pumping down again. The reasons behind this procedure are briefly reiterated later when this has a bearing on the manner of presentation.

TABLE 9

The following is a very brief commentary on the sequence of operations involved in experimental analyses 1-14.

EXPERIMENTAL ANALYSIS CODE NUMBERS	PROCEDURE PRIOR TO ANALYSIS	COMMENTS ON THE MASS SPECTROMETER ANALYSES
1.	(i) 'Clean' iron film formed.	(i) CO, N_2, and H_2O quantities high due to filament and sample outgassing.
	(ii) Liquid nitrogen trap applied.	(ii) Unusual n C_5F_{12} cracking pattern presumably due to interaction with 'clean' iron film.
	(iii) Pump isolated.	
	(iv) n C_5F_{12} introduced into chamber.	
	(v) Analyse gases.	
2.	(i) Reduce pressure.	(i) Unusual n C_5F_{12} cracking pattern.
	(ii) Repeat analysis.	

EXPERIMENTAL ANALYSIS CODE NUMBERS	PROCEDURE PRIOR TO ANALYSIS	COMMENTS ON MASS SPECTROMETRY ANALYSES
3.	(i) Repeat analysis.	(i) Unusual n C_5F_{12} cracking pattern.
4.	(i) Repeat analysis.	(i) Unusual n C_5F_{12} cracking pattern.
5.	(i) Carry out pressure change experiments. (ii) Repeat analysis. (iii) Repeat pressure change experiments.	(i) Complete change in the cracking pattern.
6.	(i) Repeat analysis checking on individual peaks.	(i) Previous trends confirmed.
7.	(i) Repeat analysis.	(i) Previous trends confirmed.
8.	(i) n C_5F_{12} introduced into chamber. (ii) 'Clean' iron film formed. (iii) Liquid nitrogen trap applied.	Results non-representative (i) Too high a pressure in reaction.chamber for M.S. to operate correctly. (ii) Liquid nitrogen trap not continuously maintained cold. (iii) Insufficient iron film formed.

EXPERIMENTAL ANALYSIS CODE NUMBERS	PROCEDURE PRIOR TO ANALYSIS	COMMENTS ON MASS SPECTROMETRY ANALYSES
8. Cont.	(iv) Pump in operation. (v) Analyse gases.	
9.	(i) Repeat analysis.	(i) Ditto experiment 8.
10.	(i) n C_5F_{12} introduced into chamber. (ii) Liquid nitrogen trap applied. (iii) Pump in operation. (iv) Analyse gases.	(i) The normal n C_5F_{12} cracking pattern produced.
11.	(i) Close pump valve. (ii) Repeat analysis.	(i) The normal n C_5F_{12} cracking pattern produced.
12.	(i) 'Clean' iron film formed. (ii) Open pump valve. (iii) Repeat analysis.	(i) Insufficient iron vapourised to form coherent mirror. (ii) Considerable O_2 & N_2 released from filaments (iii) Slight change in n C_5F_{12} cracking pattern.

EXPERIMENTAL ANALYSIS CODE NUMBERS	PROCEDURE PRIOR TO ANALYSIS	COMMENTS ON MASS SPECTROMETRY ANALYSES
13.	(i) Allow traps to warm up then re-cool.	
	(ii) Reduce pressure then close valve.	Ditto experiment 12
	(iii) Repeat analysis.	
14.	(i) Introduce more sample.	(i) CF fragments increasing in volume.
	(ii) Repeat analysis.	

A complete record of all the mass spectrometer analyses is given in TABLE 10 and later summarised in FIGS. 50 and 51.

In TABLE 10 the ascending order of mass ratios for the various molecular or atomic fragments detected in the analysis are presented in the two left hand columns along with an indication of their chemical structure (species). Then follow various columns of molecular abundance values all adjusted to be relative to the base peak concentration at $m/_e 69$ which was nominally made 100%. The only exception to this was analysis 5 which, due to the apparent magnitude of the SiF_3 fragment required the base peak to be readjusted to $m/_e 85$ (i.e. mass number SiF_3). Included in this table are abundance values quoted in literature[152,153,154] for standard mass spectrometer analyses of $n\text{-}C_5F_{12}$ along with independent control analyses carried out on an M.S.9. high resolution instrument. For interpretation and comparison purposes comparative cracking patterns[152,153,154] of $C_1\text{-}C_5$ perfluorinated alkanes, alkenes and SiF_4 are presented in TABLE 11.

In FIG. 50 selected examples have been arranged in logical sequence and allocated letters A-F for easy reference. Using this format the progressive changes in chemical structure of $n\text{-}C_5F_{12}$ when in the presence of 'clean' iron may be readily deduced from the changing cracking patterns.

TABLE 10.

MASS SPECTROMETER CRACKING PATTERNS FOR nC_5F_{12}. WITH AND WITHOUT THE PRESENCE OF CLEAN IRON.

m/e	SPECIES	RELATIVE ABUNDANCE															
		N.B.S. CRACKING PATTERN	M.S.9 CRACKING PATTERN	EXPERIMENTAL CODE NUMBERS. 1	2	3	4	5	6	7	8	9	10	11	12	13	14
12	C	–	–	26	11·3	1		115			1·61	2	1·6	5·6	28·8	503	371
13		–	–	–	–	–		2·9			0·2	–	–	0·2	1·2	9·5	2·2
14	N	–	–	6	5	–		96·5			0·81	1	0·7	4·9	7·6	123	233
15		–	–	4	–	–		5·2			1·01	0·8	0·5	3·3	6·4	52	17·3
16	O	–	–	28	6·7	1		86·5			2·2	2·4	3·5	7·9	20·8	126	69
17		–	–	48	12·1	–		14·4			2·8	9·8	6·6	4	0·5	29·3	25·4
18	H_2O	–	–	150	42·0	2		57·5			10·1	37·2	23·4	14·7	254	104	112
19	F	0·08	–	2	0·8	–		4·0			0·6	0·6	0·2	0·2	0·4	–	–
20		–	–	40	23	3		57·5			17·3	17	5·5	4·8	10·4	9·5	6·4
22		–	–	8	1·25	–		11·5			–	–	0·2	–	0·8	–	–
24		–	–	–	0·4	–		–			2·4	0·6	0·2	0·5	1·6	–	–
27		–	–	–	1·25	–		–			1	1·2	0·6	–	1·4	–	–
28	CO N_2	–	–	400	83	14		173			27·6	59·1	20·7	37·8	282	4000	640
29		–	–	52	4·2	–		86·5			0·8	1	0·6	6·7	4	148	138
30		–	–	12	0·8	–		31·5			–	–	0·2	1·9	0·3	–	25·9
31	CF	6·50	10·50	60	62	12		13·2	55·5		63·3	54	15·1	15·3	8·0	18·9	34·5
32	O_2	–	–	–	1·25	–		–			–	1·2	0·4	0·4	0·1	–	–
33		–	–	–	0·6	–		14·4			–	–	–	–	–	–	–
41		–	–	10	–	–		–			–	0·2	–	–	0·6	–	–
43	C_2F	–	–	1	0·3	–		5·2			0·2	0·2	–	–	–	–	–
44	CO_2(SiO)	–	–	10	50	15	18	115			2·2	4	4·6	12·1	40	15·7	8·6
47		–	–	–	–	–	–	6·7			–	–	–	–	–	–	–
50	CF_2	2·27	3·67	5	14·5	2·5	2·8	1·5			6·1	5·6	28	3	2·4	2·5	3·1
51		–	–	–	2·1	–	–	0·75			1	–	–	–	–	–	–
55	C_2F	0·06	0·20	–	0·4	–	–	–			0·2	0·6	0·06	0·05	0·1	0·4	0·2
62	C_2F_2	0·29	0·55	–	1·6	–	–	–			1·2	1·2	0·3	0·35	0·1	0·7	1·1
66		–	–	–	–	–	–	1·5			–	–	–	–	–	–	–
69	CF_3	100	100	100	100	100	100	9·6	100	100	100	100	100	100	100	100	100
74	C_3F_2	0·21	0·55	–	1·6	–	–	1·5			1·2	1·2	0·1	0·5	0·1	0·5	0·7
81	C_2F_3	0·49	1·10	–	1·6	–	–	3·75			1	0·8	0·4	0·4	0·4	0·2	0·3
85	C_3F_3	–	–	–	10	2	2·8	100			–	–	0·06	–	–	–	0·5
86	C_4F_2																
87																	
93	C_3F_3	1·60	2·76	–	3·3	1	1·4	–			1·8	1·8	1	1·1	1	0·7	0·6
100	C_2F_4	6·45	12·70	5	40	10	8·5	4·7		67·5	12·3	10	7	6·5	6·2	5	4·7
105	C_4F_3	–	–	–	–	–	–	1·5		2·78	–	–	–	–	–	–	–
112	C_3F_4	0·29	0·55	–	5	1·5	1·4	–		9·9	–	–	1·6	1·6	1·2	1·1	1·4
119	C_2F_5	29·9	31·50	5	74·5	18	17	0·75		11·4	26·2	22·4	15·2	14·2	15·3	12·5	9·5
131	C_3F_5	6·56	9·40	–	13·3	4·5	4·3	1·5		17·6	5·9	5	3·6	3·3	3·3	2·1	2·4
143	C_4F_5	0·02	–	–	3	1	–	–		9·5	1	1·2	1·7	1·2	0·5	0·5	0·3
150	C_2F_6	1·15	2·20	–	6·4	1·5	1·4	1·5		16·2	1·6	1·4	0·9	0·9	1	0·7	0·5
169	C_3F_7	10·50	12·15	–	16·7	5	4·3	–			6·1	5	3·4	3·2	3·3	2·9	2·0
181	C_4F_7	3·29	3·67	–	0·5	1	1·4	–			1·6	1·6	1·2	1	1·2	0·5	0·5

TABLE 11. COMPARATIVE MASS SPECTROMETER CRACKING PATTERNS FOR C_1–C_5 PERFLUORINATED ALKANES AND ALKENES AND SiF_4 (PRINCIPLE PEAKS ONLY)[17,18,19]

m/e	SPECIES	(m.s.10) n-C_5F_{12}(c)	C_4F_{10}	C_3F_8	C_2F_6	CF_4	n-C_5F_{10}	n-C_4F_8	C_3F_6	C_2F_4	cyclo C_5F_{10}	cyclo C_4F_8	octafluoromethylpropene C_4F_8	hexafluoro 1,3 butadiene C_4F_6	hexafluoro 2 butyne C_4F_6	hexafluorocyclobutene C_4F_6	octafluoro 2 pentyne C_5F_8	SiF_4	cyclo C_5F_{10}	dodecafluoro 2 methyl butane C_5F_{12}	(n-C_5F_{12}/deionisation) TABLE 10 2	(n-C_5F_{12}/deionisation) TABLE 10 5
		RELATIVE ABUNDANCE																				
12	C	1.6		2.4	1.5				12.6	7.7				6.8		7.0					11.3	1150
19	F	0.2			1.2	6.7												1.9			0.8	40
20		5.5																			23.0	57.2
22		0.2																			1.25	11.5
26		0.2																			0.4	—
27		0.6																			1.25	—
28	CO/N_2	20.7																4.0			83.0	173.0
29		0.6																			4.2	86.5
30		0.2																			0.8	31.5
31	CF	15.1	12.2	28.8	18.3	4.9		70.2	100	100	23.3	54.2	58.9	49.6	53.4	64.0	17.1		23.3	6.5	62.0	13.2
32	O_2	0.4																			1.25	—
33		—																3.7			0.8	14.4
41		—																			—	—
43	C_2F	—																			0.8	5.2
44	CO_2 / SiO	14.6																			50.0	1150
47		—																3.2			—	6.7
50	CF_2	2.8	4.2	9.3	10.1	11.8		7.7		30.8	5.1	13.2							5.1		14.5	1.5
51		—																			2.1	0.75
55	C_3F	0.06												6.1	15.2		5.8				0.4	—
62	C_2F_2	0.3																			1.6	—
66		—																0.5			—	1.5
69	CF_3	100	100	100	100	100		36.5	77.1	3.6	16.2	24.6	100		42.1	7.7	43.5		15.2	100	100	9.6
74	C_3F_2	0.1												11.5	21.5	8.6	100				1.6	1.5
81	C_2F_3	0.4							14.2	73.1											1.6	3.75
85	SiF_3	—																100			10	100
86	C_4F_2	1.0																5.2				
87		—																3.4				
93	C_3F_3	1.0						12.9			9.7	6.5	30.0	100	100	100	37.2		9.7	2.8	3.3	—
100	C_2F_4	7.0	8.4	6.6					36.1	43.1	23.8	100							23.8	3.5	40.0	6.7
104		—																1.5			—	—
105	C_4F_3	—																			—	1.5
112	C_3F_4	1.6											11.2	10.5							5.0	—
119	C_2F_5	15.2	18.3	9.0	41.3															16.3	74.5	0.75
124		—															17.8				—	—
131	C_3F_5	3.6	8.4					100	72.0		100	86.7	15.0						100	8.3	13.3	1.5
132		—										2.7									—	—
143	C_4F_5	1.7													82.0	18.6	100				3.0	—
150	C_3F_6	0.9							28.6												5.4	1.5
162		—												29.9	39.5	26.2					—	—
169	C_3F_7	3.4		24.6																	16.7	—
181	C_4F_7	1.2						11.9			14.4		73.3						14.4	4.5	0.5	—
193		—															46.1				—	—
200		—						8.8					18.7								—	—

It should be noted that cracking patterns B and C of the $n\text{-}C_5F_{12}$ in and out of the apparatus compare reasonable wellwith the fragmentation values quoted by various accredited sources[152,153,154] and summarised in A. After approximately ten minutes exposure to 'clean' iron however a new pattern D appears which finally ends up in the form E after about fifty minutes. It must be noted that C, D and E are not consecutive results although D and E were obtained in the same run and the latter are more fully described in FIG. 51.

If the experiments had been so arranged that the 'control' analysis C of $n\text{-}C_5F_{12}$ had been done immediately prior to the formation of the clean iron film then any remaining sample gas would have been subjected to the widely reported dispersal gettering effect[137] complicating the analysis of fragments generated by chemisorption or contact gettering recorded later. In other words the action of vapourised iron would have been one of physically burying or chemically reacting with any near-by gas molecules in the course of its passage to condensation on the reaction chamber walls thus hindering interpretation of later events.

As mentioned in the commentary on analysis 5 (TABLE 9) pressure change experiments were carried out before and after the mass spectrometer analysis resulting in a reproducible 4.66×10^{-2} N m^{-2} $\longrightarrow$ 8.26×10^{-2} N m^{-2} pressure increase in the former case and 4.8×10^{-2} N m^{-2} $\longrightarrow$ 5.6×10^{-2} N m^{-2} in the later. These measurements were made on a Pirani gauge specially adapted to stand up to high temperature bake-out procedures and which had formerly been calibrated to equivalent dry air pressures.

In a separate experiment clean iron films were formed on microscope slides positioned inside the reaction vessel and then stereoscan pictures taken on removal. These of course must have been oxidised but nevertheless reveal something of the surface texture and film thickness 13.8 - 26.7 μm (See FIG. 49).

FIG 50 – COMPARISON OF MASS SPECTROMETER ANALYSES

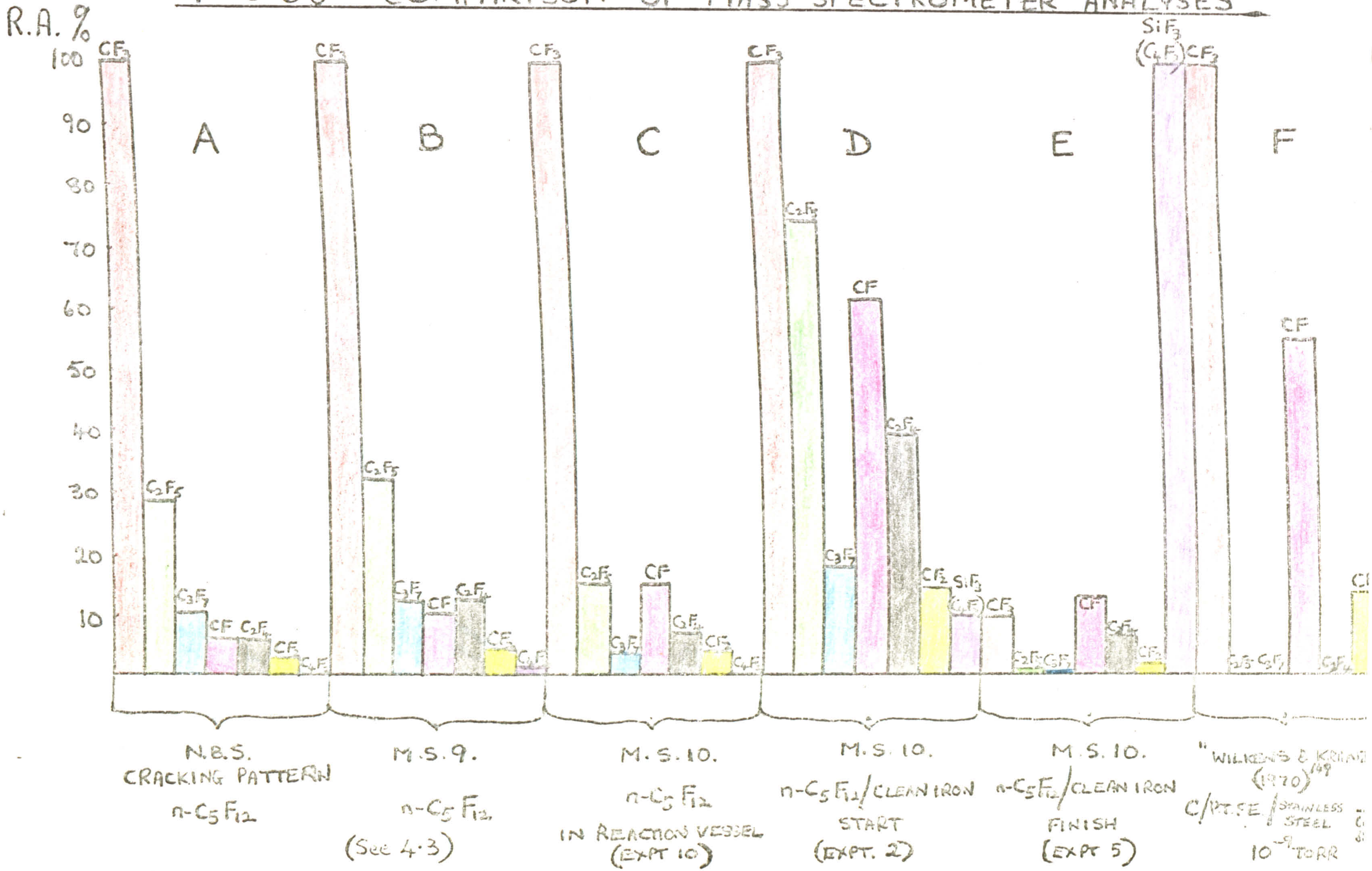

FIG 51. — n-C_5F_{12} CRACKING PATTERN OBTAINED IN PRESENCE OF CLEAN IRON

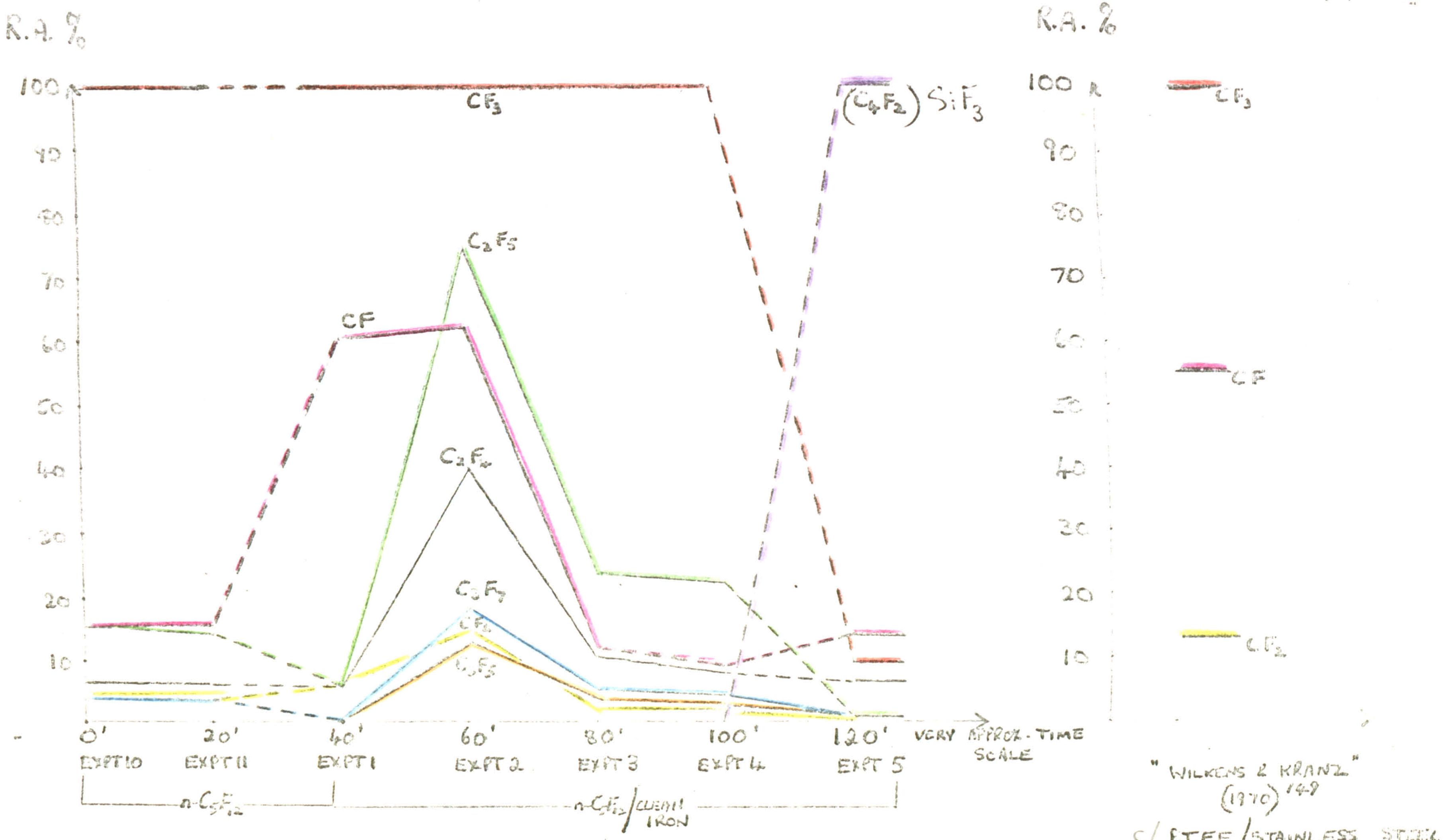

"WILKINS & KRANZ" (1970) 149

C/P.T.F.E./STAINLESS STEEL

4.5.2 Interpretation of Results

4.5.2.1. Limitations of the M.S.10 mass spectrometer in relation to the present work and some of the factors controlling interpretation of results.

If the mass spectrometer were able to give quantitative information on the molecular peak (i.e. $\frac{m}{e}$ 288) of n-C_5F_{12} it could have been deduced[144 (P.26)] from observing the relative abundance of associated isotope peaks whether this was the main species entering the instrument before cracking in the head. This is because the molecular ion peak in the mass spectrum is the one corresponding to the ion containing the most abundant isotopes. As the M.S.10 resolving power is severely limited at $\frac{m}{e}$ 200 only relative changes in abundance could be observed in the lower molecular weight range. These fragments were the result of further cracking in the head of the spectrometer itself (see fig. 52). The present discussions are therefore merely a qualitative comparison of fragmentation patterns X and X+Y (up to a maximum $\frac{m}{e}$ value of 200).

Since the proportion of molecules ionised in the spectrometer head is very low[144 (P.28)] the probability of collision with a neutral molecule and consequential intermolecular reaction is potentially significant. Fortunately it can be shown that the abundance of these ions is proportional to $\sqrt{\text{sample pressure}}$ and so the effect would be negligible in the prevailing low pressure conditions (given that the constant of proportionality is small).

4.5.2.2 Assessment of the fragmentation process.

4.5.2.2.1 Introduction

The results show that when n-C_5F_{12} is introduced on to a clean iron film formed under U.H.V. conditions then the resulting mass spectrometer cracking pattern is totally different from the one produced in a control experiment without the film present. Clearly the explanation lies in one of two

1. Analysis of gas before "clean" iron formation.

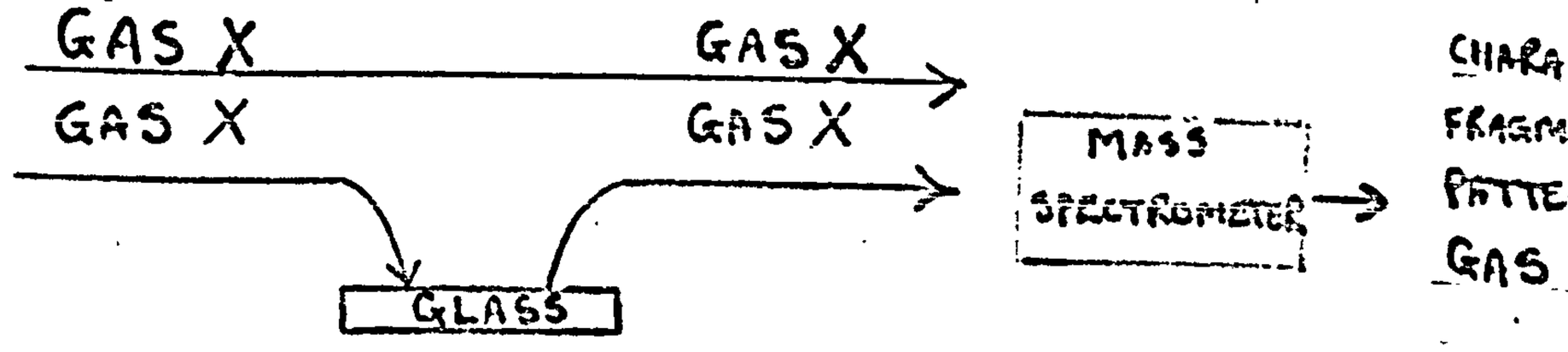

2. Analysis of gas after "clean" iron formation.

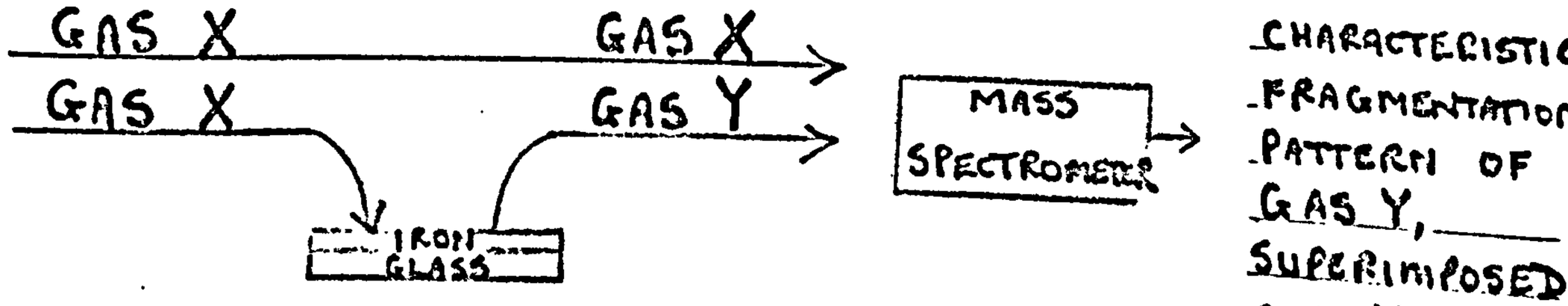

FIG 52.

The Origin of Metastable Peaks.

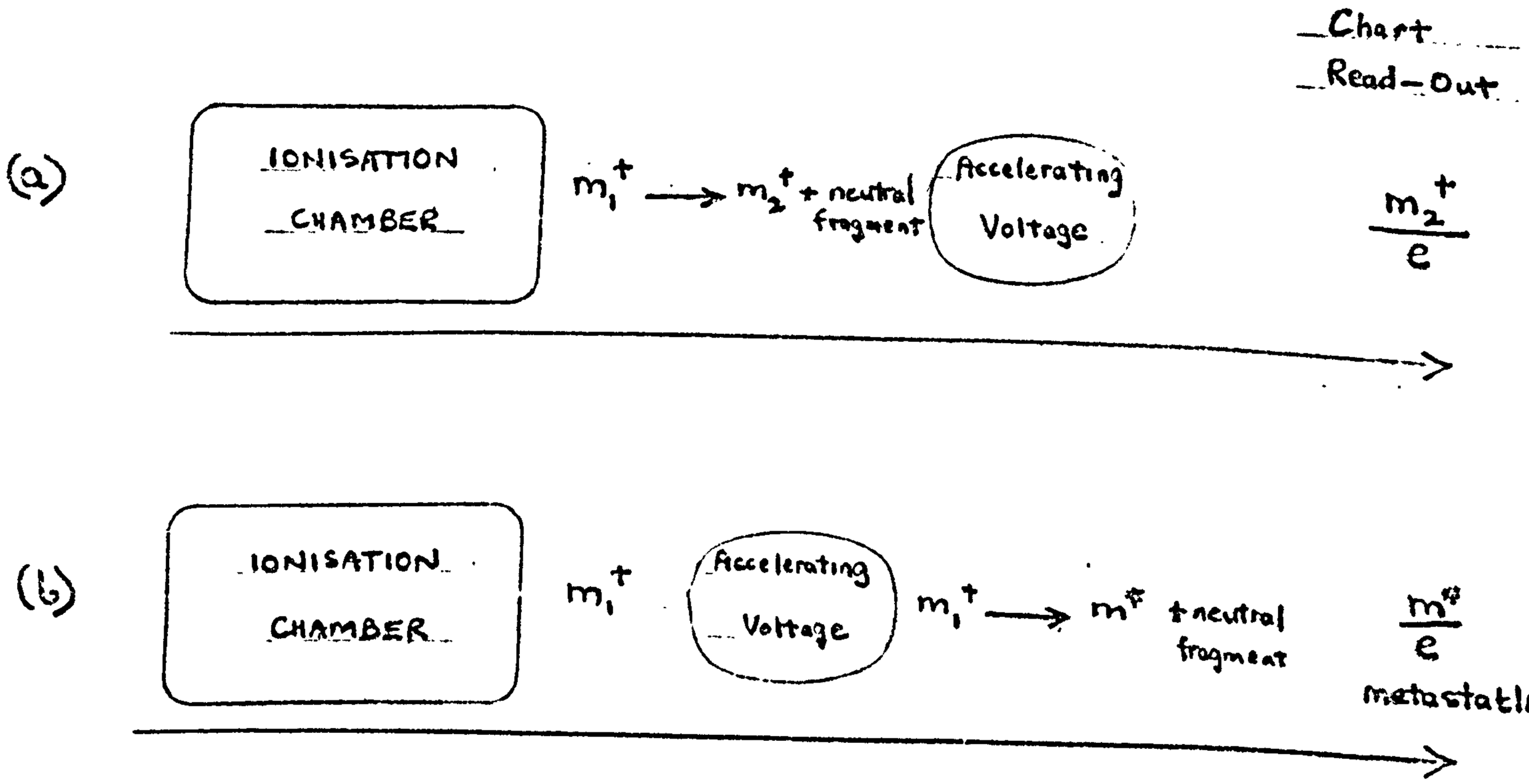

FIG. 53.

alternatives. Either the n-C_5F_{12} is fragmenting abnormally after entering the spectrometer or before. The likely breakdown of ions produced in the former case may be partially detected[145 (P.251) 144 (P.29)] by metastable peak analysis (see fig. 53). In case (a) the ion m_1^+ fragments before the accelerating voltage is applied producing a new ion m_2^+ and a neutral molecule. This new ion is normal and is recorded on the chart read-out as $\frac{m_2}{e}$. If however m_1^+ fragments after acceleration as in case (b) then part of the original kinetic energy is carried away by the neutral fragment and so although of similar type to m_2^+ it has less energy and appears lower on the read out as $\frac{m}{e}^*$. This particular transition gives rise to the metastable peak. Mathematically the values of m_1^+ m_2^+ and m^* can be related to each other by the approximate formula $\frac{(m_2)^2}{m_1} = m^*$ ——— (1)

To aid interpretation of the present results four basic rules were obtained from the literature.

(1) m_1 and m_2 are much larger than m^* Ref. 145 (P.253)

(2) neutral fragments are given off as an entity Ref. 145 (P.253)

(3) $m_1 - m_2$ can not lie between $\frac{m}{e}$ 2 - 15 Ref. 144 (P.31)

(4) if strongest peak is unity then, $\frac{m^*}{m_1 m_2} \simeq$ 0.01 Ref. 145 (P.256)

As a first step in the elimination procedure it was assumed that unidentified peaks in experiments 2 and 5 were potentially metastable. Then assuming that the most prominent peaks in the spectrum were potentially m_1^+ or m_2^+ species, possible transitions of the type $m_1^+ \longrightarrow m_2^+$ and neutral fragment were calculated. This involved firstly working out values of m_1 by substituting possible values of m_2 and m^* in equation (1) and then repeating the procedure with all the possible combinations of m_1 and m^* to arrive at values for m_2.

Over 114 separate calculations were required. Next non-rational values of either m_1^+ or m_2^+ were eliminated by checking $\frac{m}{e}$ values for carbon/fluorine containing fragments. Similarly non-rational values of the neutral fragment were removed by applying rule (2). This brought the number of possible transitions down to 16. Finally by applying rule (4) only one transition possibility remained and even this was very marginal and occured only in experiment 2. (i.e. 'D' in fig. 50).

$$C_2F_4^+ \longrightarrow CF_2^+ + CF_2$$
$$(m_e^* 100) \qquad (m_e^* 50)$$

Assuming $m^* = 26$

$$m_1^+ = 100$$

$$m_2^+ \ (Cal^d) = 50.99$$

This transition is feasible if one allows a 4% error in the measurement of the position of the proposed metastable peak. Furthermore, comparing analysis C and E with D in fig.50 then it would not be unreasonable to propose that the abnormally high value of CF_2 in D is at least in part due to the breakdown of the C_2F_4 fragment in the spectrometer. As a corollary it follows that the C_2F_4 fragment intensity would in fact have been even higher but for this transition.

Thus it appears that the abnormally high values of the $C_2F_5^+$, $C_3F_7^+$, CF^+, $C_2F_4^+$ peaks in experiment 2 and the SiF_3^+ peak in experiment 5 are most likely attributable to the presence of a clean iron surface promoting catalytic breakdown of nC_5F_{12}.

4.5.2.2.2 Sorption at metal surfaces

In view of the work quoted earlier regarding the apparent reactivity of clean iron it is reasonable to assume that an energy rearrangement is possible on the surface via a sorption process. A review of gas adsorption at metal interfaces has recently been written by Hayward[141 (P.225)] and this summarises much of the relevant theory associated with this process.

Physical adsorption can occur to some degree with all gas/solid combinations (under the correct conditions) due to the universal action of dispersion forces. Electric fields at the surface of solids can also contribute up to 20% of the binding energy and this is accompanied by a drop

in work function for the material in question. As a general rule the heats of physical adsorption may be regarded as of the same order as the heats of lique-faction of the gases concerned e.g. usually in the region of (10 k cals/Mole) $.42 kJ.mol^{-1}$.

Metal surfaces in particular, however, can behave rather like a conventional free radical and gases can interact chemically without appreciable disruption of the bonding within the solid network. This process is known as chemisorption. Unfortunately the nature of the surface forces which cause chemisorption are not well understood and even elementary statements of theory tend to be polemic. Generally the heats of adsorption are higher than for physical adsorption e.g.(50-100 k.cals.$mole^{-1}$)210-420 $kJ\ mol^{-1}$. but tail off rapidly as reaction proceeds. Also in contrast to physical adsorption the work function of the metal usually rises[141 (P.96)]

Absorption processes have not been considered in the present context because these are only considered important when the absorbing species is very small e.g. hydrogen or nitrogen atoms [141(P.234)]

4.5.2.2.3 The electronic theory of metals and metal surfaces

The most fundamental treatment of the electronic structure of metals is found in the "Band theory". This employs molecular orbitals which extend over the whole of the metal crystal.[141 (P.235)150]. It is difficult to apply the principles postulated however to surface problems involving localised bonds. Consequently the alternative approach involving "valence bond theory" has been adopted in the present instance. This considers the metal crystal as a giant covalent molecule [150 (P.17)] in which each atom is bound to its neighbours by resonating covalent bonds. The emergence of various potentially bonding orbitals[151, 141(P.256)] on the metal surface can thus be described as in FIG. 54 which although strictly speaking is for face centred cubic metals

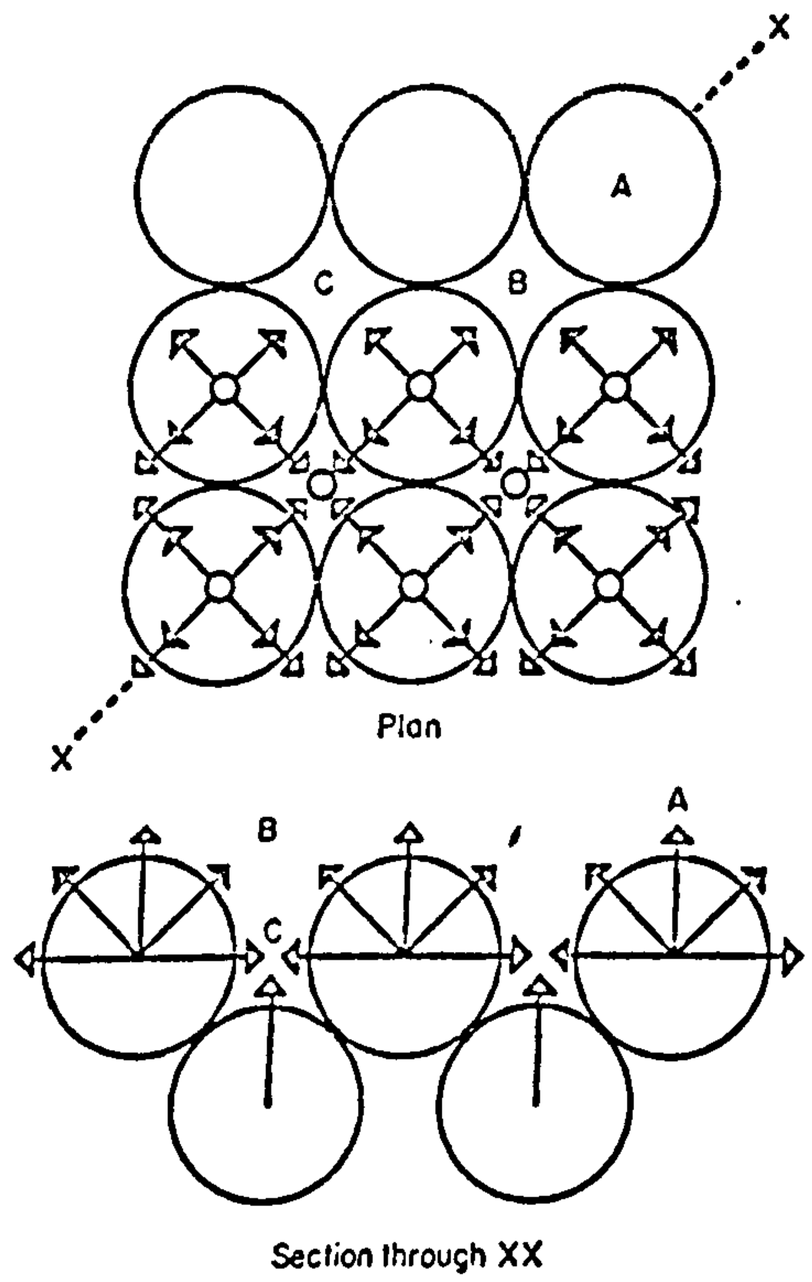

FIG. 54 Representations of the emergence of orbital lobes in the (100) face of face-centred cubic metals. Open circles – atomic orbitals emerging at right angles to plane of paper; open arrowheads – atomic orbitals within plane of paper; filled arrowheads – bonding orbitals within plane of paper in elevation, but emerging at 45° to it in the plan. (After Bond, 1966.)

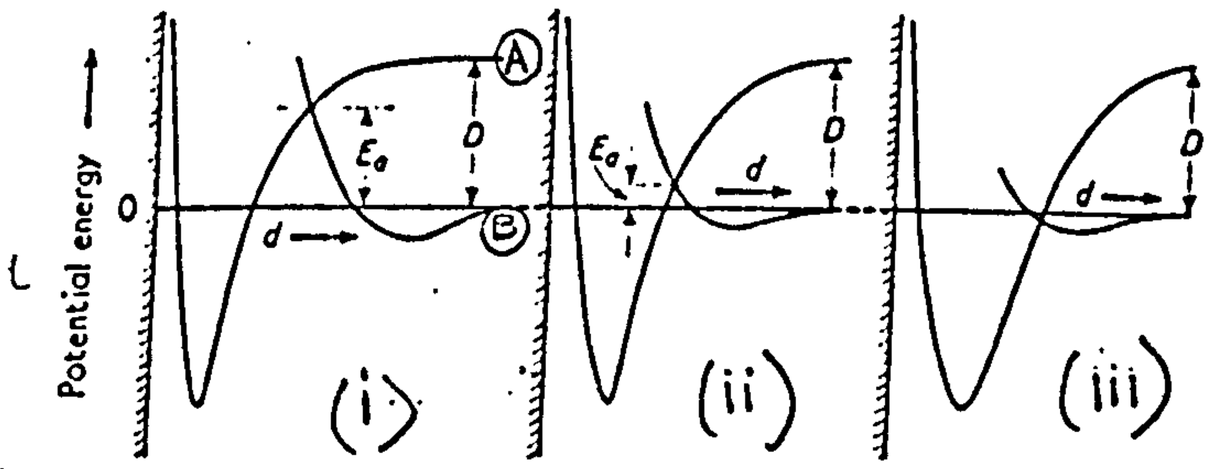

FIG. 55 The dependence of the activation energy for chemisorption on the shapes and positions of the relevant potential energy curves.

(f.c.c.) the same principles can be applied to the body centred cubic (b.c.c.) structures found with iron.[141 (P.256)]. In fact the non-close packed face shown in FIG. 54 is also possible with b.c.c. iron[121].

4.5.2.2.4. The role of the surface in catalytic degradation

For the present discussion the clean iron surface may conveniently be regarded as a heterogenous catalyst. In terms of the "Absolute Rate Theory", therefore, the catalytic iron lowers the potential energy barrier between reactants and products:[150 (P.4)] in other words it stabilises the transition state involved. Thus, (assuming the n-C_5F_{12} chemisorbs on the iron surface) the clean iron acts as an energy sink allowing the degradation path of n-C_5F_{12} (proposed later) to proceed more easily. This process can be more readily visualised by reference [150(P.51)] to FIG.55. This is an adaption of the familiar potential energy bonding diagram the vertical axis being the distance of the absorbing molecule from the clean iron surface. Curve A represents a chemisorption process and B a physical adsorption process. The most energetically favourable path for the approaching n-C_5F_{12} molecule is, initially, along Curve B and then, at the point of intersection, along the A curve. This process involves surmounting the activation energy of chemisorption equal to Ea. The presence of the clean iron thus effectively changes the potential energy diagram from (i) to (ii) or even (iii).

Again, following current theoretical concepts [150(P.5)] it is likely that the surface of the iron can play an important geometric role in aligning the n-C_5F_{12} molecule in such a way as to favour disassocation. In other words the three dimensional arrangement of molecules at the adsorption point is such that the n-C_5F_{12} molecule can approach the surface iron atoms sufficiently closely for the full catalytic effect to operate. <u>N.B.</u> Branched molecules would have difficulty in lying flat on the iron surface resulting in a reduced number or carbon atoms getting close enough to the iron for interaction.

4.5.2.2.5 An analysis of the mass spectrometer cracking patterns found when n-C_5F_{12} comes in contact with clean iron at U.H.V.

Essentially the problem under discussion is why does the cracking pattern for n-C_5F_{12} change from C (FIGS. 50 & 51 and TABLE 10) to D when clean iron is present and finally after a number of intermediate stages change further to E after condensation and revapourisation of any reaction products.

At this point the interpretation may be conveniently divided into three major phases.

Firstly the cracking pattern C (FIG.50 and experiment 10 TABLE 10) is fairly typical of the fragmentation of the n-C_5F_{12} molecule when passed through a standard mass spectrometer. This conclusion is readily arrived at by comparing C with analysis B (M.S.9 TABLE 10 which were results obtained from a high resolution mass spectrometer on a control sample of n-C_5F_{12}. Further confirmation may be obtained by comparing C with A which is a standard analysis found in the literature.[152,153,154] Thus it may be said that when clean iron is absent and n-C_5F_{12} is introduced into the apparatus then no molecular cracking is taking place other than when the material is analysed in the spectrometer itself.

Secondly when a clean iron mirror is present in the apparatus and n-C_5F_{12} is introduced on to it the cracking pattern immediately changes from C to D. Presumably this must mean that one is now observing the cracking pattern of n-C_5F_{12} along with at least one major new type of gas molecule produced by interaction with the clean iron. (FIG52). Clearly one of three processes could be occuring to produce this effect. Since the $C_2F_5^+$ fragment has increased the most relative to CF_3^+ then the new gas might be assumed to have its base peak at m/e 119. But, checking the literature tables for molecules producing base peaks at m/e 119 (TABLE 11) there are no cracking patterns that fit closely enough to confirm the hypothesis. Alternatively it may be argued that as $C_2F_4^+$ has increased the most relative to its own original concentration then the new molecule might have its base peak at m/e 100. In this case octafluorocyclobutane (C_4F_8) is a possibility (TABLE 11) but unfortunately even allowing for a mixture

with nC_5F_{12} the average cracking pattern does not successfully account for the high proportion of $C_2F_5^+$ and $C_3F_7^+$ in the analysis. The most likely explanation of the D cracking pattern however is that by some process a cracking pattern very similar to nC_5F_{12} is being produced but with the overall proportion of CF_3^+ being reduced by interactions in the spectrometer head. The coreactant with the CF_3^+ ion in this case could very likely be CF_2 that is known to be stable for at least a few seconds. Thus the following reaction sequence is possible following the principles cited by Bond [150 (P.413)] for formic acid degradation

$$nC_5F_{12} + 1^* \longrightarrow C_4F_{10} + :CF_2 + 1^*$$

$$CF_2 + CF_3^+ \longrightarrow C_2F_5^+$$

N.B. 1^* is the notation for a catalyst ('clean' iron) reaction site

Obviously other combinations of CF_2 with fragmentation ions are possible but since CF_3^+ is the most abundant species obtained from the cracking of nC_5F_{12} in the spectrometer head then the generation of $C_2F_5^+$ ions seems to be, on balance, more probable.

The cracking pattern for C_4F_{10} when considered in conjunction with nC_5F_{12} and the CF_3^+ removal process compares reasonably well in terms of the order of the most abundant fragments (TABLE 11). The fit is certainly not a perfect one but in the light of fragmentation patterns quoted in the literature for perfluorinated alkanes and alkenes C_1-C_5 this explanation seems the only one at all feasible.

The third major type of cracking pattern to be interpreted is that shown by E. Once again a complete change has taken place, presumably as a result of the condensation and revapourisation of the clean iron reaction products in the vapour trap (FIGS. 50 & 51 and TABLE 10). Between m/e 85-87 a new parent peak has appeared that can be resolved by reference to associated peaks. This is necessary because of the poor resolution of the m.s.10 instrument when dealing with the substantial peaks in the range m/e 85-87 which are close together and

obviously swamped by one very large peak somewhere in the middle. This is probably due to the base peak associated with a SiF_4 cracking pattern and would give rise to a parent peak at m/e 85 and subsidiary peaks at m/e 87, 28, 33, 47 and 19 (TABLE 11). All of these occur in experiment 5 but not all in experiment 10 (TABLE 10). Thus it would be more reasonable to assume that reaction products from the clean iron/n-C_5F_{12} are attacking the borosilicate glass than for a very large increase in the unstable C_4F_2 molecule (F-C≡C-C≡C-F) found at m/e 86. It is conceivable that the reactive fragment interacting with the glass is a diradical difluoromethylene (F-$\dot{C}$-F) or difluorocarbene ($:CF_2$) that can appear more easily due to the lower activation energy encountered in removing itself from the end of a perfluorinated alkane.[146 (P.3428)] Using the concept of thermal bond dissociation energies, once a carbon/carbon bond has been broken. [for uncatalysed nC_5F_{12} requiring at least (87 k cals/mole) 365 k J mol^{-1} 146(P.3427)] then it can be shown that the subsequent energy for removing one CF_2 unit can be as low as (44 k cals/mole) 185 k J mol^{-1} [146(P.3428)]

$$\overset{86}{}\quad\overset{86}{}\quad\overset{85}{}\quad\overset{78}{}\quad\overset{44}{}$$

e.g. $R - CF_2 - CF_2 - CF_2 - CF_2 - CF_2^{\bullet}$

Thus assuming that the clean iron is functioning as a catalyst to thermal degradation and assuming equal lowering of activation energy all along the nC_5F_{12} molecule then elision of a CF_2 fragment is highly likely and indeed has been postulated for the thermal breakdown of P.T.F.E. and other perfluorinated molecules.[146,147,148]. A chain reaction or "unzipping" process, however, is likely to be hindered here because unlike P.T.F.E. when the chain length is small the bond energies increase quite dramatically.

e.g. $CF_3 \overset{122}{—} F \gg CF_3 \overset{94}{—} CF_3 > CF_3 \overset{91}{—} CF_2CF_3$

$> CF_3CF_2 \overset{88}{—} CF_2CF_3 > CF_3CF_2 \overset{87}{—} CF_2CF_2CF_3$

This tentatively supports the earlier hypothesis which proposed (in the absence of strong evidence to the contrary) the formation of C_4F_{10}. After elision of one CF_2 unit from the nC_5F_{12} recombination could occur leaving behind the shortened perfluorinated alkane.

The reaction mechanism could follow one of two routes according to the nature of the transition state formed in conjunction with the clean iron surface. (FIG.56).

This reaction scheme includes the metastable transition referred to earlier of $C_2F_4^+ \longrightarrow CF_2^+ + CF_2$ and is not unreasonable providing one postulates that the high level of $C_2F_4^+$ ions in experiment 2 is partially due to the recombination of CF_2 radicals.

It is interesting to note in conclusion that WILKENS AND KRANZ[149] have reported similar relative concentrations of CF_3, CF and CF_2 wear fragments from carbon filled P.T.F.E. sliding on stainless steel in U.H.V. as were found in the present work with nC_5F_{12} on clean iron. This can be seen by comparing D and F cracking patterns in FIG.50 and FIG. 51. In D however certain additional fragments such as C_2F_5, C_3F_7, C_2F_4 etc. also appeared in fairly large quantities and so direct correlations between the two experiments are not perfect. Nevertheless the similar relative proportions of these common fragments can hardly be fortuitous and are open to one of two explanations. Either the mode of mechano-chemical rupture of P.T.F.E. is essentially similar to that of a thermally degrading perfluorinated alkane or the wear of P.T.F.E. under U.H.V. conditions is being catalysed by the worn surface of stainless steel unable to replenish its natural oxide layers that are being progressively removed by the tribological process. The first of these explanations would seem to be the most plausible because of the conspicuous absence of C_2F_5 etc. fragments in the WILKENS AND KRANZ[149] experiments. Thus it can be argued that, in very general terms at least, any weak links in the

FIG 56. A HYPOTHETICAL REACTION PATH FOR THE CATALYTICALLY INDUCED BREAKDOWN OF nC_5F_{12} ON CLEAN IRON

ROUTE 1

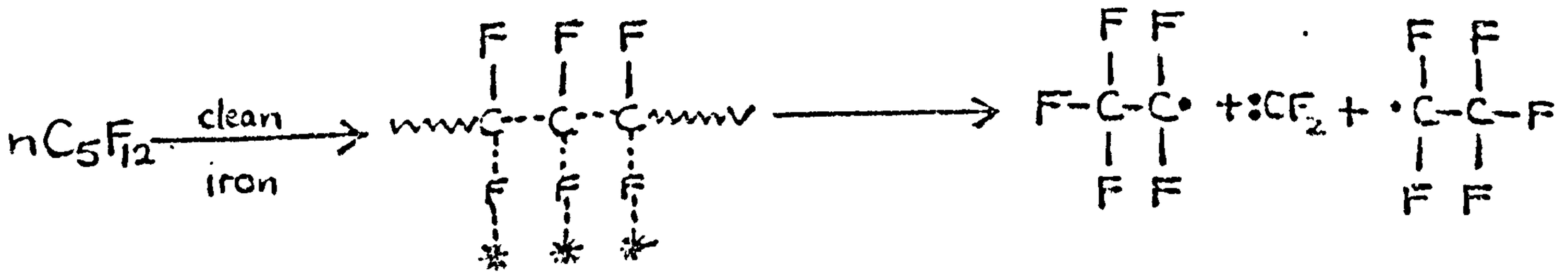

Then, $C_2F_5\cdot + \cdot C_2F_5 \xrightarrow{\text{recombination}} nC_4F_{10}$

Also,

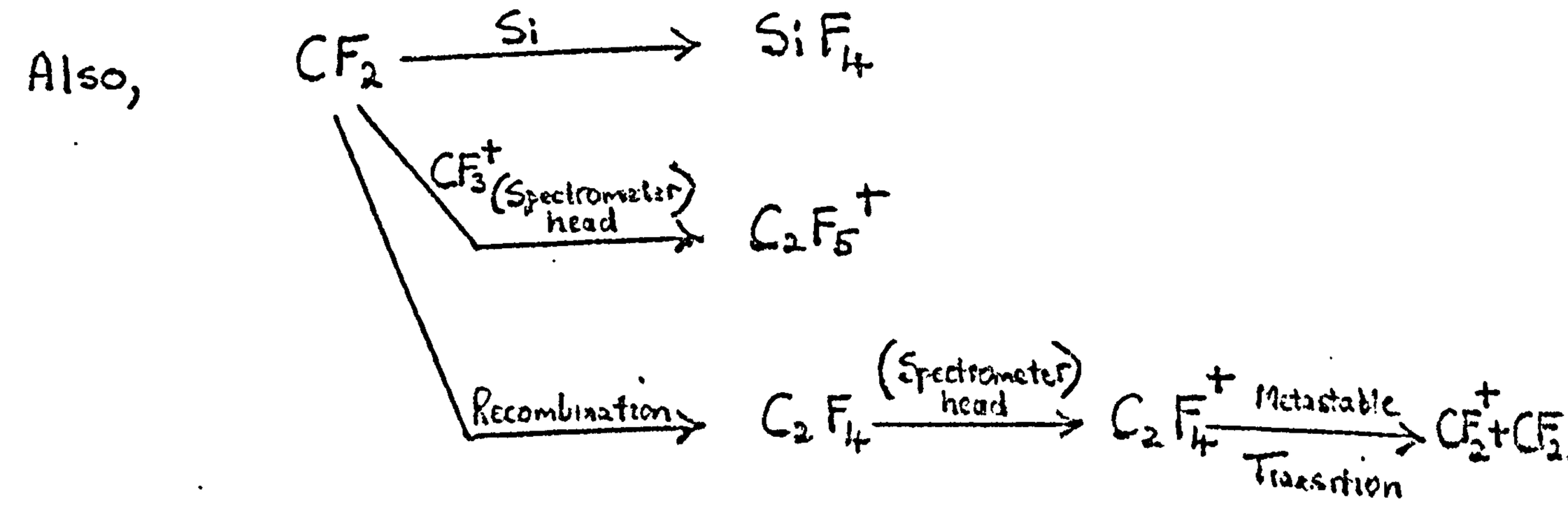

ROUTE 2

⟶ proceed as per ROUTE 1..

P.T.F.E. molecule are just as likely to be open to rupture by energy from mechanical agencies as thermal. The alternative possibility of the stainless steel acting as a catalyst under these U.H.V. conditions can only be ascertained by further experimentation that would involve repeating both experiments in the same vacuum chamber. One of the most important considerations would be that the same mass spectrometer be used in such a fashion that the flight paths of carbon/fluorine fragments en route to the cracking head were both the same. This would reduce the risk of any integrating or disintegrating short life time fragments producing different cracking patterns merely because of the different flight times involved in reaching the ionisation chamber.

4.6 Specific Conclusions (for SECTION TWO).

(1) Oxide free 'clean' iron appears to act as catalyst for the breakdown of nC_5F_{12} at room temperature and under U.H.V. conditions.

(2) A hypothetical reaction path is proposed involving the elision of a CF_2 fragment after the nC_5F_{12} molecule has passed through a transition state on the clean iron surface. (See FIG56)

(3) One of the proposed reaction products, $:CF_2$, is highly reactive and is capable of removing Si from the Borosilicate (Pyrex) glass walls of the reaction chamber.

(4) It is possible that under the correct conditions the thermal breakdown of P.T.F.E. could be induced by the catalytic action of clean iron generated by a wearing or fatigue process.

(5) Further long term research work is necessary to confirm and qualify the above hypotheses.

5. GENERAL CONCLUSIONS.

Viewed as a whole the work described has established some significant and previously unresearched facts about the chemical and physical changes that are likely to occur at polymer/mild steel sliding interfaces. An interesting picture emerges that is largely complimentary to existing concepts.

For example, it has been demonstrated that for P.V.C. (under the conditions chosen) the wear process is intimately linked with mechano-chemical surface change rather than other possible alternatives such as thermal degradation. Obviously in sliding situations these various types of degradation process can never be entirely divorced from each other but here the evidence clearly points to the former as being the rate controlling factor. Furthermore, the evidence was derived from data eminating from surface conditions where one would have expected both abrasive (oxide break-up), adhesive (transfer films) and fatigue (initial lumpy wear debris) wear processes to be operating in varying degrees according to the countersurface and environment involved . Thus in dry wear conditions and in the absence of corrosive fluids etc. the degradation characteristics of polymers similar to P.V.C. and Cl^{d}P.V.C. may be conveniently interpreted in terms of mechano-chemical principles. This in turn leads to an endorsement of the importance of well established 'wear' parameters such as surface temperature and countersurface profile hardness and rigidity. These must necessarily be considered in conjunction with the viscoelastic properties of the thermoplastics used. For example, as the temperature goes up so does the likelihood of mechano-chemical energy being dissipated by molecular chains slipping past one another rather than by initiating chain scission. As a result the polymer suffers a smaller drop in molecular weight than otherwise would have been the case. Conversely the presence of hard rigid, intact, countersurface oxides appears to facilitate

the transfer of mechano-chemical energy across the interface resulting in polymer wear debris of relatively lower molecular weight.

A further consequence of the present work is an enlarged understanding of the role of mild steel countersurfaces in polymer wear processes. As a result of the experimental transition from surfaces possessing thick oxides to no oxides at all the corresponding interpretations have to be adjusted accordingly. At one extreme the mechanical properties and mechano-chemical history of the materials plays the predominant role; at the other the catalytic nature of 'clean' iron becomes increasingly significant.

In the case of 100nm oxides the wear rates of polymers slid against them seemed to depend heavily on two factors, oxide tenacity and oxide type. If the oxide remained intact then its smooth hard profile appeared to be linked with low polymer wear. If the oxide broke up, and providing no fine transfer films were present, then Fe_3O_4 was observed to promote a beneficial polishing action that contrasted markedly with the coarser, harmfully abrasive action of $\alpha Fe_2O_3/Fe_3O_4$ oxide particles. To some extent these latter effects may be related to the mechanical properties of the individual oxide crystals and the way in which they shatter under applied stress.

At the other end of the scale, when oxides are absent from an iron surface, catalytic forces have been demonstrated to be very important. This is not only from the point of view of breaking down hydrocarbon materials[138] but also in the present context, promoting the degradation of normally very stable inert materials (such as nC_5F_{12}) that are structurally similar to P.T.F.E. Thus under extreme conditions where 'clean' iron surfaces are likely to be produced and maintained in that state for some

length of time (such as in the low pressure environment of space craft) the chemistry of the surface alone could well become as critical as the chemical and physical side-effects of the wear process itself.

APPENDIX 1

The Vacuum Furnace

The Furnace consisted of a 50cm x 33cm diameter vacuum chamber heated internally by a 300-400 watt electric heater and cooled externally by a water jacket.

The whole apparatus was a modified version of the Edwards Speedivac $\left(\frac{1}{2}\text{ lb.}\right)$ 0.23 kg Melting Vacuum Furnace and is shown overleaf. The centrally pivoting crucible was removed along with various shields and baffles and replaced by a new heating element wound on a silica glass former. Four strands of 1.0 mm. diameter nickel/chrome was chosen as a filament material in preference to tungster due to oxidation in the operating $\left(10^{-1}\text{-}10^{-2}\text{ torr}\right)\triangleq$ 10-1.0 Nm^{-2} vacuum region. (Initial experiments had shown that use of tungsten wire promoted contamination by tungsten oxide (WO_2) on the mild steel specimen surface). The filament was wound around a silica glass grooved former and mounted vertically on a table inside the furnace. This allowed the mild steel drum to be positioned inside it promoting a uniform temperature build up on the surface. The temperature was measured by a chromel/alumel thermocouple placed next to the specimen surface and with read-out on a Scalamp galvanometer. An estimate of the temperature was made by referring to a calibration curve plotted using the same thermocouple in a standard air furnace. The range required for the present experiments was $(200\text{-}500^{\circ}C)$ 473-773K and required a heater current of 10-32A at 15-25V. Externally the walls of the main vessel were continuously water-cooled preventing distortion by thermal expansion.

The vacuum chamber pumping arrangement consisted of a standard rotary backing pump and oil diffusion pump linked in series. As the maximum vacuum required was $\left(10^{-2}\text{ torr}\right)\triangleq$ 1.0 Nm^{-2} air was leaked into the system by a bleed valve positioned below the main chamber. This reduced any possibility of oil contamination that might have been promoted by operating the backing pump alone.

THE VACUUM FURNACE

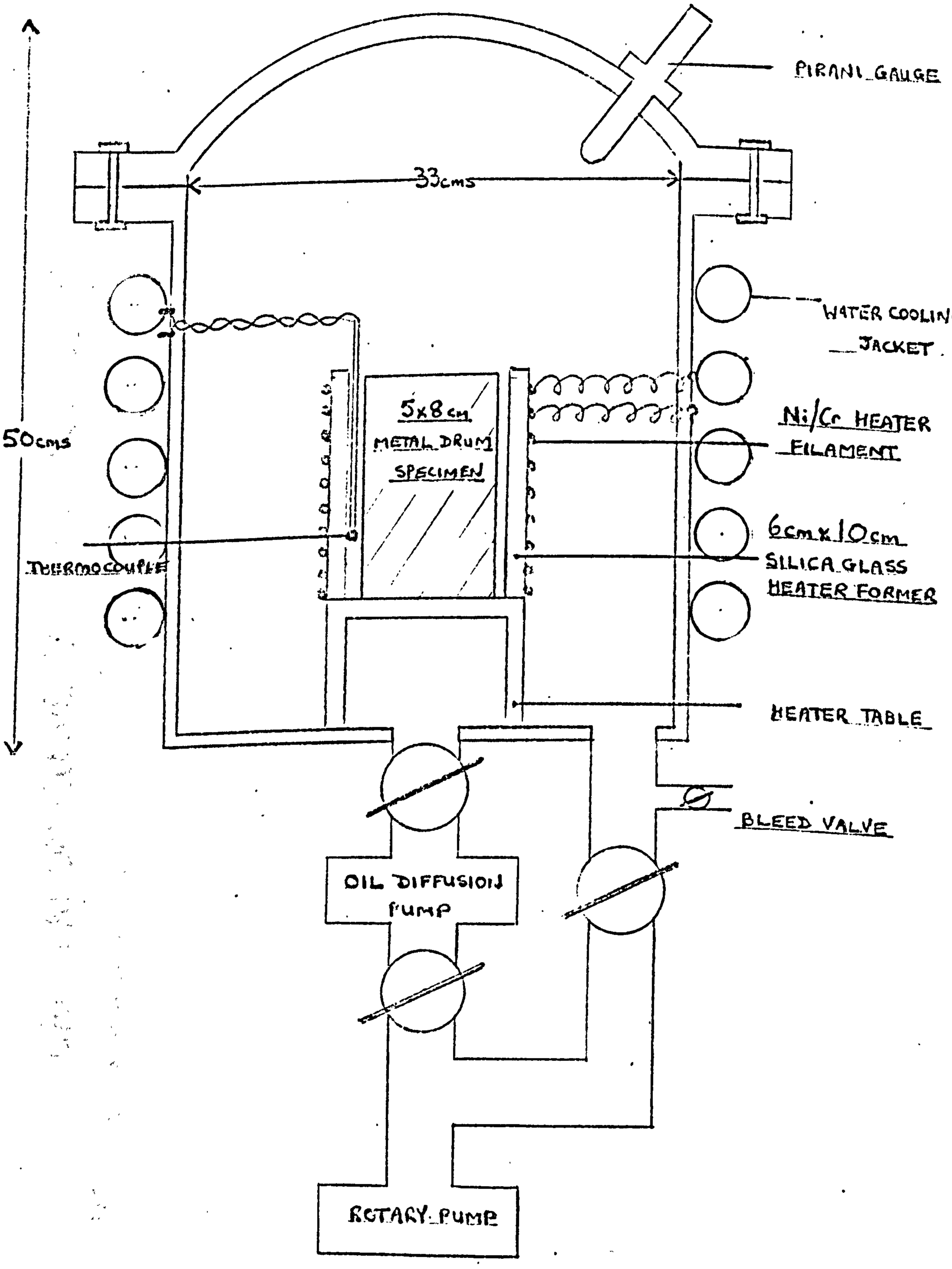

CALIBRATION CURVE VACUUM FURNACE THERMOCOUPLE

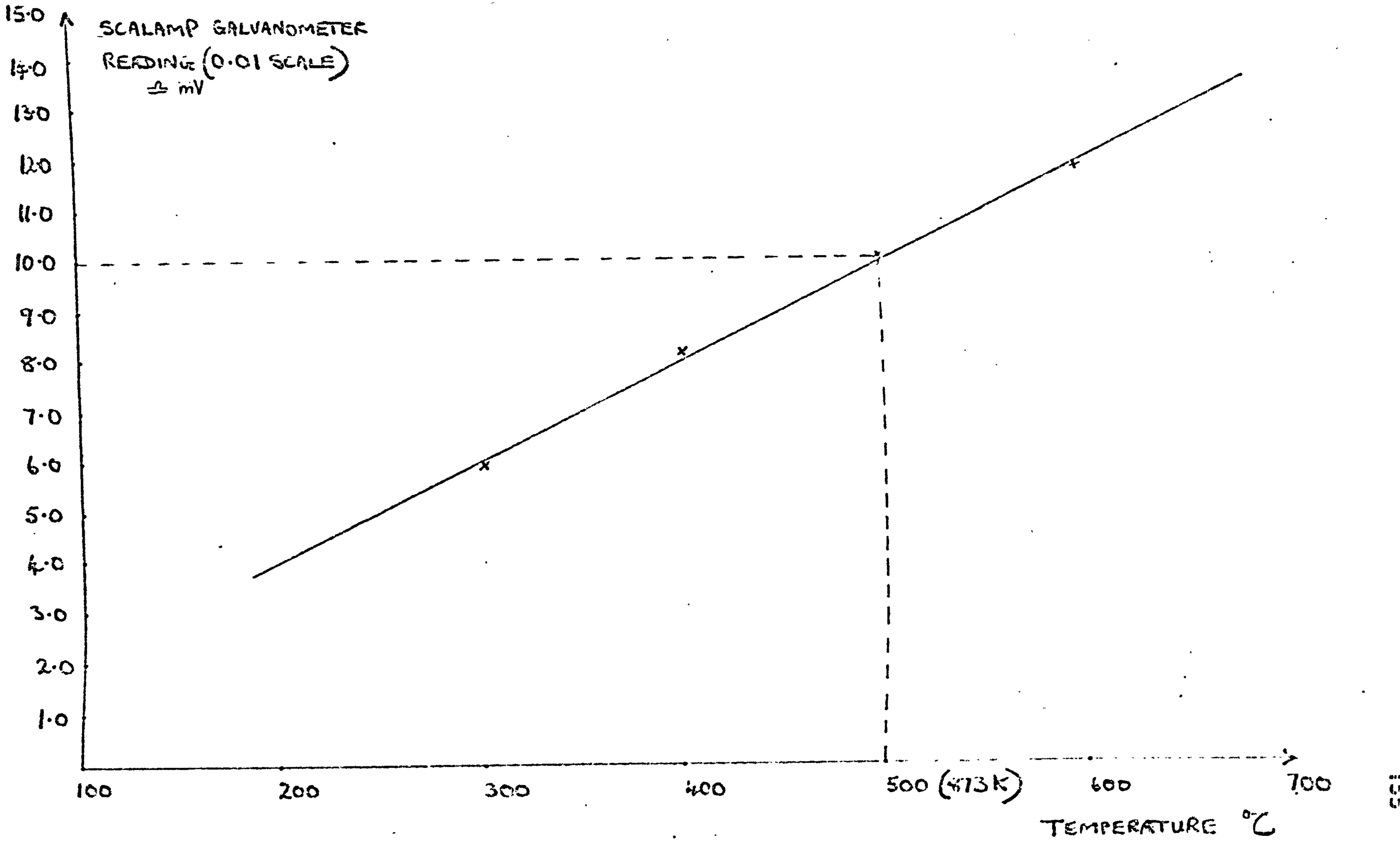

APPENDIX 2

Gel Permeation Chromatography

2.1 The principles

This is a technique for determining the molecular weight distributions of a diluted solution of polydisperse polymer by gel filtration.[132,133,134]

Typically the apparatus consists of a 1200mm long column of cross-linked polystyrene gel material being continually flushed with solvent. A 0.1-2 wt.% solution of the polymer material in the same solvent is injected into the stream and passed through the column. Unimpeded by the gel the larger molecules pass through first whereas smaller fragments take longer according to the polystyrene pore size. Detection is by differential refractometry because concentration $\propto$ refractive index for dilute solutions. Automatically a concentration versus elution volume graph is plotted and calibration spikes are superimposed on it for each $(5\ c\ c)\ 5\times10^{-6}\ m^3$ passed. The exact molecular weight at each point can only be determined by previous calibration of the column using monodisperse sample material or by monodisperse polystyrene and applying appropriate conversion factors. The resolution of G.P.C. apparatus is not infinite and even monodisperse material tends to produce Gaussian bell-shaped curves. Hence polydisperse material is a composite Gaussian Curve of all the components. The height of the curve is not necessarily proportional to the molecular weight at that point as the molecular weight of components on either side of it tend to influence the value. Similarly exagerated effects of very large or very small components must be allowed for in initially packing the column and in this instance two separate ones were used.

2.2 The application

Polymeric debris from the wear rate experiments was stored in sealed glass containers. Only fragments from the same or identical experiments were kept together. When 0.01 - 0.2 grams had been collected the polymer was put through the R.A.P.R.A. G.P.C. column for molecular weight analysis.

The operating concentrations were 0.2% in tetrahydrofuran at (25° C) 298K passing through the column at 1 ml/min. The instrument sensitivity was set at 8X and one of two separate columns were used. Column A was designed to be more accurate for lower molecular weight samples and column B more accurate for the higher molecular weight materials.

The pore size packing for each column was as follows:-

Column A.	(100-350 Å)	10-35 n m.
	(700-2000 Å)	70-200 n m.
	($5-15 \times 10^3$ Å)	$5-15 \times 10^2$ n m.
	($7-50 \times 10^5$ Å)	$7-50 \times 10^4$ n m.
Column B.	(700-2000 Å)	70-200 n m.
	($1.5-5.0 \times 10^4$ Å)	$1.5 - 5.0 \times 10^3$ n m.
	($7 - 50 \times 10^5$ Å)	$7-50 \times 10^4$ n m
	($5 - 10 \times 10^6$ Å)	$5-10 \times 10^5$ n m

Because the G.P.C. machine could not be calibrated directly for P.V.C., the Q factor method of interpretation was adopted giving 'A' values. These are values obtained using the extended chain length of polystyrene in angstrom units for calibration. An idea of the molecular weights of Mn, Mw, amd Mz were obtained by multiplying these A values by the factor Q, the molecular weight per angstrom for the material under consideration. For P.V.C. the Q. factor is 25.1. The polydispersity of the samples was expressed by the N : W : Z ratio. i.e. The ratio if number average m.wt., to weight average m.wt., to 'Z' average m.wt. (see RESULTS/DISCUSSION for definitions). A useful introduction to the calculation of molecular weight distributions and the various average molecular weights from the chromatograms and calibration curves produced from using G.P.C. equipment has recently appeared by COOPER[134] and also PICKETT[135] et al.

APPENDIX 3

Infra-Red Attenuated Total Reflectance Absorption Spectrophotometry

3.1 The Principles

The instruments used in the present work were a Unicam SP 200 infra red spectrophotometer with an attached R.I.I.C. Tr 25 A.T.R. unit.

A beam of infra-red energy is made to pass through a thallous bromide-iodide prism against which the specimens are clamped in close optical contact.[20] The angle at which the beam enters the crystal is such that total internal reflection takes place about twenty five times along the polymer/prism interface.

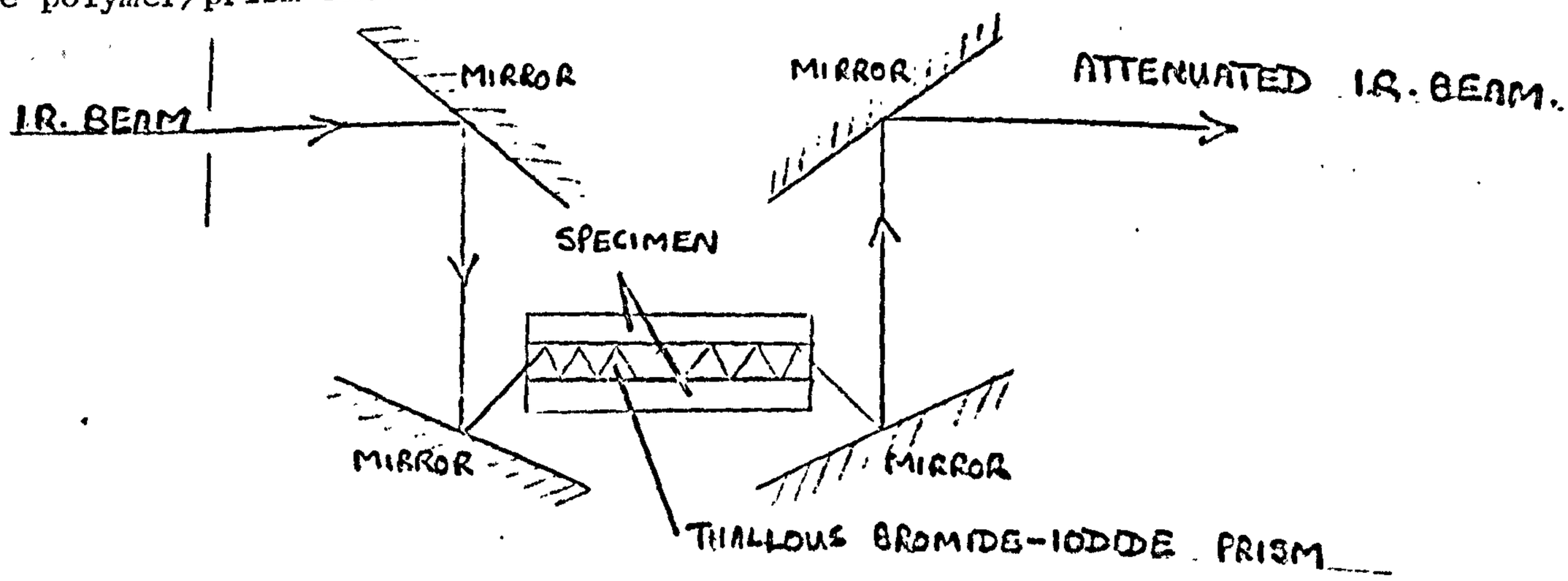

Since in such circumstances the infra-red beam only penetrates the interface to a distance of the order of one wavelength (2-15μm) the emergent beam is attenuated with the absorption characteristics of the polymer surface only.

3.2 The Application

As the wear rate experiments proceeded strips of polymer of varying character were removed by tweezers from the metal drums* and mounted, with the metal/polymer interface side upwards, on adhesive tape. When a sufficient area of backed polymer had been collected (approx. two pieces 4 x 1 cm.) these were fitted as an intimately contacting "sandwich" alongside the A.T.R. prism, such that the polymer was physically contacting the thallous bromide - iodide (KRS-5) crystal. Infra red energy of wavelength

2 - 15 μm was passed through the prism in the usual way such that approximately twenty five internal reflections at 45° incidence took place and hence the polymer penetrated to a depth of 2 - 15 μm. The reference beam was attentuated in each case to allow two scans of the infra-red region, one giving a transmittance value of approximately 30% and the other 60% at 5 μm. Thus two charts were obtained of each specimen the first giving 'on scale' peaks over the entire 2 - 16 μm wavelength region and the other 'on scale' accentuated peaks in the 5 - 10 μm area only resulting in greater resolution. In all cases to compensate for the high percentage of energy loss the incident infra-red beam was pre-set to a value of 3E.

* N.B. Only loose polymer debris being pushed out of the wear track was collected (see measurement of wear rate).

3.3 Infra-Red Spectrophotomctry Absorption Spectra of P.V.C.

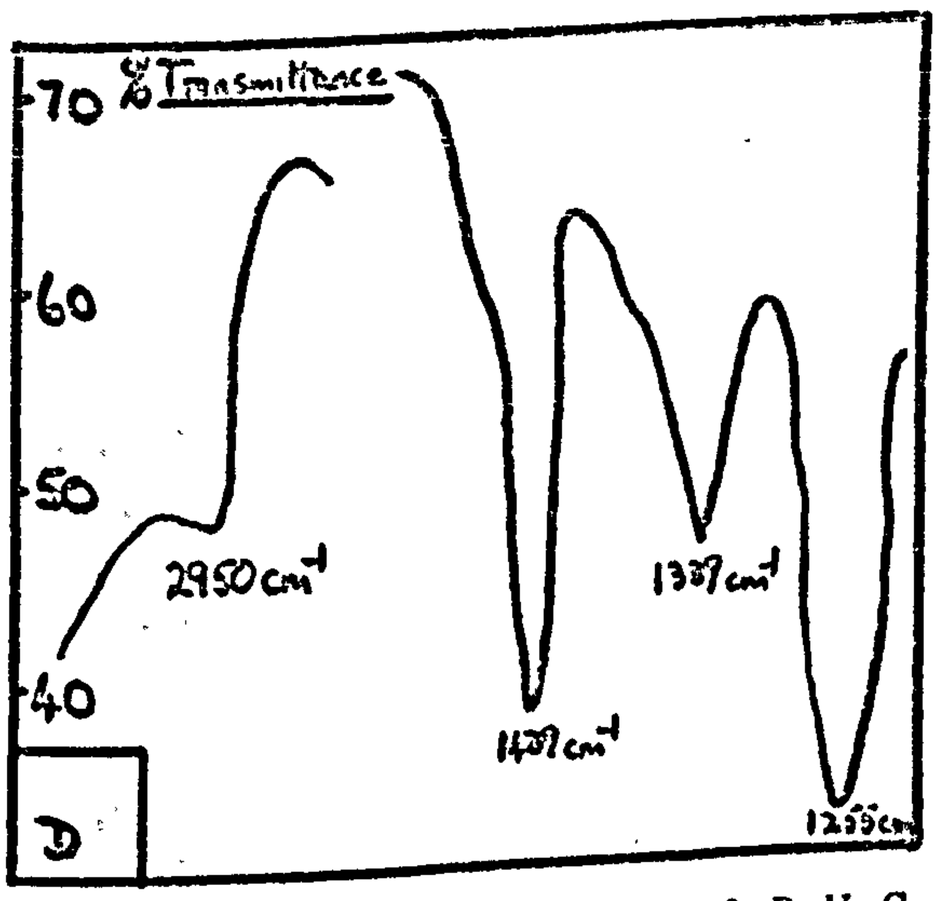

Standard control sample of P.V.C (stabilised with 2% dibasic lead stearate).

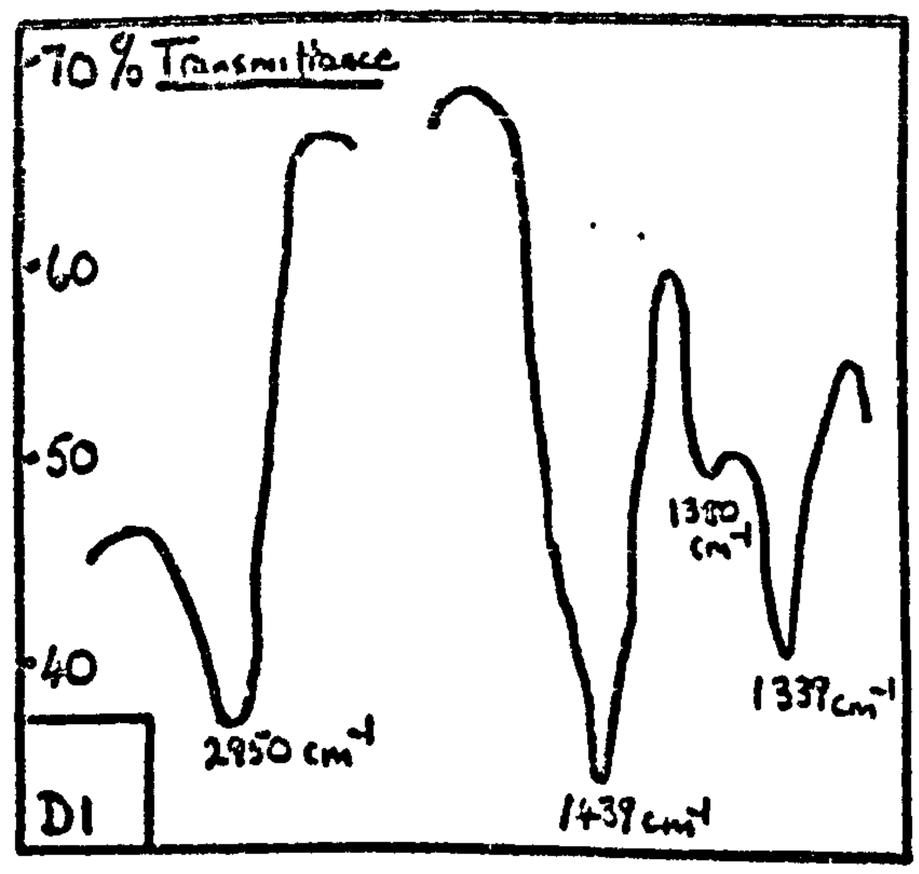

Stabilised P.V.C. slid on mild steel.

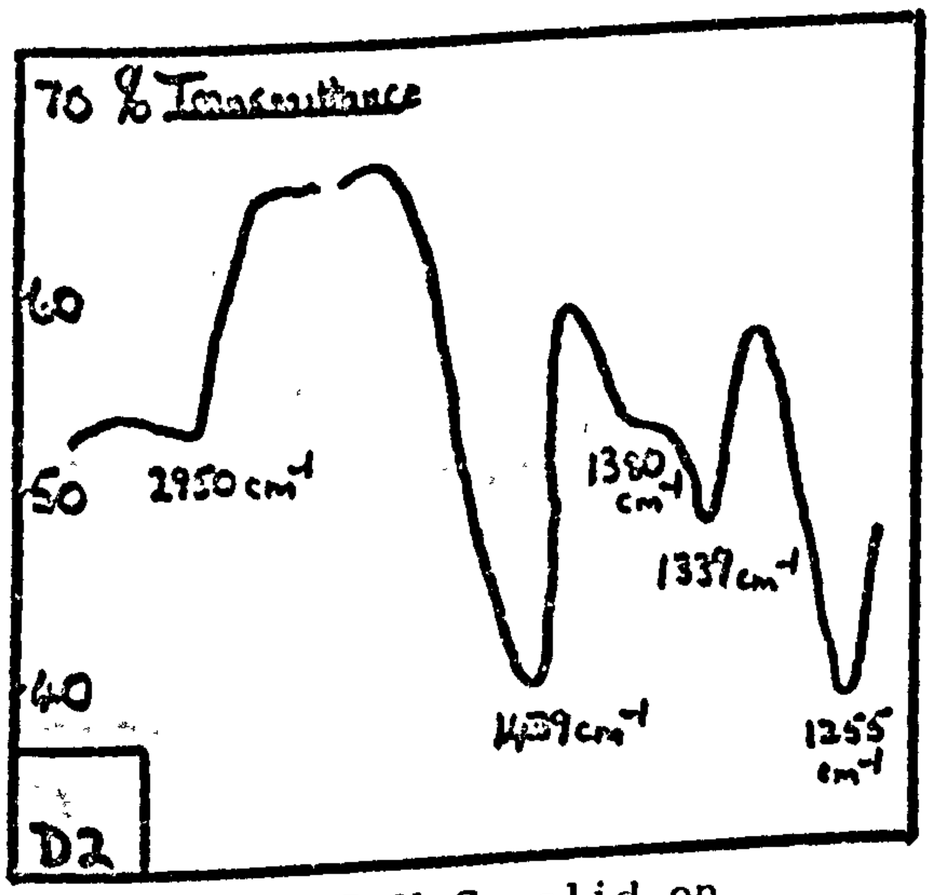

Stabilised P.V.C. slid on 100 nm thick Fe_3O_4 oxide.

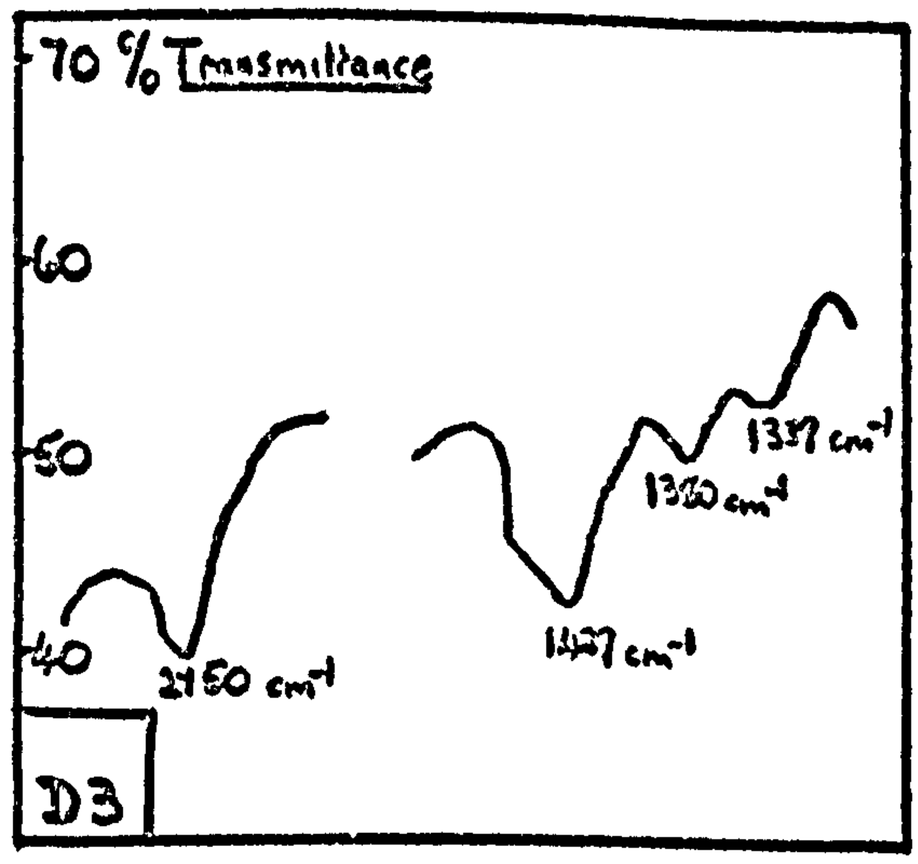

Stabilised P.V.C. slid on 100 nm thick Fe_3O_4 / Fe_2O_3 oxide.

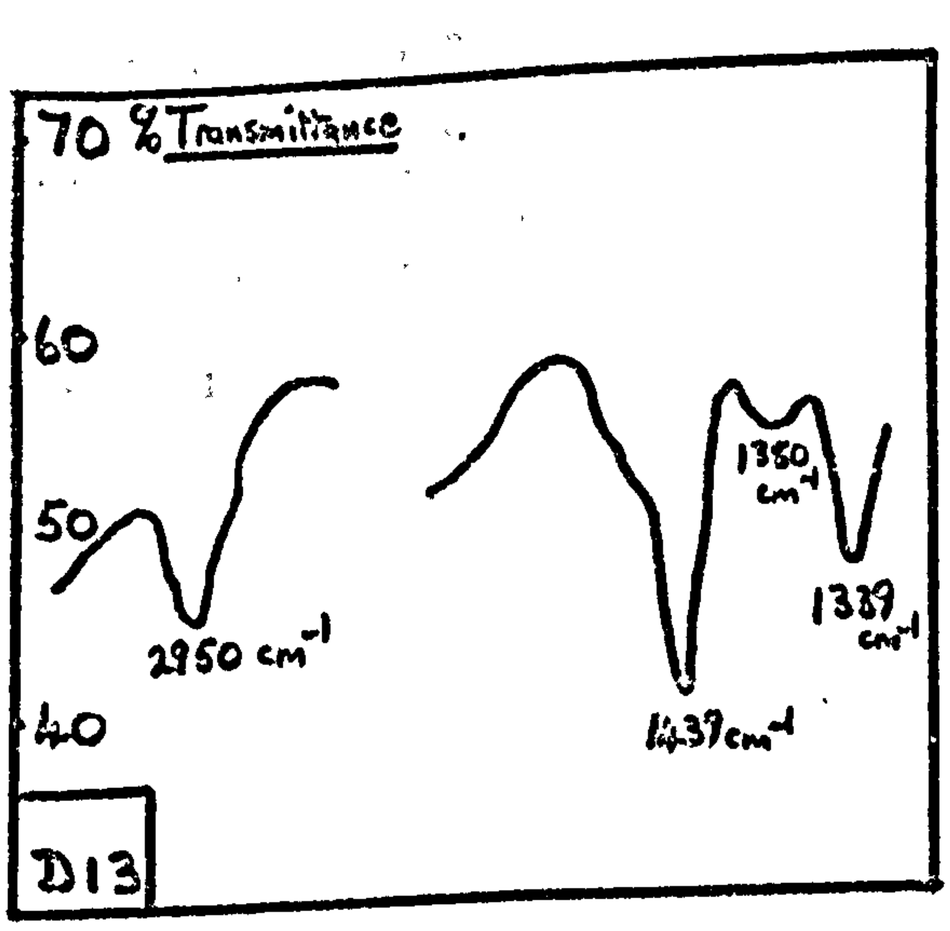

Stabilised P.V.C. slid on mild steel (15.7 N load).

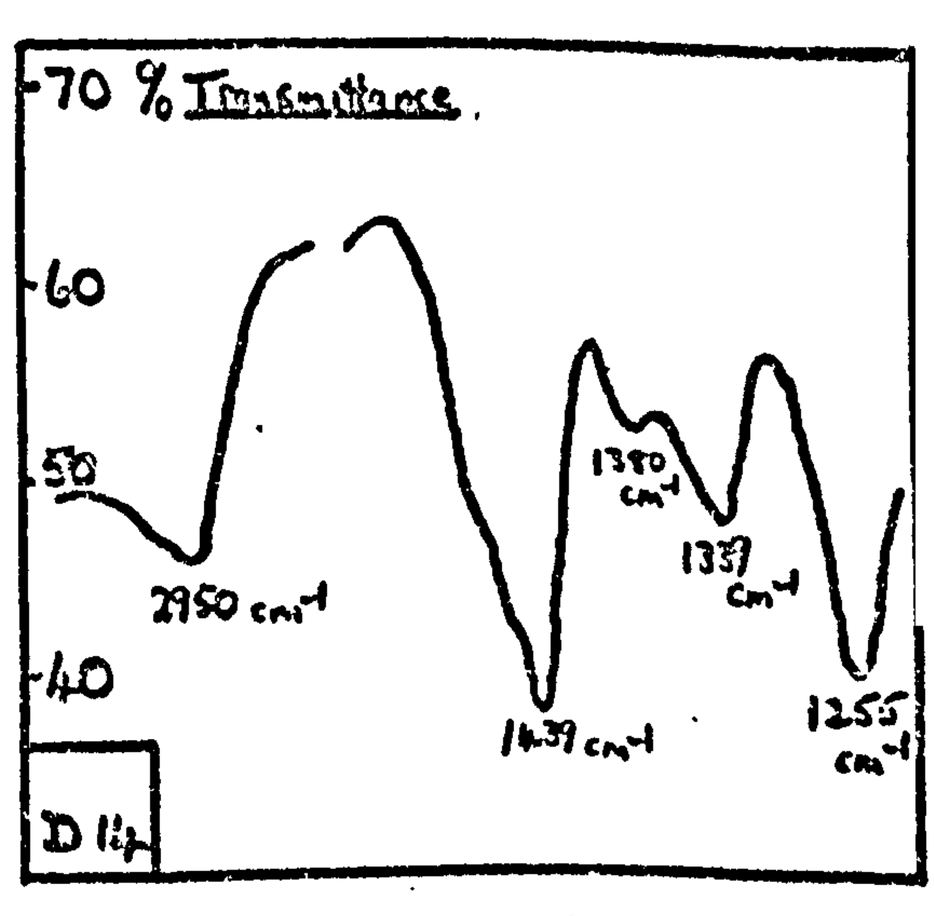

Stabilised P.V.C. slid on mild steel (3.9 N load).

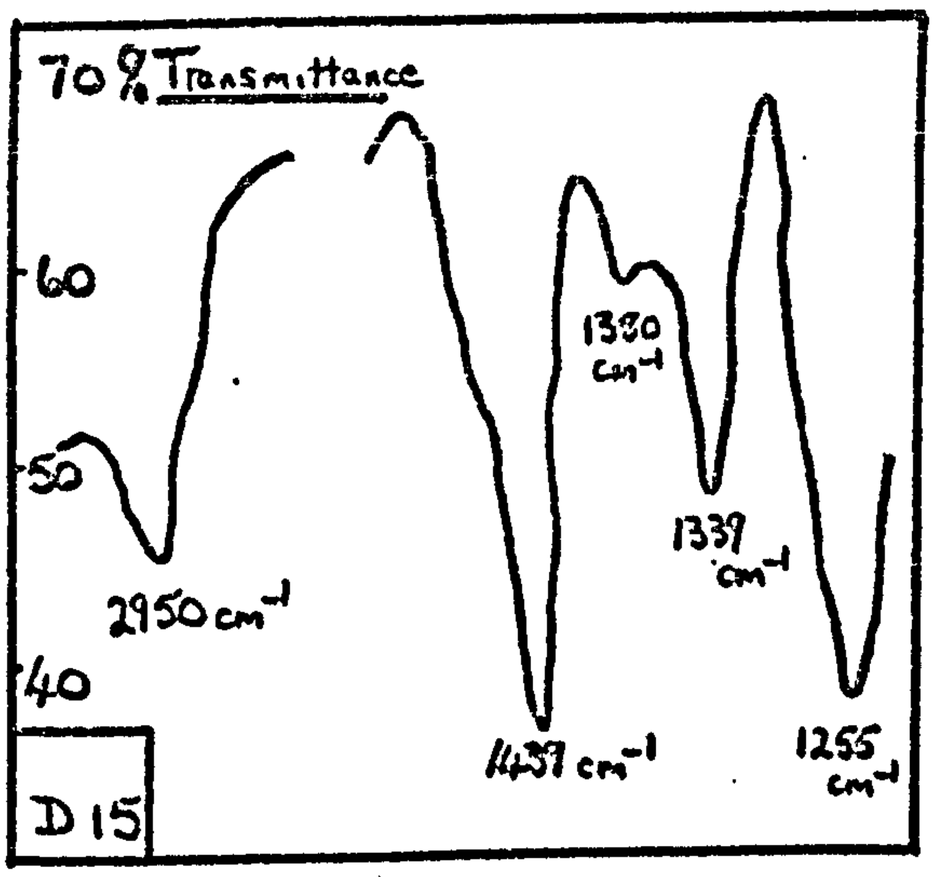

Stabilised P.V.C. slid on mild steel (at 2.88 ms^{-1} sliding speed.)

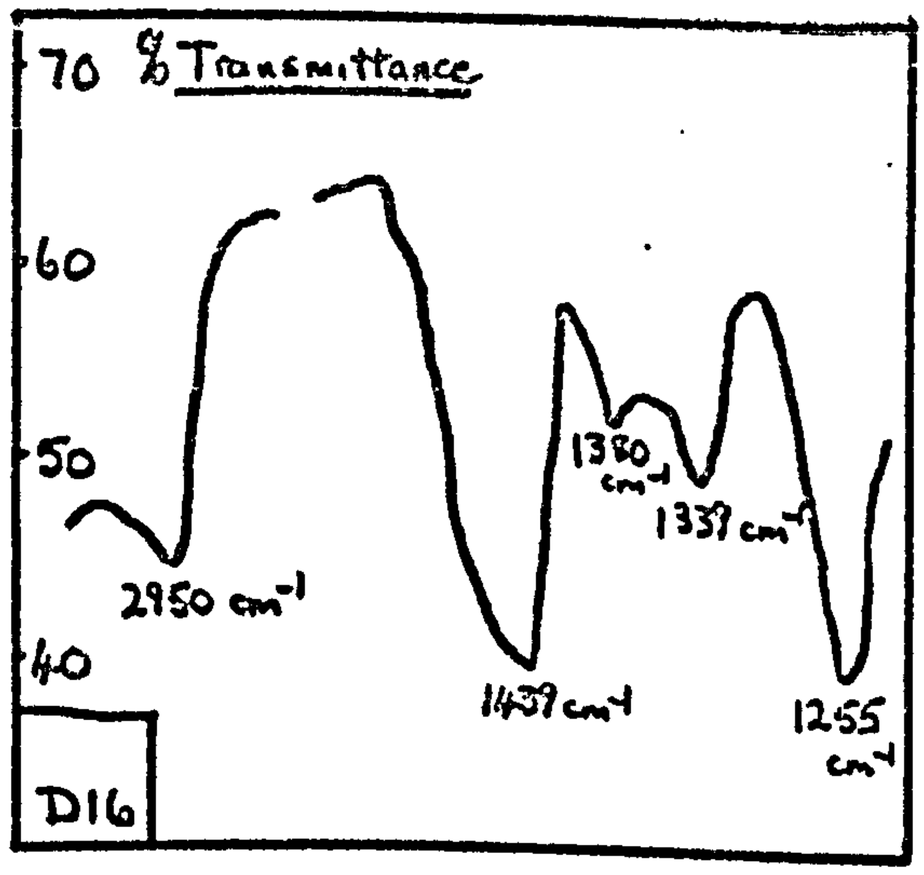

Stabilised P.V.C. slid on mild steel (at 5.33 ms^{-1} sliding speed).

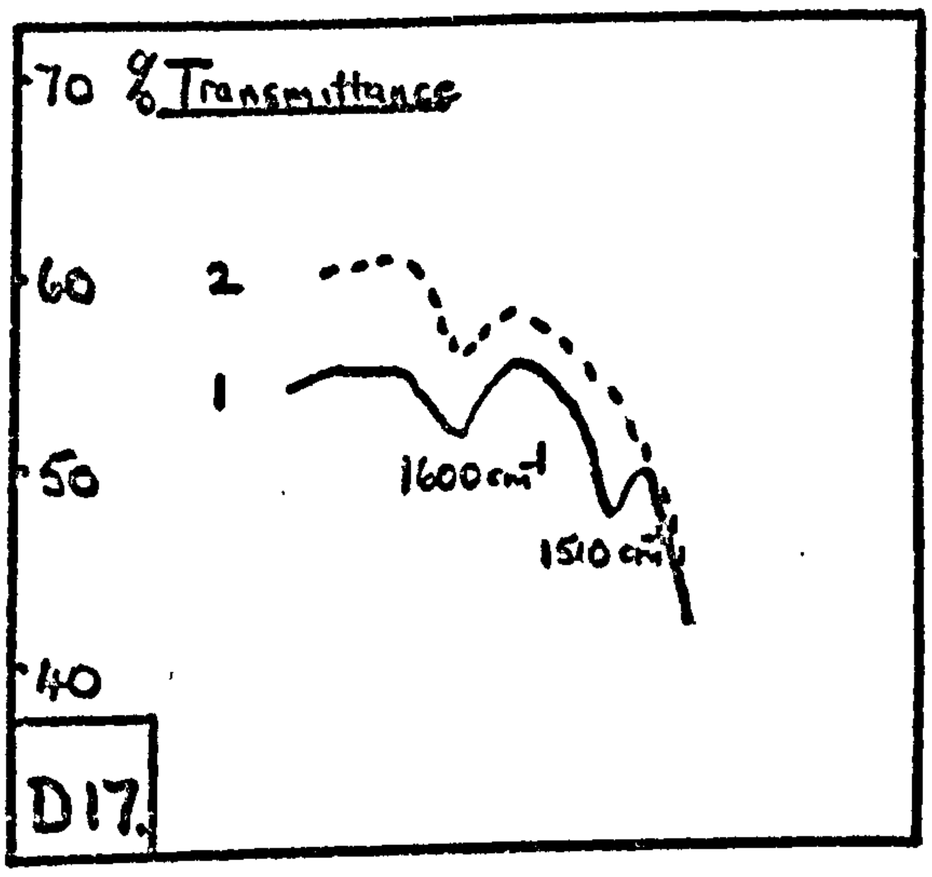

Absorption through:-

(1) —— 73.0 μm thick P.V.C. film (stabilised with 2% dibasic lead stearate).

(2) ---- 106.0 μm thick P.V.C. film (unstabilised).

Unless otherwise stated the wear debris analysed came from experiments in which P.V.C. flats were slid at 1.44 ms^{-1} against mild steel rotating drums with a surface finish of 0.075 m (c.l.a.) and a loading of 8.83N. Only the salient features of the various spectra have been presented to enable easy cross reference. The % transmittance ordinates have been included on the graphs for comparison of relative peak heights alone (i.e. qualitative analysis) and do not necessarily have any 'absolute' significance in this particular context. The various peaks are individually labelled with the appropriate wave numbers (i.e. the reciprocal of wave-length) at which the absorption occurred.

SEE TABLE 2. IN RESULTS/DISCUSSION SECTION for ancillary detail.

APPENDIX 4

U.V. Spectroscopic Analysis.

4.1 The Application

As it is possible for P.V.C. to degrade by more than one mechanism (e.g. mechanical chain scission or chemical evolution of H Cl) U.V. spectroscopic analysis was employed in order to differentiate between the two possibilities. It is known that when H Cl is evolved from the P.V.C. molecule increased conjugation occurs along the backbone chain producing a polyene structure. Changes of this character are readily detected by U.V. absorption techniques which generate spectra characterised by increased absorption peak intensity, wave shifts or peaks at an increased number of wave lengths. In the present case a very basic simple qualitative indication of any increase in P.V.C. conjugation in the worn P.V.C. samples was required.. Correspondingly 3 solutions of P.V.C. in tetrahydroforan solvent were made up initially at 1.0% dilution. The first was a P.V.C. control sample, the second P.V.C. wear debris and the third a heavily thermally degraded P.V.C. sample (493K 2hrs.) The appropriately diluted solutions were placed in turn in silica cells alongside a pure solvent reference cell inside a Unicam SP 800 U.V. Spectrophotometer. U.V. energy of wavelength 200-450 nm was passed through the specimens and characteristic absorbance patterns recorded automatically on a chart.

4.2 Ultra-Violet Spectrophotometry Absorption Spectra of P.V.C.

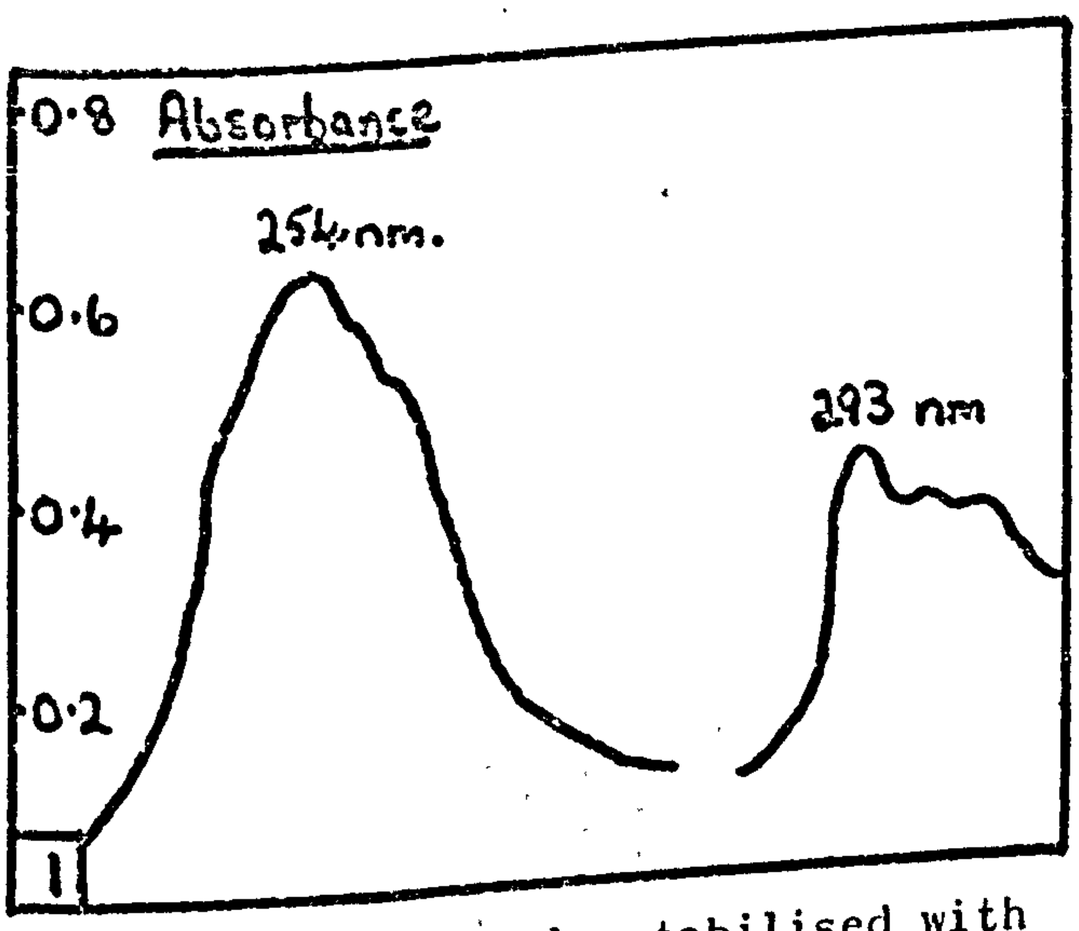

P.V.C. control sample stabilised with 2% dibasic lead stearate and dissolved as a 1% solution in T.H.F.

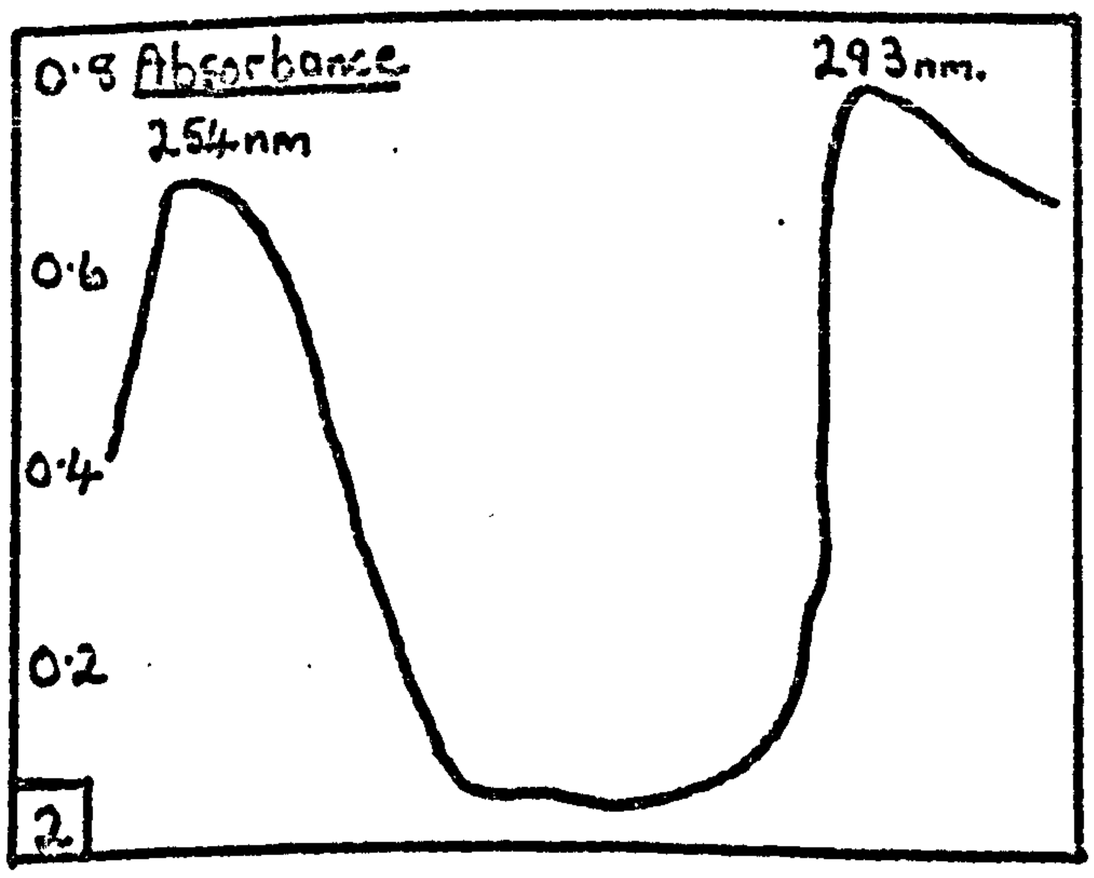

Stabilised P.V.C. thermally degraded for 2 hours at 500 K and dissolved as a 1% solution in T.H.F.

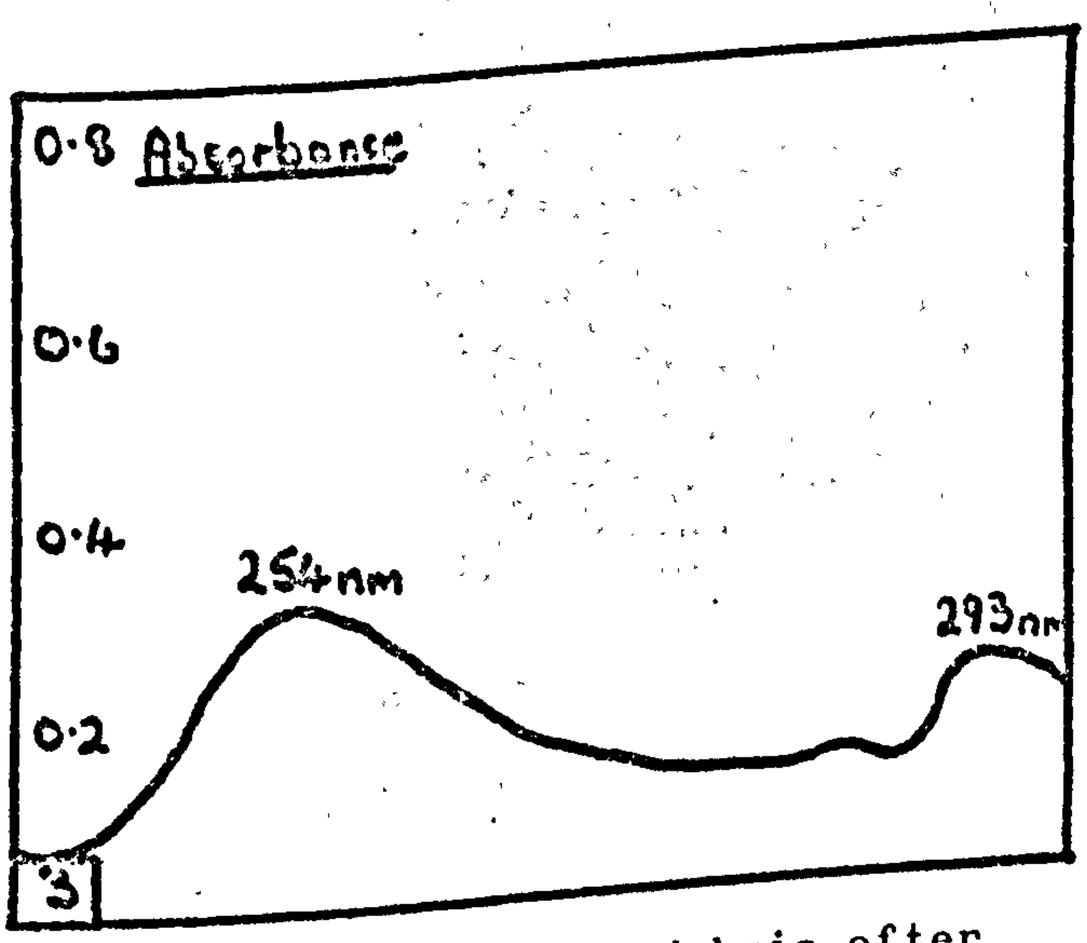

Stabilised P.V.C. wear debris after sliding at 1.44ms^{-1} on a mild steel drum with a 0.075 m (c.l.a.) surface finish for 30 minutes and an 8.83 N loading.

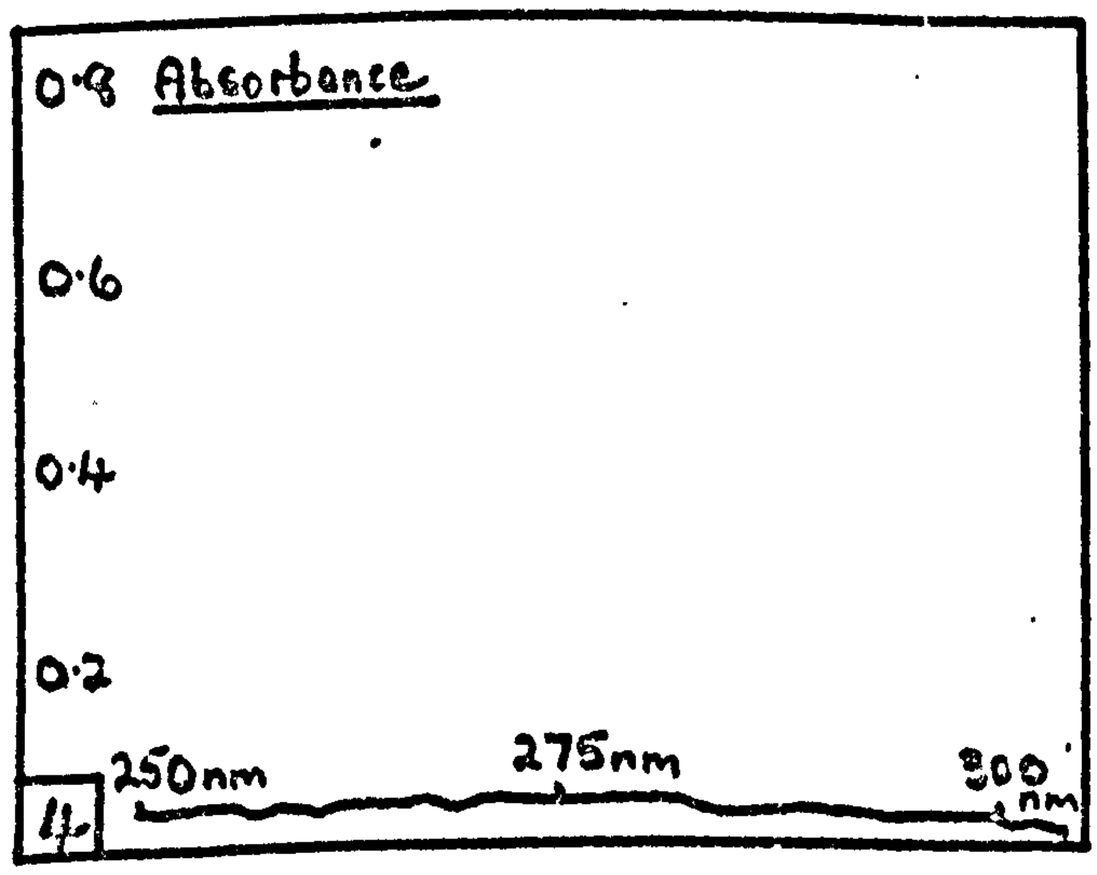

T.H.F. solvent control sample.

SEE TABLE 3 in RESULTS/DISCUSSION SECTION for ancillary detail.

APPENDIX 5

The Detection of Thin Films on Mild Steel

Taken as a whole the wear experiments showed that it is fundamentally important to establish the nature of materials on the planes of rupture. Thin films were frequently found left on the surface of the metal after polymeric materials had slid across them.

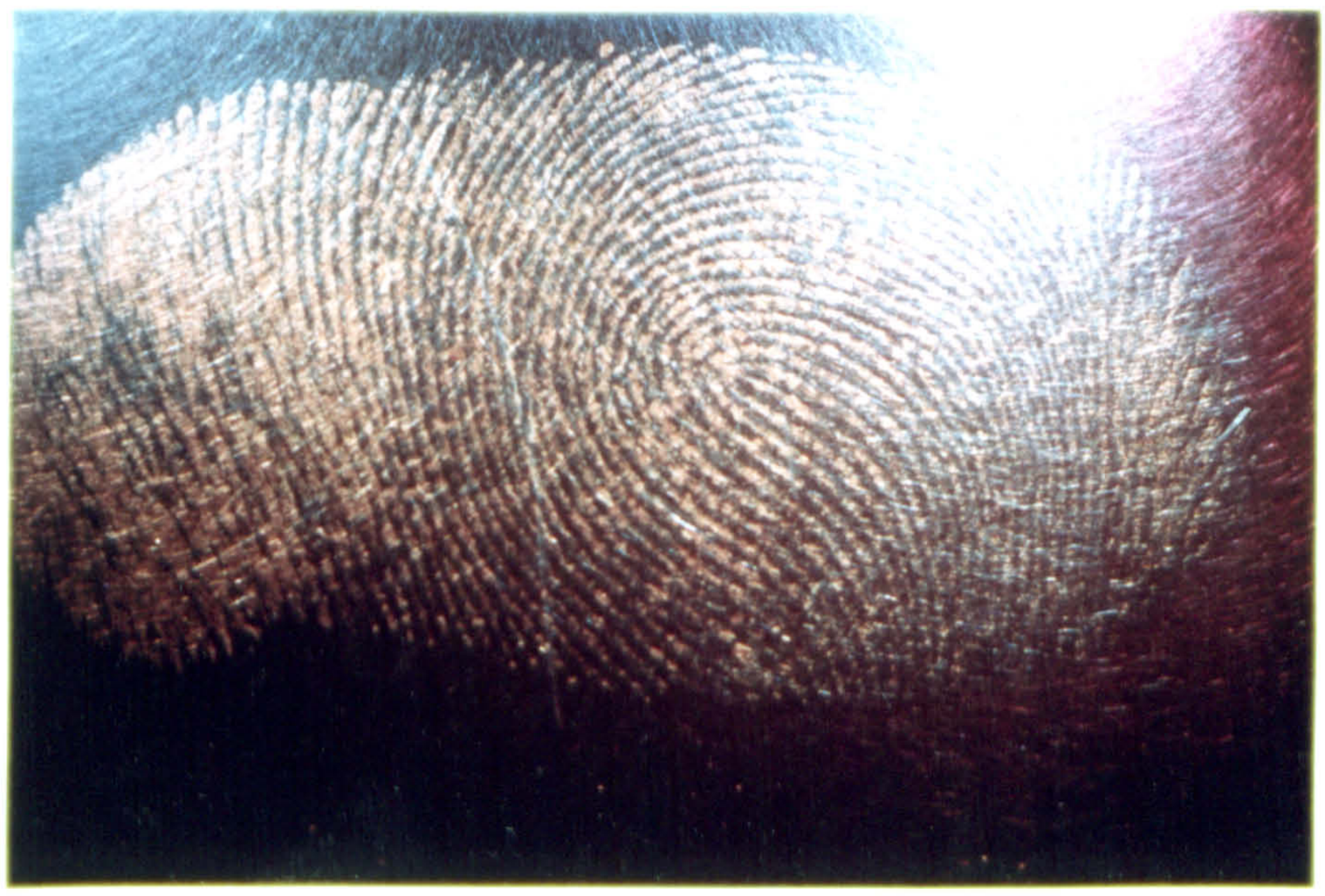

A thumbprint on mild steel showing up distinctly due to the development of oxide interference colours (propagated by heat treatment in an air furnace for 30 minutes at 750K)

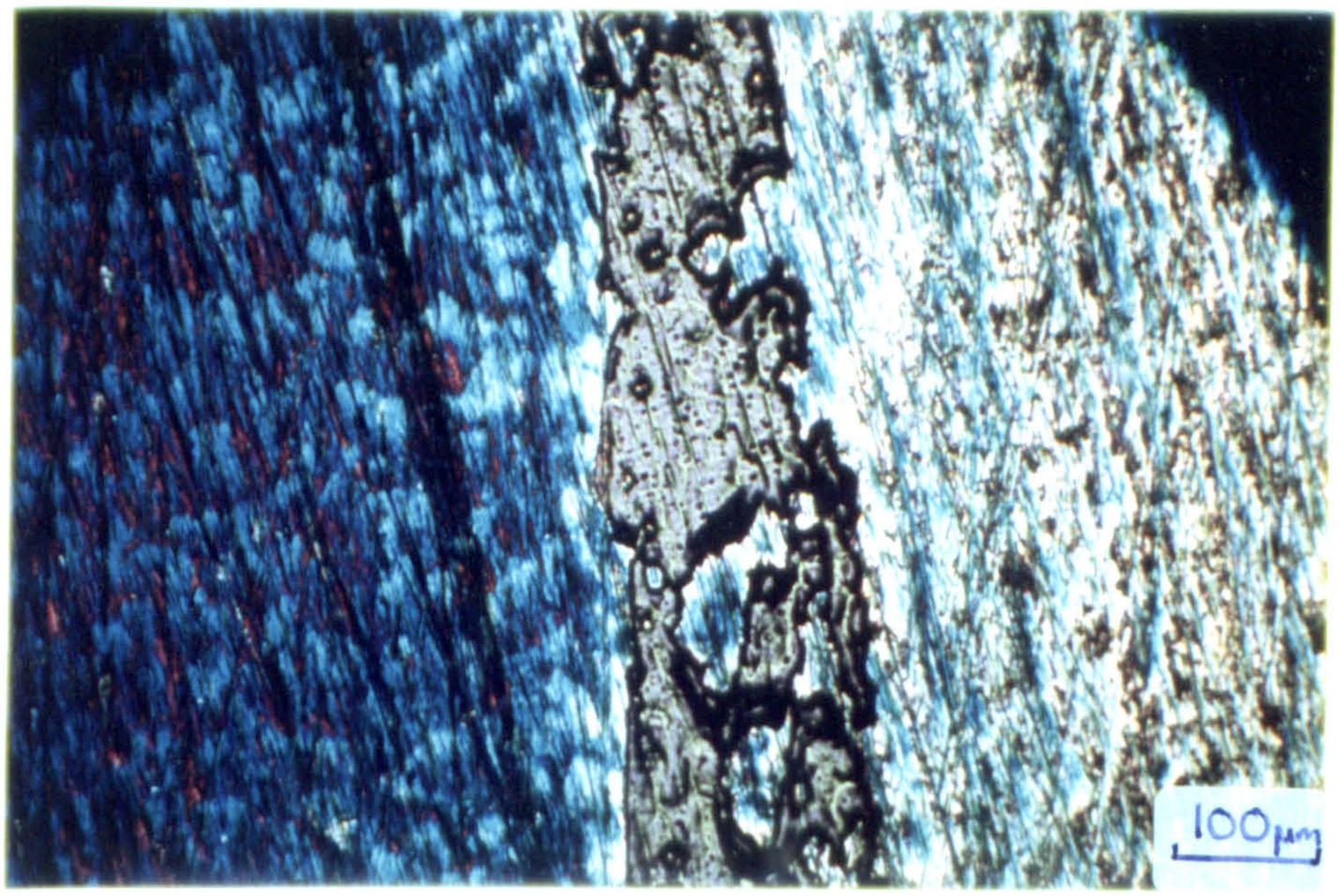

P.V.C. wear debris shown up distinctly on a mild steel substrate by subjecting the specimen to the heat treatment described in the text.

Although sensitive microscopic techniques were found necessary to establish the existence of these films an original method was especially developed to simplify this procedure. This involved heating the mild steel drums in air or vacuum for controlled times in a furnace at 750K. According to the conditions either ferrosoferric oxide (Fe_3O_4) or ferric oxide (Fe_2O_3) layers formed producing the well known interference colours culminating in a deep blue hue at approximately 100nm[36]. The thin film of material over the track inhibited or altered the rate of oxide growth and therefore appeared quite distinctly in a different colour (see PHOTOGRAPHS). This could also have been due to some chemical attack from degradation products in the polymer surface (though later analyses did not confirm this). (See RESULTS/DISCUSSION)

130 (P.20)

Such evidence gave no direct indication of film thickness but calibration tests were made with appropriately diluted solutions or dispersions of P.V.C. and P.T.F.E. Some care was necessary with highly diluted solutions because the residue from solvents was found also to alter the oxidation rate though to a much lesser degree. The results suggested that films as thin as 2-10nm may be readily detected and crude estimates of thickness made by comparison with wear tracks.

Thus this new 'oxide suppression' technique proved very valuable in initially establishing the presence of thin transfer films that are referred to repeatedly in the following discussions.

In each of the polymer systems studied some degree of transfer effect was observed by this method either as a precursor to macro deposition e.g. Cl.P.V.C., or as a thin film in its own right e.g. P.T.F.E.. Further details are described in the discussion under the individual descriptions of each wearing system.

APPENDIX 6

The Computation and Analysis of Polymer Wear Rate Data

6.1 The Application

The wear rates of the polymer specimens were calculated by taking weight loss measurements every 600s (ten minutes) and plotting the appropriate curves. These are given for reference in the following 6.2 subsection with the code numbers 1-46, matching those used in TABLES 5 & 6 (See RESULTS/DISCUSSION). Each graph contains several curves representing up to three seperate (but otherwise identical) runs on the same countersurface drum under the same conditions and in the same station. (See APPARATUS and EXPERIMENTAL PROCEDURE).

In order to establish mathematically the validity of the results obtained, a thorough statistical analysis was applied using a computer. The results of the analysis are shown in TABLE 6 and demonstrate that almost without exception a high degree of correlation exists between the weight loss versus time curves where they are drawn collectively on the same graph.

Secondly the t-test[117 (P.227)] method was applied to the results of wear rates from similar experiments performed on different drums in different stations. Effectively this compared the significance between different experiments. For example, comparing experiments 1 and 2 there is a 2-5% significance value. This means that there is only a 2-5% chance that the similarity of the wear curves could have occurred by chance, therefore the two sets of results are mathematically significant. Whilst in some cases the results of the same experiment performed in different stations were indeed found to be significantly similar,

e.g experiments 3 and 4, in others this was definitely not the case, e.g experiments 17 and 18. This suggested that the vibrational characteristics of individual stations must be taken into account when interpreting i.e. individual results are strictly relative and not necessarily absolute. It must be noted, however, that just because the rectilinear lengths of the curves are relatively displaced from each other along the 'weight' loss axis (reflected as poor t-test results) this does not necessarily mean that their slopes (i.e. wear rates) are substantially different (allowing for initial ambiguities). In fact an examination of the graphs shows that most of the wear rate curves approximate to a straight line after an initial 10 - 20 minutes running in period. Thus the usual methods of finding the best average value to the slope were adopted using the generally accepted 'least squares' criterion[117] (P. 277-285, P. 293).

In the first instance this enabled the average wear rate to be calculated in the form of g/s. By simple conversion factors involving the specific gravities of the various plastics used these values were converted to cm^3/cm (i.e. volume of material removed per unit distance slid).

6.2 Polymer Wear Rate Graphs

1.

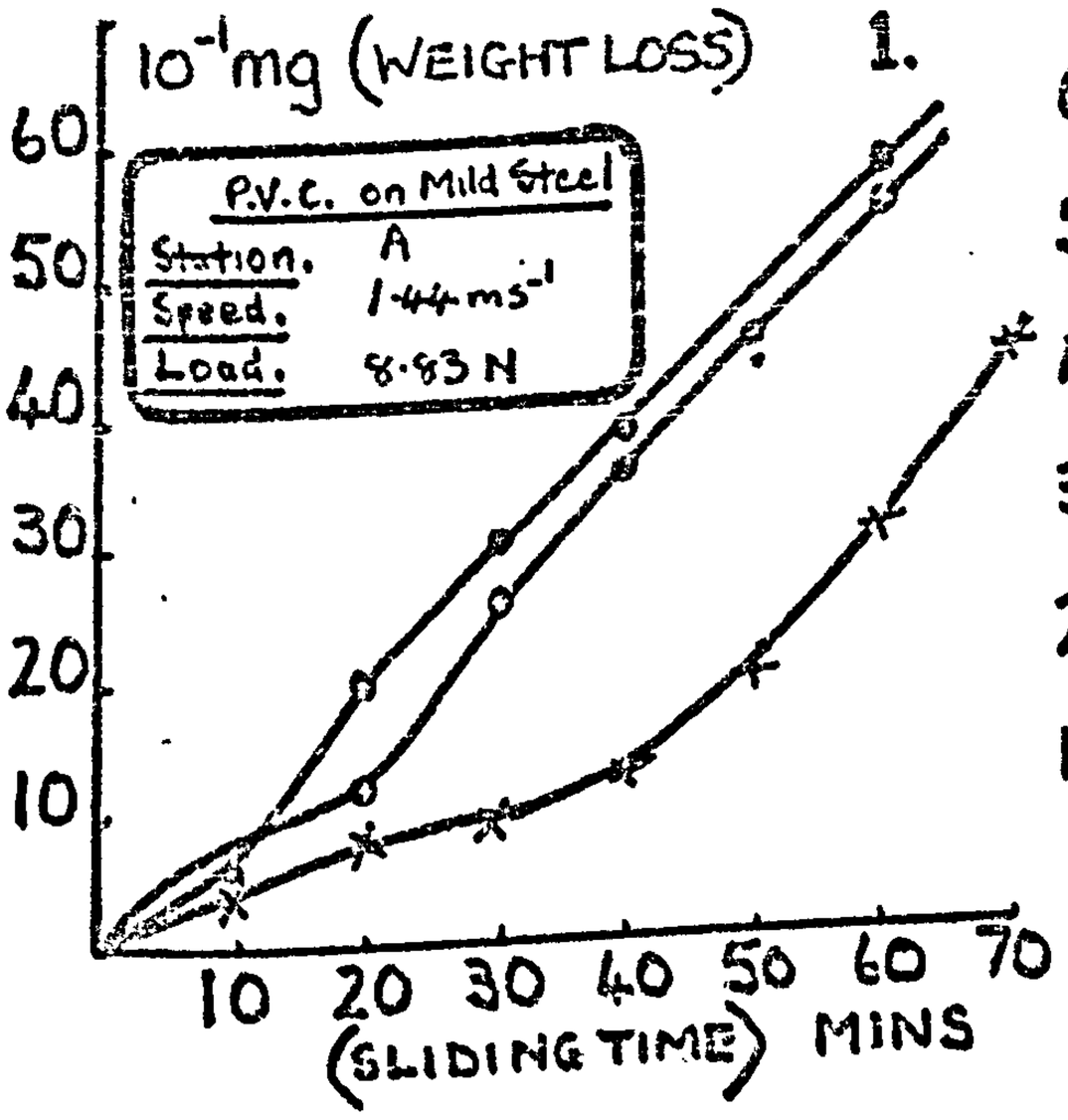

2.

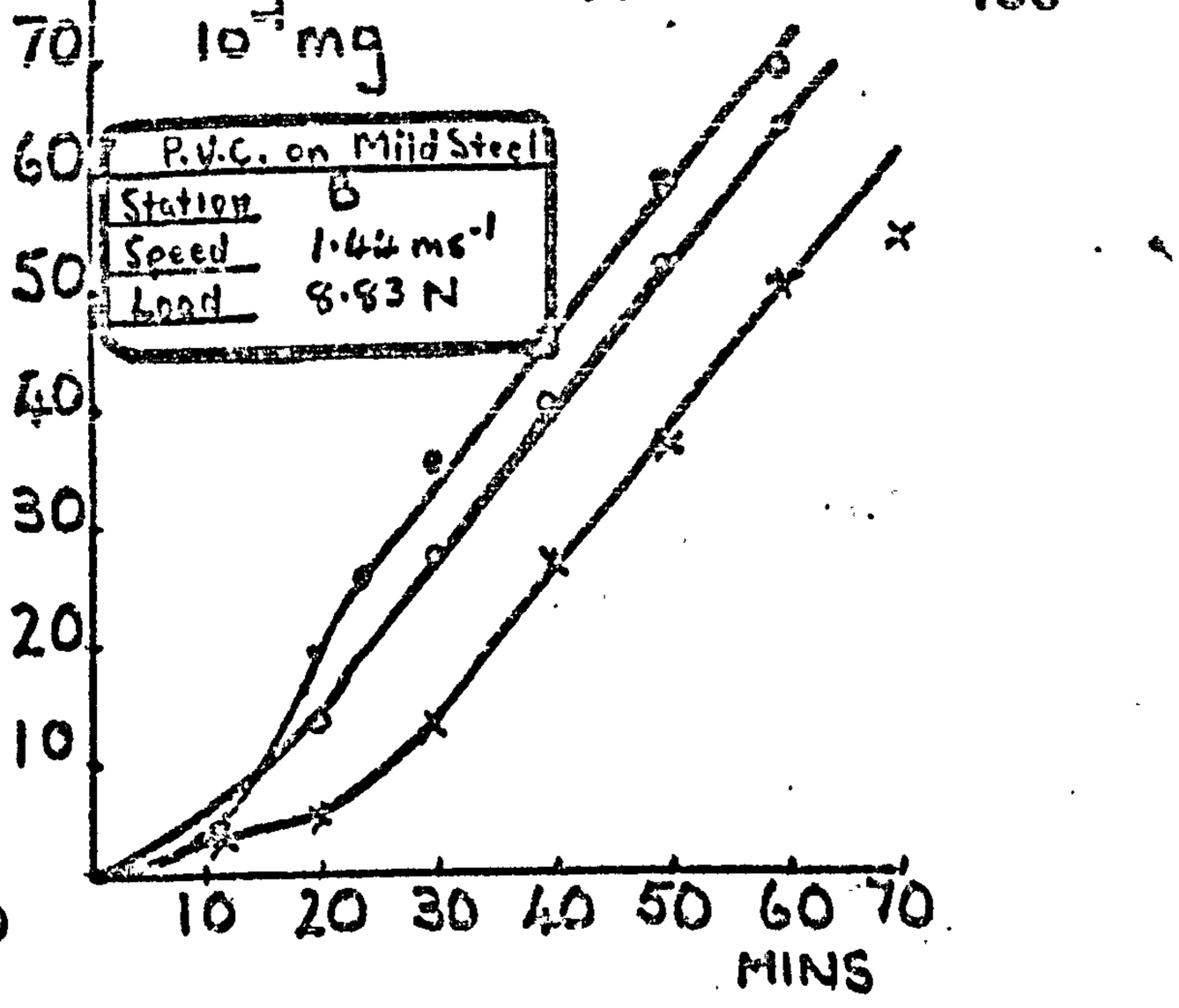

3.

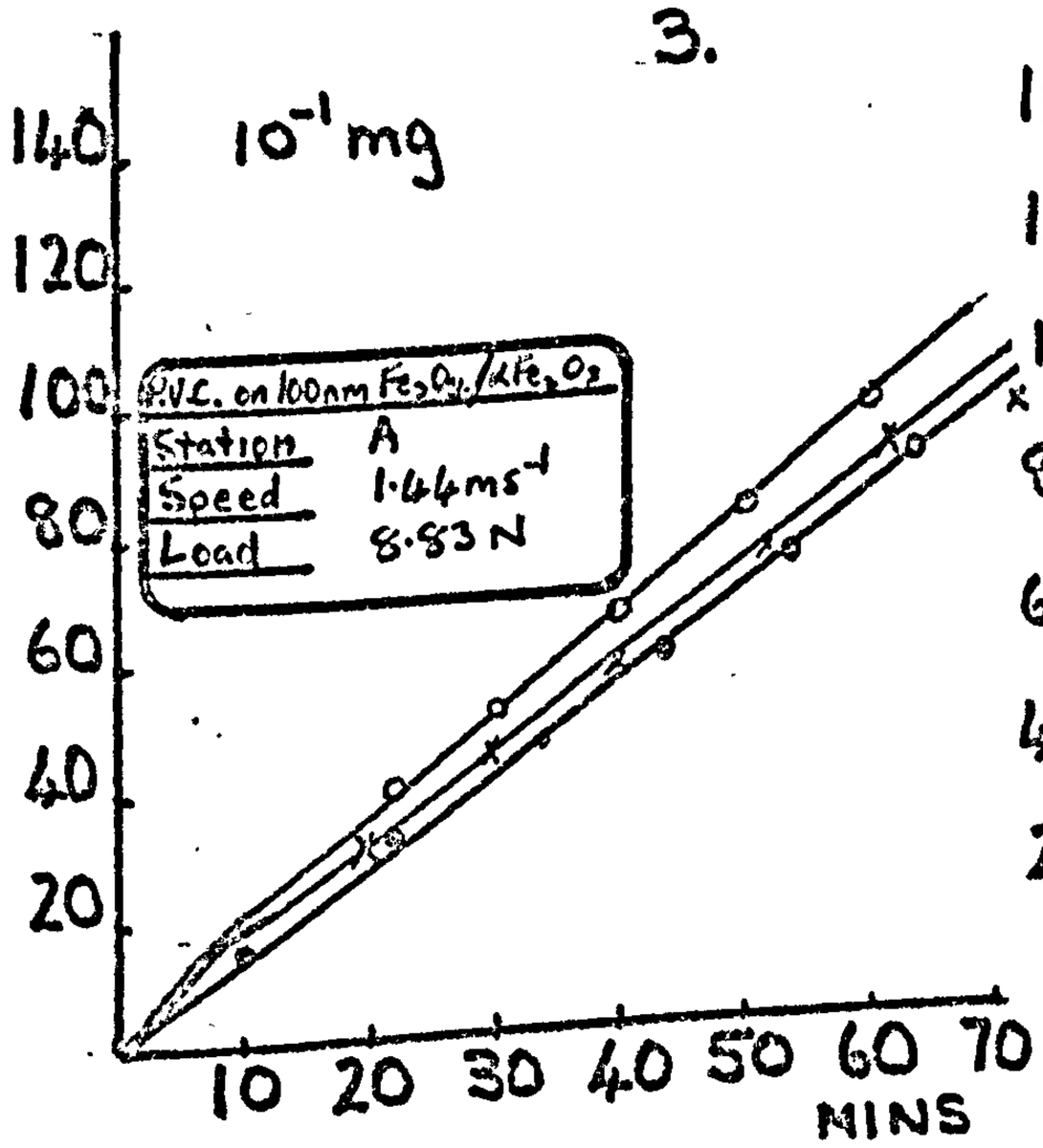

4.

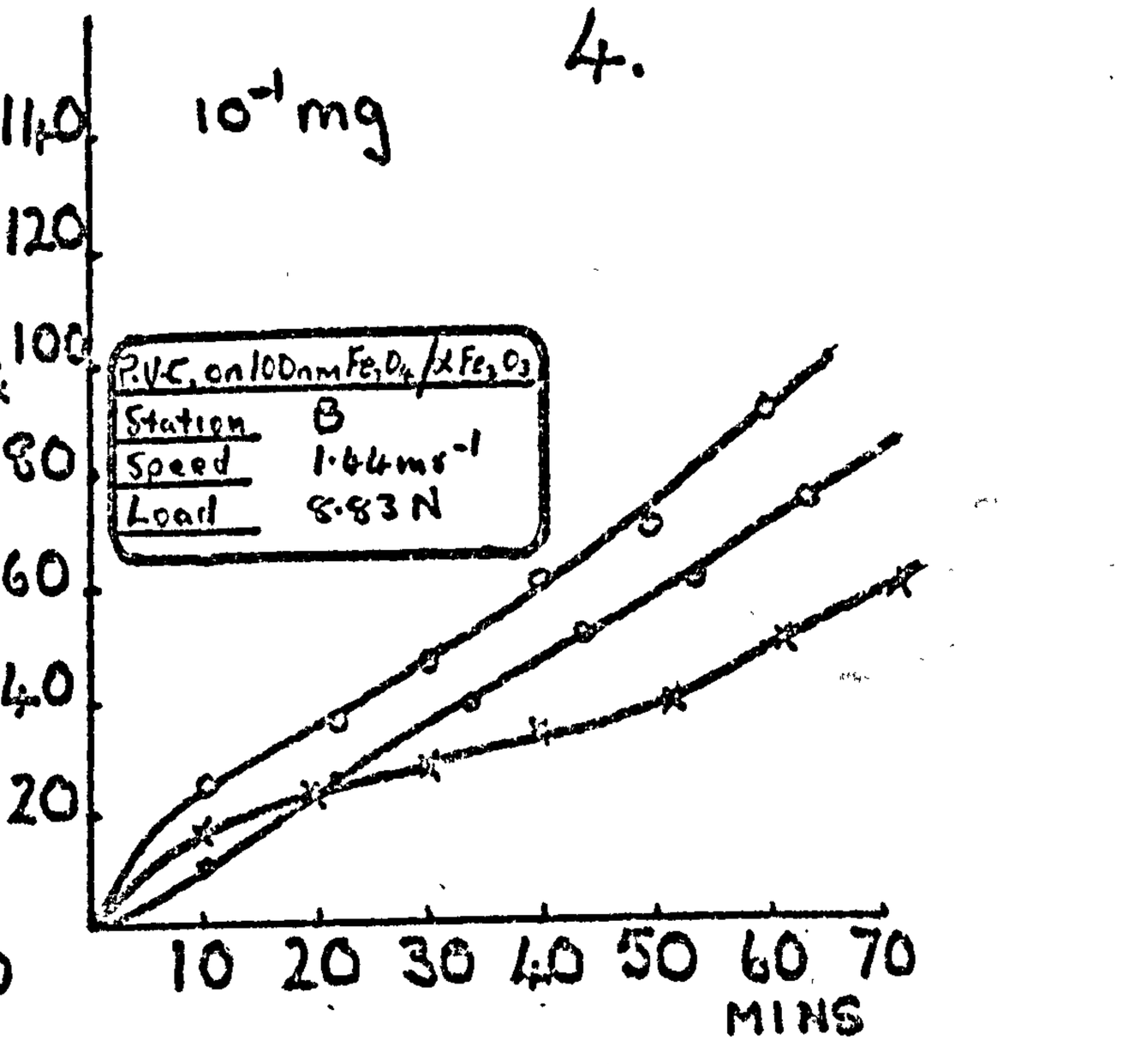

5.

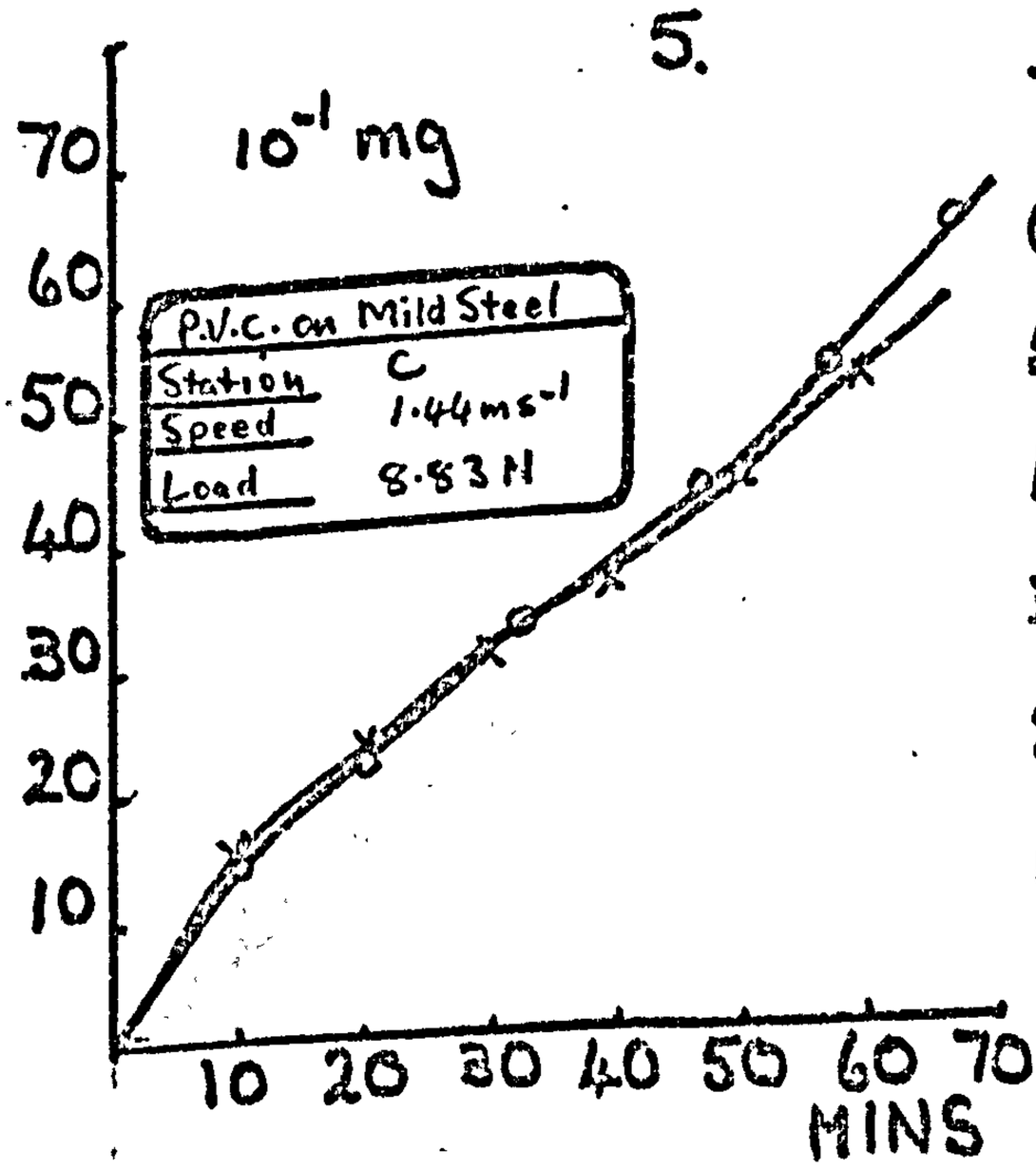

6.

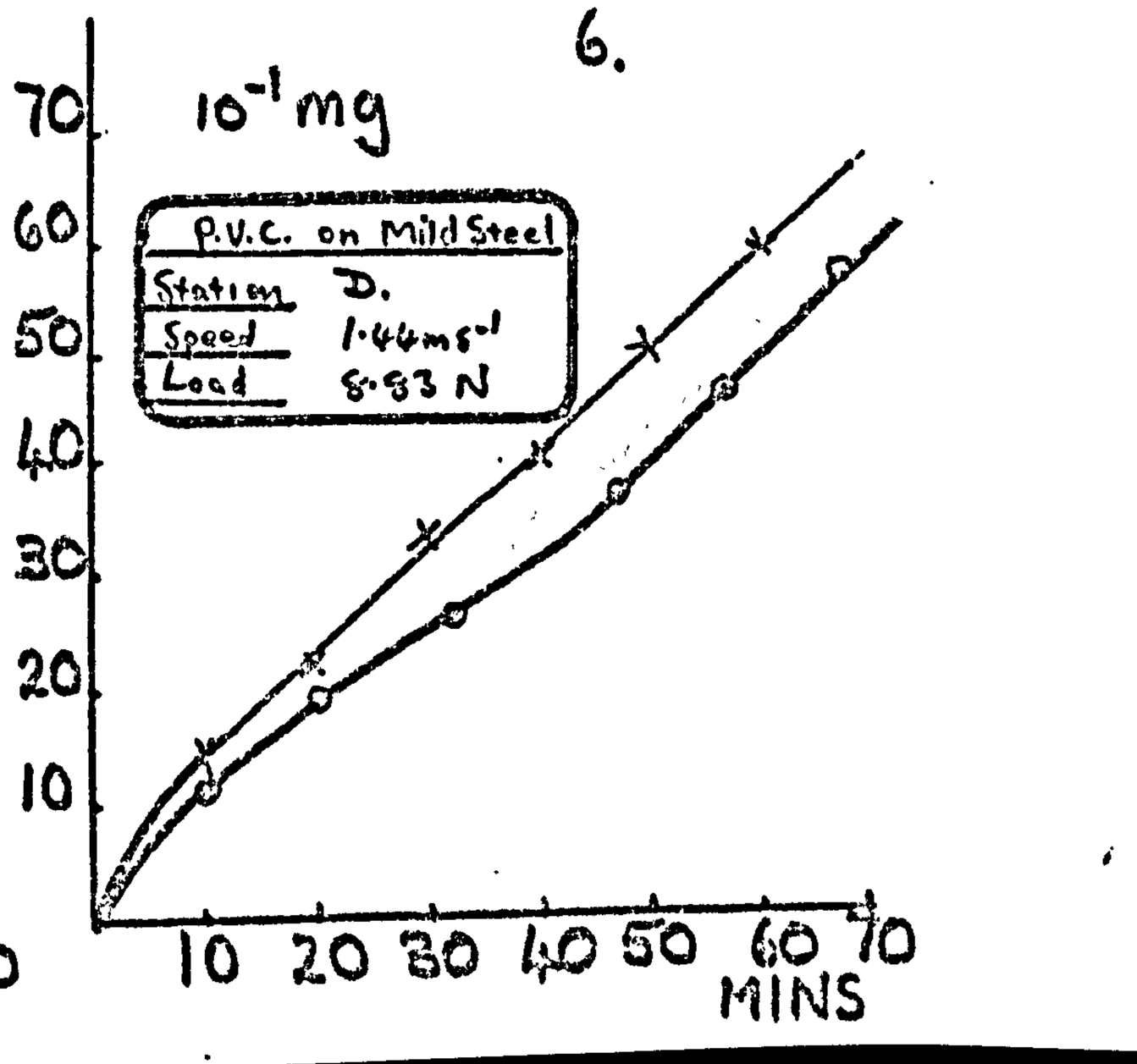

7.

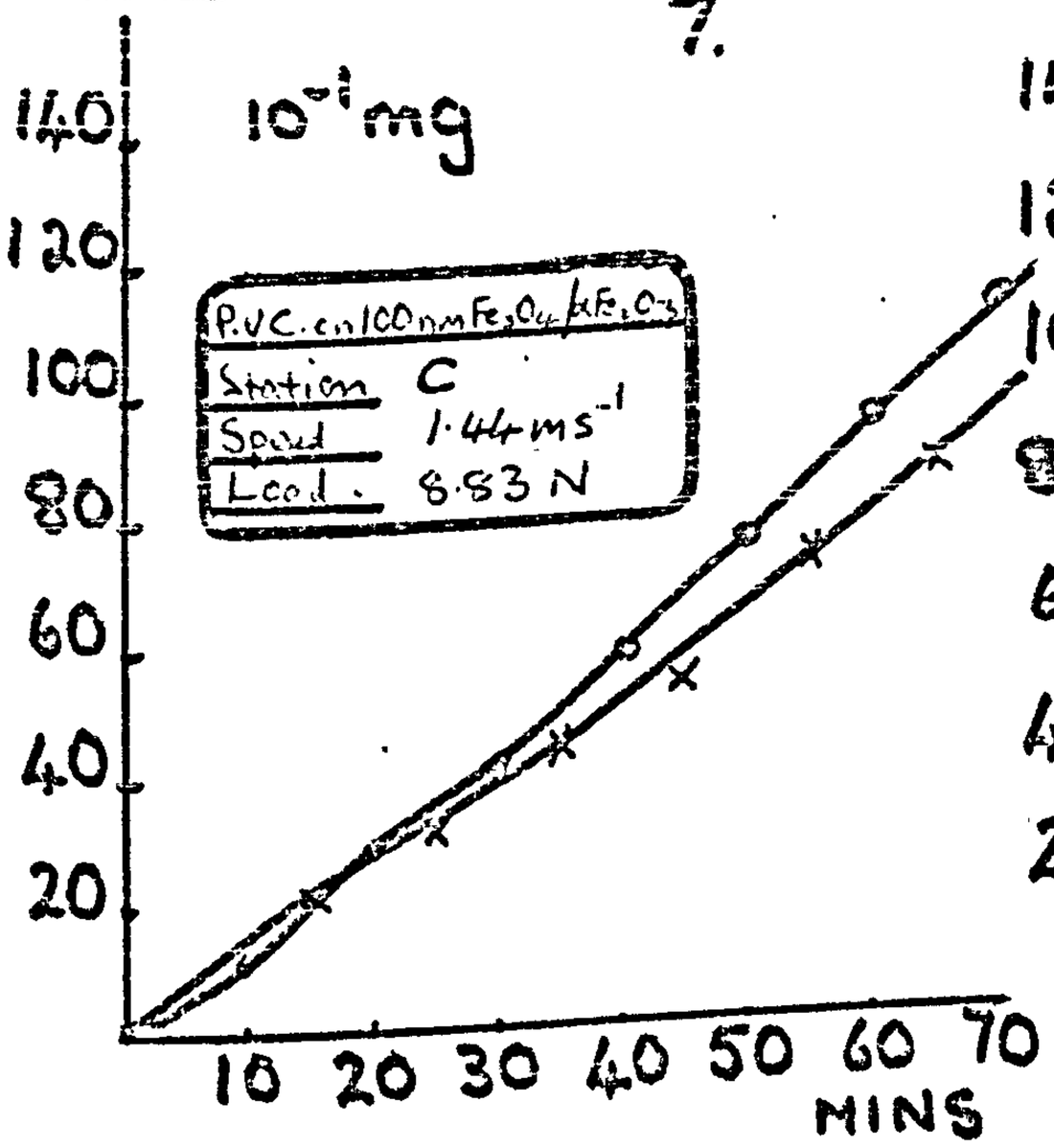
10^{-1} mg
140
120
100
80
60
40
20
P.V.C. on 100nm Fe_3O_4/αFe_2O_3
Station C
Speed $1.44 ms^{-1}$
Load 8.83 N
10 20 30 40 50 60 70
MINS

8.

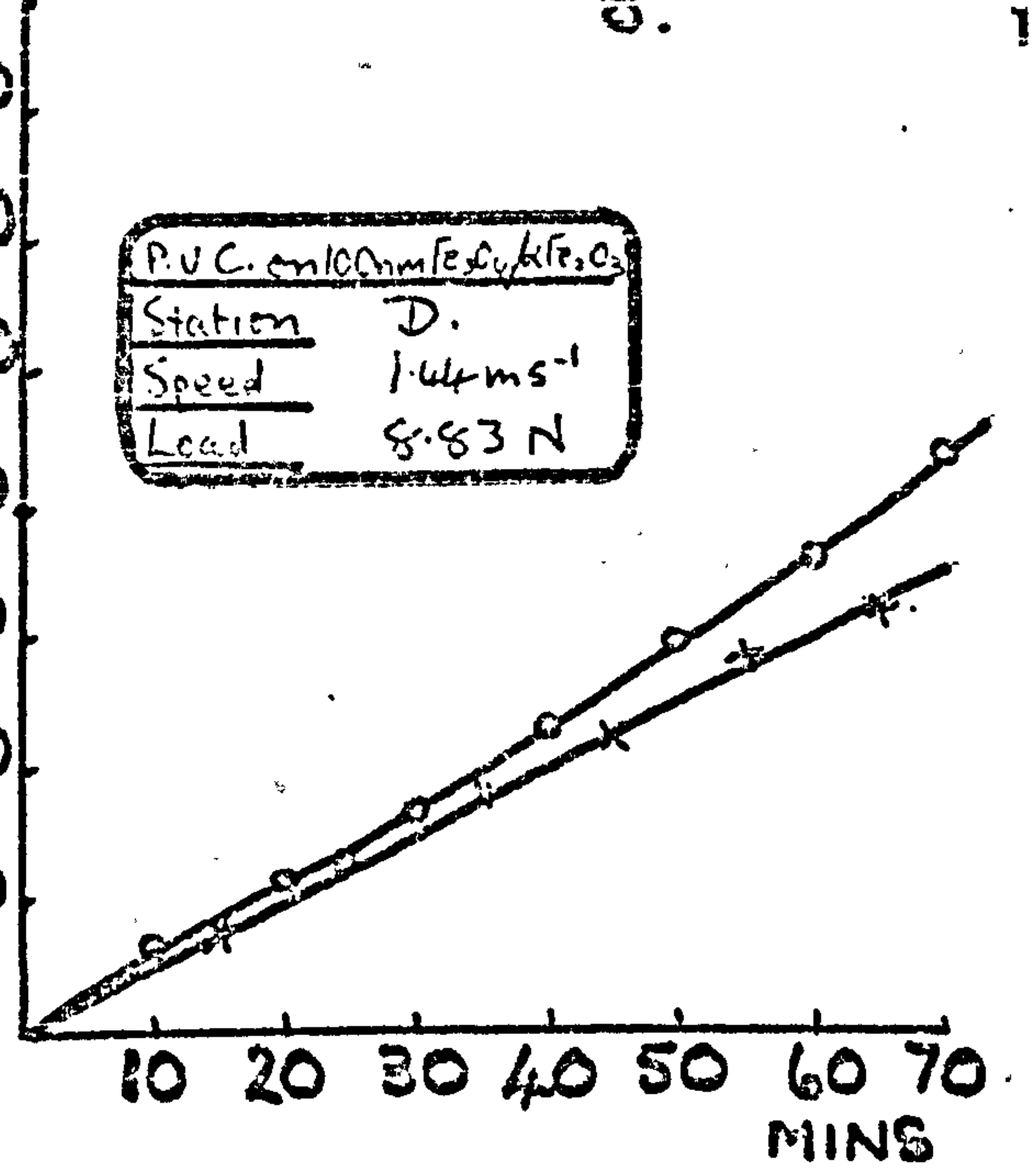
140
120
100
80
60
40
20
P.V.C. on 100nm Fe_3O_4/αFe_2O_3
Station D.
Speed $1.44 ms^{-1}$
Load 8.83 N
10 20 30 40 50 60 70
MINS

9.

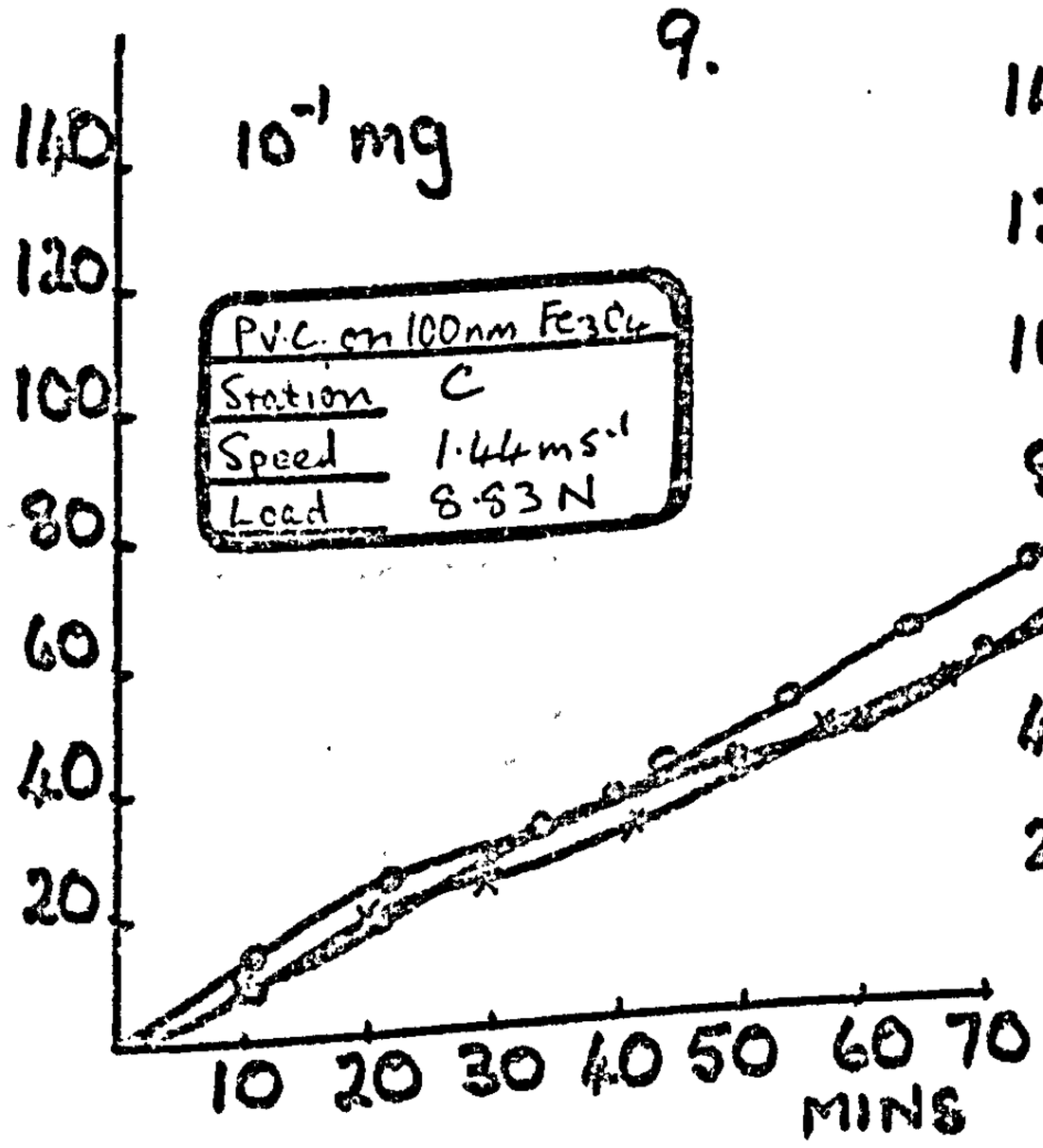
10^{-1} mg
140
120
100
80
60
40
20
P.V.C. on 100nm Fe_3O_4
Station C
Speed $1.44 ms^{-1}$
Load 8.83 N
10 20 30 40 50 60 70
MINS

10.

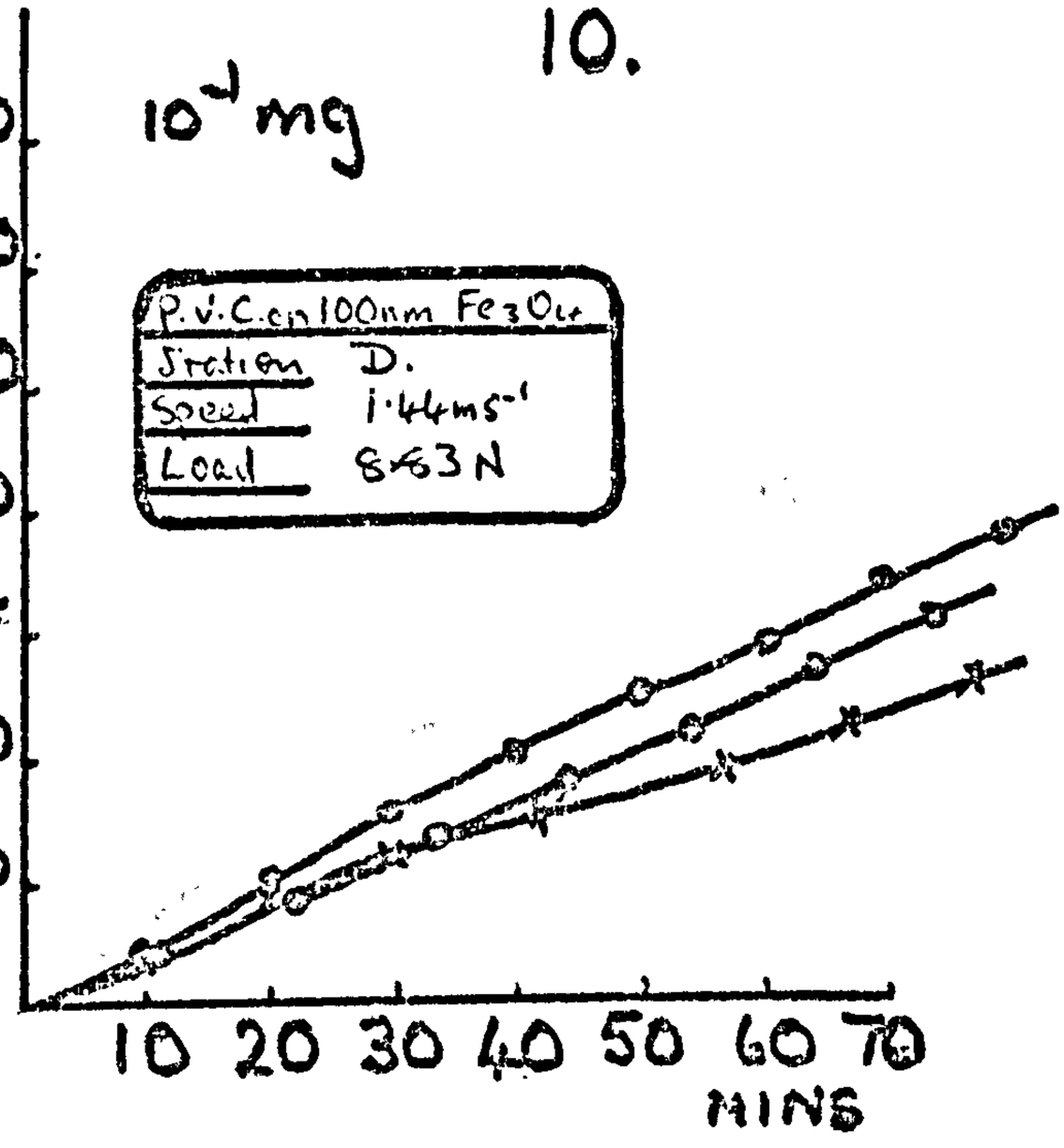
10^{-1} mg
140
120
100
80
60
40
20
P.V.C. on 100nm Fe_3O_4
Station D.
Speed $1.44 ms^{-1}$
Load 8.83 N
10 20 30 40 50 60 70
MINS

11.

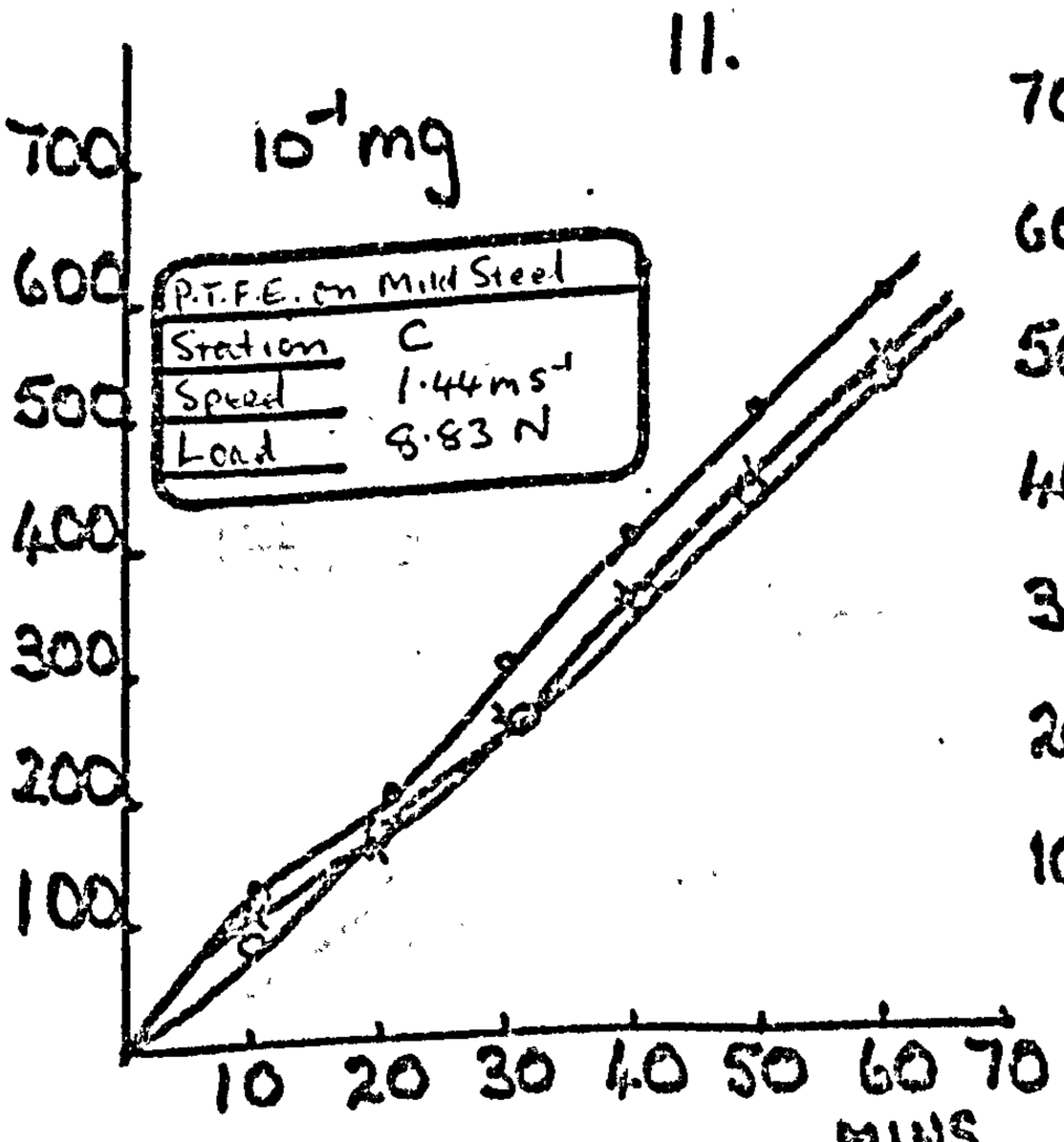
700
600
500
400
300
200
100
10^{-1} mg
P.T.F.E. on Mild Steel
Station C
Speed $1.44 ms^{-1}$
Load 8.83 N
10 20 30 40 50 60 70
MINS

12.

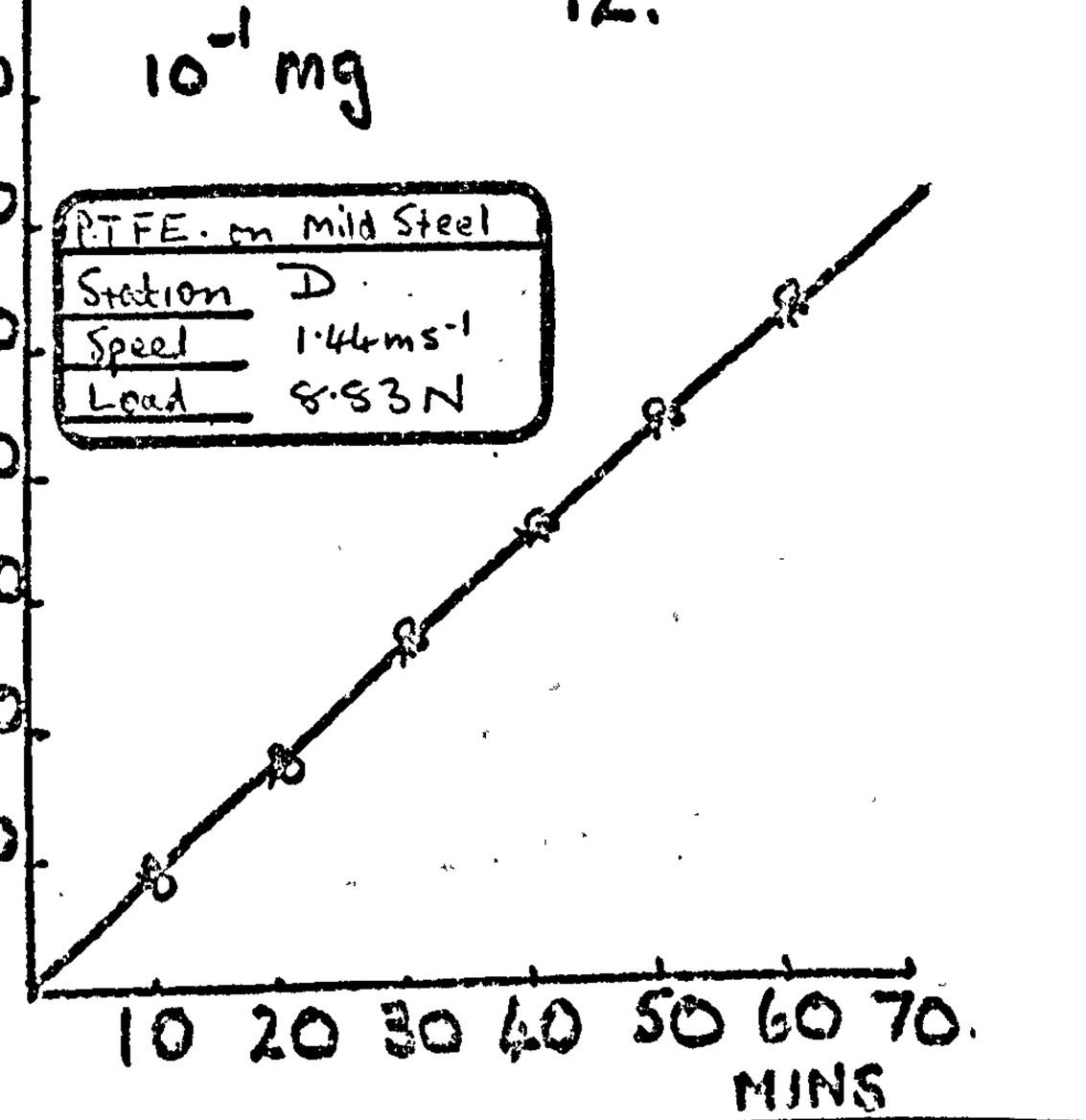
700
600
500
400
300
200
100
10^{-1} mg
P.T.F.E. on Mild Steel
Station D
Speed $1.44 ms^{-1}$
Load 8.83 N
10 20 30 40 50 60 70
MINS

13.

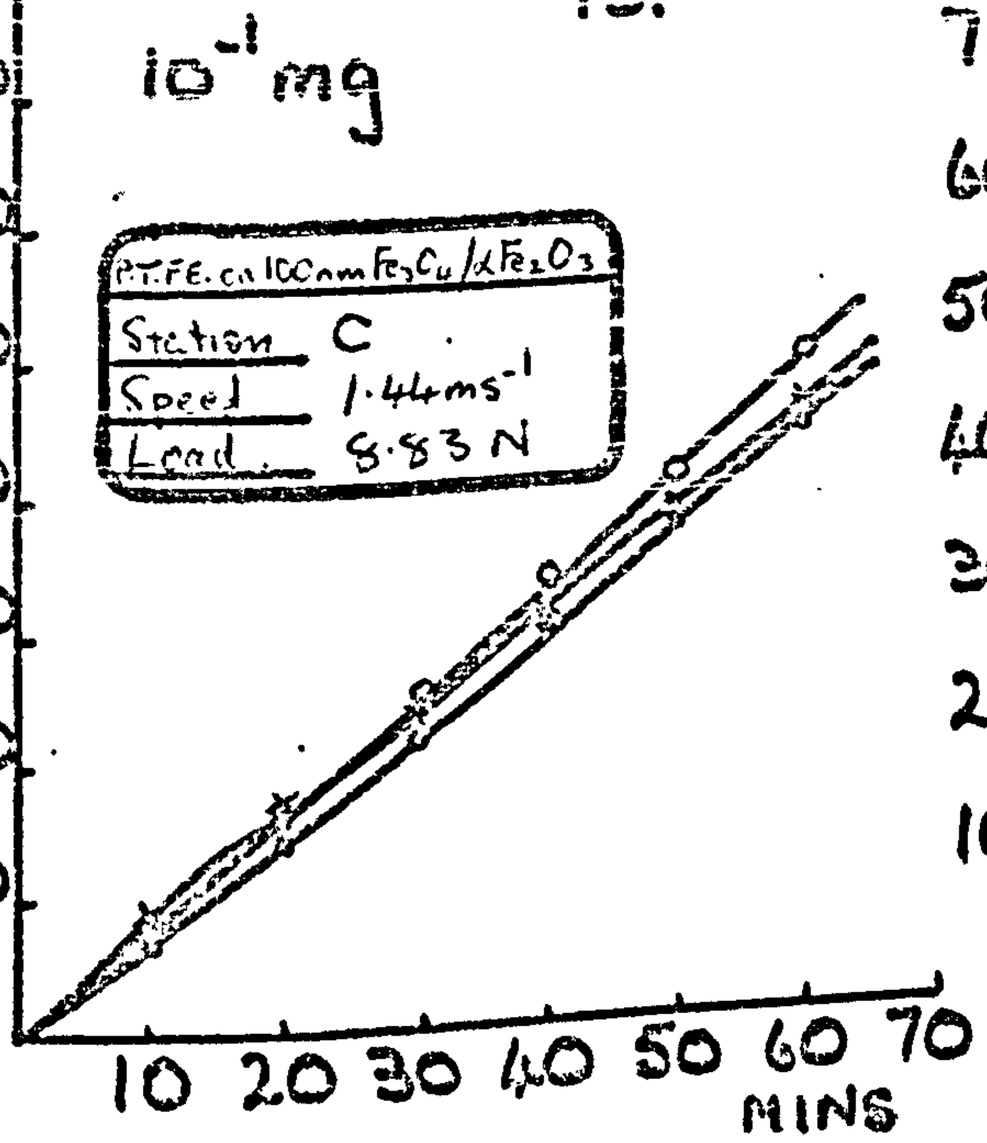

14.

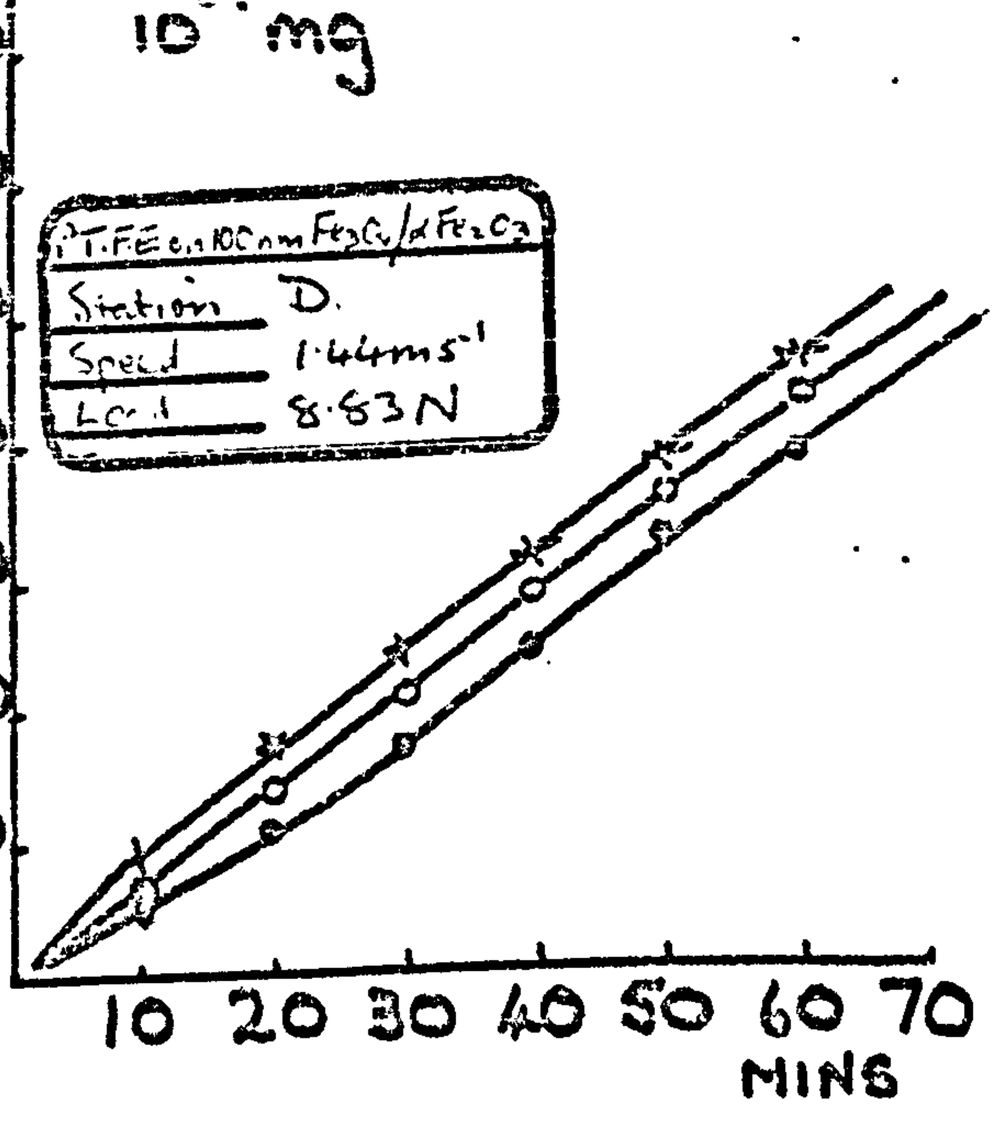

15.

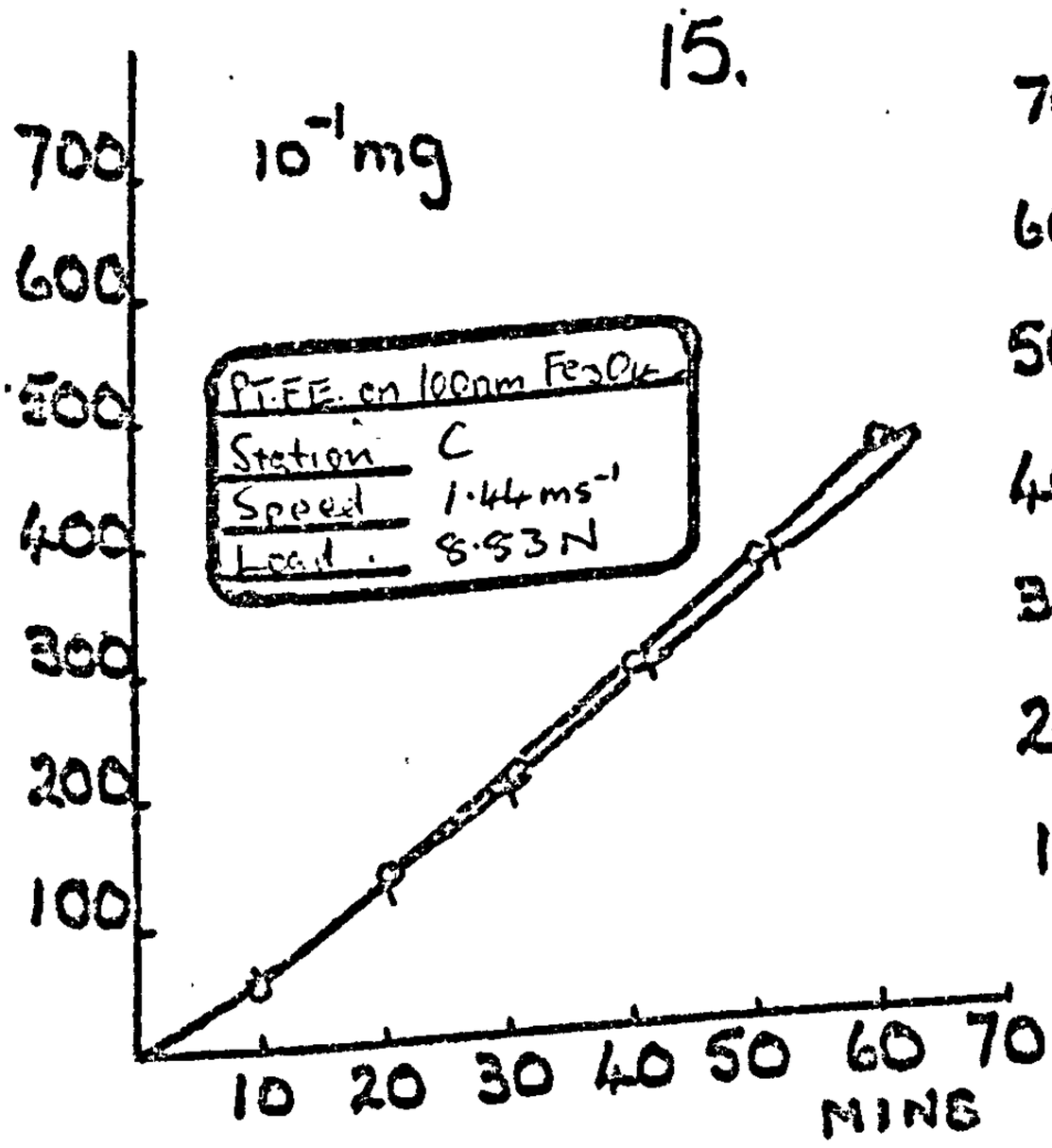

16.

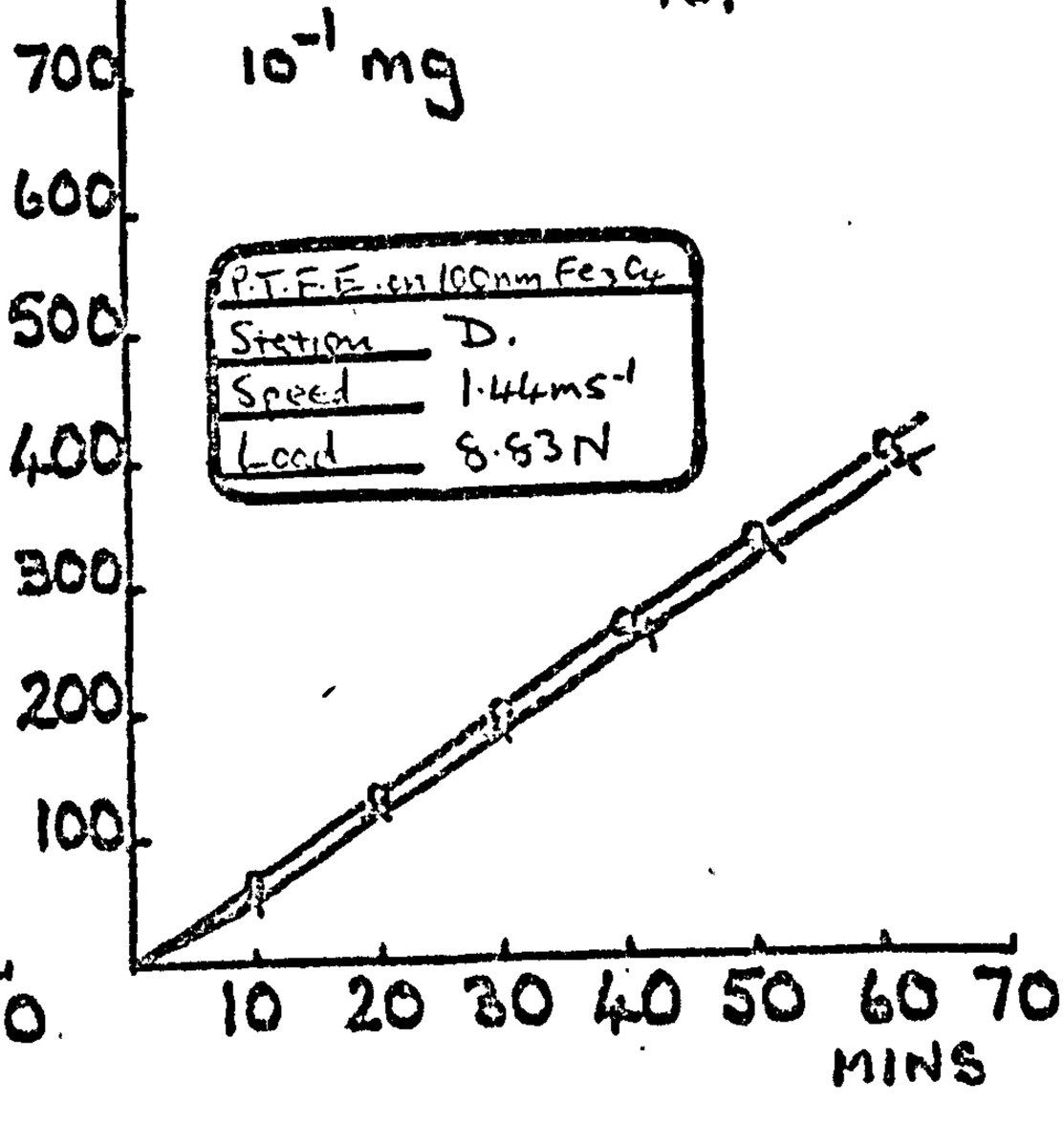

17.

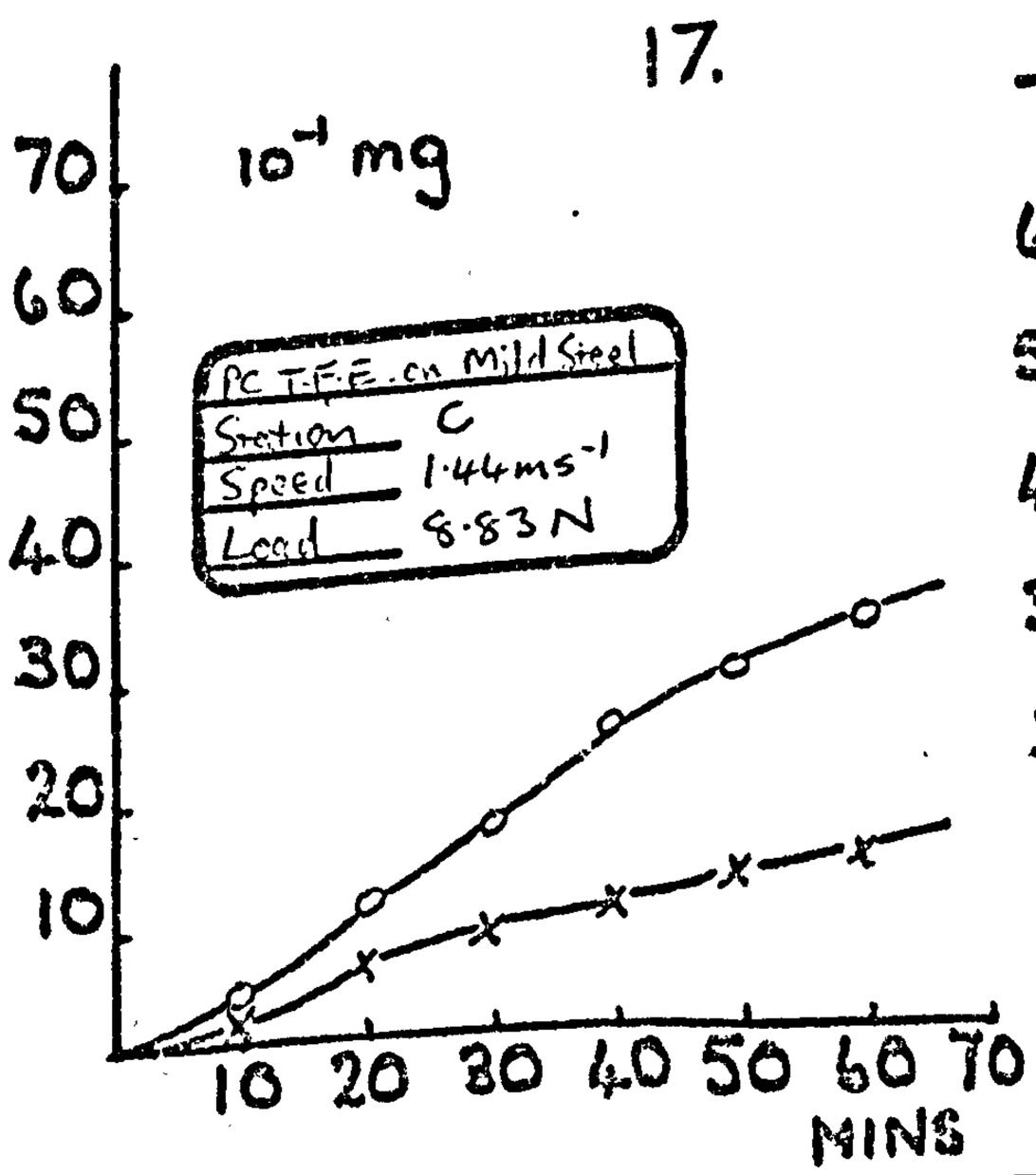

18.

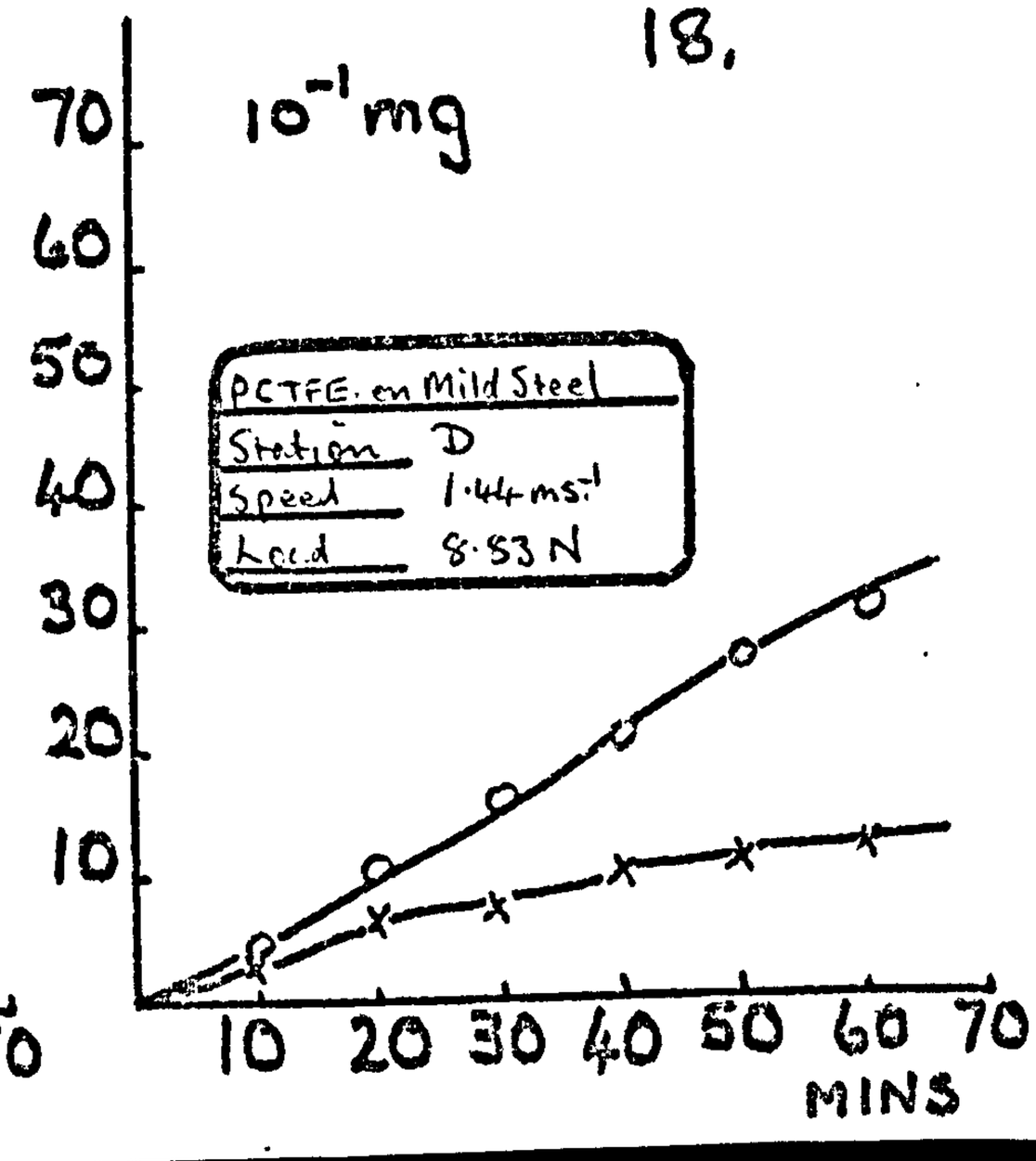

19.

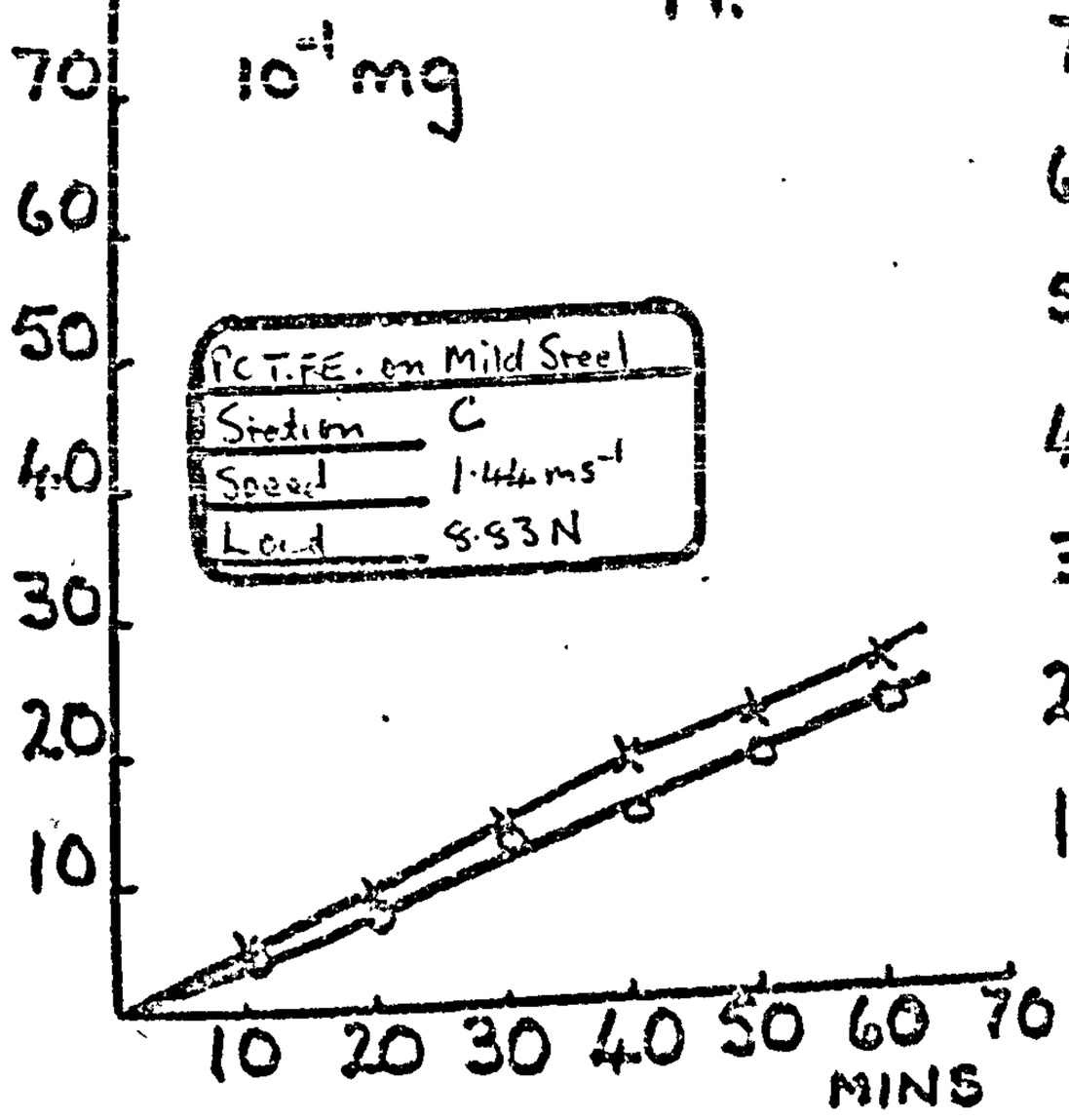

20.

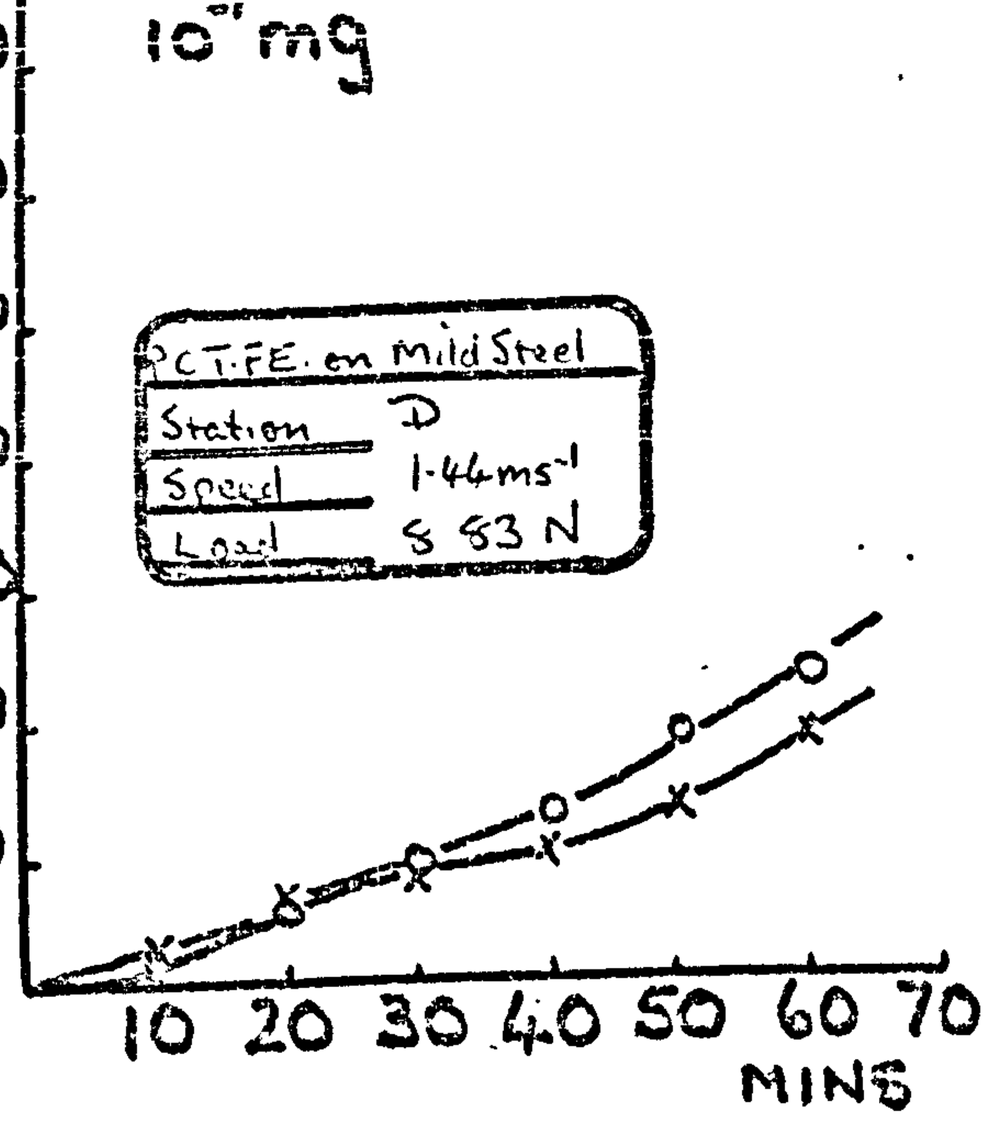

21.

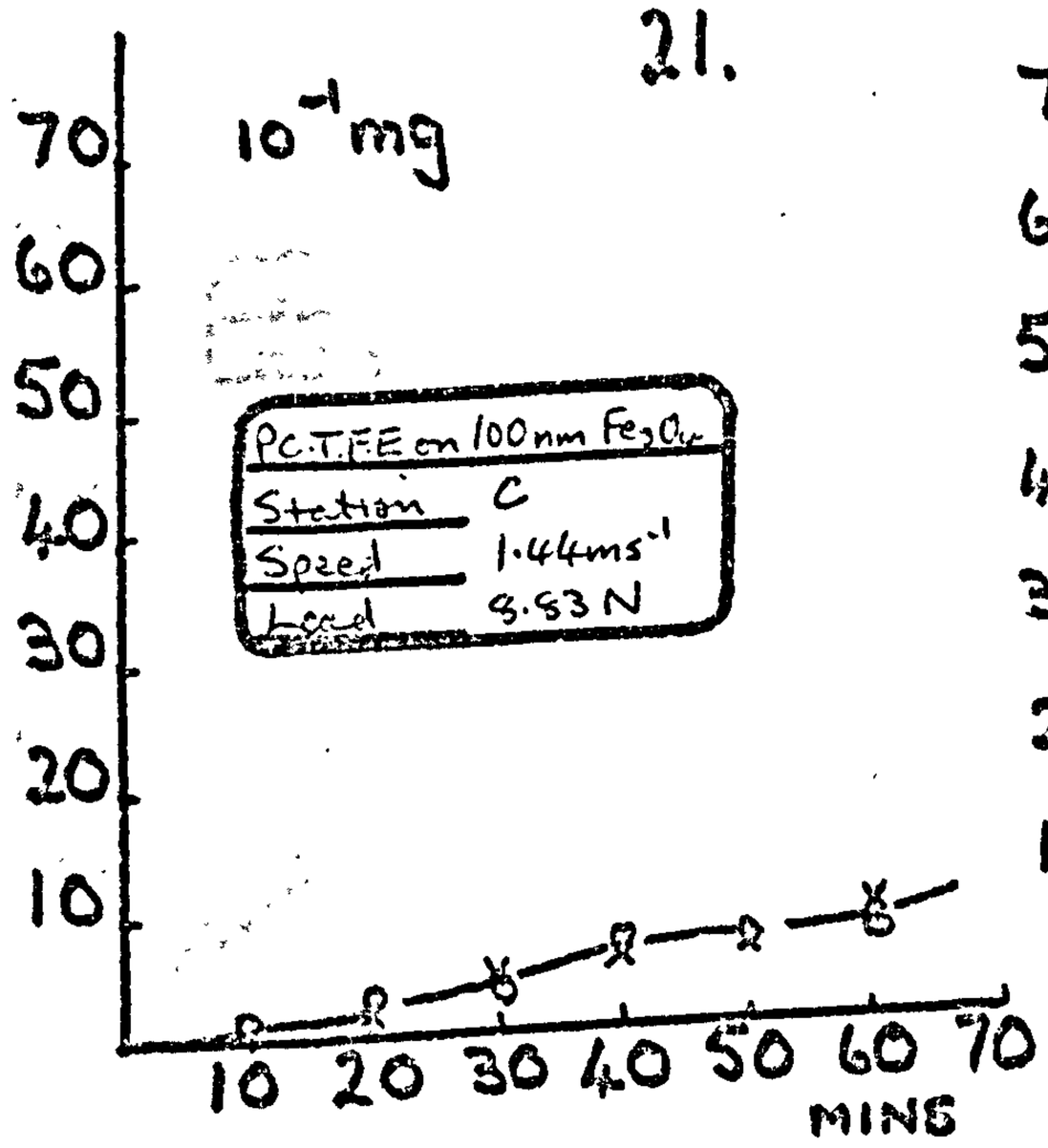

22.

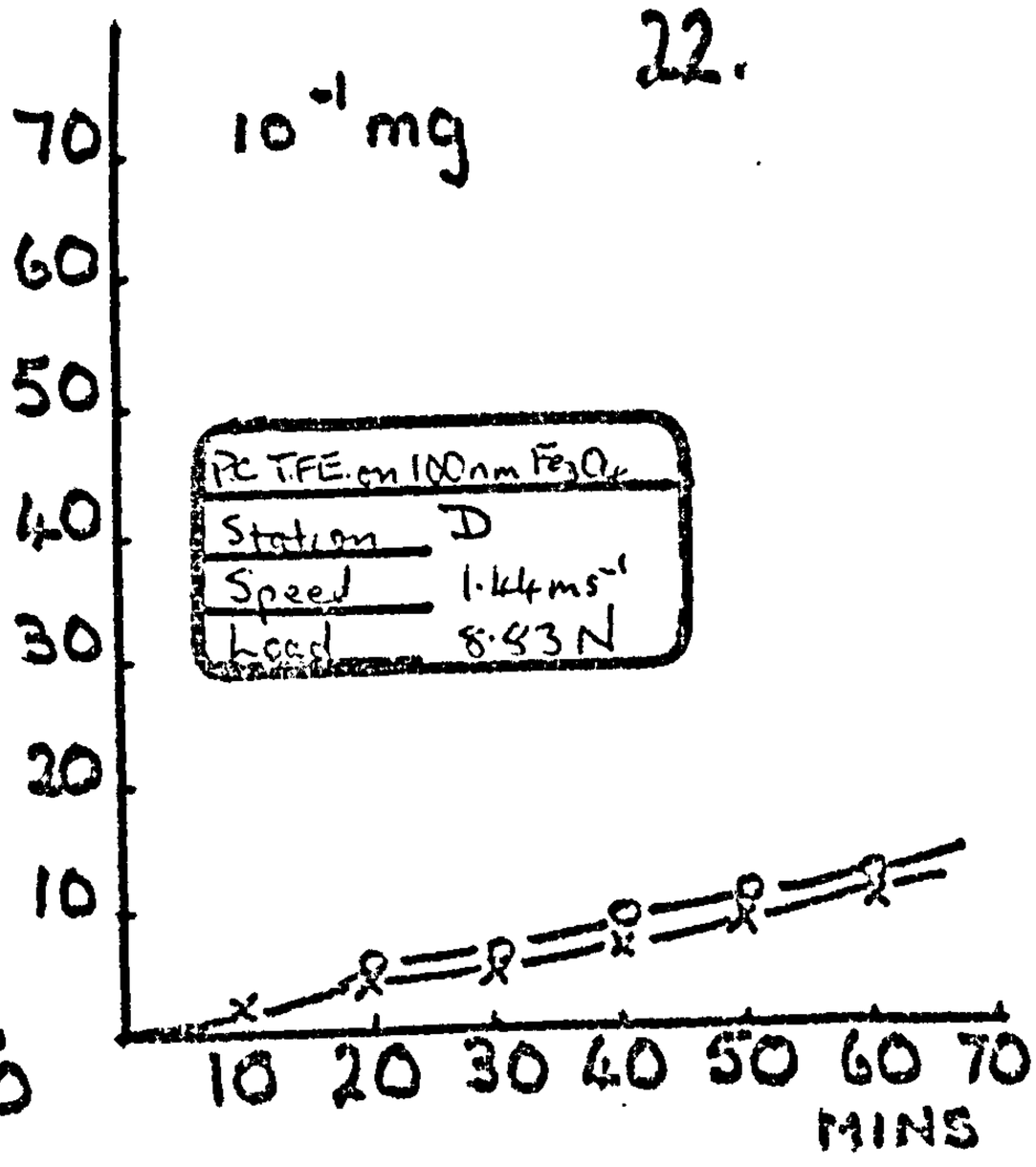

23.

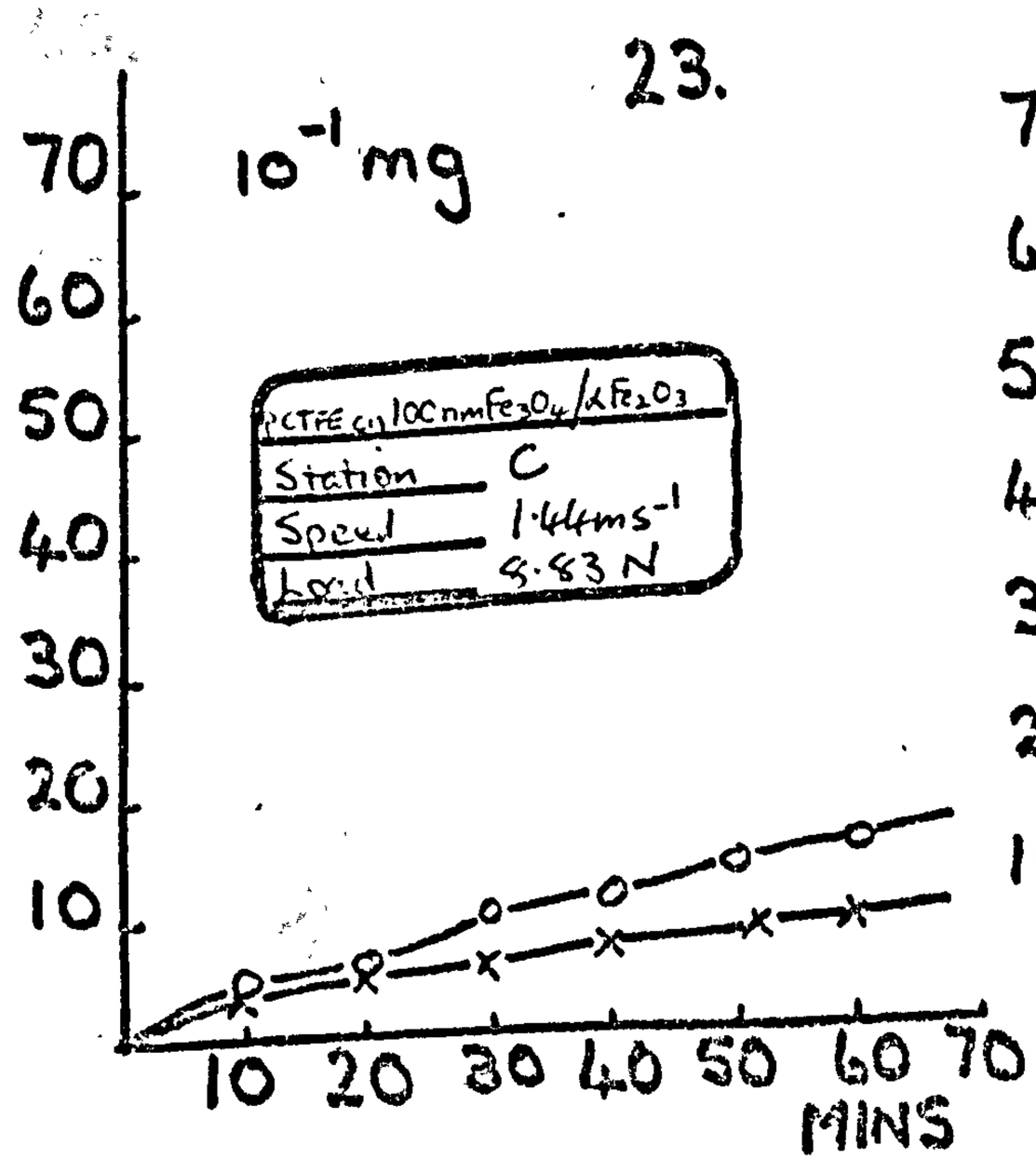

24.

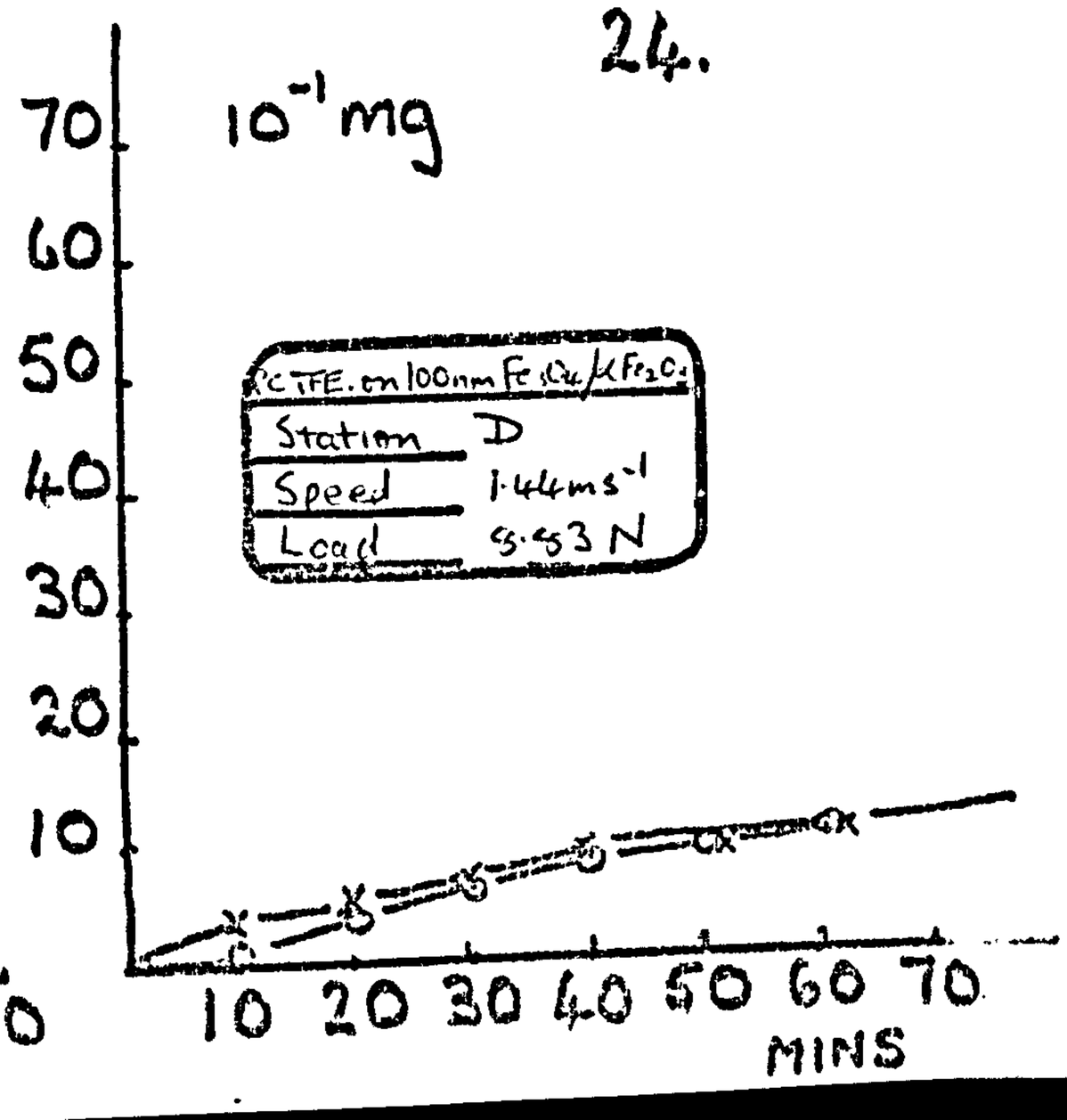

25.

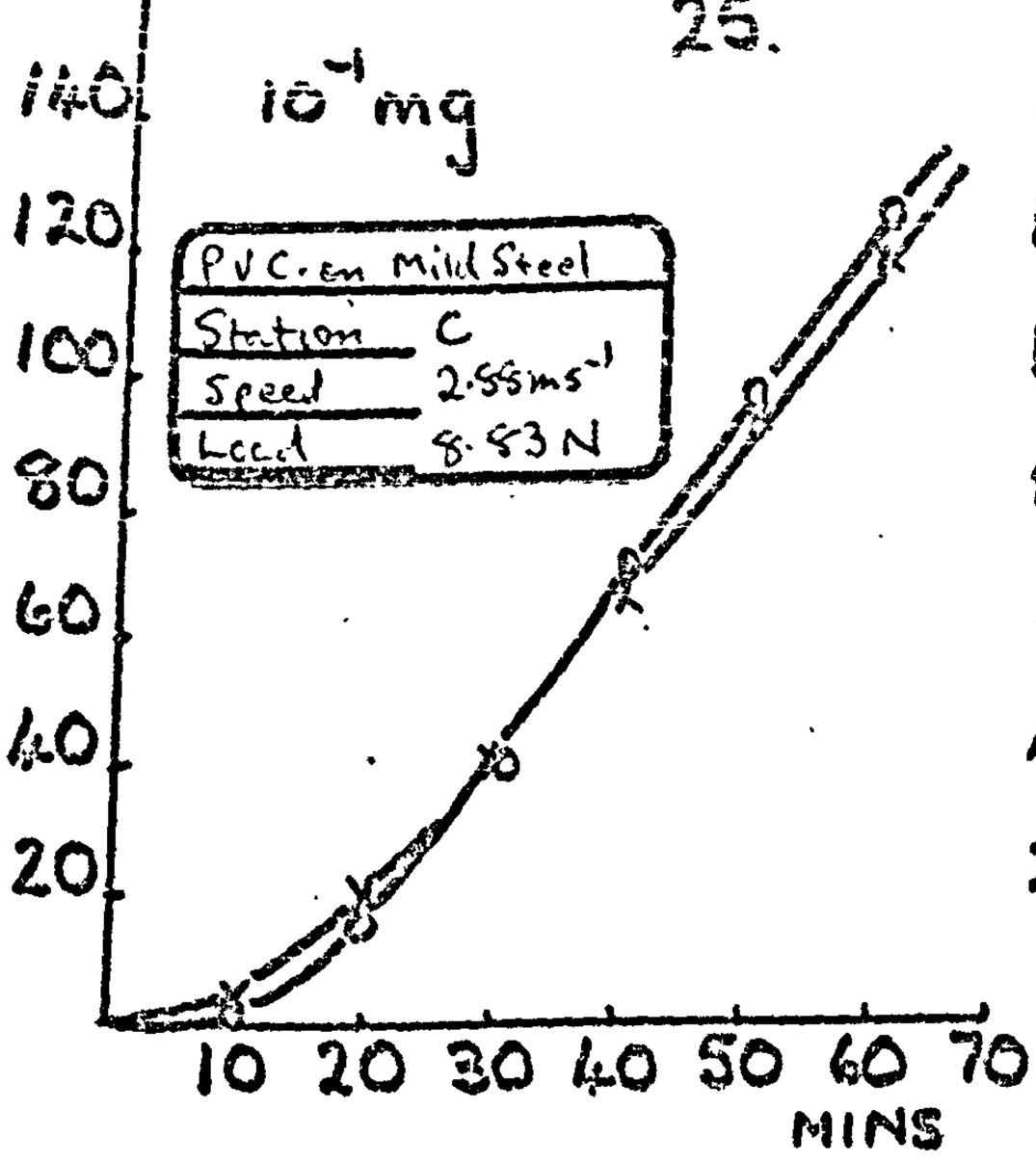

26.

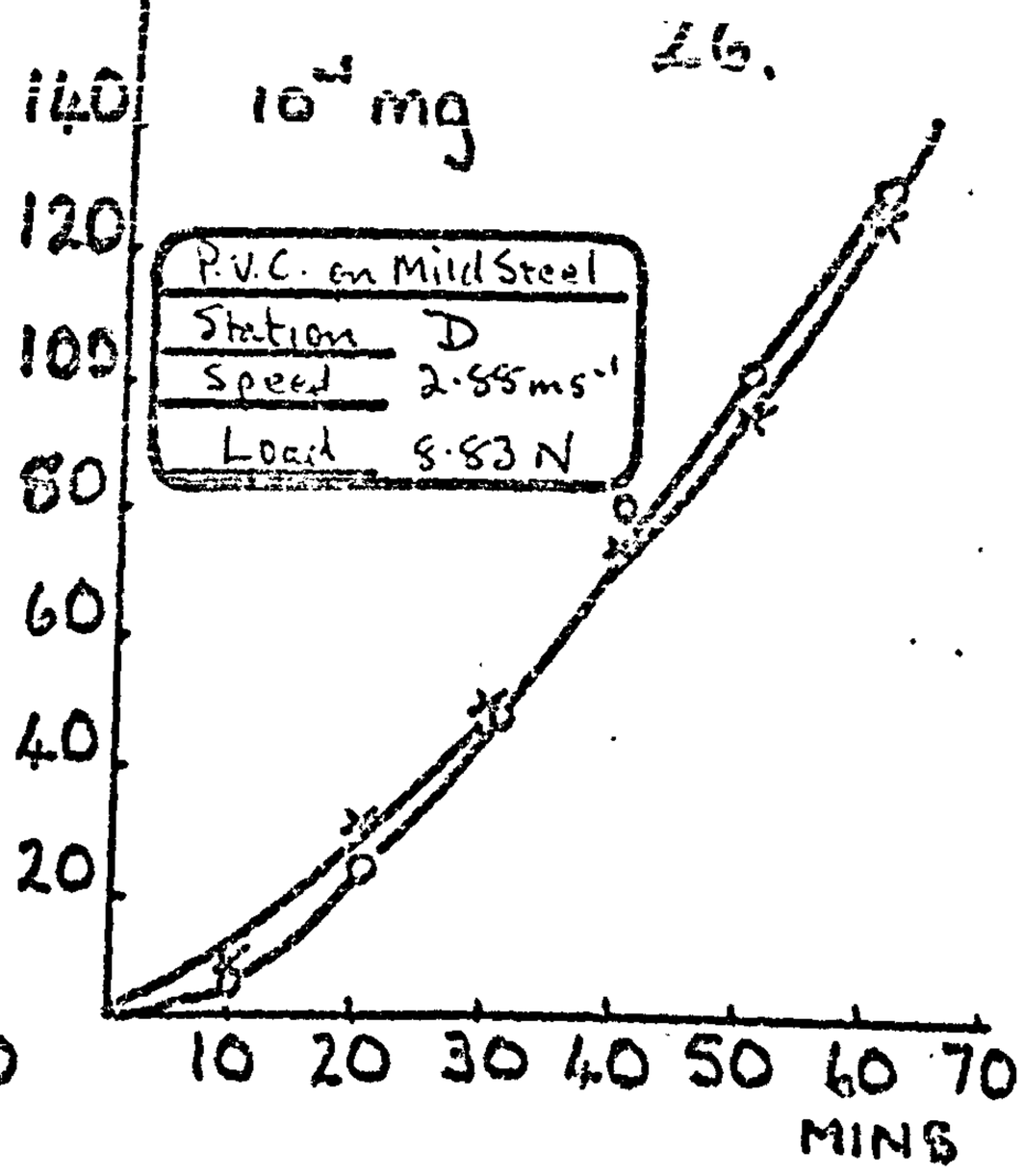

27.

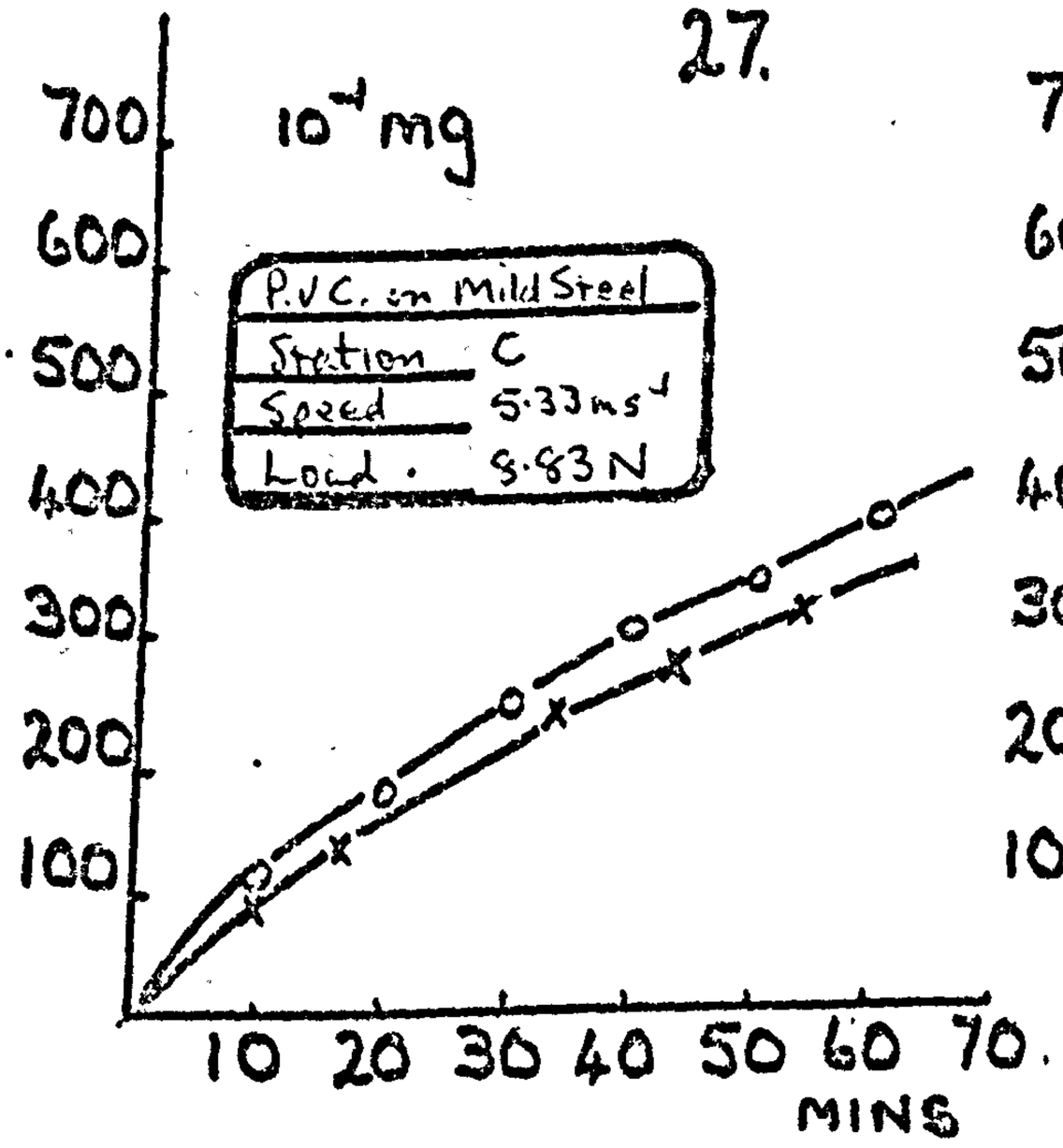

28.

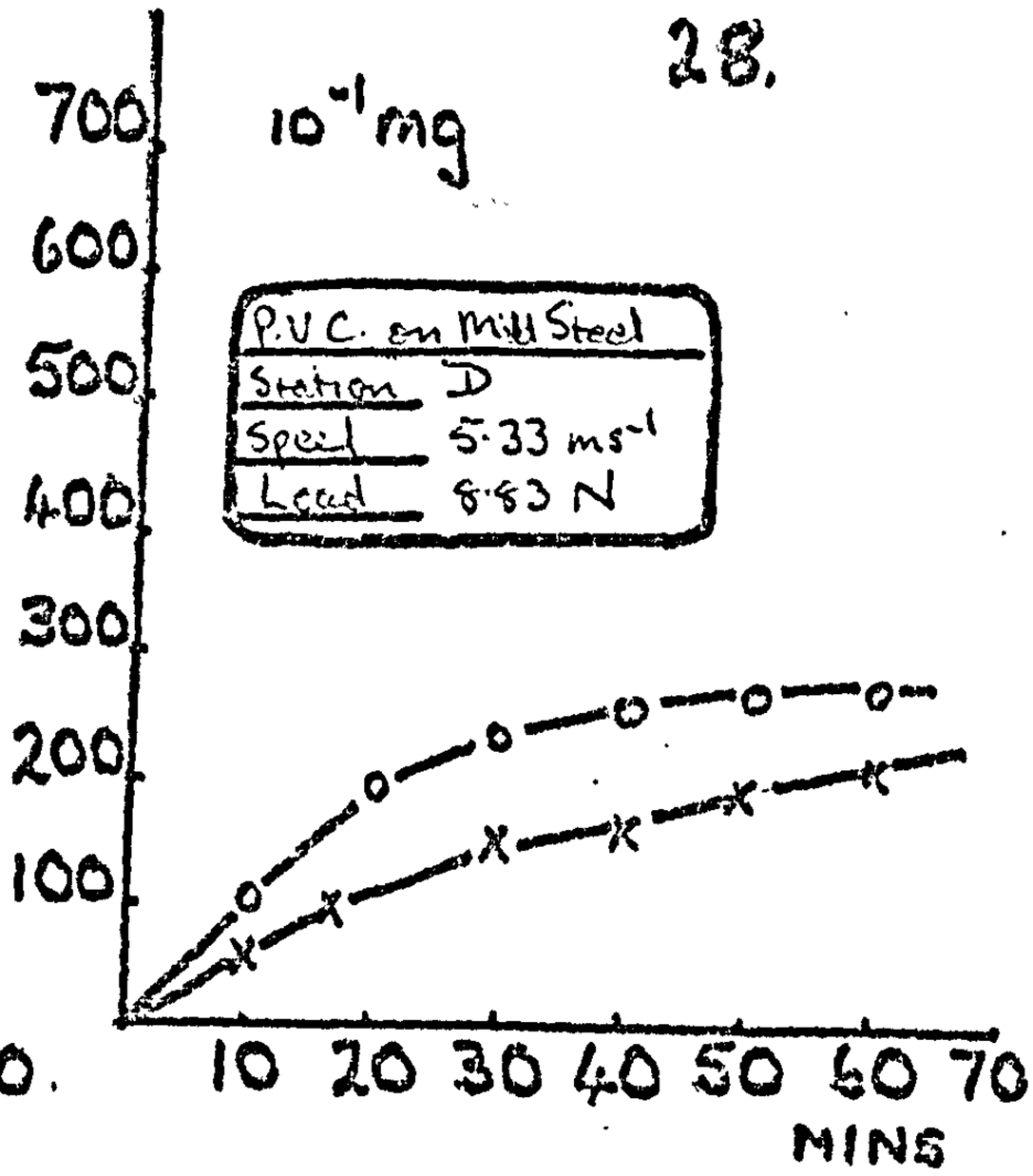

29.

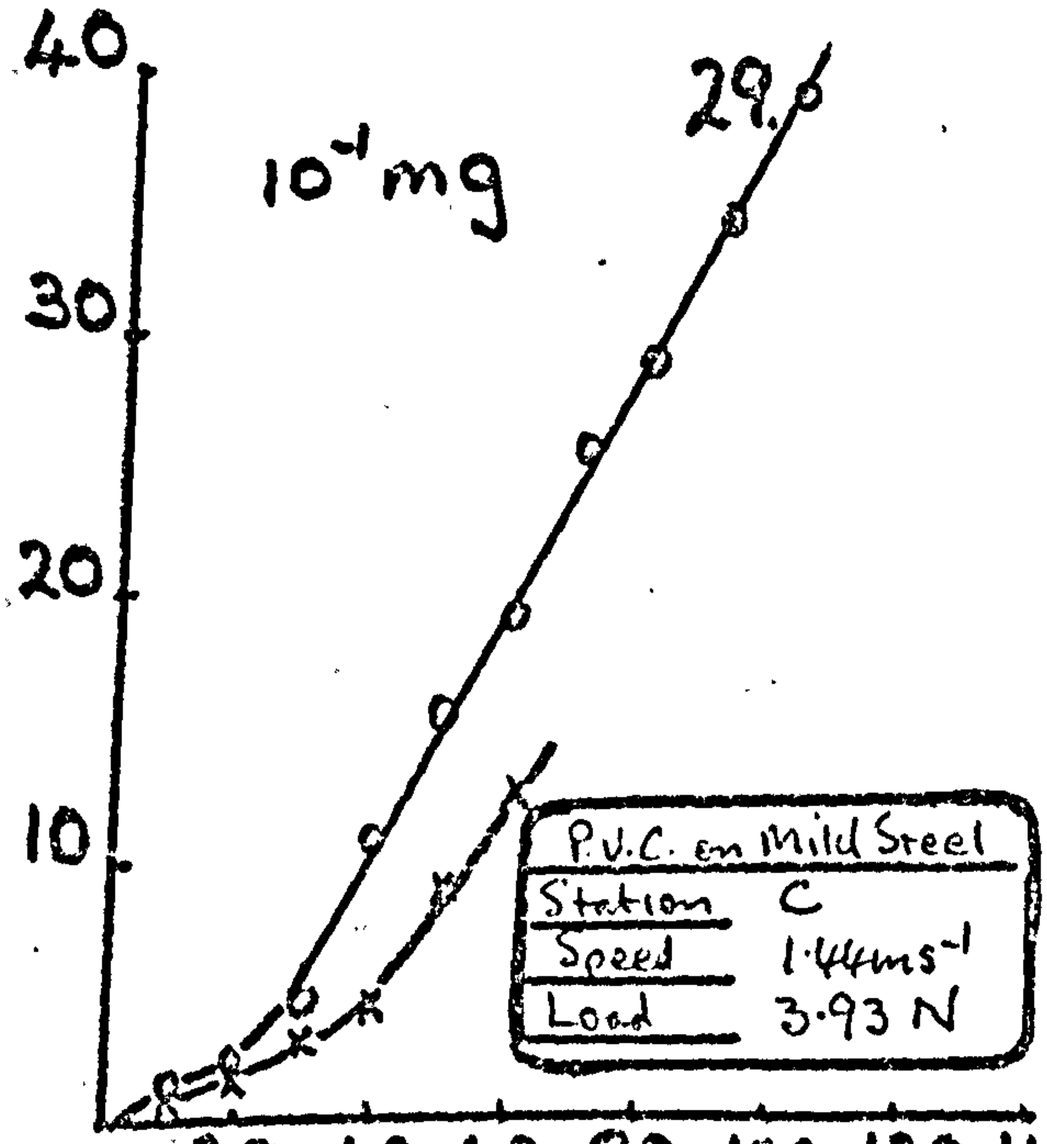

30.

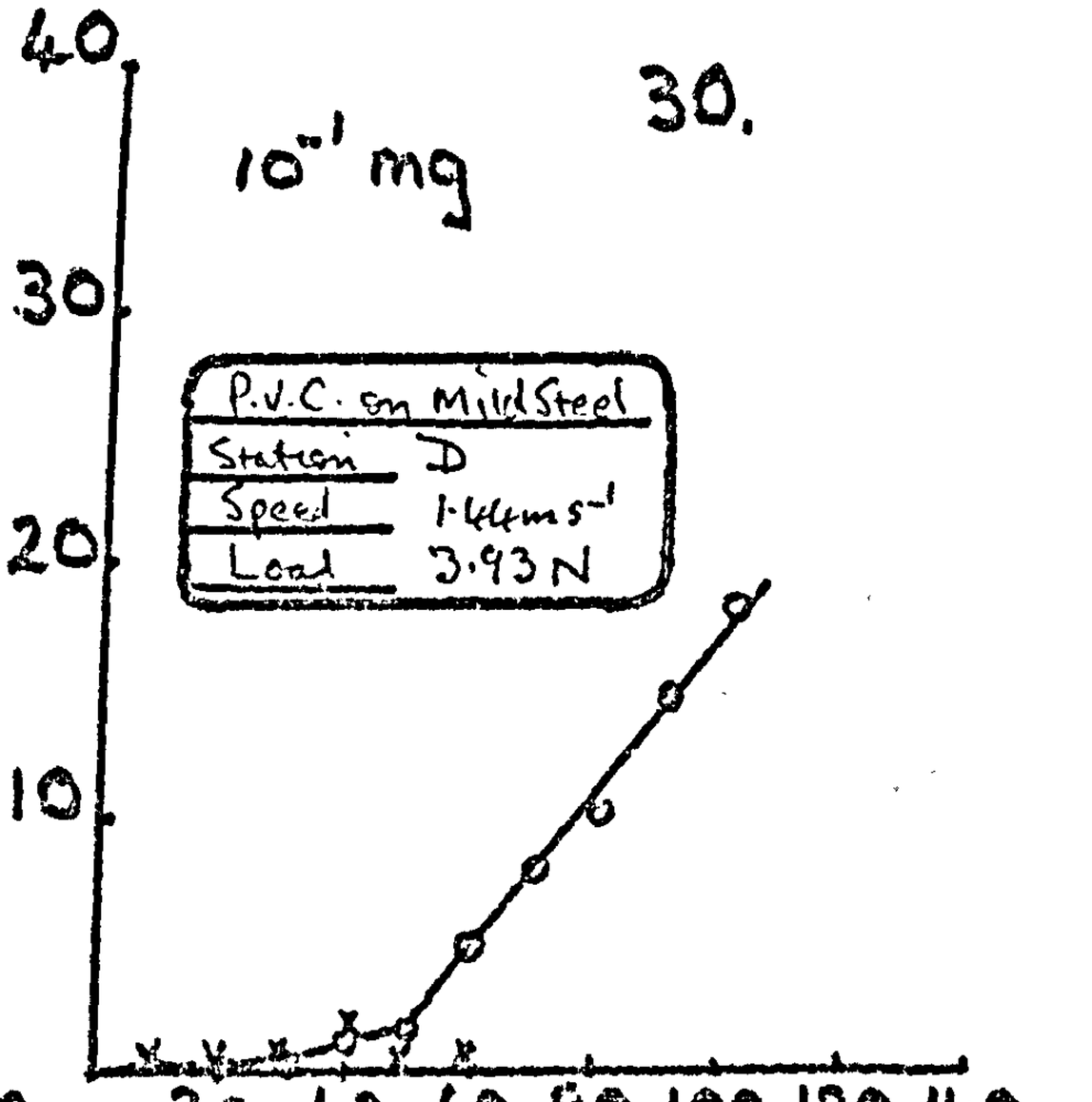

31.

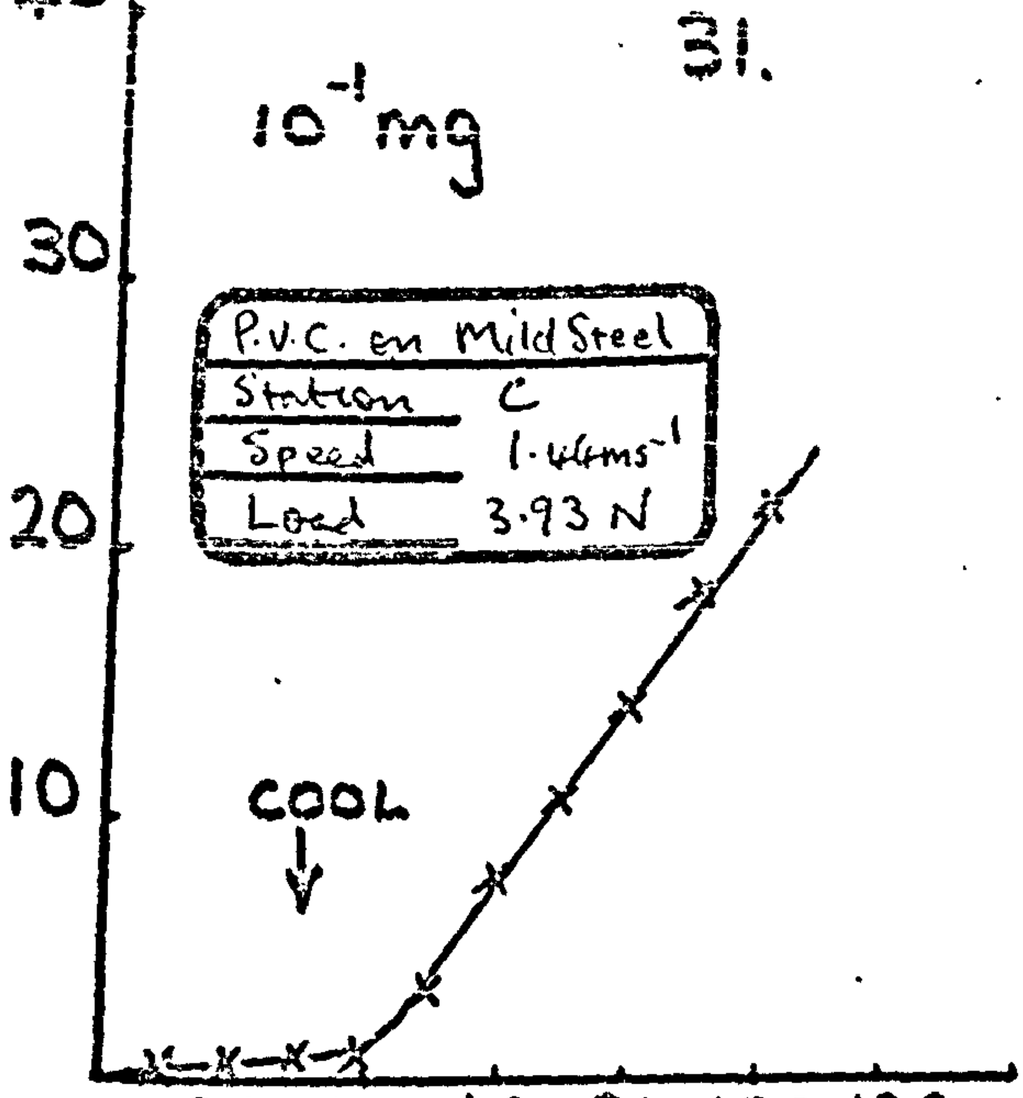

32.

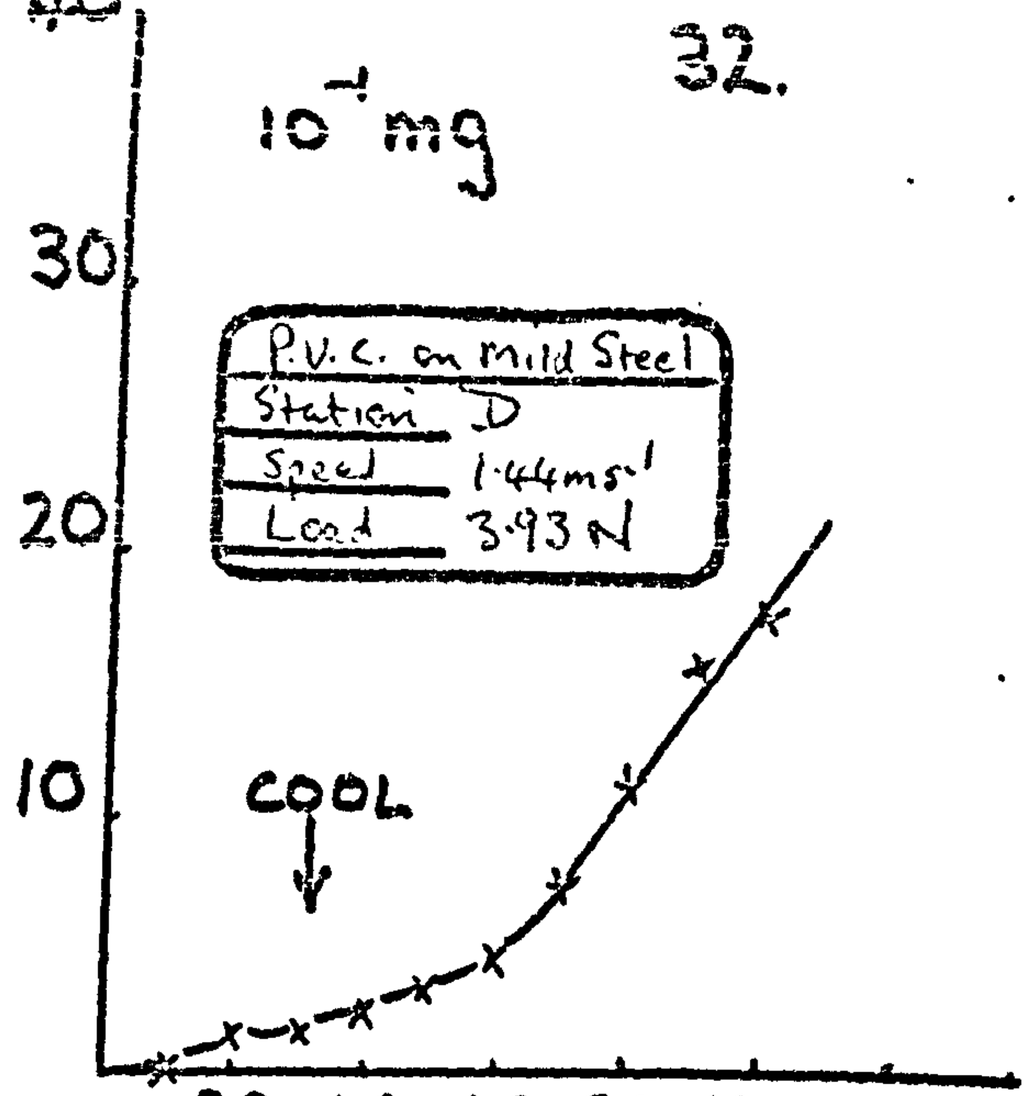

33.

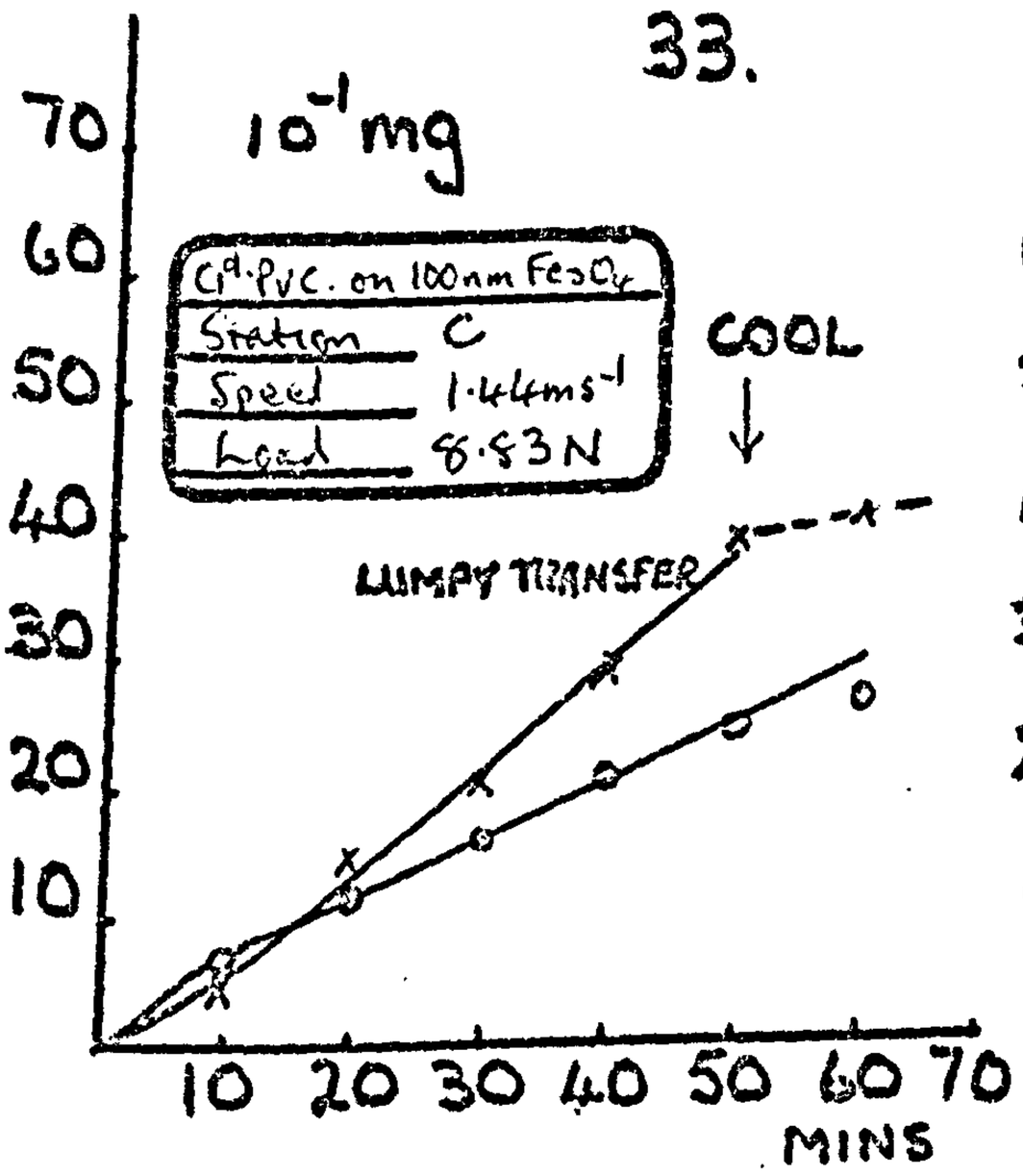

34.

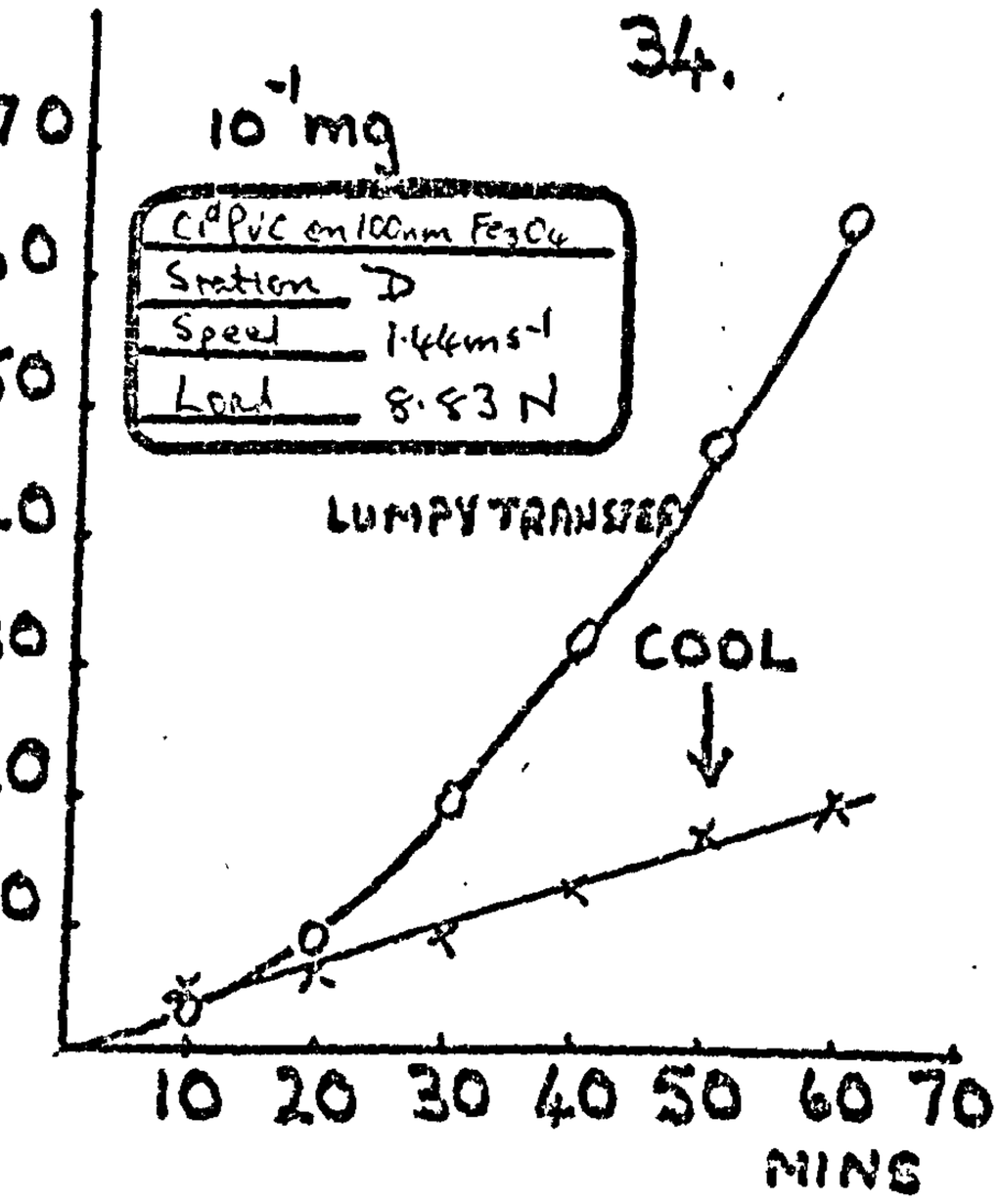

35.

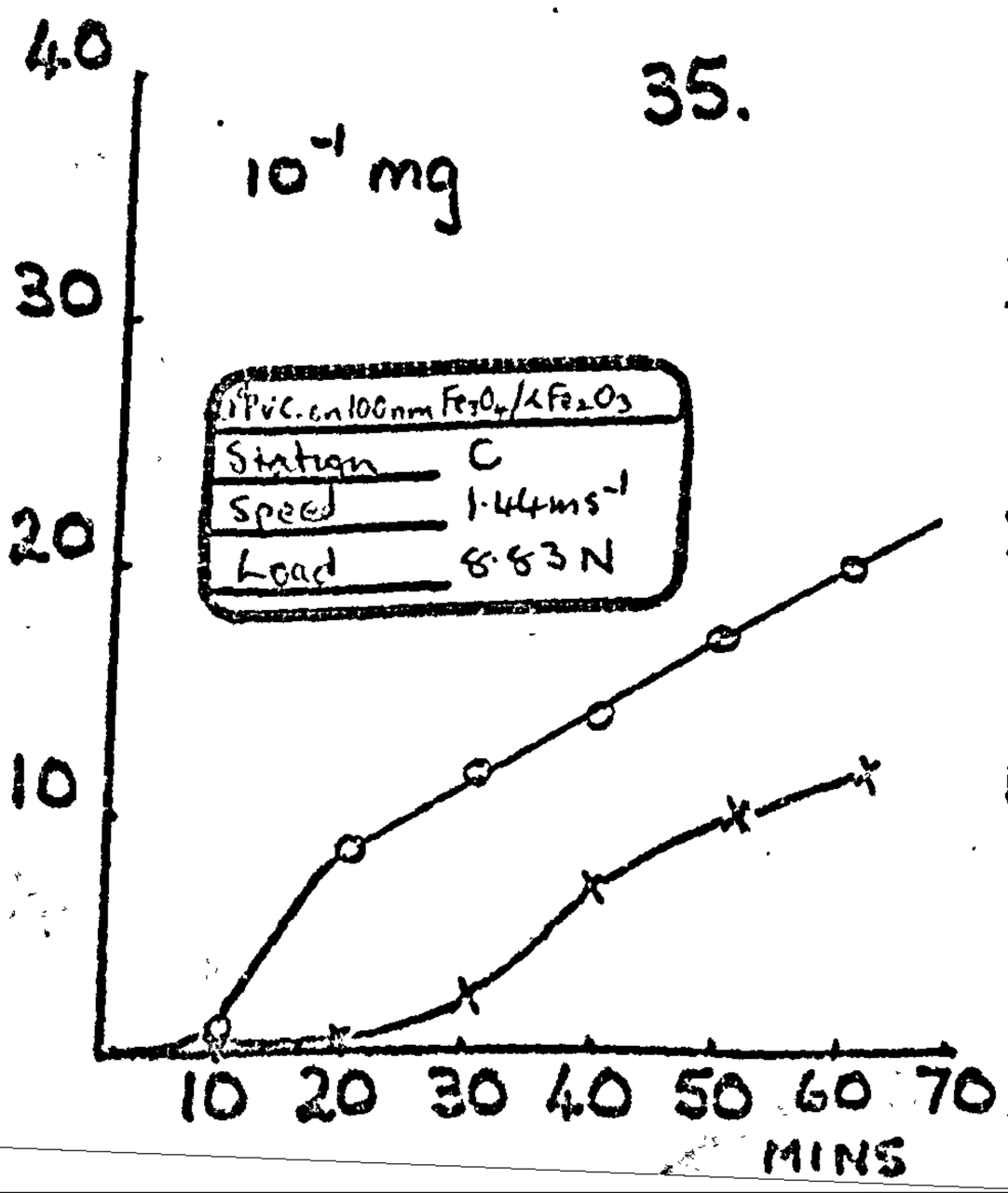

36.

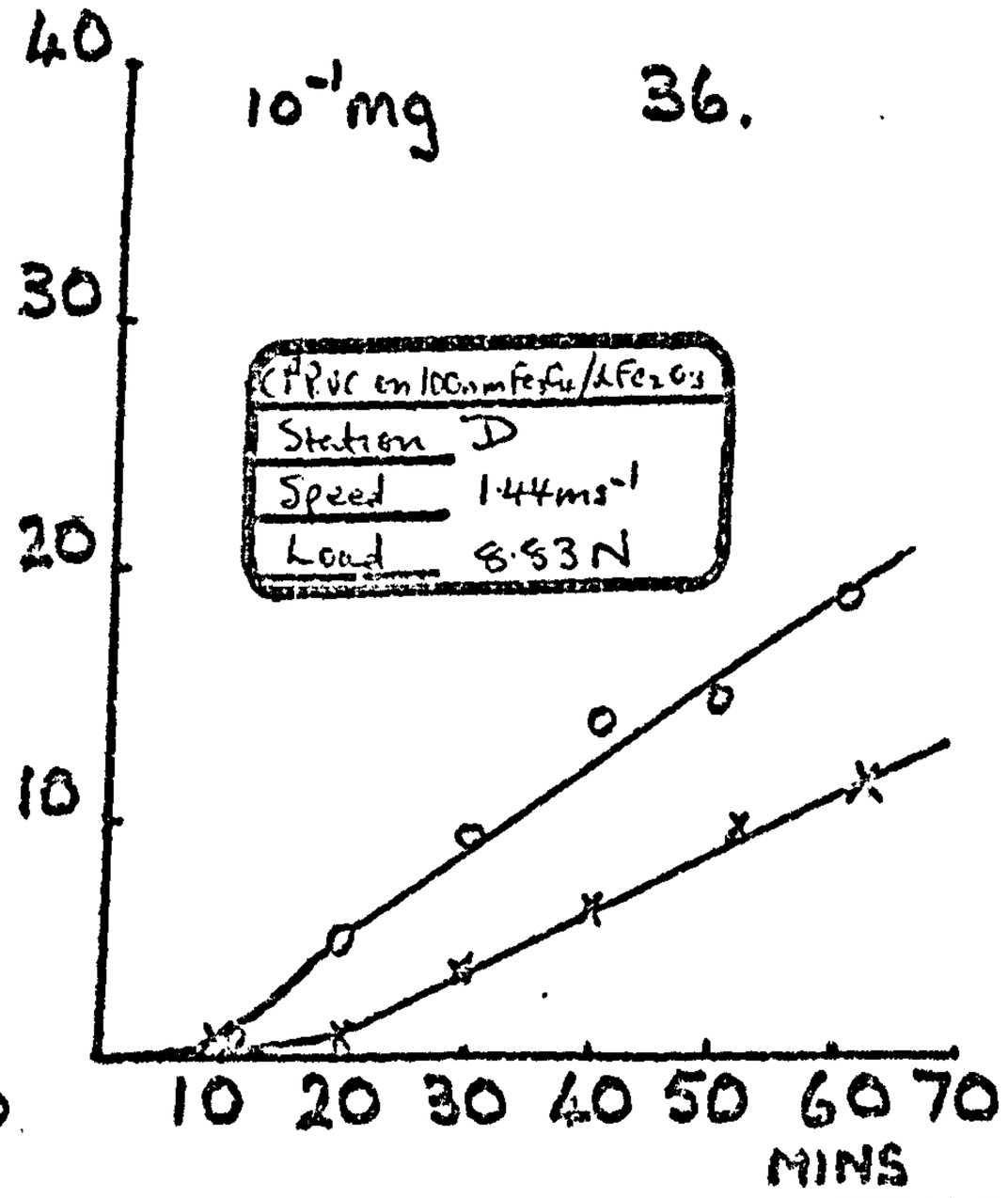

31.

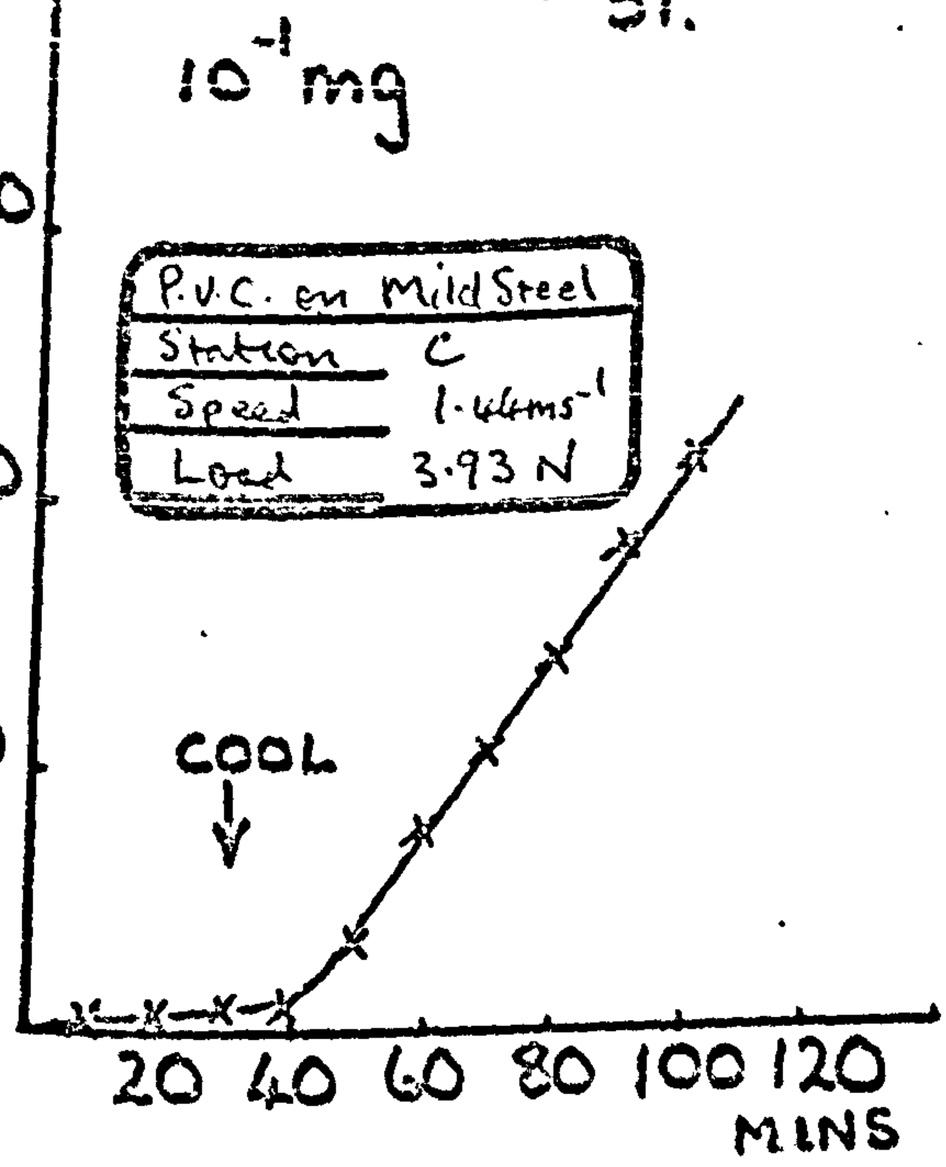

32.

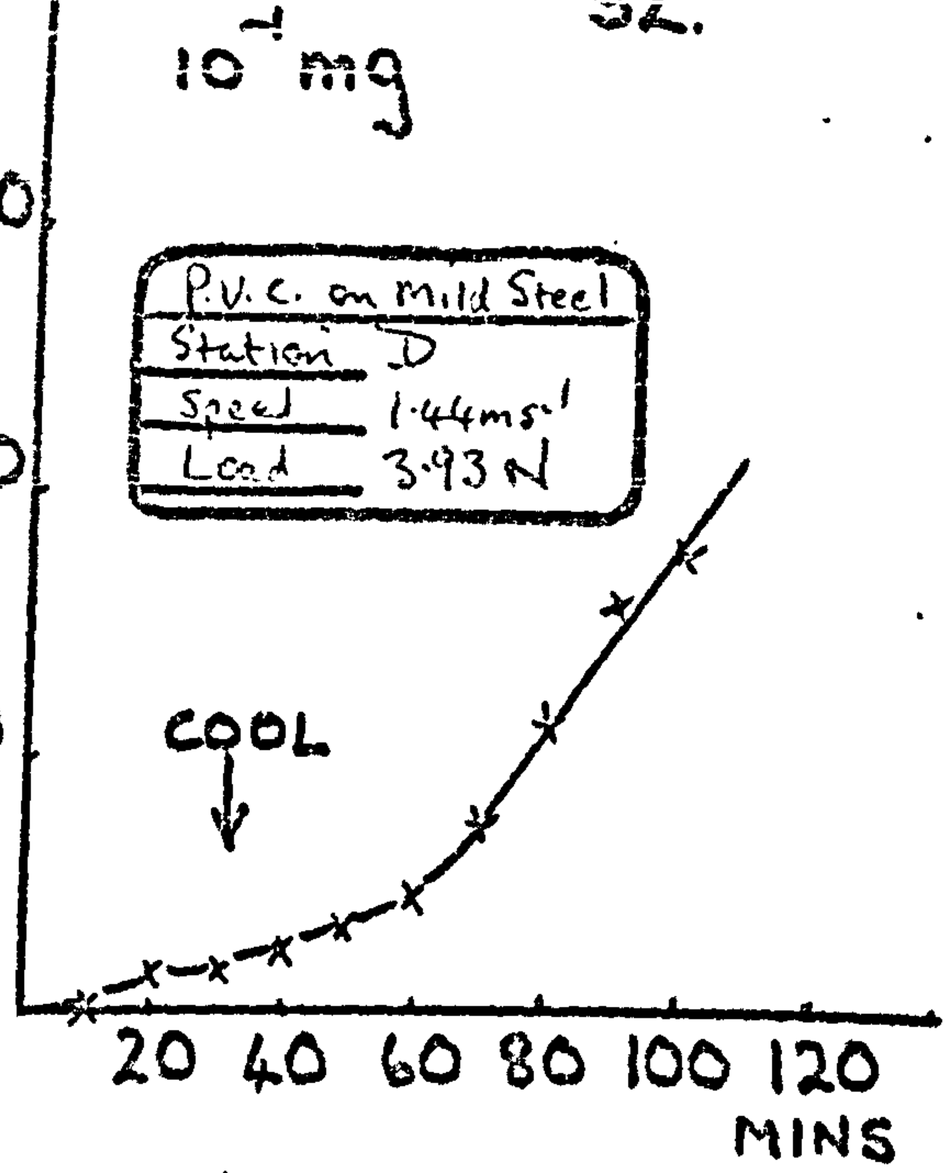

33.

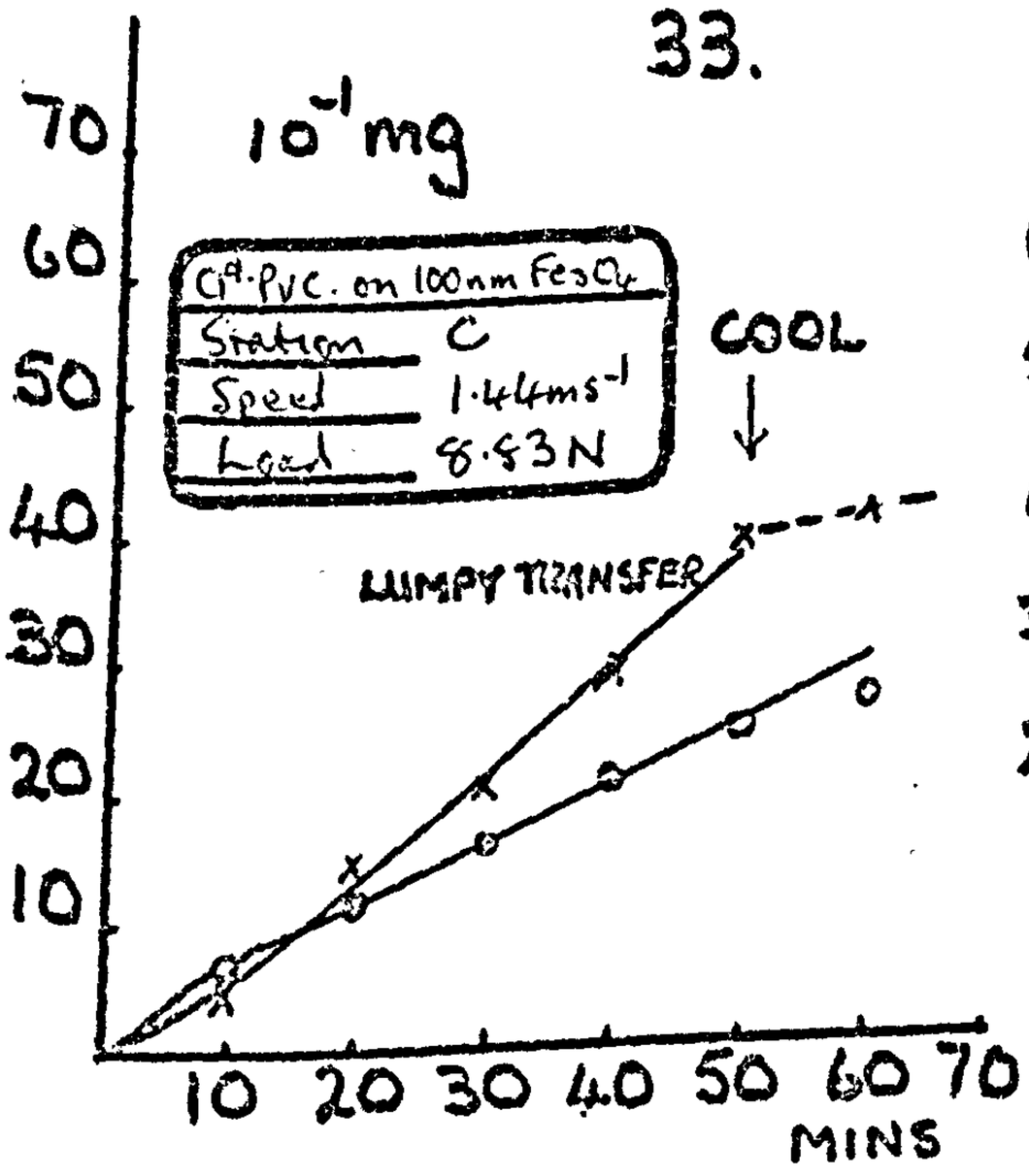

34.

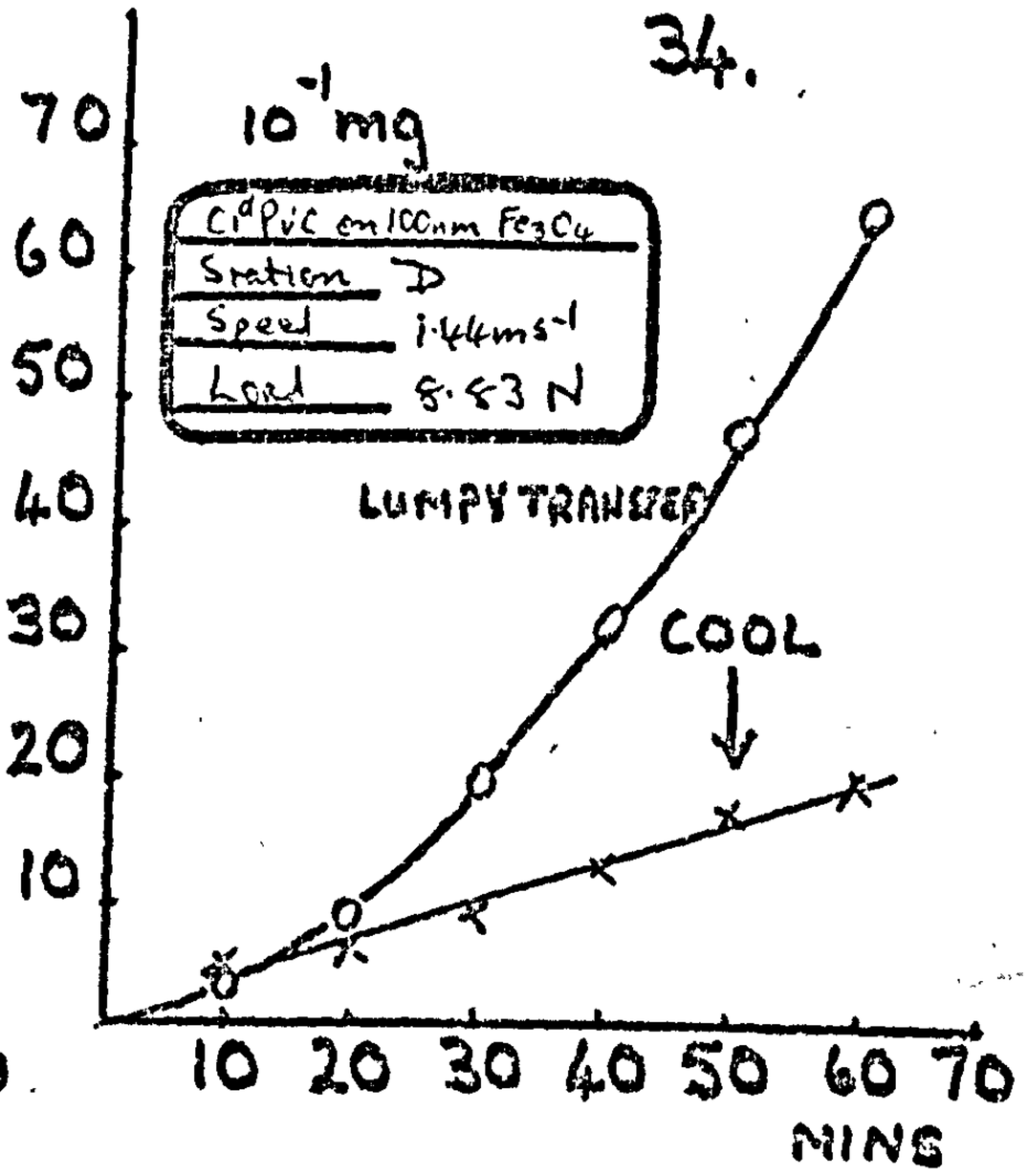

35.

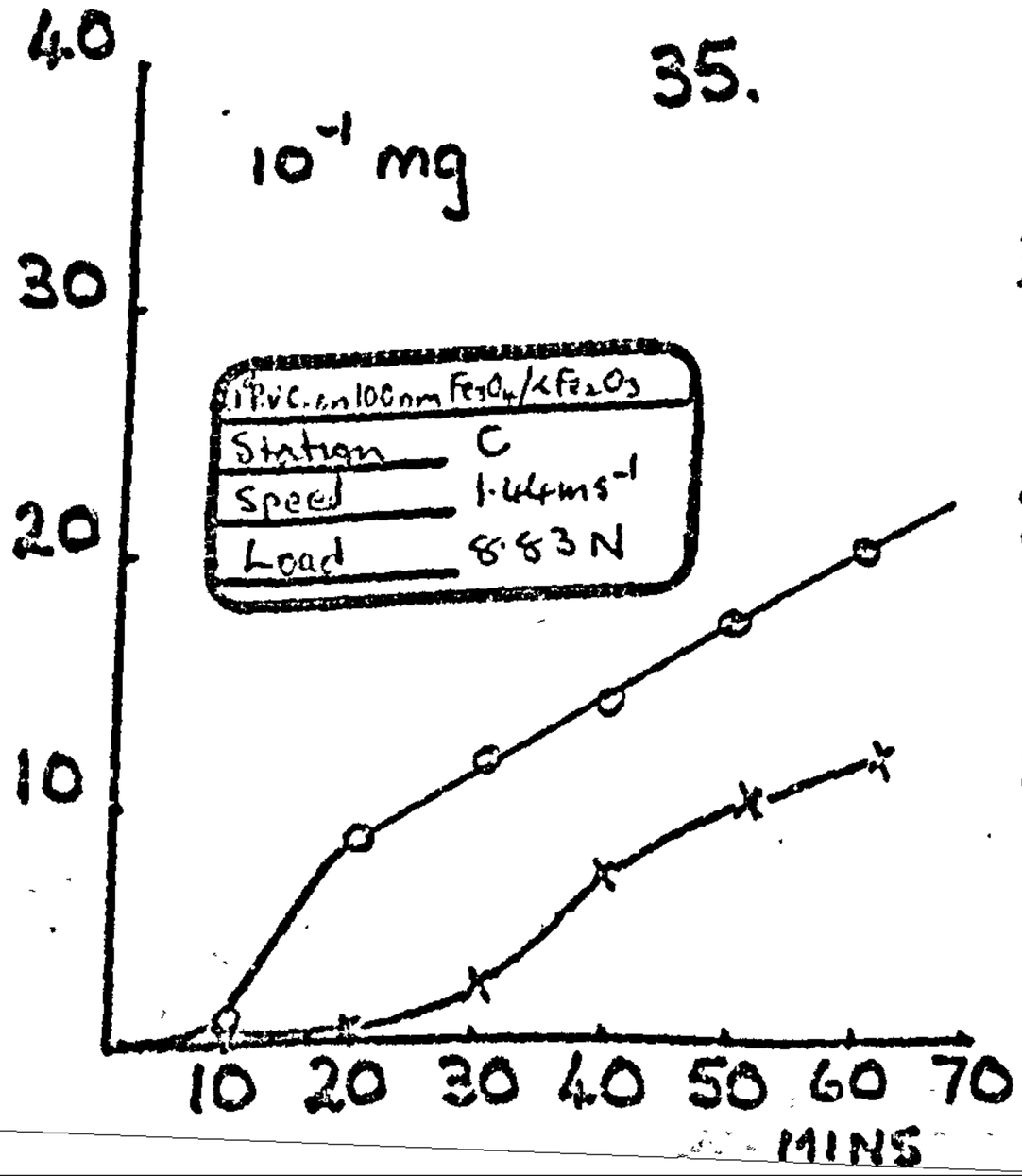

36.

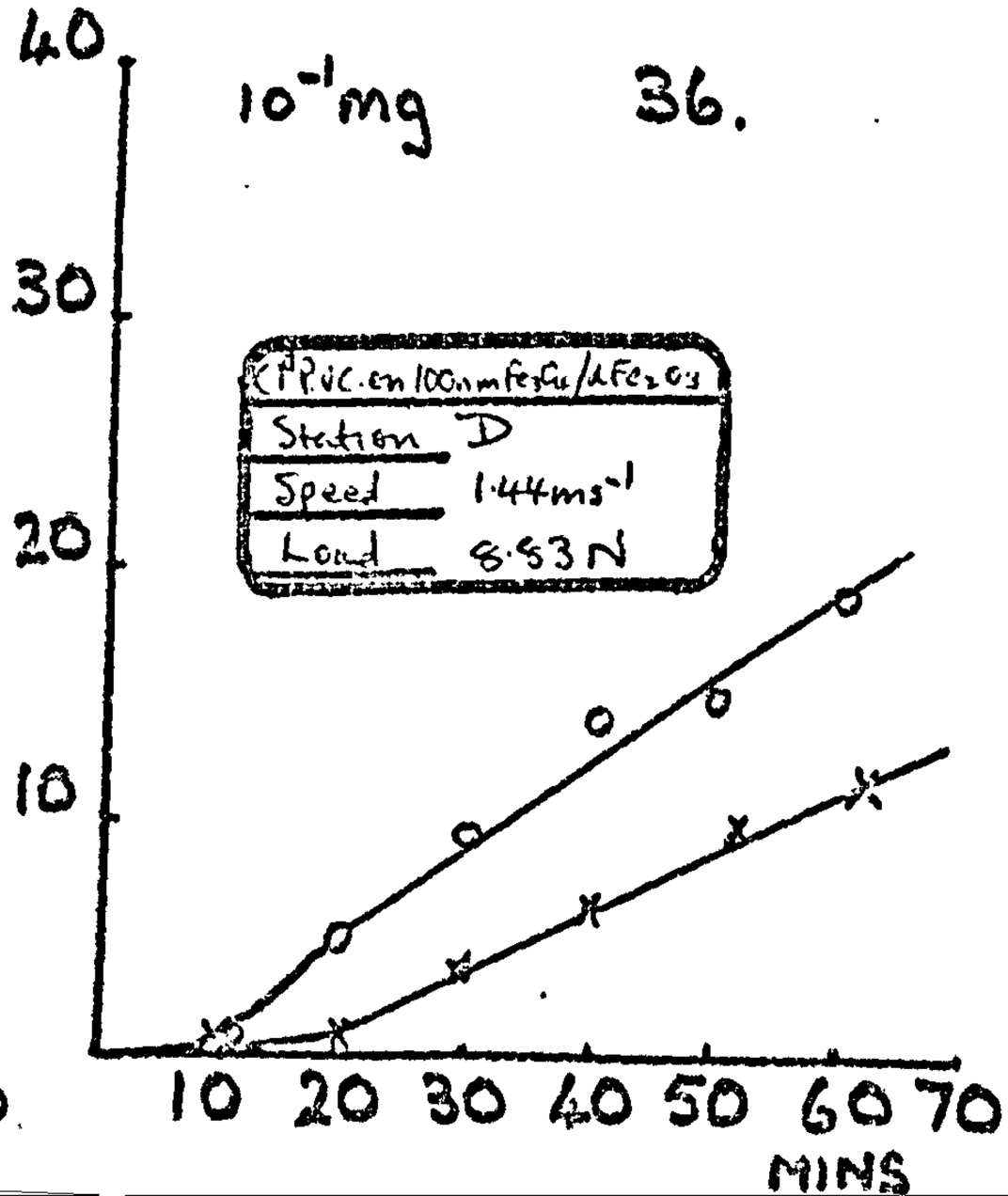

37.

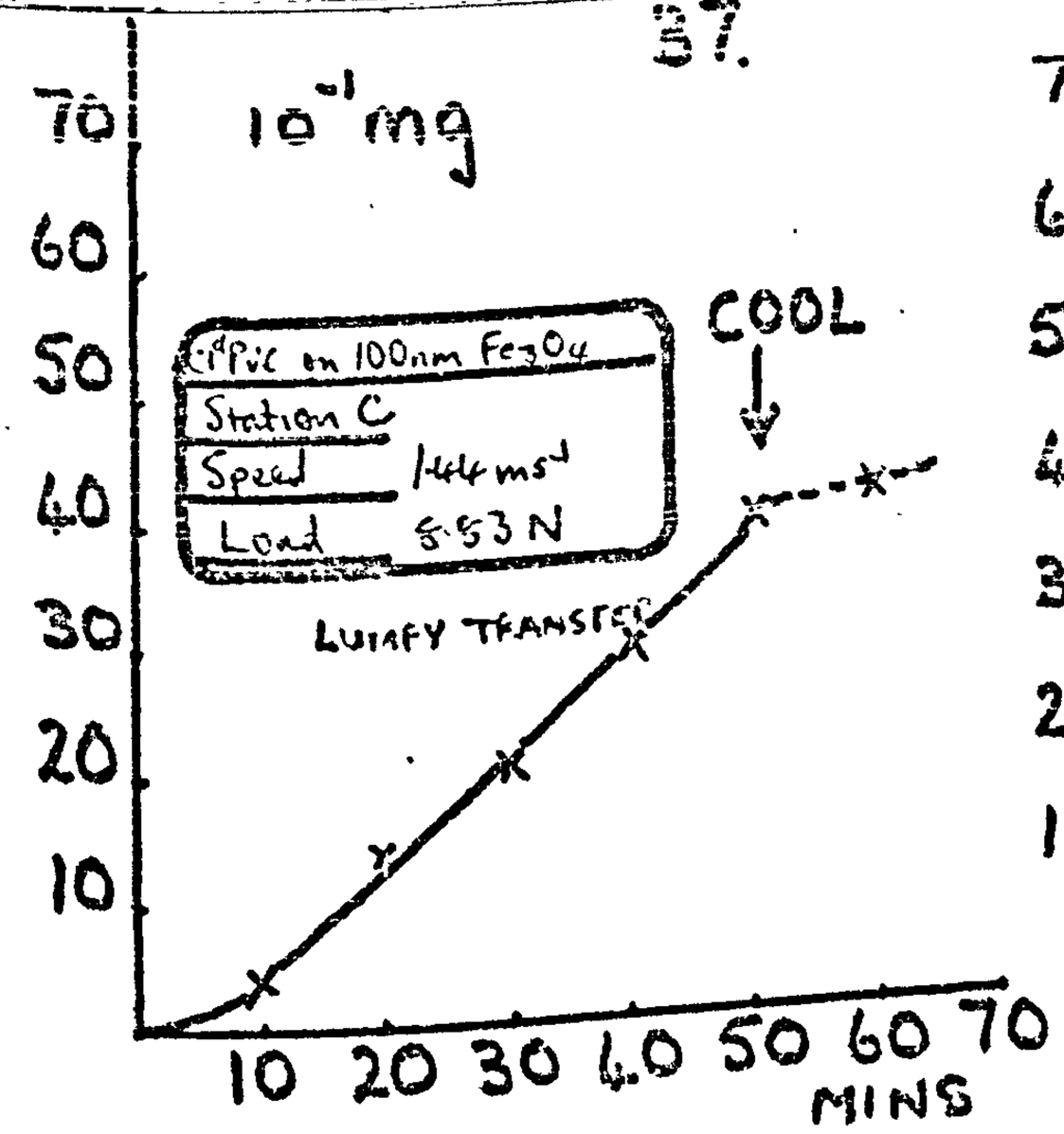

38.

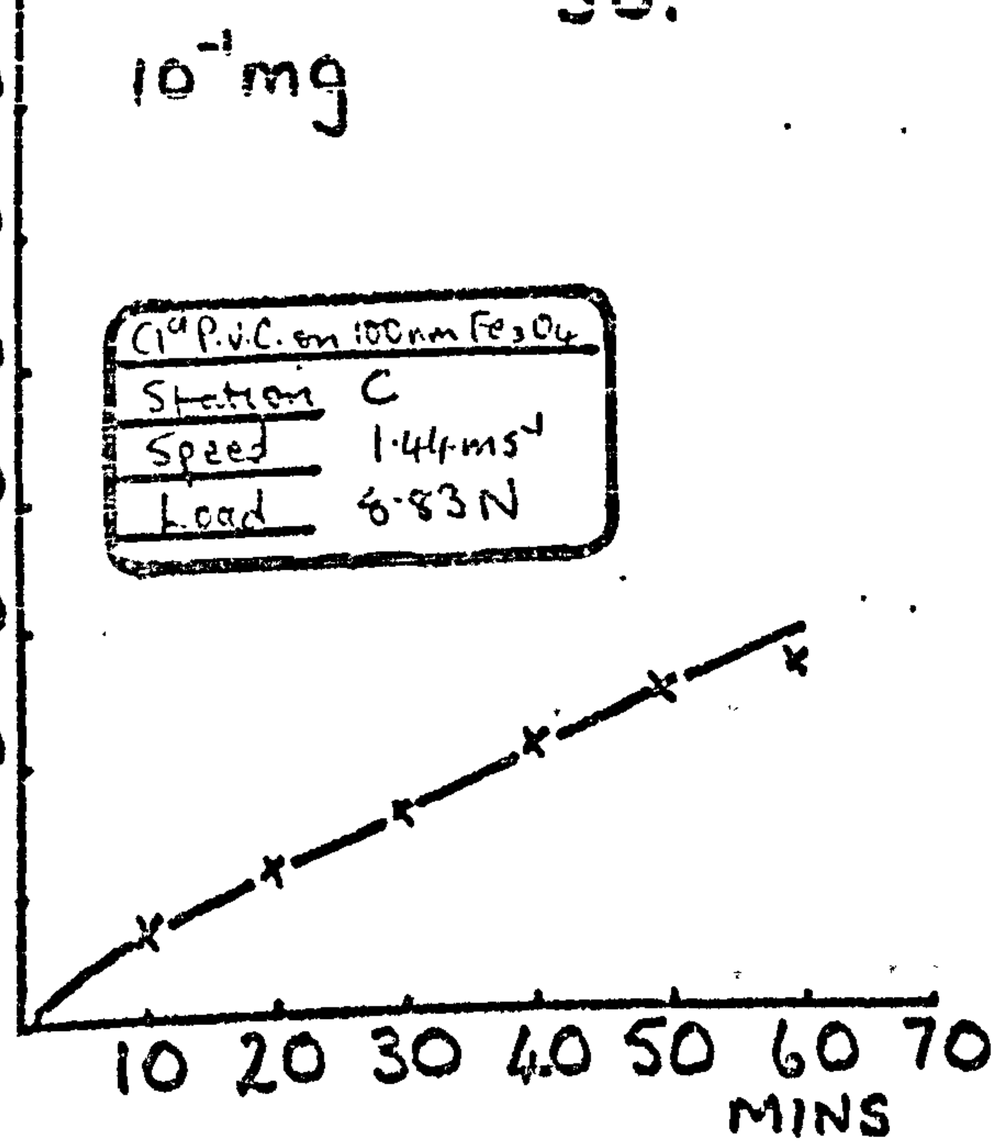

39.

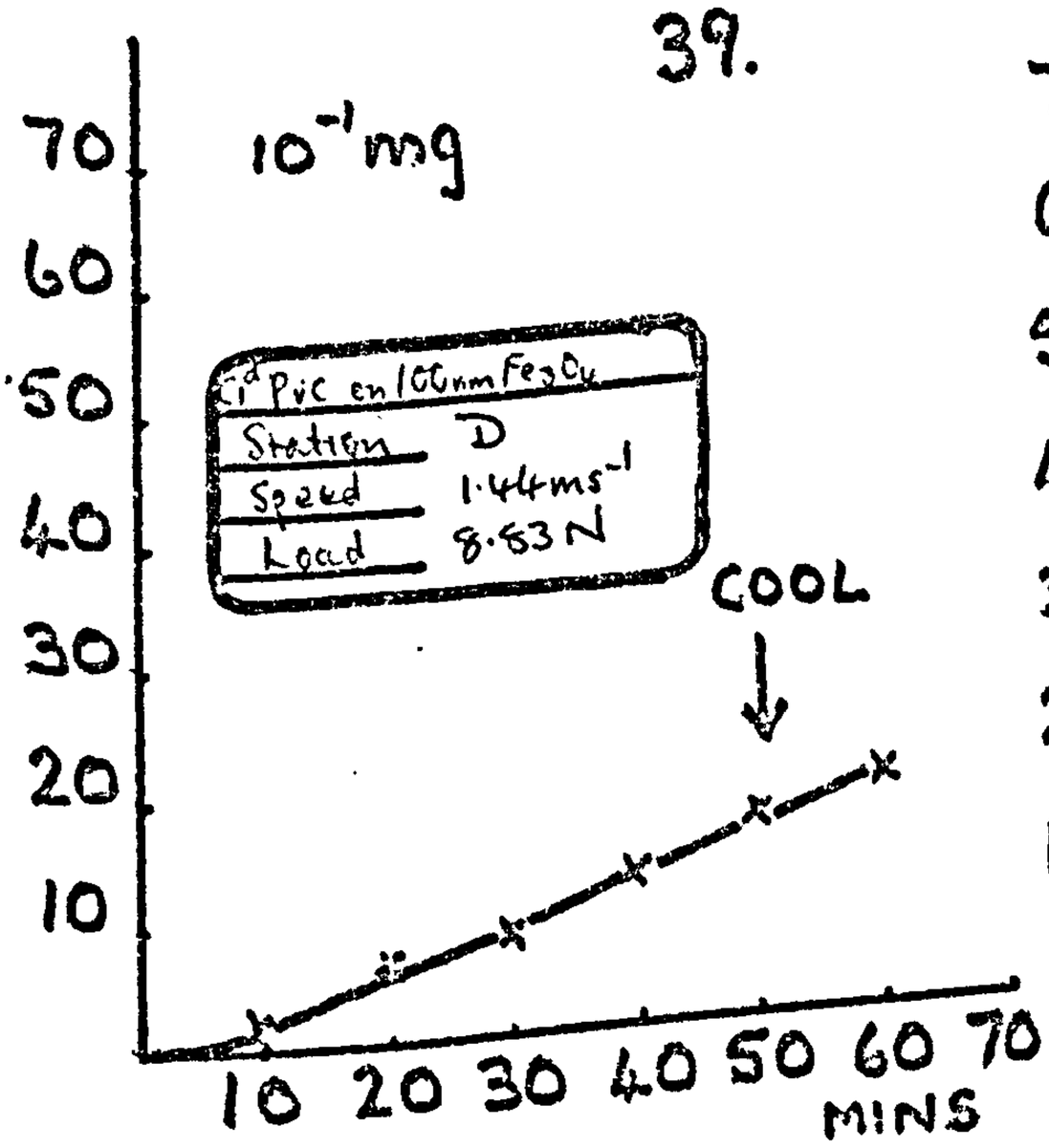

40.

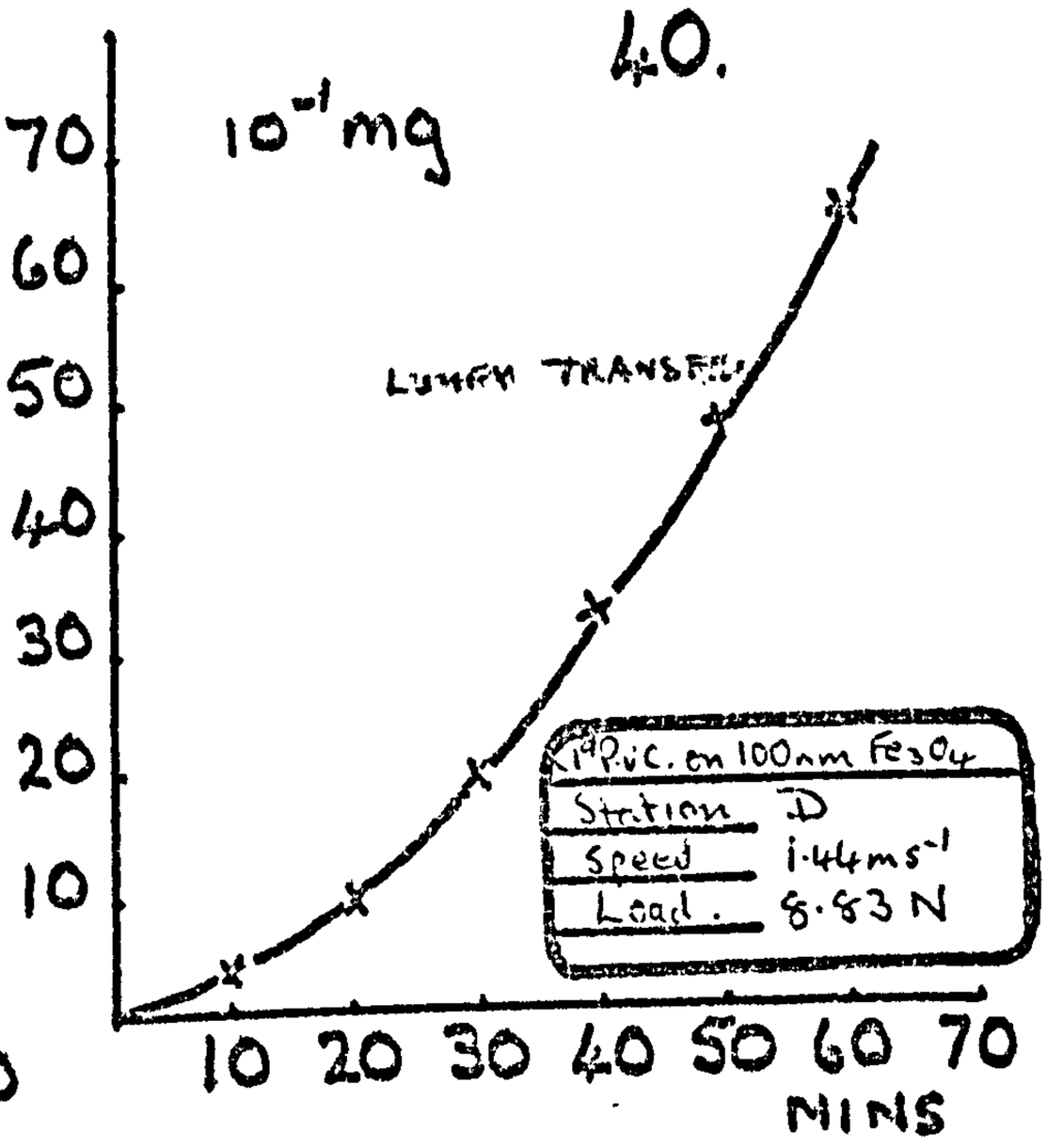

43.

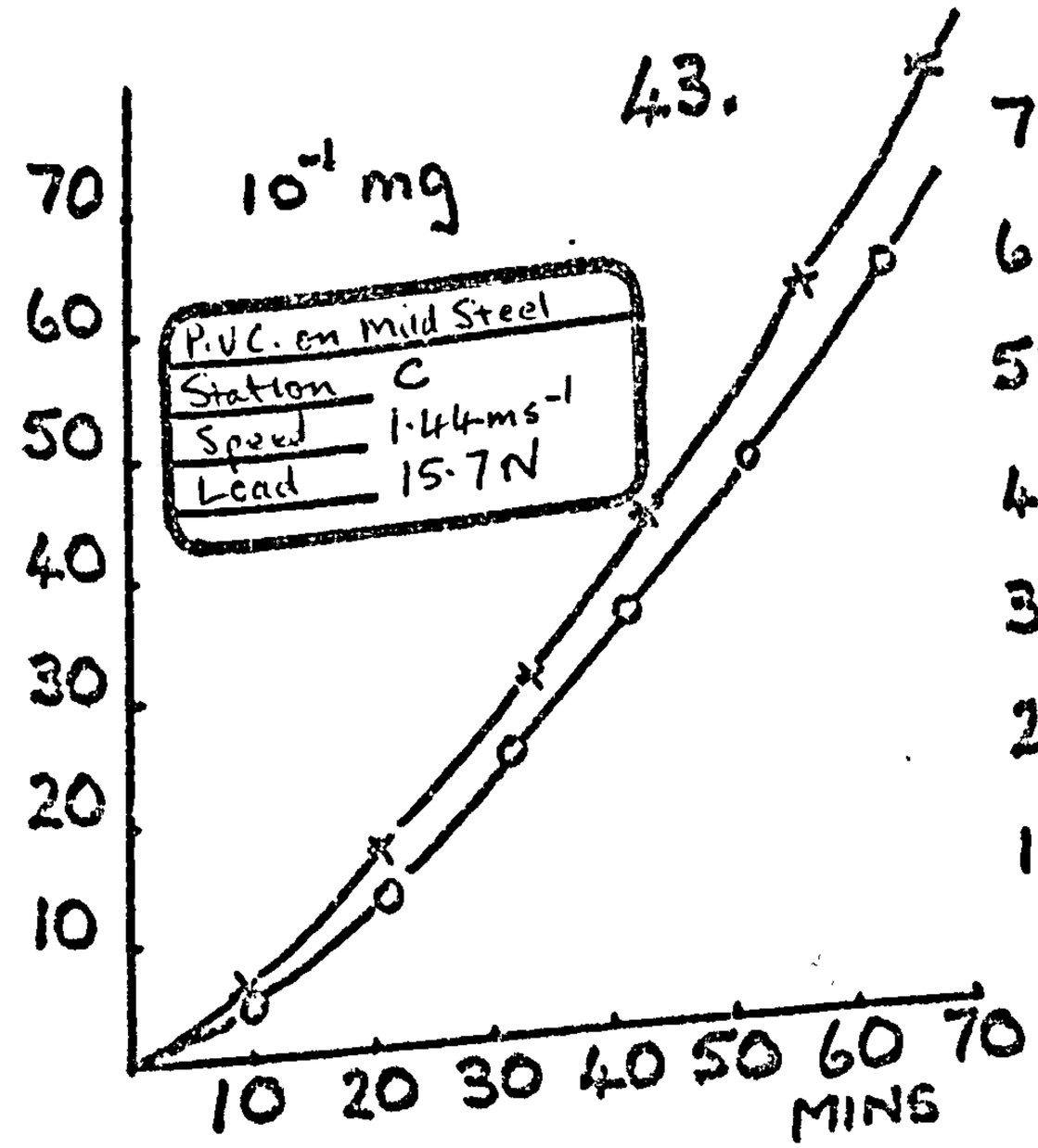

44.

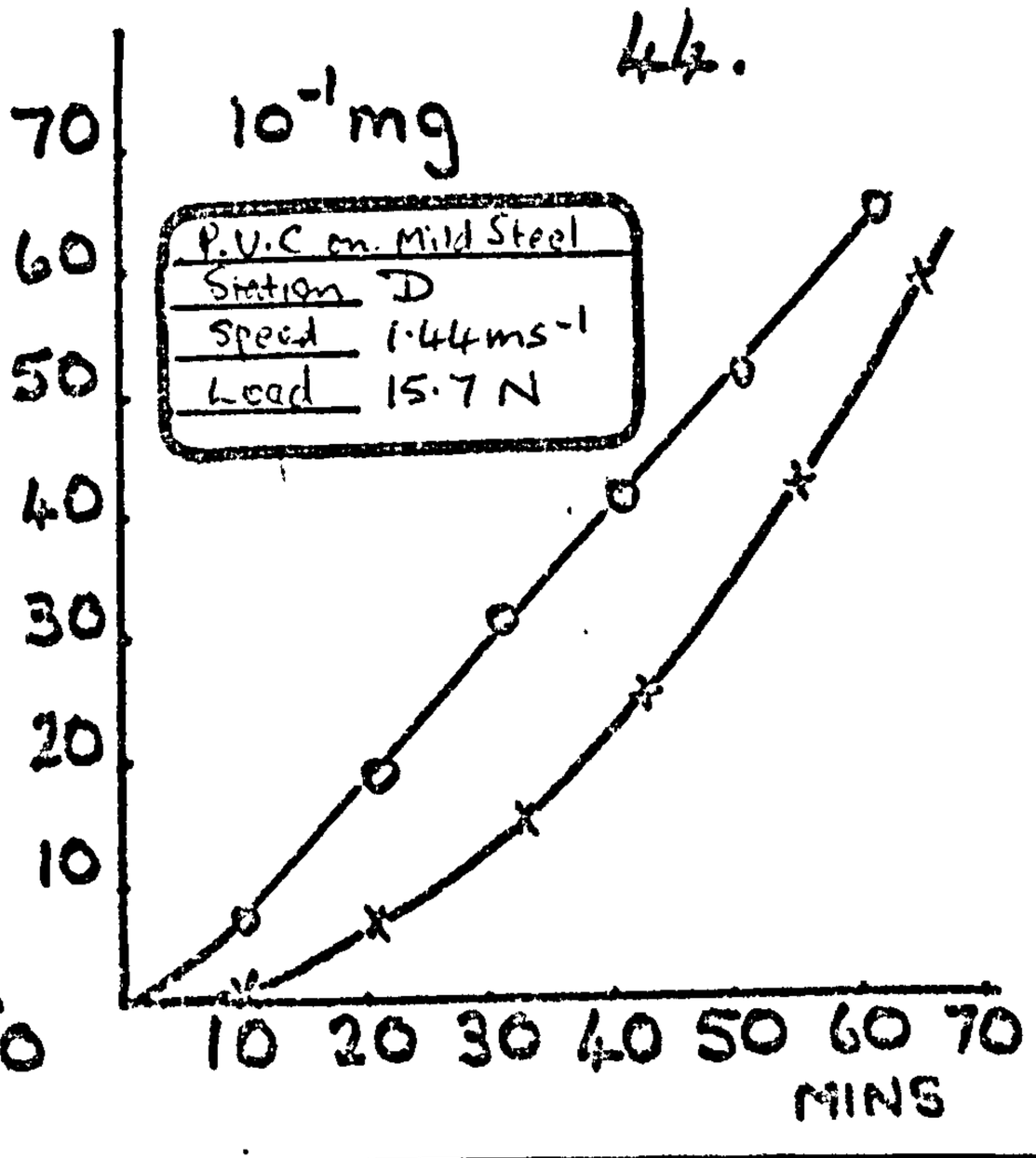

45.

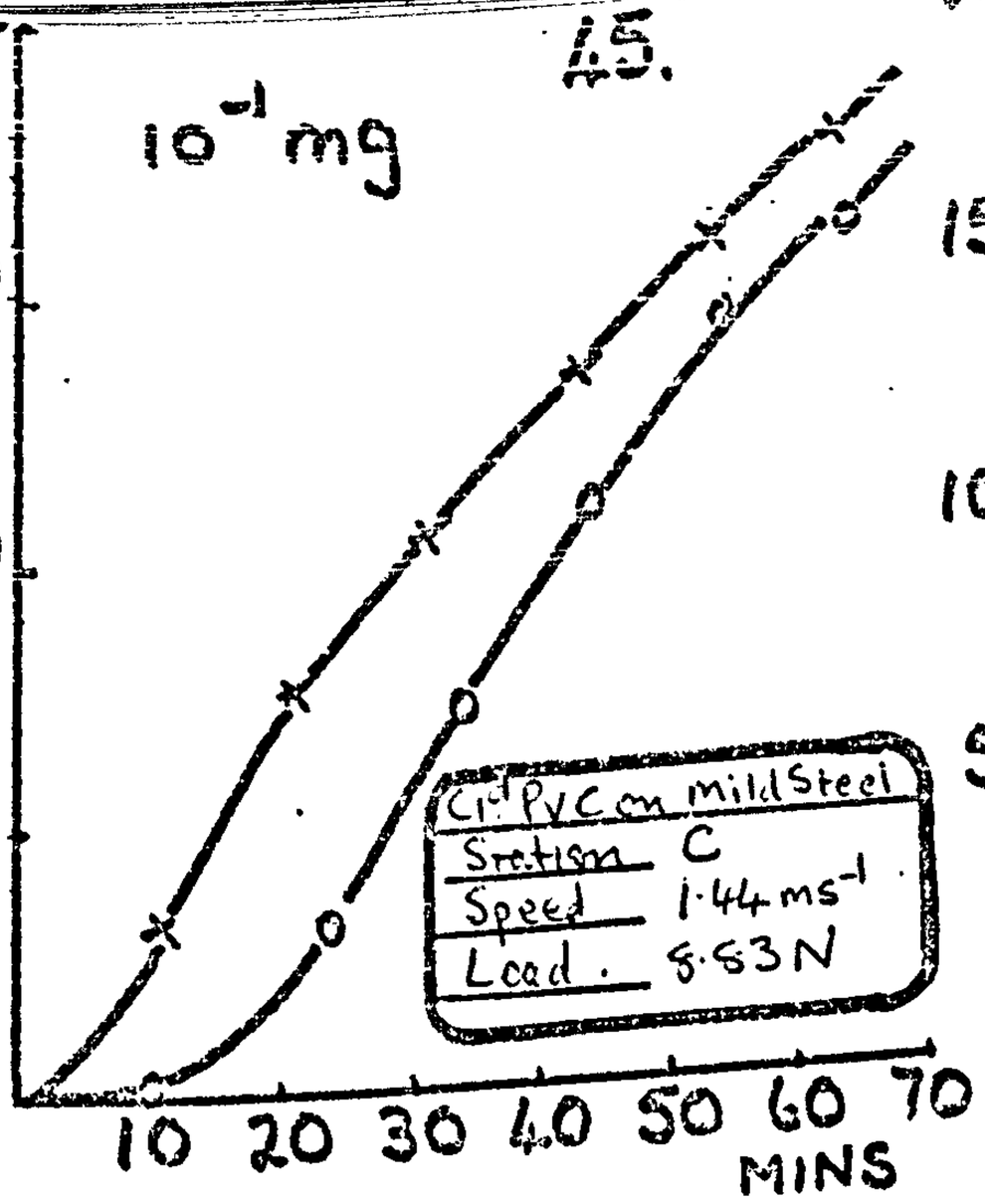
10^{-1} mg
150
100
50
10 20 30 40 50 60 70
MINS
Cl^{d} PVC on mild Steel
Station C
Speed 1·44 ms^{-1}
Load 5·53 N

46.

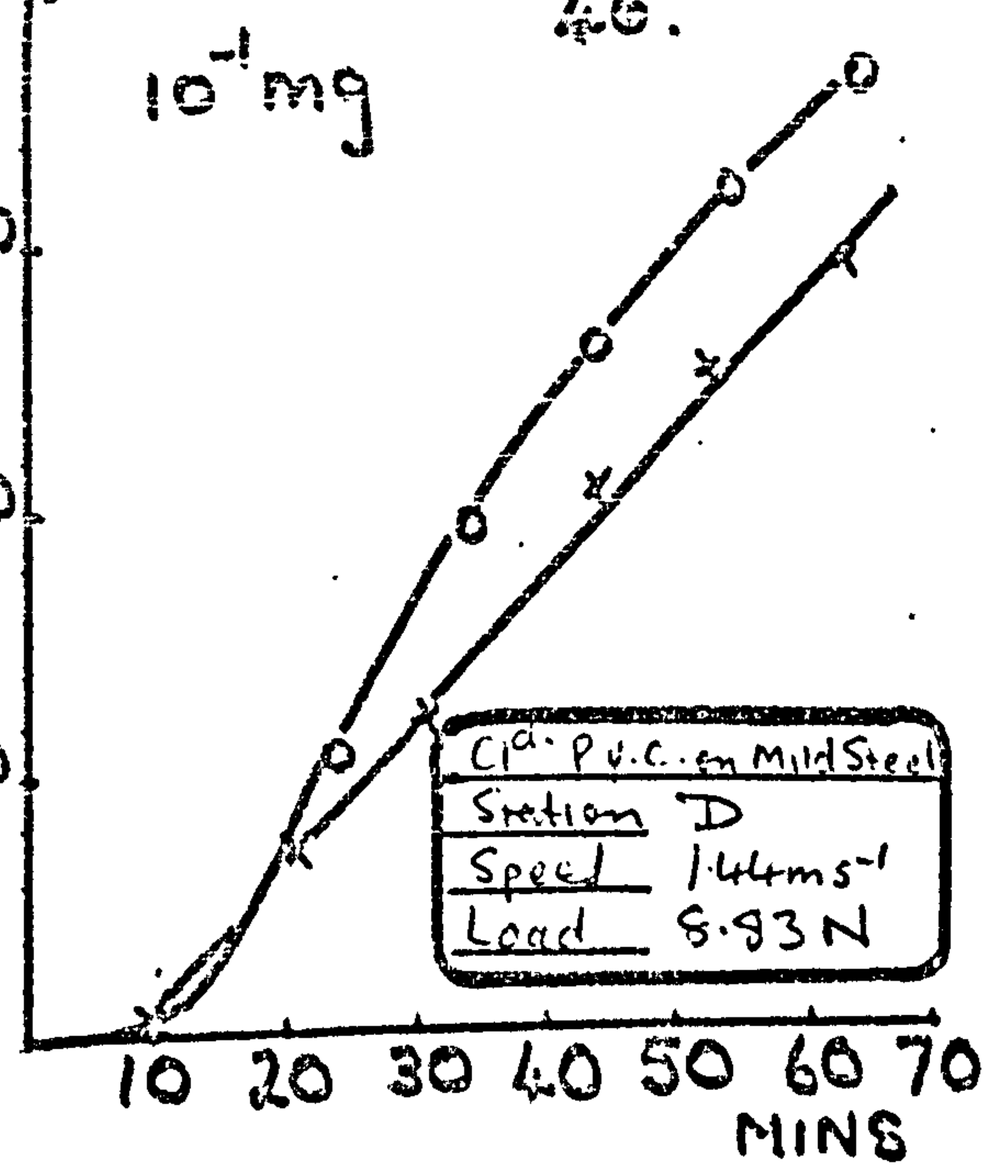
10^{-1} mg
150
100
50
10 20 30 40 50 60 70
MINS
Cl^{d} P.V.C. on Mild Steel
Station D
Speed 1·44 ms^{-1}
Load 5·93 N

APPENDIX 7

Electron and X-Ray Diffraction Analysis

7.1 The Application

7.1.1 X-ray diffraction analysis

Standard powder camera techniques were employed to obtain X-ray diffraction lines from the oxide specimens. As already described (See SAMPLE PREPARATION AND ANALYSIS) the oxides produced on steel in air or vacuum furnaces were removed and rolled into thin rods 0.3 - 0.5 mm in diameter. These were mounted centrally in the powder camera, lined up in front of the X-ray source, and the device for slowly and continuously rotating the specimen (whilst exposed to X-rays) was set in motion. Due to the interplanar spacing of iron oxides and their X-ray diffraction characteristics the radiation required in this instance was that produced by electrons bombarding a cobalt target fitted with an iron filter. Characteristically at 26 k.V. and 10 m A this produced X-ray radiation of $K\alpha_1 = (1.78\ \mathring{A})$ 0.178 n m. and $K\alpha_2 = (1.79\ \mathring{A})$ 0.179 n m.

Exposure times were varied between 5 and 10 hours.

Indexing of the values of the d lines both qualitatively and quantitatively was carried out in the first instance using an appropriate "d line" rule and later, more accurately, by incorporating a Joyce recording microdensitometer. The ratio of longitudinal pen movement to film scan movement was increased to 2 : 1 to improve resulution. Confirmation of characteristic d line patterns for each type of oxide was made by reference to A.S.T.M. powder diffraction files.

7.1.2 Electron diffraction analysis

Whereas X-rays can characteristically penetrate to a depth of 10 μ m in crystal, electron beams commonly used in diffraction work (80 - 100 kV) tend not to pass beyond the top 5 - 100 n m of surface. Hence electron diffraction was used to confirm earlier work on the nature of the surface oxides.

Transmission electron diffraction rings were obtained on an A.E.I. E.M.6G electron microscope by examining selected areas of mild steel surface removed by standard extraction replica techniques and carbon coating. The results were recorded on plates and then the diameter of the rings 'D' measured in the usual way. The microdensitometer was again used to aid this process but this time on a scale extension of 5 : 1. Knowing the camera constant $L\lambda$, for the electron microscope these 'D' measurements were converted to 'd' line interplanar spacing values using the formula $\frac{Dxd}{2} = L\lambda$ where L is the effective camera length and λ the wavelength of the electron beam[21].

Reference to A.S.T.M. powder diffraction files confirmed the presence of particular surface oxides.

7.2 Tables of results.

7.2.1 X-ray diffraction.

SAMPLE Code/History	d	I/I_1	A.S.T.M. I/I_1 Fe_3O_4	A.S.T.M I/I_1 αFe_2O_3	A.S.T.M. I/I_1 FeO	REMARKS
X 7	2.53	100	100	—		
	1.48	29.5	85	—		
	2.096	29.5	70	—		Fe_3O_4
Oxide on mild	1.61	24	85	—		+
steel produced	2.966	24	70	—		a trace αFe_2O_3
in a vacuum						
furnace.	2.69	5.5	—	100		
X10	2.53	100	100	50		
	1.48	59.2	85	—		
	2.69	45.4	—	100		
Oxide on mild	2.96	40.7	70	—		
steel produced	1.61	39.8	85	—		$Fe_3O_4/\alpha Fe_2O_3$
in an air	2.096	35.2	70	—		
furnace.	1.69	21.3	—	60		
	1.84	16.7	—	40		
	3.66	16.7	—	25		
X13	2.53	100	100			
	1.48	58	85			
	1.61	36.8	85			Fe_3O_4
	2.96	33.4	70			
magnetite	2.09	31.6	70			
Sample	1.049	21.0	40			
	1.09	19.3	60			
	4.85	12.3	40			
				100		
X14	2.69	100		50		
	2.51	82		60		
	1.69	68.5		40		αFe_2O_3
	1.84	55		25		
Haematite	3.66	51.2		30		
Sample	2.20	50		35		
	1.45	46.4		35		
	1.48	39.1				
X15	2.53	100	100	(50)		
	1.48	46.8	85	35		
	2.96	31.9	70			
1:1	2.09	27.6	70			
	1.61	26.6	85			
Magnetite/Haematite	2.69	17.0	—	100		
Sample	1.091	14.9	60			
	4.85	11.7	40			
				60		
	1.69					

Where,
d = interplanar crystal spacing x10nm(Å)
I = 'd' line intensity (arbitarily in cms)
I/I_1 = relative intensity

A.S.T.M. $\frac{I}{I_1}$ Fe_3O_4 = Relative intensities quoted by the American Society for Testing and Materials powder diffraction file

7.2 Tables of results

7.2.2 Electron diffraction

SAMPLE Code/History	D	d	A.S.T.M 'd' Fe_3O_4	A.S.T.M 'd' αFe_2O_3	A.S.T.M 'd' FeO	REMARKS
E 14 Quick on mild steel produced in a vacuum furnace.	1·22 1·92 2·09 1·802 2·8 3·52	2·53 1·61 1·48 1·71 1·12 0·85	2·53 1·61 1·48 1·71 1·12 0·85			Fe_3O_4
E 16 Oxide on mild steel produced in an arc furnace	1·02 1·18 1·4 1:62 1:82 2·04 2·32 2·74	3·03 2·62 2·21 1·91 1·695 1·51 1·33 1·13	2·966 1·712 1·483 1·327 1·21	2·69 2·201 1·838 1·69 1·484	1·52	$Fe_3O_4/\alpha Fe_2O_3$ + trace FeO

Where,

D = Electron diffraction ring diameter (arbitarily in cms.)

d = Interplanes crystal spacing x 10nm (Å)

A.S.T.M. 'd' Fe_3O_4 = 'd' lines quoted by the American Society for Testing and Materials (for Fe_3O_4 etc.).

APPENDIX 8

Micro-Hardness Testing

8.1 The application

The standard procedure was adopted for measuring the Vickers Hardness Number (V.H.N.) on a modified M.55 microscope. The specimens were prepared in the form of 2.5cm diameter discs and heated accordingly to produce the appropriate 100nm oxide layers. Similarly the mild steel control was cleaned and polished to the same specification as the drums used in the wear experiments. A minimum loading of 10 g was found to produce an accurately measurable indentation in both mild steel and oxide. Even this loading however, was sufficiently high to press the indenter to a depth of approximately 10μm which was considerably greater than the outside oxide layer 0.1μm deep. Thus the V.H.N. values obtained only serve as a very approximate indication of relative hardness. Indeed it has been recorded[90] that in the case of organic coatings the hardness values are influenced by the hardness of the substrate if the indenter makes an impression greater than 1/10th of the layer thickness let alone being allowed to pass right through it! Similarly in the case of Rockwell hardness tests both side flow and punching through of the surface layers can produce low readings[91].

APPENDIX 9

Calculations.

(1) Q/ What is the time required to form a monolayer of oxygen on the inside surface of the reaction chamber assuming a constant supply of oxygen?

Given: (i) Pressure = 1.33×10^{-8} N m^{-2} (10^{-10} torr) = P_1

(ii) O_2 incidence rate at 1.33×10^{-4} N m^{-2} (10^{-6} torr) = 3.6×10^{14} molecules $cm^{-2} s^{-1}$ = I

(iii) Molecular density for monolayer of O_2 = 8.7×10^{14} cm^{-2} = D

A/ If 1.33×10^{-4} N m^{-2} (10^{-6} torr) = P_2

then the molecular incidence rate at 1.33×10^{-8} N m^{-2} pressure

$$= \frac{P_1}{P_2} \times I$$

Therefore the time for O_2 monolayer formation on mild steel at U.H.V.

$$= \frac{D}{\frac{P_1 \times I \times 60^2}{P_2}} \text{ hrs.}$$

$$= \underline{\underline{6.7 \text{ hrs.}}}$$

NB./ Ancillary data from Ref. 137 (p.655)

(2) Q/ Is there sufficient oxygen in the reaction vessel under U.H.V. conditions to form a monolayer of oxygen on a clean iron film?

Given: (i) Pressure = 1.33×10^{-8} N m^{-2} (10^{-10} torr) = P_1

(ii) Ambient temperature = 293K = K_1

(iii) Number of molecules per cm^3 = $9.656 \times 10^{18} \times Pmm$

$$= \frac{N \times P_1}{K_1} \qquad K$$

(iv) Radius of reaction vessel = 5cms = r_1

(v) Length of associated glass and metal tubing = 100 cms = 1

(vi) Radius of associated glass and metal tubing = 0.63 cms = r_2

(vii) The molecular density for a monolayer of O_2 = 8.7×10^{14} molecules cm^{-2} = D

A/ The total volume of the reaction vessel

$$= \frac{4}{3} \pi r_1^2 + 1 \pi r_2^2 = V$$

The surface area of the clean iron films = $4 \pi r_1^2$ = A

Therefore the total number of molecules of oxygen in the vessel at 293K and 1.33×10^{-8} N m^{-2} (10^{-10} torr) assuming only O_2 present.

$$= V \times N \times \frac{P_1}{K_1}$$

$$= \underline{2.12 \times 10^9 \text{ molecules}} \qquad \text{——— (1)}$$

(2) continued....

The total number of oxygen molecules required to form a monolayer on the clean iron surface

$$= A \times D$$

$$= \underline{2.73 \times 10^{17} \text{ molecules}} \qquad (2)$$

By comparing the results (1) and (2) it can be seen that if the clean iron film is prepared under U.H.V. conditions it could never become completely oxidised (even after 6-7 hours) due to the insufficient number of oxygen molecules available.

NB/ Ancillary data from Ref. 137 (p. 8).

(3) Q/ How quickly does a monolayer of oxygen take to form on mild steel at room temperature and 1.02×10^2 k N m^{-2} (760 mm Hg) pressure.

Given: (i) O_2 incidence rate at 1.33×10^{-4} N m^{-2} (10^{-6} torr)
$= 3.6 \times 10^{14}$ molecules $cm^{-2} s^{-1} = I$

(ii) Molecular density for monolayer
$O_2 = 8.7 \times 10^{14} cm^{-2} = D$

(iii) Pressure of 1.33×10^{-4} N m^{-2} (10^{-6} torr) $= P_2$

(iv) Pressure of 1.02×10^2 k N m^{-2} (760mm Hg) $= P_3$

A/ O_2 incidence rate at 1.02×10^2 k N m^{-2} (760 mm Hg)

$$= \frac{P_3}{P_2} \times I \text{ molecules } cm^{-2} s^{-1}$$

Therefore time for a monolayer of O_2 to form on mild steel at typically ambient temperature and pressure

$$= \frac{D}{\frac{P_3 \times I}{P_2}} \text{ seconds}$$

$$= \underline{3.2 \text{ ns}}$$

ACKNOWLEDGEMENTS

I should like to thank my Supervisor, Dr. M.W. Pascoe, for all the help, encouragement, valuable advice and friendship afforded to me over the last three years along with the Head of Department, Prof. W.A. Holmes-Walker, and the Science Research Council for providing the funds.

Thanks are also due to Mrs. D. Sadler and Miss A.E. West and their respective staff for the efficient and prompt way they dealt with my many requirements and I should especially like to mention Mr. Mrs. T R.Cullingford for their unfailing kindness and practical help. I am also indebted to Dr. H. Naylor, Dr. P.T. Davies and Mr. D. W. Morecroft of Shell Research Ltd. for lending their 'clean iron' apparatus and to Prof. G.C. Bond and Dr. D.N. Waters for interesting discussions. I also acknowledge the extremely efficient Brunel Library staff and Mr. L.J.Maisey of R.A.P.R.A. (P.S.C.C.) for help with samples and G.P.C. and D.S.C. analyses.

Finally, and certainly not least, to my wife Jackie for sacrificing so much to help and encourage me in addition to the major task of typing most of the script - thank you. I am sure that time will show that it was all worth it.

REFERENCES

1. C. J. SPEERSCHNEIDER, The role of filler geometrical shape in wear and friction of filled PTFE, Wear, 5 (1962) 392-399.

2. K. R. MAKINSON AND D. TABOR, The friction and transfer of P.T.F.E. Proc. Roy. Soc., A281 (1964) 49-61.

3. J. K. LANCASTER, R.A.E. Report T.R. 68045, 1968.

4. R. HARGREAVES AND D. H. TANTAM, The performanace of some plain bearing materials under boundary conditions at low temperatures, Proc. Inst. Mech. Engrs., 175 (20) (1961) 941-954.

5. J. P. GILTROW AND J. K. LANCASTER, R.A.E. Report 69060, 1969.

6. D. H. BUCKLEY AND R. L. JOHNSON, NASA Report T.N.-D-2073, 1963.

7. G. C. PRATT, Recent developments in PTFE-based dry bearing materials treatments, Proc. Inst. Mech. Engrs., 181 (1966) 132-143.

8. R. G. BAYER, Prediction of wear in a sliding system, Wear, 11 (1967) 319-332.

9. G. VINOGRADOV, V. A. MUSTAFAEV AND YU. YA. PODOLSKY, Wear, 8 (1965) 358-373.

10. C. M. POOLEY, personal communication.

11. G. C. PRATT, Plastics as bearing materials with particular reference to PTFE, Plastics Inst. J., 32 (1964) 255-260.

12. B. V. DERYAGIN, Zhur. Tekk. Fiz., 24 (1954) 1354-1357.

13. S. M. SKINNER, R. L. SAVAGE AND J. E. PUTZLER, J. Appl. Phys., 24 (1953) 438-450.

14. D. E. PACKHAM, The adhesion of polyethylene to high-energy surfaces, Adhesion Conference, City University, 19th March, 1970.

15. H. SLINEY, NASA Technical Note T.N.-D5301, 1969.

16. W. HIRST, Basic mechanisms of wear, Proc. Inst. Mech. Engrs., 182 (1967/68).

17. J. K. LANCASTER AND M. KERRIDGE, Proc. Roy. Soc., A 236 (1956) 250-264.

18. A. W. J. DE GEE AND J. H. ZAAT, Wear, 5 (1962) 257-274.

19. R. H. BROWN AND E. J. A. ARMAREGO, Wear, 6 (1963) 106-117.

20. J. K. LANCASTER, R.A.E. Report 65102, 1965.

21. H. LEE AND K. NEVILLE, Handbook of Epoxy Resins, McGraw-Hill, New York, 1967.

22. H. KRAUSE, S. L. COSGROVE AND C. M. ALLEN, Phthalocyanines as high-temperature lubricants, J. Chem. Eng. Data, 6 (1) (1961) 112-118.

23. G. SALOMON, A.BEGELINGER AND A. W. J. DE GEE, Frictional properties phthalocyanine pigments, Wear, 10 (1967) 383.

24. J. F. ARCHARD, The temperature of rubbing surface, Wear, 2 (1958/59) 438-455.

25. E. RABINOWICZ, Friction and Wear of Materials, Wiley, New York, 1965.

26. R. B. LEWIS, Predicting bearing performance of filled Teflon T.F.E. resins, ASME Paper 66, WA/RP-1, 1966.

27. C. F. LINDAY, Friction and wear tests at high rubbing speeds, VDIZ, 109 (16) (1967) 722-727.

28. AWATANI AND R. KIMURA, Wear properties of plastics, J. Soc. Mech. Engrs., 11 (1968) 939-947.

29. M. D. BEZBAROD'KO AND L. I. SHABAROV, Friction of steel on plastics, Soviet Plastics, 9 (1965) 30-36.

30. Filled PTFE properties and application design data, I.C.I. Technical Service Note F.13. 1969.

31. R. J. STEIJN, Sliding experiments with PTFE, ASLE Trans., 11 (1968) 235-247.

32. J.FARCHARD AND W. HIRST, The wear of materials under unlubricated conditions, Proc. Roy. Soc., A236 (1956) 397-409.

33. D. DRAIGOR, Soviet Mater. Sci., 2 (1) (1966) 47-48.

34. E. RABINOWICZ, Variation of friction and wear of solid lubricant films with film thickness, ASLE Trans., 10 (1967) 1-10.

35. A. W. J. DE GEE, Influence of oxide films on friction and wear during sliding, Materialprüf., 9 (5) (1967) 166-169.

36. R. L. JOHNSON, M. B. PETERSON AND M. A. SWIKERT, NACA TN 2366, 1951.

37. D. DRAIGOR, O. D. KNAB AND V.A. DANILENKO, A method of investigating sintered material surfaces, Soviet Mater. Sci., 2 (1) (1966) 49-50.

38. A. T. MALE, C. F. HINSLEY AND G. ROWE, Frictional properties of metal oxides at high temperature, Wear, 11 (1968) 233.

39. R. M. REIHSMANN, Quantum Inc. Report, AD 402 082, 1963.

40. J. K. LANCASTER, Composite self-lubricating bearing materials, Proc. Inst. Mech. Engrs., Pt.1., 182 (1967-68).

41. A. A. MILNE, Wear, 1 (1957) 92-103.

42. Symposium on Electron beam irradiation, Imperial College, London, 1967.

43. W. WILKENS AND O. KRANZ, Wear, 15 (1970) 215-227.

44. G. J. L. GRIFFIN AND D. K. MAJUMDAR, J. Appl. Cryst., 3 (1970) 400.

45. G. A. GOROKHOVSKII, Mechanico-chemical dispersion of metals in dynamic contact with polymers, Soviet Mater. Sci., 1 (5) (1965) 365-367.

46. G. A. GOROKHOVSKII AND I. I. AGULOV, Structural changes in iron operating in contact with polymers, Soviet Mater. Sci., 2 (1) (1966) 78-81.

47. F. P. BOWDEN, Fundamentals of Gas-Surface Interactions, Academic Press, New York, 1967.

48. C. ROWE AND J. DICKERT, ASLE Trans., 10 (1967) 85-90.

49. W. CAMPBELL AND R. LEE, Polymer formation on sliding metals in air saturated with organic vapours, ASLE Trans., 5 (1962) 91-104.

50. S. W. CHAIKIN, On frictional Polymer, Wear, 10 (1967) 49-60.

51. D. TABOR AND R. WILLIS, Thin film lubrication with substituted silicones: the role of physical and chemical factors, Wear, 11 (1967) 145-162.

52. D. TABOR AND R. WILLIS, The formation of silicone polymer films on metal surfaces at high temperatures and their boundary lubricating properties, Wear, 13 (1969) 413-442.

53. A. E. JEMMETT, Chemical behaviour of siloxanes at metal interfaces, Tribology, 1 (3) (1968) 173-177; and 1 (4) (1968) 237.

54. A. A. KOUTKOV AND D. TABOR, Tribology, 1 (1970) 163-164.

55. D. SCOTT, Wear, 13 (1969) 1-2.

56. A.R. LANSDOWN, Tribology News, 12 (1970) 5.

57. N. ISTOMIN AND R. MATVEEVSKII, Anti-friction compounds based on PTFE and lead, Russian Eng. J. Vol. L 2 (1970) 58.

58. Plastic Coatings Ltd. Guildford, Surrey.

59. D. SCOTT, J. BLACKWELL, P. McCULLOGH AND E. MILLS, Composite Materials for roller bearing cages, Wear 15 (1970) 257-269.

60. G. V. VINOGRADOV, Effect of temperature on friction and adhesion of crystalline polymers, Wear, 16 (1970) 213-219.

61. J. K. LANCASTER, Estimation of the limiting P.V. relationships for thermoplastic materials, Tribology, May (1971) 82-86.

62. H. UETZ AND H. BRECKEL, Friction and wear tests on PTFE, I.C.I. Translation TR 10.210, Wear, 10 (1967) 185-198.

63. A. SELWOOD, The topography of rough surfaces, Wear, 5 (1962) 148-157.

64. E. FINKEN, Surface roughness in wear, Wear, 6 (1963) 293-302.

65. D. R. GABE, Methods of measuring surface roughness, Metallurgin LXXII (1965) No. 429.

66. G. GOROKHOVSKII, L. BEZRUK, P. SEVERIN AND M. DUDNIK, The effect of structural orientation on the wear characteristics of PTFE, 1968, I.C.I. Translation TR 10.311 (1966).

67. A. B. WINTERBOTTOM, Optical studies of the oxidation of iron at temperatures in the range of 20-265°C, J. Iron and Steel Inst. 165 (1950) 9-22.

68. W. E. BOGGS, R. H. KACHIK AND G. E. PALLISSIER, Effect of oxygen pressure on the oxidation of zone-refined iron, J. Elect. Chem. Soc., 112, 6 (1965) 539.

69. A. KNAPPWOST AND H. WOCHNOWSKI, Sliding of mild steel under vibrating load, Tribology News, May (1972).

70. ASTM, X-ray Powder Diffraction File 13-534.

71. T. F. J. QUINN, The applications of modern physical techniques to tribology, Newnes-Butterworths (1971) P.140.

72. P. J. ALISON AND H. WILMAN, The differential behaviour of hexagonal and cubic metals in their friction, wear and work-hardening during abrasion, Brit. J. Appl. Phys., 15 (1964) 281.

73, D. H. BUCKLEY AND R. L. JOHNSON, Friction and wear of hexagonal metals and alloys as related to crystal structure and lattice parameters in vacuum, A.S.L.E. Conf. Oct. 18-20 (1965).

74. F. P. BOWDEN AND D. TABOR, Friction and lubrication, Methuen Monograph P.33 (1967).

75. J. R. WHITEHEAD, Surface deformation and friction of metals at light loads, Proc. Roy. Soc. A (1950) 201 109.

76. E. RABINOWICZ, Lubrication of metal surfaces by oxide films, A.S.L.E. Trans. 10 400-407, (1967).

77. M. COCKS, Surface oxide films in intermetallic contacts, Nature (1952) 70 203.

78. R. W. WILSON, Influence of oxide films on metallic friction, Proj. Roy. Soc., (1952) 212 450.

79. A. J. M. MOORE AND W. J. TEGART, Effect of hardness on breakdown of oxide films, Proc. Roy. Soc., A (1952) 212 252.

80. T. SPALVINS, Frictional characteristics of sputtered solid film lubricants, NASA TMX 52 819 (1970)

81. R. F. HORAN, Studies of low friction coatings for vulcanised elastomers, Quantum Inc. Report AD 443 073 (1964).

82. W. R. MOORE, Introduction to polymer chemistry, University of London Press, (1963) P.90.

83. Improving adhesive bond strength in polymers by surface treatment, Techlink No. 512, Feb. (1970).

84. K. MACKENZIE AND A. E. JEMMETT, Polymer Shear stability, Wear, 17 (1971) 389-398.

85. D. W. MORECROFT, Reactions of Octadecane and decoic acid with clean iron surfaces, Conf. Swansea Tribology Centre, Jan. (1971).

86. F. G. ROUNDS, Some environmental factors affecting surface coating formation with lubricating oil additives, A.S.L.E. Lubrication Conf. Oct. 18-20 (1965).

87. G. C. MARKS, J. L. BENTON AND C. M. THOMAS, The thermal degradation of P.V.C. in a nitrogen atmosphere, S.C.I. Monograph 26 (1966/67) 204. 223

88. A. K. OSBORNE, An encyclopeadia of the iron and steel industry, 2nd Edit. The Technical Press (1967) 423.

89. G. R. BOOKER, J. NORBURY AND A. L. SUTTON, X-ray diffraction studies on precipitates and inclusions in steels using an extraction replica technique, B. J. Appl. Phys., 8 (1957) 55.

90. P. FINK-JENSEN, Hardness testing of organic coatings, Butterworths (1965) 250, 258.

91. V. E. LYSAGHT, Indentation hardness testing, Reinhold (1949) 162.

92. A. D. CROSS AND R. A. JONES, An introduction to practical infra-red spectroscopy, Butterworths (1969) 73.

93. L. REICH AND S. STIVALA, Elements of polymer degradation, McGraw-Hill (1971) 46.

94. F. W. BILLMEYER, Characterisation of molecular weight distributions in high polymers, J. Pol. Sc. C. 8 (1965) 161-178.

95. J. HASLAM AND H. A. WILLIS, Identification and analysis of plastics, Iliffe (1965) 156.

96. N. K. BARAMBOLM, Mechano-chemistry of polymers, Maclaren (1964).

97. D. BAUM AND L. H. WARTMAN, J. Pol. Sc. 28 (1958) 537.

98. W. C. GEDDES, The mechanism of P.V.C. degradation, R.A.P.R.A. Tech. Review No. 31 (1966).

99. P. MEARES, Polymers - structure and bulk properties, D. Van. Nostrand (1967).

100. C. M. POOLEY AND D. TABOR, Transfer of P.T.F.E. and related polymers in a sliding experiment, Nature Phy. Sc. 237 (1972) 88.

101. M. GORDON, The structure and physical properties of high polymers, (1957) 92, P.I. Monograph.

102. B. KE., Newer methods of polymer characterisation, Interscience (1964) 440.

103. S. B. RATNER, Soviet Plastics 7 (1964) 37.

104. J. K. LANCASTER, Polymer-based bearing materials - the role of fillers and fibre reinforcement in wear, M.S.C. Conf. Brunel University, April, (1972).

105. J. A. BRYDSON, Plastics materials, Iliffe (1966)

106. British Plastics 39 1 (1966).

107. F. CHEVASSUS AND R. DE BROUTELLES, The stabilization of P.V.C. Arnold (1963)

108. S. L. MADORSKY, Thermal degradation of organic polymers, Interscience (1964).

109. J. KRAMER, Z. Physik 128 538 (1950).

110. L. GRUNBERG, Proc. Phys. Soc. 66 (1953) 153.

111. C. F. BERSCH, et al, J. Res. Nat. Bur. Stand. 60 481 (1958).

112. T. WEXLER AND D. CORNILESCU IUPAC Int. Symp. Macromol. Chem. Prague (1965), Reprint 614.

113. S. OHNISHA, Y. NAKAJIMA AND I. NITTA, J. App. Pol. Sc. 6 639 (1962)

114. A. KONISHI, Nippon Kagaku Zasshi 78 1517 (1958) S.L.A. Trans. 60-18459.

115. E. J. ARLMAN, J. Pol. Sc. 12 547 (1954)

116. B. BRAUN AND M. THALLMAIER, IUPAC Int. Symp. Macromol. Chem. Prague (1965) Reprint 279.

117. M. J. MORONEY, Facts from Figures, Pelican (1968).

118. A. K. OSBORNE, An Encyclopaedia of the iron and steel industry, 2nd Edit. The Technical Press (1967) 423.

119. W. E. HANFORD AND R. M. JOYCE, Polytetrafluororthylene J.A.C.S. 68 2082 (1946)

120. A. W. J. DE GEE AND A. BEGELINGER, See Solomon Proc. Inst. Mech. Eng. (1965/66) 180 (Pt 3K).

121. R. E. REED-HILL, Physical Metallurgy Principles, Van Nostrand Reinhold (1970), 6.

122. D. MARGERISON AND G. C. EAST, Introduction to polymer chemistry, Pergamon (1967) 166.

123. D. REDDY AND B. S. NAU, Wear testing, Brit. Hydromechanics Res. Assn. TN 940 (1968).

124. M. ANTLER, Wear 7 (1964) 181.

125. M. COCKS, J. Appl. Phys. 33 (1962) 2152-2161.

126. M. ANTLER, ASLE Trans. 5 (1962) 297-307.

127. C. M. ALLEN AND E. DRAUGLIS, Wear 14 (1969) 363-384.

128. J. T. BURWELL, Wear 1 (1957) 119-141.

129. J. K. LANCASTER, Basic mechanisms of friction and wear of polymers, P.I. Conf. Plastics In Bearings, Solihull, Feb. (1973).

130. U. R. EVANS, The corrosion and oxidation of metals, Arnold (1967)

131. A. F. WELLS, Structural inorganic chemistry Oxford (1950).

132. Encyclopeadia of Polymer Science and Technology (1967) 241.

133. H. DETERMANN, Gel chromatography, Springer-Verlag (1968).

134. A. R. COOPER, Gel permeation chromatography Chem. Brit. March (1973)

135. H. E. PICKETT, M. J. R. CANTOW AND J.F. JOHNSON, J. App. Pol. Sc. 10 (1966) 917 - 924.

136. F. P. CLARK, Handbook of Physical Constants. Geolog. Soc. Am. Memoir 97, (1966) 463.

137. S. DUSHMAN, 'Scientific Foundations of the vacuum technique' J. Wiley (1958) (a) P.656 (b) P.655 (c) P.8.

138. D. W. MORECROFT, Reactions of octadecane and decoic acid with clean iron surfaces. Conf. on chemical effects at Bearing Surfaces, Swansea Tribology Centre, Jan. 6-8, (1971)

139. R. W. ROBERTS, Trans. Fara. Soc. 58 (1962) 1159.

140. P. A. REDHEAD, Can. J. Physics. 42 (1964) 886.

141. J. R. ANDERSON, (Editor) Chemisorbtion and reactions on metallic films, Vols. 1 and 2. Academic Press (1971).

142. V. PONEC, Preparation of ultra-clean substrate surfaces, P. 485.

143. R. E. BANKS, Fluorocarbons and their derivitives, Macdonald (1970) 12

144. H. C. HILL, Introduction to mass spectrometry, Heyden (1969)

145. J. H. BEYNON, Mass spectrometry and its applications to organic chemistry, Elsevier (1960) (a) P. 251 (b) P. 253 (c) P. 256.

146. L. A. ERREDE, The application of simple equations for caluculating bond dissociation energies to the thermal degradation of fluorocarbons, J. Org. Chem. 27 (1962) 3425.

147. R. K. STEUNENBERG, AND G. H. CADY, J. Am. Chem. Soc. 74 (1952) 4165

148. G. H. CADY, Proc. Chem. Soc. April (1960) 133.

149. W. WILKENS AND O. KRANZ, Wear 15 (1970) 215-227.

150. G. C. BOND, Catalysis by metals, Academic Press (1962).

151. G. C. BOND, Dis. Fara. Soc. 41 200 (1966).

152. A. CORNU AND R. MASSOT, Compilation of mass spectrometry data, Heyden (1966)

153. Eight Peak Index of Mass Spectra, M.S. Data Centre, A.W.R.E., Aldermarston. Vol. 2 Table 3 (1970).

154. A.S.T.M. Index of Mass Spectral Data, STP 356 (1969).

155. J. C. HENNIKER, Infra-red spectrophotometry of industrial polymers, Academic Press (1967).

156. K. ANDREWS, D. DYSON AND S. KEOWN, Interpretation of electron diffraction patterns, Hilger & Watts (1967).